

## Porous Conductive Textiles for Wearable Electronics

Yichun Ding<sup>1,5,6 §</sup>, Jinxing Jiang<sup>1, §</sup>, Yingsi Wu<sup>1, §</sup>, Yaokang Zhang<sup>1, §</sup>, Junhua Zhou<sup>1, §</sup>, Yufei Zhang<sup>1, §</sup>, Qiyao Huang<sup>1,3 \*</sup>, Zijian Zheng<sup>1,2,3,4 \*</sup>

<sup>1</sup> School of Fashion and Textiles, The Hong Kong Polytechnic University, Hung Hom, Kowloon, Hong Kong SAR 999077, P. R. China

<sup>2</sup> Department of Applied Biology and Chemical Technology, Faculty of Science, The Hong Kong Polytechnic University, Hung Hom, Kowloon, Hong Kong SAR 999077, P. R. China

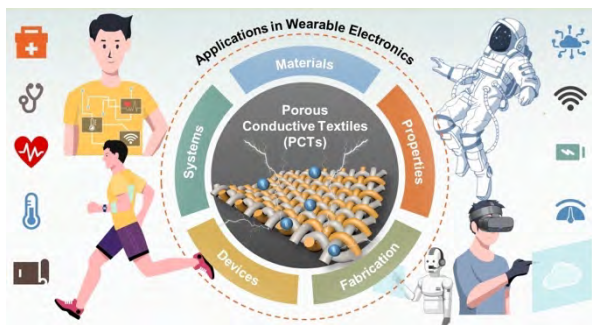
<sup>3</sup> Research Institute for Intelligent Wearable Systems, The Hong Kong Polytechnic University, Hong Kong SAR 999077, P. R. China

<sup>4</sup> Research Institute for Smart Energy, The Hong Kong Polytechnic University, Hong Kong SAR 999077, P. R. China

<sup>5</sup> Fujian Institute of Research on the Structure of Matter, Chinese Academy of Sciences Fuzhou, Fujian 350108, P.R. China

<sup>6</sup> Fujian Science & Technology Innovation Laboratory for Optoelectronic Information of China, Fuzhou, Fujian 350108, P.R. China

## TOC graphic



## ABSTRACT

Over the years, researchers have made significant strides in the development of novel flexible/stretchable and conductive materials, enabling the creation of cutting-edge electronic devices for wearable applications. Among these, porous conductive textiles (PCTs) have emerged as an ideal material platform for wearable electronics, owing to their light weight, flexibility, permeability, and wearing comfort. This review aims to present a comprehensive overview of the progress and state of the arts of utilizing PCTs for the design and fabrication of a wide variety of wearable electronic devices and their integrated wearable systems. To begin with, we elucidate how PCTs revolutionize the form factors of wearable electronics. We then discuss the preparation strategies of PCTs, in terms of the raw materials, fabrication processes, and the key properties. Afterward, we provide detailed illustrations of how PCTs are used as basic building blocks to design and fabricate a wide variety of intrinsically flexible or stretchable devices, including sensors, actuators, therapeutic devices, energy harvesting and storage devices, and displays. We further describe the techniques and strategies for wearable electronic systems either by hybridizing conventional off-the-shelf rigid electronic components with PCTs, or by integrating multiple fibrous devices made of PCTs. Subsequently, we highlight some important wearable application scenarios in healthcare, sports and training, converging technologies, and professional specialists. At the end of the review, we discuss the challenges and perspectives on future research directions and give overall conclusions. As the demand for more personalized and interconnected devices continues to grow, PCT-based wearables hold immense potential to redefine the landscape of wearable technology and reshape the way we live, work, and play.

## **CONTENTS**

### **1. Introduction**

### **2. Materials and Methods to Fabricate PCTs**

#### **2.1 Textile Materials**

#### **2.2 Conductive Materials**

##### **2.2.1 Conducting Polymers**

##### **2.2.2 Carbon Materials**

##### **2.2.3 Metals**

#### **2.3 Fabrication of PCTs**

##### **2.3.1 Fabrication of PCTs from Intrinsically Conductive Textile Materials**

##### **2.3.2 Fabrication of PCTs from Non-Conductive Textile Materials**

##### **2.3.3 Patterning**

#### **2.4 Strategies to Endow Flexibility/Stretchability**

##### **2.4.1 Stretchable Textile Structures**

##### **2.4.2 Intrinsically Stretchable Materials**

#### **2.5 Key Properties of PCTs**

##### **2.5.1 Conductivity**

##### **2.5.2 Mechanical Properties**

##### **2.5.3 Comfortability**

### **3. Wearable Devices based on PCTs**

#### **3.1 Sensors**

##### **3.1.1 Biophysical Sensors**

##### **3.1.2 Chemical and Biological Sensors**

##### **3.1.3 Electrophysiological Sensors**

#### **3.2 Actuators**

##### **3.2.1 Electrical Actuation**

##### **3.2.2 Thermal Actuation**

##### **3.2.3 Solvent Actuation**

#### **3.3 Therapeutic Devices**

##### **3.3.1 Thermotherapy**

##### **3.3.2 Electrical Stimulation**

##### **3.3.3 Drug Delivery**

#### **3.4 Energy Harvest and Storage Devices**

##### **3.4.1 Solar Cells**

- 3.4.2 Generators
  - 3.4.3 Wireless Energy Harvesting
  - 3.4.4 Biofuel Cells
  - 3.4.5 Supercapacitors
  - 3.4.6 Batteries
- 3.5 Displays
  - 3.5.1 Light-Emitting Devices
  - 3.5.2 Electrochromic Devices
- 4. Integrated Wearable Systems based on PCTs
  - 4.1 Hybridizing Microelectronics with PCTs
    - 4.1.1 Microelectronics Integrated Hybrid Systems
    - 4.1.2 Connection of Rigid Electronics on Textiles
  - 4.2 Integrating Fibrous Devices Made of PCTs
    - 4.2.1 Functional Fibrous Devices Integrated Systems
    - 4.2.2 Fabrication Methods of Fibrous Devices
    - 4.2.3 Assembly and Connection of Fibrous Devices
  - 4.3 Optimizing Wearable Durability and Performance
    - 4.3.1 Bonding Strength Enhancement
    - 4.3.2 Strain Engineering
    - 4.3.3 Encapsulation
    - 4.3.4 Multilayer Electronics on PCTs
  - 4.4 System Integration
    - 4.4.1 Integrated Circuits
    - 4.4.2 Wireless Communications
    - 4.4.3 Machine Learning
- 5. Application Scenarios
  - 5.1 Health Monitoring and Theranostics
  - 5.2 Exercises and Sports
  - 5.3 Converging Technologies
    - 5.3.1 Human-Machine Interaction
    - 5.3.2 Extended Reality
    - 5.3.3 Internets of Things
  - 5.4 Extreme Environments

6. Challenges and Perspectives

7. Conclusions

Author Information

Corresponding Author

Authors

Author Contributions

Notes

Biographies

Acknowledgments

Abbreviations Used

References

## 1. INTRODUCTION

Wearable electronics are electronic devices designed to be worn on various parts of human body such as heads and hands, and to offer electronic functionalities such as sensing, actuating, data transmission, and energy harvesting and storage.<sup>1-3</sup> Over the years, a diverse range of wearable electronics have been introduced to the market, spanning various fields such as communication and entertainment, sports and health monitoring, clinical and rehabilitation, education, military, and aerospace. These wearable products, with a total market worth over USD 81 billion in 2022, have significantly contributed to improving convenience, productivity, and wellness to humans and society.<sup>4-6</sup> Yet, limited to the materials and technologies available, wearable products nowadays are designed and manufactured in the formats where rigid electronic components are attached on or to flexible and wearable soft supports, belts, or adhesives. These designs lack wearing comfort and conformability for long-term on-body applications.<sup>7, 8</sup> The mechanical mismatch between rigid electronic devices and human body also impedes the epidermal interfacing, resulting in a deficiency, particularly in the reliability of signal collection and transmission from the human body.<sup>9, 10</sup>

Over the past two decades, various strategies have been proposed to revolutionize the form factors of wearable electronics. The vision is to create new-generation electronic devices that can not only maintain their functionality throughout multiple flexing or stretching cycles but also possess promising wearing comfort, conformability, and even skin biocompatibility for long-term wearable applications.<sup>11, 12</sup> To this end, there are mainly two approaches: making flexible/stretchable structures and developing soft materials. For the former, rigid silicone-based electronics can be reconstructed into ultrathin or wavy configurations to achieve the desired flexibility or stretchability.<sup>13-18</sup> For the latter, a variety of intrinsically soft materials, such as polymeric thin films, foils, paper sheets, and textile materials, have been incorporated with electronic counterparts for the assembly of flexible or even stretchable electronic devices.<sup>19-23</sup> Pioneering prototypes of such flexible or stretchable electronics include multifunctional sensors,<sup>24-28</sup> actuators,<sup>29</sup> transistors,<sup>30, 31</sup> energy storage devices,<sup>32-37</sup> and energy harvesters.<sup>38, 39</sup> Further advancement in device integration has allowed the creation of soft electronic systems that can be comfortably and conformably applied to human bodies, and perform functions similar to conventional rigid-type wearable products.<sup>40-43</sup>

Since wearable electronics are mostly in contact with human bodies, textiles are deemed to be a suitable platform for daily and long-term applications.<sup>44</sup> Textiles refer to materials and

structures that are composed of fibers. From the viewpoint of materials, the raw materials of textiles, *i.e.*, fibers, are generally characterized by good flexibility and fineness, which therefore can offer textiles great softness, large surface areas, and high porosity.<sup>45</sup> These properties are highly beneficial for the development of wearable devices, where electronic materials can be embedded into the porous textile structures without compromising the electronic performance and the textile softness potentially.<sup>46, 47</sup> In addition, textiles can be fabricated from either natural or synthetic fiber materials, and then processed into one-dimensional (1D) yarns, two-dimensional (2D) fabrics, and three-dimensional (3D) composites.<sup>48</sup> In comparison to planar-type soft materials (*e.g.*, thin films, paper sheets, metal foils), soft and porous textiles demonstrate advantageous multiscale hierarchical structures with a higher degree of materials diversity, leading to greater conformability to different shapes of objects.<sup>21</sup> Consequently, integrating electronics with textile materials and structures enables the creation of textile-based wearable electronics that are capable of providing electronic functions while maintaining superior softness, comfortability, and conformability to human bodies.<sup>49</sup> From the viewpoint of manufacture, textile industry is one of the largest industries that comprises of high-throughput and high-speed processing for different fibrous materials.<sup>48, 50, 51</sup> The booming development of wearable technologies has promoted the evolution of textile industry, leading to the invention of textile technologies and production lines that are highly compatible with the integration of electronic components.<sup>52-54</sup> Such a technological revolution is highly critical for the viability of commercializing textile-based wearable electronics.<sup>47</sup> To sum up, it is an ideal strategy to utilize textile-based materials, structures, and processing technologies to develop wearable electronic devices and systems.<sup>55</sup>

Conductive materials play indispensable roles in electrical interconnection, electrode development, and system circuit fabrication. Since the majority of conventional textiles are insulating, transforming non-conductive textiles into conductive ones with desired electrically conductive properties is a pivotal process in the development of textile-based wearable electronics.<sup>56</sup> Versatile methods and techniques such as chemical synthesis/conversion, surface grafting/decorating, and physical deposition/coating can make the non-conductive textiles conductive. In general, the resulting conductive textiles can retain the porous structure characteristic of textile materials. Therefore, we herein define Porous Conductive Textiles (PCTs) as textile materials and/or structures that can not only conduct electricity but also preserve the inherent properties of textiles (*e.g.*, softness, porosity, hierarchical structures, conformability). PCTs outperform metal wires and rigid printed circuit boards (PCBs) as a soft

and conductive platform for the embodiment of electronic units.<sup>56-58</sup> They act as the soft functional electrodes integrating into clothing for continuous sensing of physical and physiological signals in an insensible manner,<sup>59-61</sup> and function as the building blocks for the fabrication of various types of wearable electronic devices.<sup>62, 63</sup> Further integration of microelectronics and wireless communication technologies can enable a textile-based intelligent electronic system with most electronic units “invisible” inside the textile materials and structures, providing a comfortable and conformable clothing platform for wearable applications including but not limited to health monitoring and theranostics, exercises and sports, virtual reality (VR), augmented reality (AR), human-machine interaction (HMI), internet of things (IoT), and even aerospace and military.<sup>9, 64, 65</sup> Ever since the early 20<sup>th</sup> century when the first generation of wearable electronics was developed by embedding rigid electronic devices and conductive threads into garments,<sup>7, 66</sup> researchers have made great efforts in the development and applications of PCTs. **Figure 1a** provides a timeline illustrating the significant advancements in the development of various formats of PCTs and their applications in wearable electronics.<sup>7, 24, 67-81</sup> The timeline categorizes these developments based on their materials and functions, offering a concise overview of the progress made over time and showcasing the evolution and diversification of PCTs as well as PCT-based wearable electronics. The increasing numbers of publications in journal articles and patents have also witnessed such rising awareness and booming technological development towards conductive textiles (**Figure 1b**). The advancements in materials science and chemistry, manufacturing, and electronic engineering continue revolutionizing PCTs, making them durable, multifunctional, and especially toward scalable manufacturing for the commercial viability of textile-based wearable electronics.



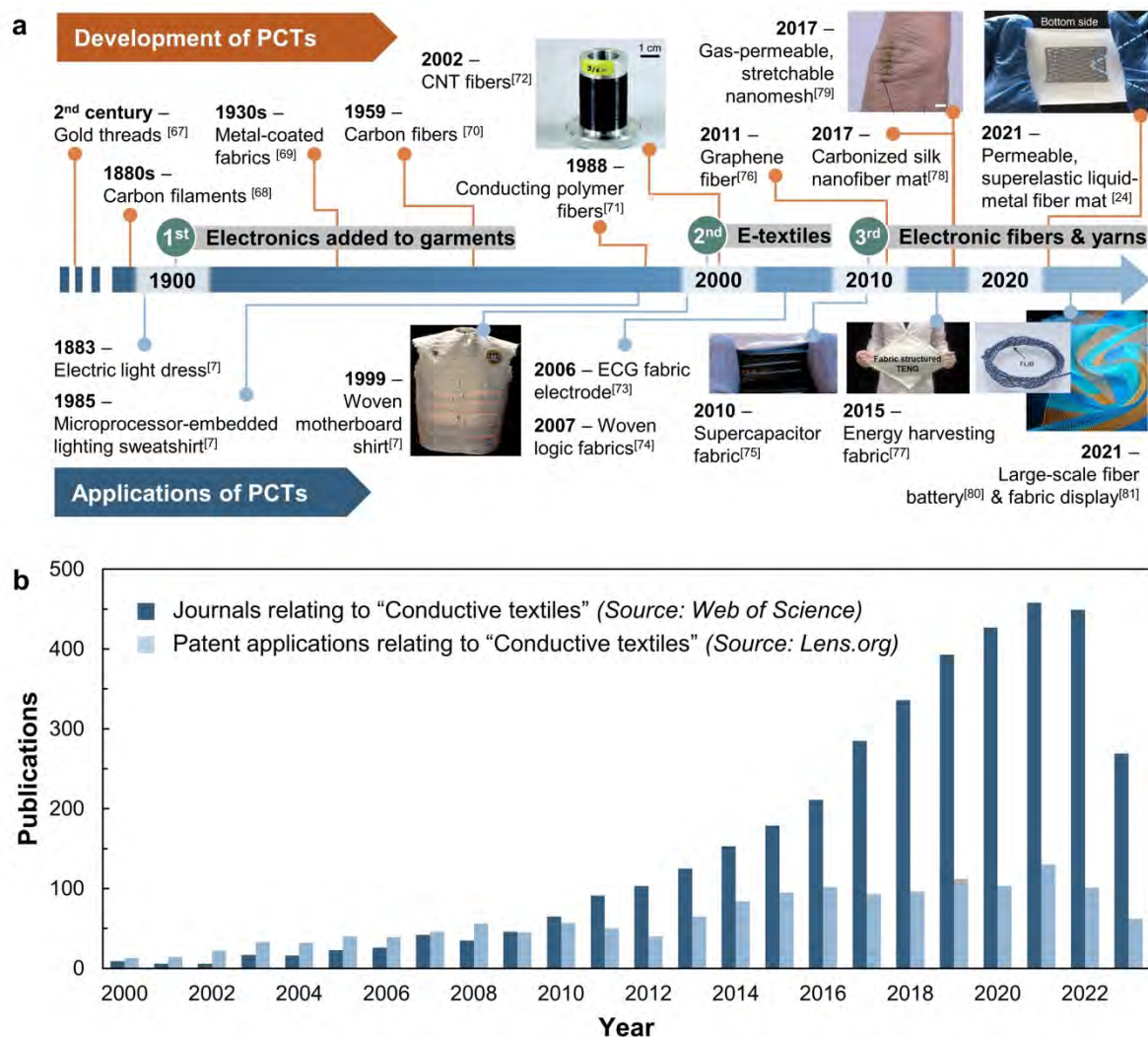


**Figure 1.** (a) Timeline showing the key development of porous conductive textiles (PCTs) and their applications in wearable electronics.<sup>7, 24, 67-81</sup> “1999-Woven motherboard shirt”, Reproduced with permission from ref. <sup>7</sup> Copyright 2016 Springer Nature. “2002-CNT (carbon nanotube) fiber”, Reproduced with permission from ref. <sup>72</sup> Copyright 2012 Royal Society of Chemistry. “2010-Supercapacitor fabric”, Reproduced with permission from ref. <sup>75</sup> Copyright 2010 American Chemical Society. “2017-Gas-permeable, stretchable nanomesh”, Reproduced with permission from ref. <sup>79</sup> Copyright 2017 Springer Nature. “2015-Energy harvesting fabric”, Reproduced with permission from ref. <sup>77</sup> Copyright 2015 American Chemical Society. “2021-Permeable, superelastic liquid-metal fiber mat”, Reproduced with permission from ref. <sup>24</sup> Copyright 2021 Springer Nature. “2021-Large-scale fiber battery & fabric display”, Reproduced with permission from ref. <sup>80, 81</sup> Copyright 2021 Springer Nature. (b) Summary of the publication records of journal articles and patent applications relating to “conductive textiles” recorded in Web of Science and Lens.org (search date: 30 Sept 2023).

In this review, we present a broad picture of the research on PCTs and their applications in wearable electronics (**Figure 2**). The review begins with an exhaustive discussion of the key materials, fabrication methods, and critical properties for PCTs (Section 2). In particular, strategies as well as their working mechanisms to impart PCTs with electrical conductivity are discussed in detail. We then comprehensively discuss all the research activities on utilizing PCTs to develop wearable electronic devices by covering the working mechanism, materials innovation, and device design in each type of device (Section 3). Taking PCTs as the building blocks, an integration of various PCT-based electronic devices, power supply, and communication units can build up a wearable electronic system that can be applied in a variety of areas, which are also thoroughly described in this review (Section 4). Then, some application scenarios including healthcare, sports and training, converging technologies, and professional specialists of PCT-based devices are illustrated (Section 5). Thereafter, the review provides a critical analysis of PCTs and PCT-based electronics in terms of their remaining challenges and future perspectives of development (Section 6). Finally, we give a thorough summary and in-depth discussion of the review (Section 7). With worldwide efforts from both academia and industries, advancement in chemistry and materials, devices fabrication, and system engineering that are elaborated in this review are expected to push forward the development of PCTs and multifunctional textile-based wearable electronics, which will soon revolutionize our lives by promoting the welfare of society as a whole.

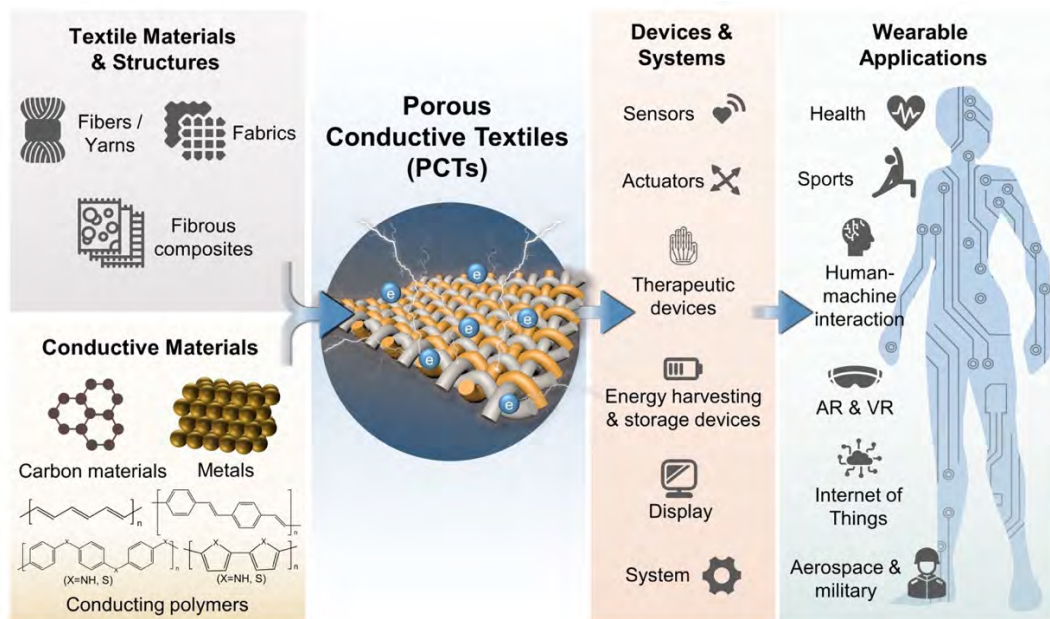


**Figure 2.** Schematic illustration showing the overall framework of the review: PCTs and their applications in wearable electronics.

## 2. MATERIALS AND METHODS TO FABRICATE PCTs

PCTs can be fabricated either by shaping intrinsically conductive materials into textiles or coating non-conductive textiles with conductive materials. Both fabrication approaches entail the utilization of diverse textile and conductive materials in different formats, along with various processing technologies. This section discusses the materials and methods that can be utilized to obtain PCTs.

### 2.1 Textile Materials

Textiles encompass a great variety of fiber-based materials including fibers, yarns, and fabrics, all of which can serve as a soft and permeable platform for the development of PCTs and subsequent wearable electronics. The smallest visible constituent of textiles is fibers, recognized by their high length-to-diameter ratio, typically greater than 100:1. In the textile industry, fibers can be classified by length, where staple fibers are short fibers with millimeter-scale length, while filaments refer to long and continuous fibers with meter scale or above. Apart from high length-to-diameter ratio, the fiber materials should have sufficient flexibility and strength for processing. Fibers can be further twisted and interlocked by a spinning process to form a continuous strand, which is also known as yarn. Fibers, yarns, or their combinations are basic components for porous fabrics.

The structures of porous fabrics obtained by conventional manufacturing processes are typically classified into three types: woven, knitted, and non-woven structures (**Figure 3**). A typical woven fabric requires two sets of interlaced yarns: longitudinal warp yarns and lateral weft yarns. The large amount of interlacement in the woven structure provides the fabric with firmness and stability, while the changeable locking angle between weft and warp yarns enables the flexibility and stretchability of woven fabrics.<sup>82</sup> Knitting refers to a group of textile structures consisting of interloped yarns. The meandering loops provide remarkable stretchability for knitted fabrics, even if the yarns of the fabric are not intrinsically stretchable. In addition to these yarn-based fabrics, there is another type of fabric classified as non-woven fabric, which is made from fibers bonded directly through various methods such as thermal, mechanical, chemical, or solvent bonding.

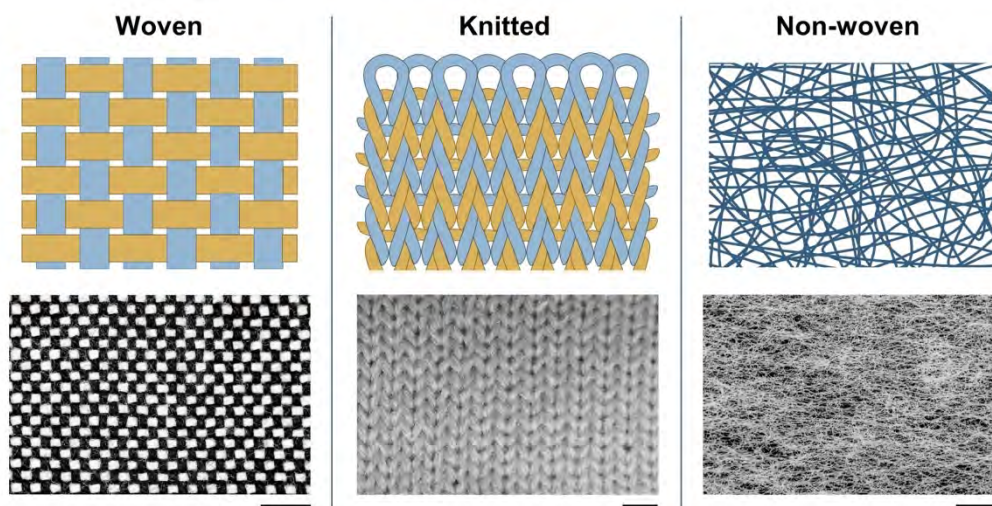


**Figure 3.** Schematic illustration (top) and digital images (bottom) showing the typical structures of porous fabrics. From left to right: woven fabric structure (scale bar: 5 mm), knitted fabric structure (scale bar: 5 mm), and non-woven fabric structure (scale bar: 1 mm).

The fiber source of textile materials can be broadly divided into two categories: natural and synthetic. Conventional natural fibers such as cotton, wool, and silk are lightweight, soft, and biocompatible. The moisture absorption property and breathability of these fibers provide enhanced comfortability for wearable electronics.<sup>83-86</sup> However, the poor chemical and abrasion resistances limit their application in some wearable electronics that require harsh chemical treatment/modification of textile substrates. On the other hand, synthetic fibers, such as nylon and polyester, show good mechanical strength and chemical resistance. As a result, synthetic fiber-based textiles have become common porous textile substrates for a great variety of wearable electronics.<sup>87-94</sup>

## 2.2 Conductive Materials

Conventional electrically conductive materials, such as conducting polymers, carbon materials, and metals are common building blocks for the construction of conductive interconnects and electrodes for wearable electronic devices and systems. Similarly, these conductive materials are indispensable in the fabrication of PCTs and textile-based wearable electronics. This subsection covers three commonly used conductive materials, elaborating on their conductive properties and the techniques employed to incorporate them with textile fibers.

### 2.2.1 Conducting Polymers

Conducting polymers refer to conjugated polymers that can conduct electricity.<sup>95</sup> For wearable

electronics, conducting polymers are ideal materials for electrodes and interconnects because of their advantageous features of lightweight, high conductivity, flexibility, and electrochemical activity.<sup>96, 97</sup> Typical conducting polymers that can be used for developing PCTs include polyanilines (PANIs), polypyrroles (PPys), and polythiophenes.<sup>98-100</sup> In their pristine state, conducting polymers are typically insulators or semiconductors with a very low conductivity of  $< 10^{-5} \text{ S cm}^{-1}$ .<sup>101, 102</sup> However, their conductivity can be boosted to a metallic level ( $> 10^4 \text{ S cm}^{-1}$ ) through appropriate doping.<sup>103, 104</sup>

Conducting polymer fibers can be produced via spinning technologies such as wet spinning, melting spinning, and electrospinning (**Figure 4**).<sup>105</sup> Wet spinning is a conventional technology employed in the textile industry to produce man-made fibers. During the wet spinning processes, solutions of conducting polymers are extruded from spinnerets into a coagulating medium (poor solvent) for producing conducting polymer-based fibers. During this process, a mutual diffusion of solvents takes place leading to the precipitation or crystallization of polymers.<sup>106</sup> Benefiting from its simple and continuous processes, wet spinning is capable of producing long and continuous filaments.<sup>107</sup> The major disadvantages of wet spinning are the requirement of a high-cost solvent recovery process and the low production rate. In melt spinning, conducting polymers or their blends are melted at high temperatures, and then extruded through the spinneret. Afterward, conducting polymer fibers are solidified immediately by a cooling process. Compared to wet spinning, melt spinning shows advantages of high production rate and high material utilization. However, melt spinning process is only compatible with thermoplastic polymeric materials for conducting polymer-based PCTs.<sup>108</sup> Generally, both the wet spinning and melt spinning processes can only produce fibers with diameters in micrometer and millimeter scales. Alternatively, the electrospinning technique is effective to produce fine conducting polymer fibers and nonwovens with the fiber diameter down to nanoscale scale. During the electrospinning process, a high direct current (DC) voltage is connected to the spinneret injected with a polymer solution. The droplet on the spinneret is extended and eventually erupts to form filaments when the electrostatic repulsion counteracts the surface tension. As the solvent evaporates, solid fibers are generated when the solution viscosity is within a certain threshold.<sup>109</sup> Electrospinning possesses advantages of simple processes and mild conditions. It is especially suitable for producing high-quality nano- and microscale fine polymeric fibers. The major disadvantages of electrospinning include low production efficiency and the use of toxic solvents.<sup>110</sup>



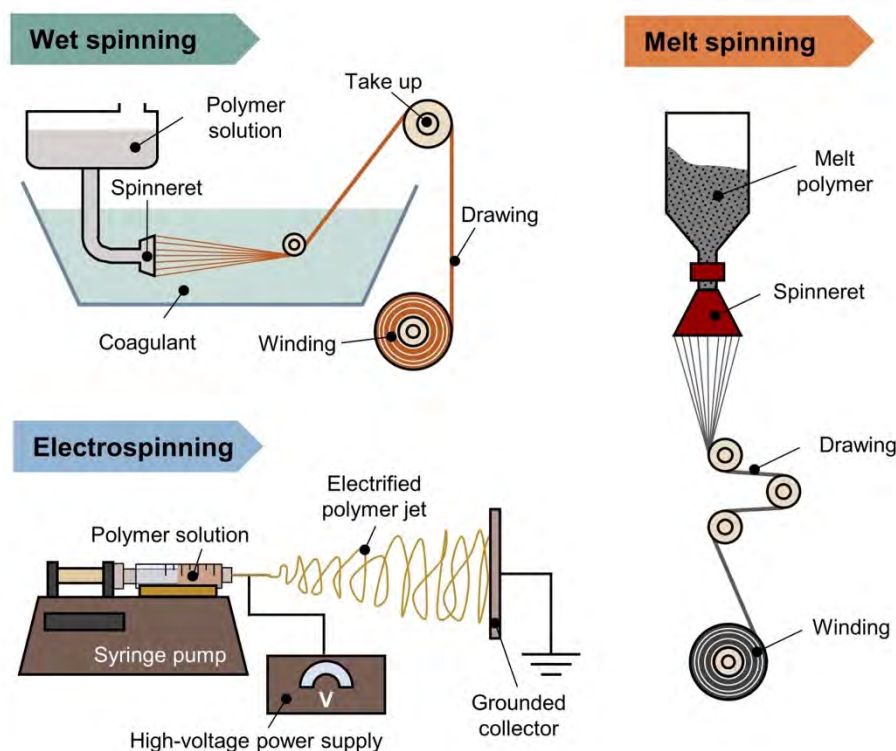


**Figure 4.** Schematic illustration showing the production of conducting polymer fibers via spinning technologies including wet spinning, melt spinning, and electrospinning.

### 2.2.2 Carbon Materials

Carbon materials show excellent chemical inertness, high mechanical robustness, and good electrical conductivity. As a result, they have been widely used for making flexible and wearable electronic devices such as Li batteries,<sup>33, 111</sup> supercapacitors,<sup>112, 113</sup> solar cells,<sup>114, 115</sup> nanogenerators,<sup>116, 117</sup> and chemical sensors.<sup>118, 119</sup> Frequently used carbon materials for PCTs in wearable electronic applications include carbon fiber, graphene, and carbon nanotubes (CNTs). Among them, the commercially available woven carbon cloth has been adopted as current collector for energy storage devices.<sup>120</sup> The carbon cloth consists of carbon yarns, which are usually produced from polymer precursors with high carbon content and high molecular weight such as polyacrylonitrile (PAN),<sup>121</sup> polyethylene (PE),<sup>122</sup> and cellulose.<sup>123</sup> Among them, PAN fibers dominate ~90% of the market for producing high-yield and high-performance carbon fibers.<sup>124, 125</sup> In the typical manufacturing process, the polymer precursors are firstly processed into fibers via spinning technologies, and then undergo a series of heat treatments, involving oxidation, carbonization, and/or graphitization to convert them into carbon fibers (as illustrated in **Figure 5**). Taking PAN as an example of polymer precursors, the initial heat treatment at 200 ~ 300 °C induces the structural change of PAN from open chain

polymers to thermally stable ladder structure.<sup>126, 127</sup> The structural change improves the thermal stability of PAN, preventing the melting of fibers during the following high-temperature carbonization process. The carbonization process at 800 ~ 3000 °C removes the non-carbon elements of PAN, turning the ladder structural PAN to carbon/graphite structure.

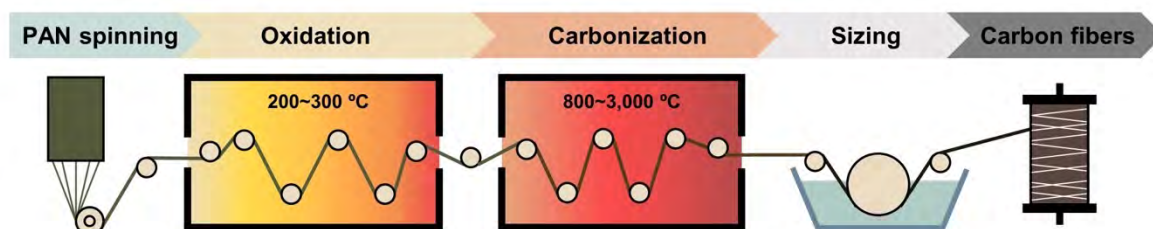


**Figure 5.** Schematic illustration showing the typical processes for fabrication of carbon fibers.

CNTs are 1D carbon materials with high mechanical strength, stiffness, and electrical conductivity.<sup>128, 129</sup> The synthesis methods of CNTs include a variety of physical and chemical approaches, such as arc discharge, laser ablation, chemical vapor deposition (CVD), electrolysis, and hydrothermal method.<sup>130, 131</sup> Similar to the fabrication of synthetic polymer fibers, CNT fibers can be produced via spinning from precursors such as liquid crystal suspension, aligned forests, and aerogels of CNTs (**Figure 6**).<sup>132</sup> The mechanical strength of spun CNT fibers is determined by multiple factors such as alignment, packing density, defects, and interfacial bonding of CNTs.<sup>133-135</sup> The excellent flexibility of CNT fibers makes them promising for E-textiles and wearable electronics.<sup>136-138</sup> The orientation behavior and high strength of CNTs also provide the possibility of constructing highly stretchable composite fibers for stretchable electronics.<sup>139, 140</sup> For example, Liu *et al.*<sup>141</sup> reported CNT-rubber sheath-core composite fibers with a high stretchability of up to 1320%, and such composite fibers showed a very small dependence of electrical resistance on strain. In addition, CNTs can serve as conductivity and strength-enhancing materials in composite fibers with polymers,<sup>142, 143</sup> metals,<sup>144, 145</sup> and metal oxides<sup>146, 147</sup> for flexible and wearable electronics.

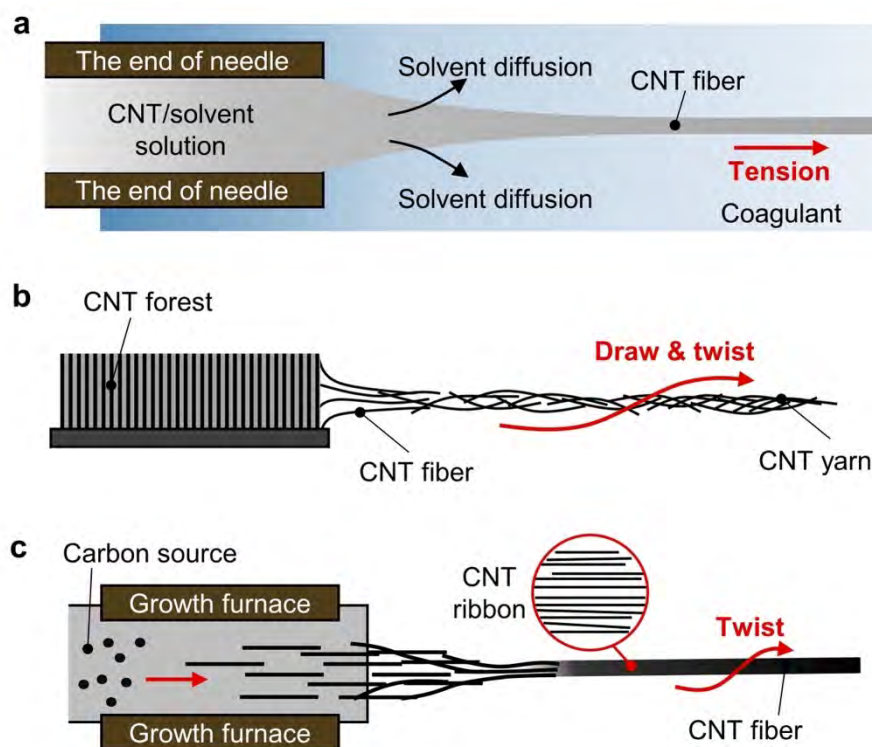


**Figure 6.** Schematic illustration showing the fabrication of CNT fibers through spinning of liquid crystal suspension (a), aligned forests (b), and aerogels of CNTs (c). Reproduced with permission from ref <sup>132</sup>. Copyright 2020 John Wiley and Sons.

Graphene, a 2D graphite material, is promising for a variety of wearable electronics because of its unique electrical, optical, thermal, and mechanical characteristics.<sup>148-152</sup> The representative methods for the synthesis of graphene include mechanical/chemical exfoliation,<sup>153, 154</sup> chemical synthesis,<sup>155, 156</sup> and CVD.<sup>157, 158</sup> Whereas the as-synthesized graphene materials are not in fibrous form, graphene oxide (GO) sheets can be assembled and aligned uniaxially into fibers.<sup>159</sup> Conventional wet spinning methods, which are highly compatible with the textile industry, can be used for large-scale fabrication of porous GO fibers from GO suspension (**Figure 7**).<sup>160, 161</sup> The GO fibers can be reduced to graphene fibers via additional processes such as chemical, laser, and thermal reduction.<sup>76, 162, 163</sup> Xin *et al.*<sup>164</sup> discovered that a post-thermal annealing process can reduce GO fibers to graphene form, by which the electrical and thermal conductivity, and tensile strength of as-spun graphene fibers are improved significantly. To make graphene-based PCTs, another strategy is mixing graphene with other materials, such as polymers,<sup>165, 166</sup> metals,<sup>167, 168</sup> and other carbon materials,<sup>169, 170</sup> to produce graphene composite fibers.<sup>171</sup> For example, Qu *et al.*<sup>172</sup> reported the synthesis of hollow graphene/conductive polymer fibers by mixing GO with conducting polymer poly(3,4-



ethylenedioxythiophene) polystyrene sulfonate (PEDOT:PSS). The doping of PEDOT:PSS improved both the tensile strength and electrical conductivity of graphene fibers. Liu *et al.*<sup>173</sup> modified metal-coated cotton yarns with GO via electrochemical deposition. The yarns were then reduced by hydrazine vapor to become Ni/rGO (reduced graphene oxide) composite electrodes for wearable supercapacitors. Graphene can also be incorporated with other carbon-based textiles to enhance their electrochemical performance and mechanical strength.<sup>174</sup> For example, Lu *et al.*<sup>175</sup> reported the fabrication of super-elastic CNT/graphene fibers via wet spinning of a mixture solution of graphene, CNT, and chlorosulfonic acid. Yang *et al.*<sup>113</sup> incorporated graphene, CNT, and conductive metal-coated textile together via a simple alternating filtration process. The composite conductive fabrics showed an areal capacitance up to  $6.2 \text{ F cm}^{-2}$ , and the authors attributed such high performance to the high surface area and good electrical conductivity of graphene and CNT.

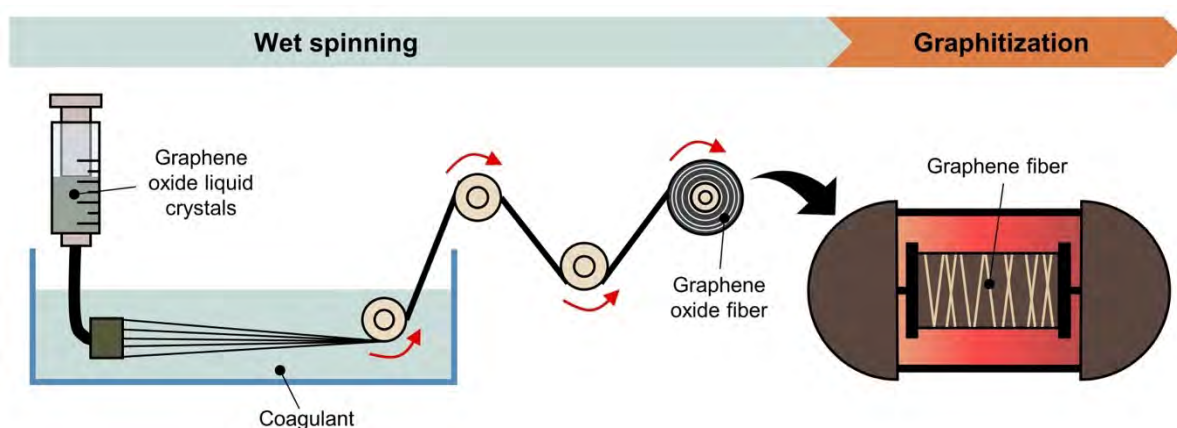


**Figure 7.** Schematic illustration showing the fabrication of graphene fibers.

### 2.2.3 Metals

Metals and alloys such as Cu, Ag, Au, Ti, and stainless steel are essential for most wearable electronics because of their high electrical conductivity ( $> 10^4 \text{ S cm}^{-1}$ ), high chemical stability, and good biocompatibility.<sup>176</sup> While bulky metal foils and thick metal films are too heavy and rigid for wearable electronics, metal nanowires (diameter  $< 200 \text{ nm}$ ) and metallic fibers (diameter of  $1 \sim 100 \text{ }\mu\text{m}$ ) show sufficient flexibility and softness that are more suitable to be incorporated into PCTs and E-textiles.<sup>177</sup>

Metallic fibers, including metals, alloys, and metal-coated textile fibers, have been commercialized for textiles and clothing applications for a long time.<sup>178, 179</sup> **Figure 8a**

schematically shows a wire drawing process that is able to make metal fibers with a fineness ranging from 50  $\mu\text{m}$  to millimeter scale. During the process, metal wires go through several drawing stones, resulting in the refinement and elongation of the metal wires. Bundle drawing is another method to produce metal filaments. In specific, a segment of solid wire (core-wire) is covered in a sacrificial alloy (usually low-carbon steel or copper) to begin the bundle drawing process. Using a rolling mill, the cladding (thin metal strip) is wrapped mechanically around the solid wire in this operation. The stiffness of metal fibers obtained via bundle drawing can be almost as high as that of carbon fibers.<sup>180</sup> Melt spinning is a common method for producing metal and metal hybrid fibers.<sup>181, 182</sup> For example, conductive fibers compositing with polymer and low-melting-point alloy can be obtained by the melt spinning process (**Figure 8b**).<sup>183</sup> Such a spinning process can preserve the connection between conductive fillers, which is usually destroyed in conventional drawing processes. As a result, the composite fibers showed a low resistivity of  $8.3 \times 10^4 \Omega \text{ m}$  with adding 2 vol% CNTs and 2 vol% low-melting-point alloy. Another approach to prepare metal composite fibers is the metallization of polymeric textile fibers via physical or chemical deposition technologies. This method enables the fabrication of wearable electronics on non-conductive textile substrates.<sup>184-186</sup> For example, PANI-coated fibers were fabricated by sputtering Au on polymethyl methacrylate (PMMA) core fibers, followed by electrochemical deposition of PANI (**Figure 8c**). Scanning electron microscope (SEM) images revealed uniform coating of metal and conducting polymer layers on the PMMA core fiber.<sup>187</sup> Chemical deposition is also a cost-efficient strategy to deposit metal thin films on textile fibers. Metal can be coated onto cotton textiles through an electroless chemical deposition method assisted by an interfacial polymer brush grafting process (**Figure 8d**). This process yielded highly conductive and flexible metal-coated cotton textiles with good adhesion between metal and cotton.<sup>188</sup>

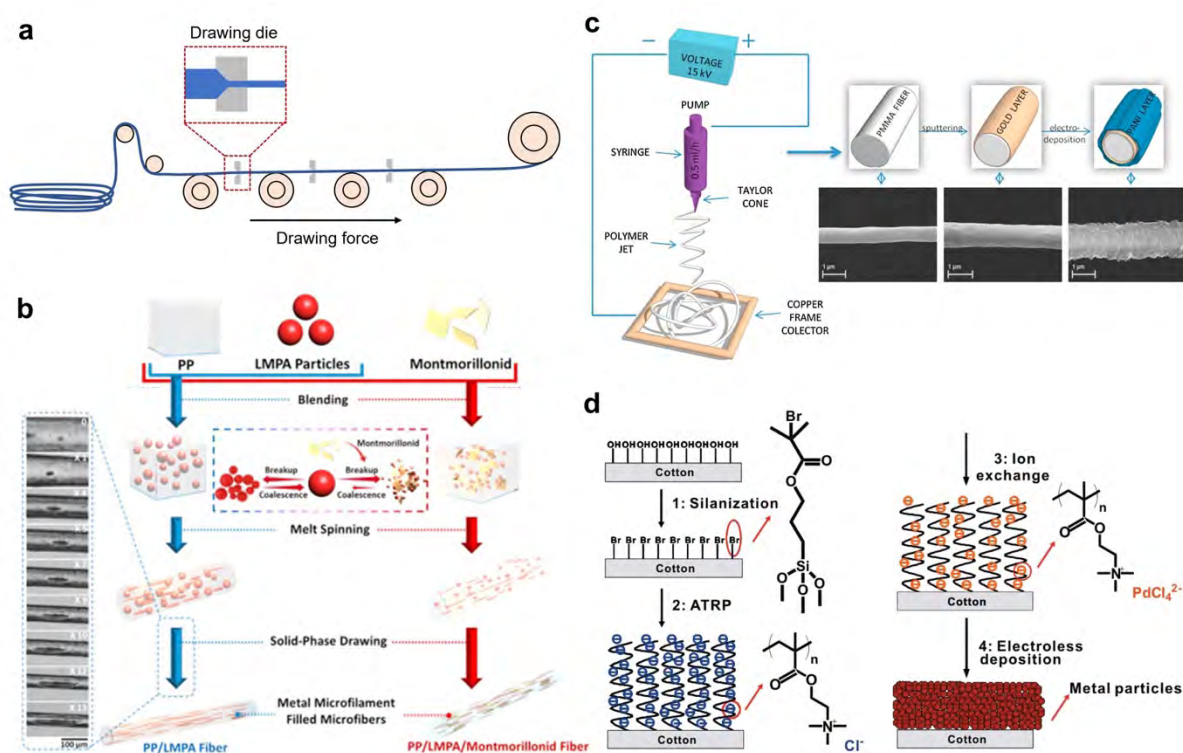


**Figure 8.** (a) Illustration of a wire drawing process for producing fine metal fibers. (b) Schematics of a melt spinning process for low melting point alloy composite fibers. Reproduced with permission from ref <sup>183</sup>. Copyright 2016 Elsevier. (c) Illustration of the fabrication process of PANI-coated PMMA fibers via electrochemical deposition. Reproduced with permission from ref <sup>187</sup>. Copyright 2016 Elsevier. (d) Polymer brush-assisted electroless metal deposition process on cotton fibers. Reproduced with permission from ref <sup>188</sup>. Copyright 2010 American Chemical Society.

Metal nanowires/nanofibers can be used as building blocks for metal-based PCTs in a smaller scale. Typically, metal nanowires show a very high aspect ratio of 1000 or larger, and a low diameter ranging from 10 to 200 nm.<sup>189</sup> The synthesis of metal nanowires usually involves the anisotropic growth of metals on hard or soft templates, through the chemical solution-phase or vapor-phase method.<sup>177</sup> The commonly used hard templates include aluminum oxides, mesoporous oxides, and CNTs.<sup>190</sup> Whereas hard template processes can yield high-quality and uniform metal nanowires, they usually suffer from tedious etching and post-treatment processes to remove residual templates after the synthesis.<sup>191</sup> On the other hand, soft template synthesis makes use of organic templates such as surfactants and polymers, which can be removed easily without complicated chemical etching or high-temperature treatment.<sup>192</sup> **Figure 9a** presents a proposed mechanism for the growth of Ag nanowires (AgNWs) in the presence

of poly(vinyl pyrrolidone) (PVP).<sup>193</sup> PVP is supposed to be a capping agent that assists the growth of pentagonal AgNWs under the confinement of five twin planes. The reaction conditions, such as temperature, stirring speed, and the duration of reactions, are critical for the synthesis of metal nanowires with high aspect ratio.<sup>194</sup> AgNWs are ideal building blocks for conductive fibers, flexible transparent electrodes, interconnects, and other components for flexible and wearable electronics because of the high conductivity and optical transparency of AgNWs networks.<sup>195</sup> In addition to AgNWs, Cu nanowires (CuNWs) are low-cost conductive building blocks for printable and wearable electronics.<sup>196</sup> **Figure 9b** shows different reaction stages during the synthesis of CuNWs via a one-pot synthesis approach.<sup>197</sup> The addition of ethylenediamine suppresses the formation of undesired octahedral Cu<sub>2</sub>O. One major challenge in the application of CuNWs arises from their susceptibility to oxidation due to their high chemical reactivity. This issue can be solved by surface passivation, doping, and alloying of CuNWs with oxidation-resistant materials such as conducting metal oxides, carbon materials, and other metals.<sup>198-200</sup> For example, Chen *et al.*<sup>201</sup> addressed this issue by electrodepositing metals (*e.g.*, Zn, Sn, and In) on the surface of CuNWs. These reactive metals form dense, transparent, and conductive metal oxide layers after plating, and thus prevent CuNWs from oxidation. Metal nanowires can be further twisted into yarns, and the twisting process is similar to that of making conventional textile yarns. For example, Mirvakili *et al.*<sup>202</sup> prepared Nb nanowire yarns by drawing Nb nanowires via a severe plastic deformation process (**Figure 9c**). The yarns showed a high ultimate tensile strength of 1.1 GPa, which is promising for actuating and artificial muscles.

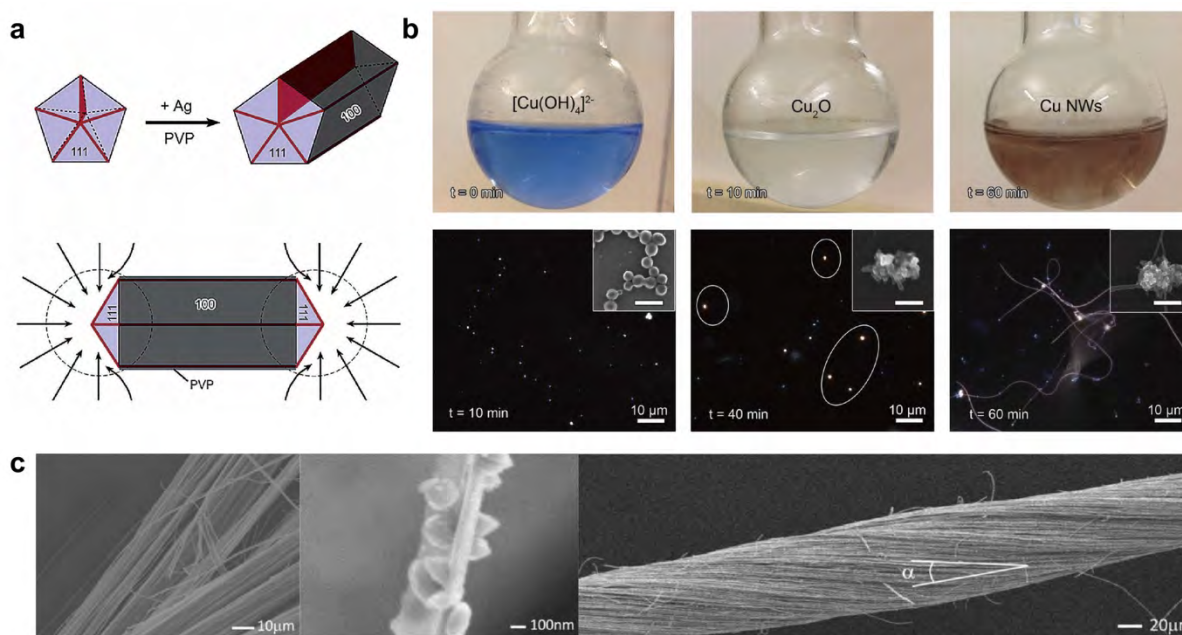


**Figure 9.** (a) Growth mechanism of pentagonal AgNW in presence of PVP. Reproduced with permission from ref <sup>193</sup>. Copyright 2003 American Chemical Society. (b) Three reaction stages during a one-pot synthesis of CuNWs. Reproduced with permission from ref <sup>197</sup>. Copyright 2014 John Wiley and Sons. (c) SEM images of Nb yarns obtained via drawing of Nb nanowires. Reproduced with permission from ref <sup>202</sup>. Copyright 2013 John Wiley and Sons.

## 2.3 Fabrication of PCTs

### 2.3.1 Fabrication of PCTs from Intrinsically Conductive Textile Materials

Intrinsically conductive textile building blocks, such as metal nanowires, carbon fibers, conducting polymer fibers, and their composites, can be assembled into conductive yarns and fabrics via conventional textile fabrication processes (**Figure 10**).<sup>203</sup> Yarn spinning refers to the process of transforming fibers into yarns, which differs from the fiber spinning processes mentioned in Section 2.1. The yarn-spinning process involves twisting or spinning fibers together to create a continuous strand of yarn with consistent diameter and strength. For example, continuous CNT yarns can be spun by directly extracting CNTs from a free-stranding CNT array (**Figure 11a**). It was estimated that a CNT array with 100  $\mu\text{m}$ -high and 1  $\text{cm}^2$  area can generate a 10 m-long CNT yarn with a diameter of 200  $\mu\text{m}$ .<sup>204</sup> The formation of a CNT yarn involves using a spinning system that consists of a motorized slider and a rotating spindle. The spindle was pulled back along the slider, which resulted in a continuous twisting and drawing of a CNT web, ensuring a constant and uniform quality of the yarn.<sup>205</sup> Post-spin twisting processes can be applied to enhance the mechanical strength of as-spun CNT yarns.

**Figure 11b** shows a flyer spinning system for producing twisted CNT yarns.<sup>206</sup> In this process, the yarn moves over a set of tensioning pins, then bends around the flyer guide, and eventually winds onto the bobbin for collection, during which it experiences significant tension. As a result, the obtained yarn has a denser composition, and the correlation between twist and strength is distinct from that of yarns created with low tension. Kim *et al.*<sup>207</sup> studied different yarn spinning and twisting structures, and applied the twisted CNT yarns for energy harvesters that convert mechanical energy to electricity (**Figure 11c**). The research results demonstrated that optimal energy generation can be achieved by adjusting the amount of yarn twist and the mixture of homochiral and heterochiral coiled yarns. Apart from twisted yarns with a single type conductive building block, different conductive fibers can be combined for specific wearable applications. **Figure 11d** shows a setup for making super-aligned CNT/PVA (polyvinyl alcohol) composite yarns. The process involves twisting a super-aligned CNT (SACNT) yarn from a SACNT array, immersing it in a PVA/DMSO (dimethyl sulfoxide) solution, and subsequently drying the composite yarn. The obtained composite yarns exhibited improved resilience to abrasions and are more durable than pure SACNT yarns, owing to the robust coupling between the CNT and PVA interface.<sup>208</sup> The twisting of CNT yarns also enabled new configurations for yarn-based electronics. **Figure 11e** shows the fabrication process of two-ply yarn supercapacitor with active material-coated CNT yarns.<sup>209</sup> The twisted structure provided high mechanical strength and flexibility, as well as a high surface area for electrochemical reactions.

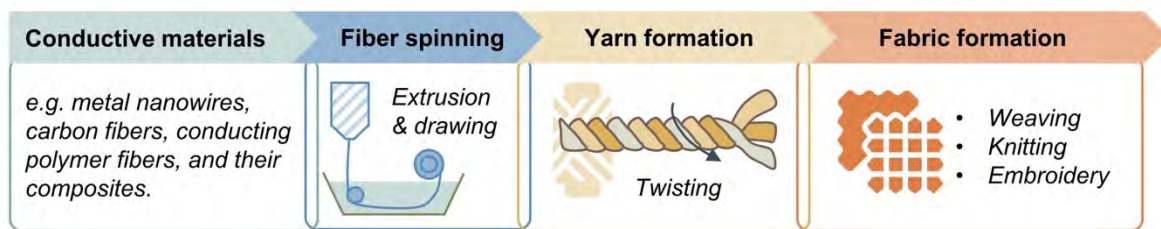


**Figure 10.** Typical processes for the development of conductive textiles from intrinsically conductive materials.



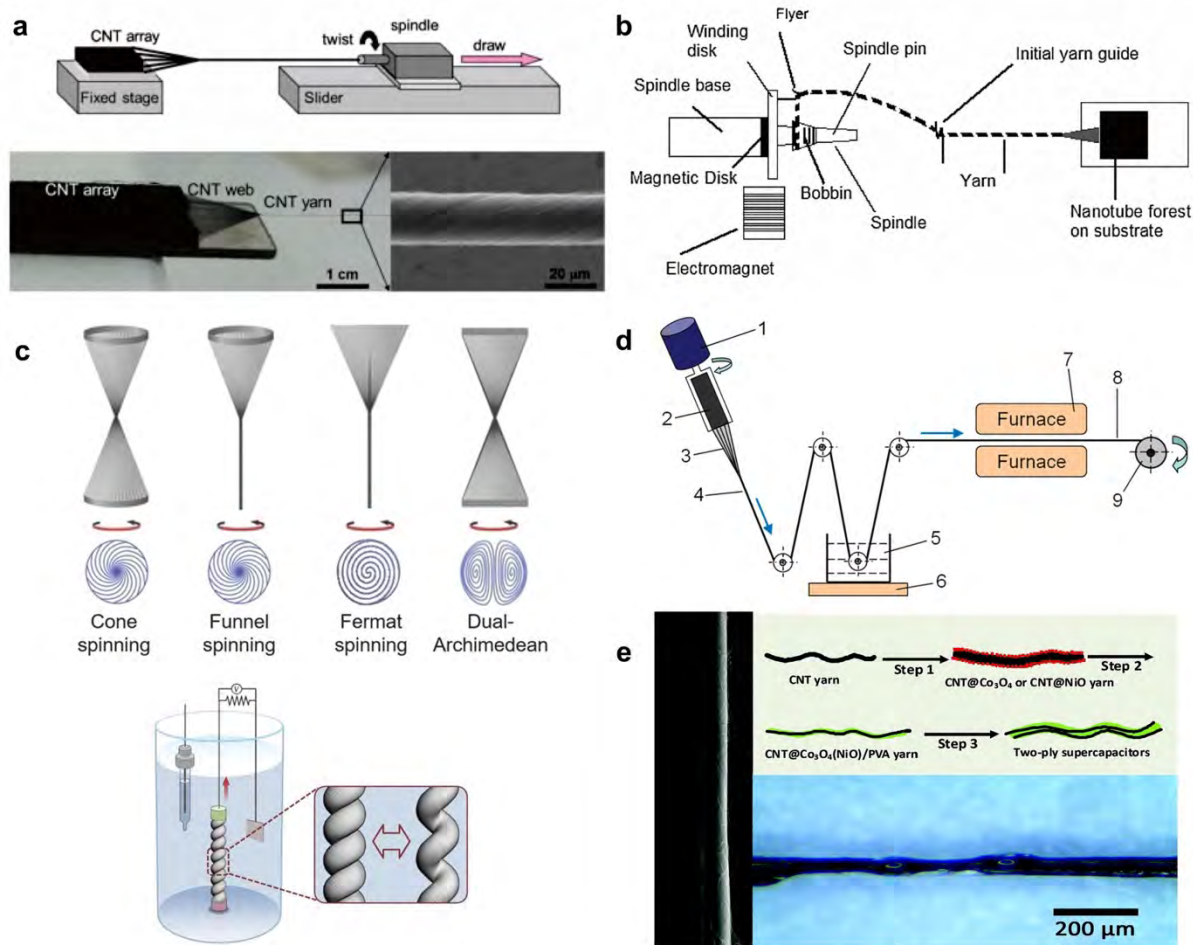


**Figure 11.** (a) Spinning process for CNT yarns from an array of CNTs. Reproduced with permission from ref <sup>205</sup>. Copyright 2012 Elsevier. (b) Illustration of a flyer spinning system for CNT yarns. Reproduced with permission from ref <sup>206</sup>. Copyright 2015 Elsevier. (c) Different CNT yarn twisting structures for harvesting mechanical energy. Reproduced with permission from ref <sup>207</sup>. Copyright 2017 American Association for the Advancement of Science. (d) Fabrication process of super-aligned CNT/PVA composite yarns. Reproduced with permission from ref <sup>208</sup>. Copyright 2010 American Chemical Society. (e) Fabrication process for a two-ply supercapacitor based on twisted CNT yarns. Reproduced with permission from ref <sup>209</sup>. Copyright 2015 John Wiley and Sons.

Whereas conductive fibers/yarns can serve as current collectors and electrodes for certain 1D wearable electronics, the majority of textile-based wearable electronics are constructed based on 2D fabrics. For example, a 2D self-powered fabric can be fabricated by the weaving of Cu-coated polyester (PET) yarn and polyimide (PI)-coated Cu-PET weft yarns (**Figure 12a**).<sup>210</sup> The process has been demonstrated to be compatible with industrial weaving machines (**Figure 12b**), through which the woven electronics can be integrated into garment accessories for

wearable respiratory monitoring (**Figure 12c**). An organic electrochemical transistor (OECT) textile can also be fabricated by weaving yarn-based OECT using a conventional weaving machine.<sup>211</sup> Knitting is another technique for manufacturing PCTs with high porosity and flexibility. **Figure 12d** shows seamless woven and knitted carbon fiber fabrics on wool garments. The knitting structure enabled the fabrication of PCTs with low resistance and high mass loading of active material, which is conducive for using as electrodes of energy storage devices such as wearable supercapacitors.<sup>212</sup> Embroidery is the art of decorating fabric or other materials by stitching using needle and thread, or sometimes with other materials like beads, sequins, or pearls. Owing to the ability of making delicated patterns on garments, embroidery holds great promise for fabricating wearable electronics, particularly for those requiring precise patterning of conductive and functional materials. **Figure 12e** illustrates the manufacturing of patterned conductive textiles with liquid metal (LM) filaments by computer-aided embroidery.<sup>213</sup> The digital embroidery technology allows for accurate and scalable reproduction of near-field inductive pattern designs.

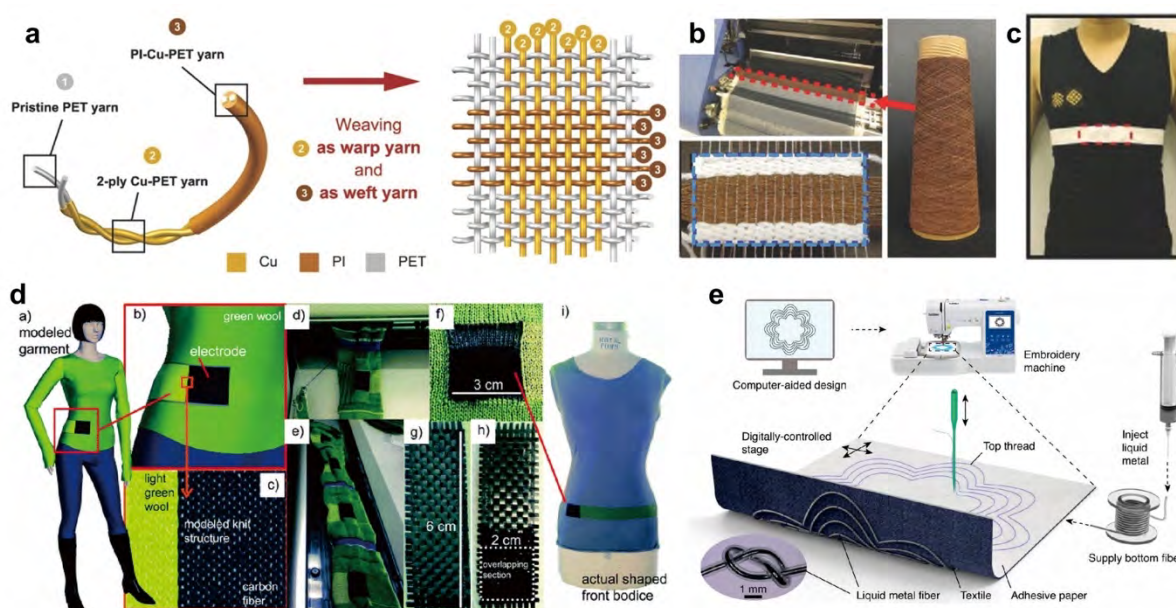


**Figure 12.** (a) Woven self-powered fabric made from Cu-PET warp yarns and PI-coated Cu-PET weft yarns. (b) Images showing the woven self-powered fabric made by industry weaving machine. (c) Chest trap integrated with the woven self-powered fabric. Reproduced with permission from ref <sup>210</sup>. Copyright 2016 John Wiley and Sons. (d) Woven and knitted carbon fiber fabrics on a wool garment for wearable electronics. Reproduced with permission from ref <sup>212</sup>. Copyright 2013 Royal Society of Chemistry. (e) Patterned LM filaments obtained via embroidery. Reproduced with permission from ref <sup>213</sup>. Copyright 2022 Springer Nature.



### 2.3.2 Fabrication of PCTs from Non-Conductive Textile Materials

In addition to obtaining PCTs from intrinsically conductive building blocks, another strategy is to deposit conductive materials onto non-conductive textiles. Metal-coated textiles have been commercialized for a wide variety of applications such as electromagnetic shielding, fashion and decoration, heat and fire resistance, and purification.<sup>214-217</sup> Conventional metal-coated textiles are obtained by vacuum deposition of thin metal layers on natural and polymeric textiles.<sup>218</sup> Thermal evaporation can also be adopted for developing metal-coated textiles. Miyamoto *et al.*<sup>79</sup> demonstrated the fabrication of Au-coated nanomesh conductors by thermal evaporation of Au on electrospun PVA nanofibers (**Figure 13a**). After deposition of Au layer on an electrospun PVA nanomesh, the PVA core fibers were removed by dissolving in water, leaving a lightweight and ultrathin Au nanomesh. The nanomesh conductors showed good conformability, which is promising for on-skin electronics.

Low-cost and high-throughput solution-based chemical deposition technologies are highly compatible with the textile industry. Catalytic electroless plating is a common approach for depositing metals such as Ni, Cu, Ag, and Au on textile substrates.<sup>219</sup> To address the adhesion issue between hard metals and soft textile substrates, interfacial modification between metals and textile substrates is critical.<sup>220, 221</sup> **Figure 13b** shows a polymer-assisted metal deposition (PAMD) method for electroless metal plating. A catalyst-affinitive polymer was grafted onto the textile substrate via free-radical polymerization to serve as both seeding and adhesive layers for metals.<sup>222</sup> Recently, Zhang *et al.*<sup>223</sup> developed a versatile method called rapid-PAMD which is capable of depositing metals (Ni, Cu, Ag, and Au) on multiple textile substrates such as cotton, polyester, Kevlar, and nylon fabrics (**Figure 13c**). In this method, the polymer modification process was shortened to less than 3 min, and no damage was caused to the mechanical strength of textile substrates. The resulting metal-coated textiles showed excellent abrasion resistance and wash durability, making them highly suitable for wearable E-textiles. Apart from conventional metals, incorporating novel metal conductors such as LMs with textile substrates is of great interests in recent years.<sup>224-226</sup> **Figure 13d** presents the fabrication of permeable and stretchable conductors by coating LM on non-woven poly(styrene-block-butadiene-block-styrene) (SBS) mats. The SBS mats were modified with Ag nanoparticles (AgNPs) to enhance the wettability of LM on textile substrate, as Ag can form alloy with LM. The combination of highly flexible LM and SBS textile resulted in super-elastic conductors that can withstand strains up to 2500%.<sup>227</sup>

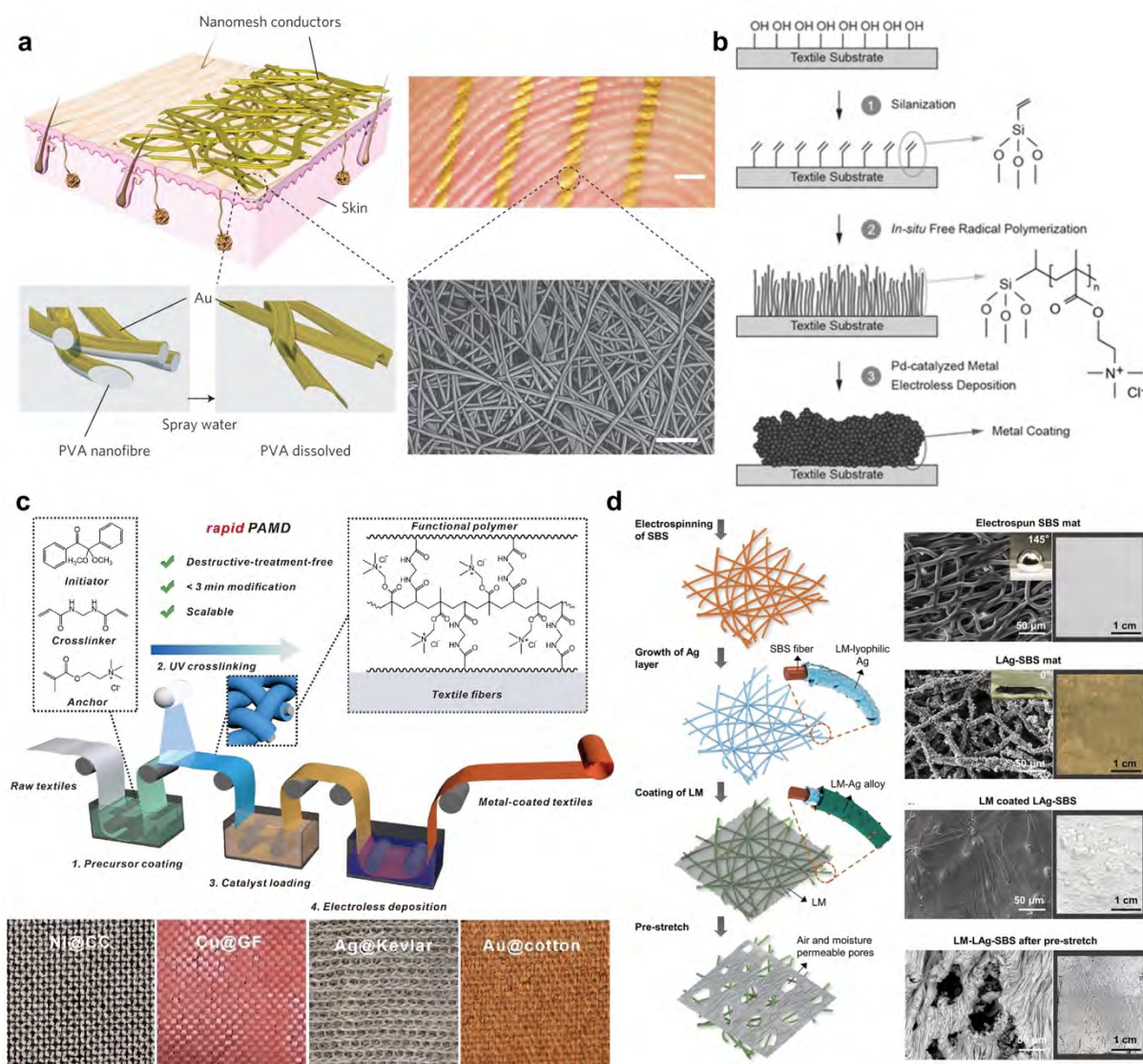


**Figure 13.** (a) Au nanomesh conductors fabricated by thermal evaporation of Au on PVA nanofibers. Reproduced with permission from ref <sup>79</sup>. Copyright 2017 Springer Nature. (b) Illustration of a PAMD process starting from radial polymerization of functional polymer. Reproduced with permission from ref <sup>222</sup>. Copyright 2014 John Wiley and Sons. (c) Rapid-PAMD process for scalable fabrication of metal-coated textiles. Reproduced with permission from ref <sup>223</sup>. Copyright 2022 American Chemical Society. (d) Fabrication of LM-coated SBS fiber mats for permeable and conductive textiles. Reproduced with permission from ref <sup>227</sup>. Copyright 2021 John Wiley and Sons.

In addition to metals, non-conductive textiles can also be coated with conducting polymers and carbon materials to make PCTs. **Figure 14a** presents a scalable pad-dry-cure process for making graphene-coated textiles, which showed a low sheet resistance of  $\sim 11.9 \Omega \text{ sq}^{-1}$ .<sup>228</sup> The sheet resistance of the graphene-coated poly-cotton fabrics remained stable even after several

cycles of machine washing. Hu *et al.*<sup>75</sup> reported stretchable, porous, and conductive CNT-coated textiles via a simple dip-coating process, through which the single-walled CNTs were uniformly coated on fabrics in both macro- and micro-scale (**Figure 14b**). The CNTs showed no obvious peeling-off after a standard tape test and a water-wash test, indicating a strong adhesion to cotton fibrils. For textile substrates that have poor affinity to carbon materials, introducing an adhesion layer between carbon materials and textiles is helpful. For example, to coat multiwalled CNTs on PET yarns, PVP was used as an adhesive material to bind CNTs and PET yarns, and an additional polystyrene-*b*-polyisoprene-*b*-polystyrene block copolymer (SIS) was employed as an encapsulation layer to improve the wear and water resistance of the conductive yarns.<sup>229</sup> Conducting polymers can be coated on non-conductive textiles via vapor deposition, solution printing/coating, and *in situ* polymerization.<sup>230-232</sup> For example, PPy-coated cotton fabrics can be prepared by an *in situ* polymerization route. The deposition of PPy was achieved via a mild two-step oxidative polymerization. This process is facile, cost-effective, and scalable, aligning well with the concept of low-cost wearable electronics.<sup>233</sup> Direct solution printing/coating of polymers is a preferred method if the polymer shows good solubility or dispersibility, and there are multiple solution coating routes such as drop-casting, dip-coating, and spray-coating can be used for coating conductive materials on non-conductive textiles (**Figure 14c**).<sup>234</sup> The crosslinked polymers served as a matrix for conductive CNT, and the composite coating exhibited good stability against harsh conditions such as bending, peeling, and washing. Apart from solution-based technologies, vapor phase polymerization is another approach to obtaining polymer-coated textiles. **Figure 14d** presents the schematical illustration and the mechanism of vapor coating of PEDOT on textile substrates.<sup>235</sup> Compared with solution-based technologies, coatings produced by vapor deposition are recognized for their ability to conform to the surface they are applied to, and the coatings are thin enough that the mechanical properties of the underlying material, rather than those of the coating, will be the most noticeable. As a result, conducting polymer-coated textiles fabricated via vapor deposition are very suitable for wearable electronics that require high flexibility, breathability, and haptic perception of fabrics.

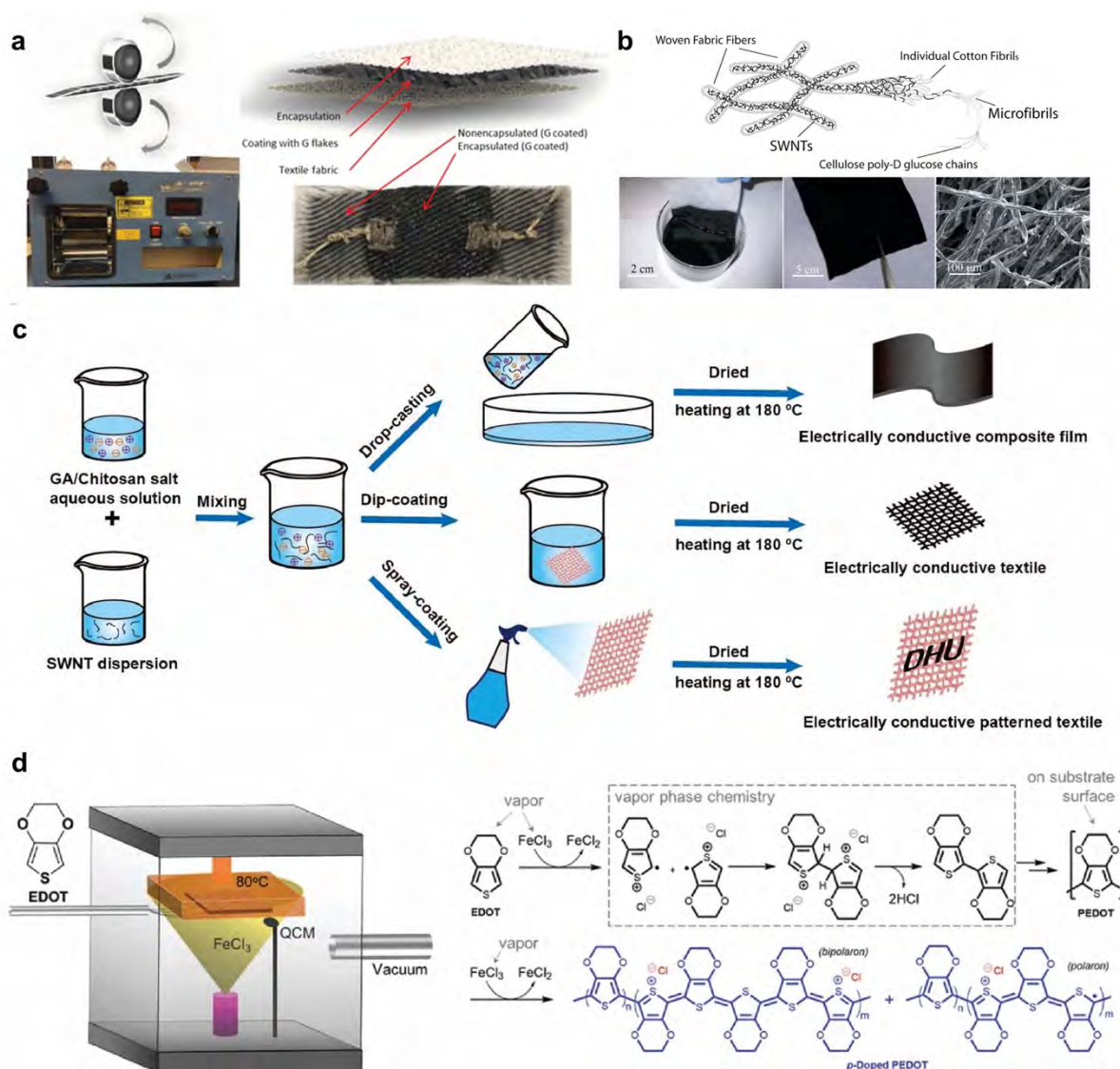


**Figure 14.** (a) Graphene-coated textiles obtained via a pad-dry-cure process. Reproduced with permission from ref <sup>228</sup>. Copyright 2020 John Wiley and Sons. (b) A dip-coating process for CNT-coated textiles. Reproduced with permission from ref <sup>75</sup>. Copyright 2010 American Chemical Society. (c) Coating of glucaric acid/chitosan polymers and CNT composites on textiles via drop casting, dip coating, and spray coating. Reproduced with permission from ref <sup>234</sup>. Copyright 2021 Elsevier. (d) Schematics and mechanism of vapor phase deposition of PEDOT on textiles. Reproduced with permission from ref <sup>235</sup>. Copyright 2017 John Wiley and Sons.

### 2.3.3 Patterning

Wearable electronics and circuits require the patterning of conductive materials on textiles. The patterning of PCTs can be done either during the formation of textiles or on existing non-conductive textiles. The patterning process can be realized via multiple conventional

technologies of textile industries, such as embroidery, screen printing, inkjet printing, and brush painting.<sup>236-239</sup> **Figure 15a** shows photographs and schematics of an embroidered F-radio frequency antenna for a smart textile system.<sup>240</sup> The Ag-coated polyamide (PA) fibers were embroidered on cotton fabric to form a square spiral structure. The system also embedded conductive fibers in asymmetrical weaving patterns, which can prevent short-circuit caused by direct contact of neighboring fibers. Screen printing is another effective approach to depositing conductive patterns on textiles. For example, Sinha *et al.*<sup>241</sup> printed conducting polymer PEDOT:PSS on non-woven PET fabrics for electrocardiography (ECG) sensors. The printed electrodes did not require any adhesives or hydrogels, providing comfort and good biocompatibility for ECG sensing. Apart from PEDOT:PSS, AgNP inks are conventional building block materials for printable electronics. Matsuhisa *et al.*<sup>242</sup> printed micrometer-sized Ag flakes on stretchable textiles as elastic conductors for wearable sensors and actuators. The sensor networks can be stretched up to 120% without sacrificing functionality. As a printing technology for depositing metals on flexible substrates, the PAMD technology is a facile approach to obtaining patterned metal electrodes on textiles. Once the catalytic precursor is fixed on selected areas of a textile via screen printing, the following metal deposition process will only take place at the catalyst-activated areas.<sup>243</sup> In addition to these traditional approaches, novel printing technologies are developed for the fabrication of high-resolution patterns on textiles. **Figure 15b** is the schematics for the fabrication of micrometer-scale resolution LM patterns on stretchable nonwoven SBS fabrics.<sup>244</sup> In a typical fabrication, LM-affinitive Ag micropatterns were transfer-printed on SBS fabrics, and LM was then wetted on areas with Ag to serve as permeable and soft microelectrodes for on-skin and implantable electronics. The high resolution, high stretchability, and good biocompatibility of LM microelectrodes enabled the implantation of bio-applications such as neural electrophysiological recording. Apart from coating and printing, the organic nature of conventional textile materials provides the possibility of obtaining conductive patterns via selective carbonization. For example, Wang *et al.*<sup>93</sup> “wrote” conductive graphene on Kevlar fabrics via laser-induced carbonization (**Figure 15c**). The laser-induced graphene showed a low electrical resistance ( $10.6\ \Omega$ ,  $2 \times 0.5\ \text{cm}^2$ ), which is sufficient for a variety of textile-based electronics such as Zn-air batteries, ECG sensors, and gas sensors.



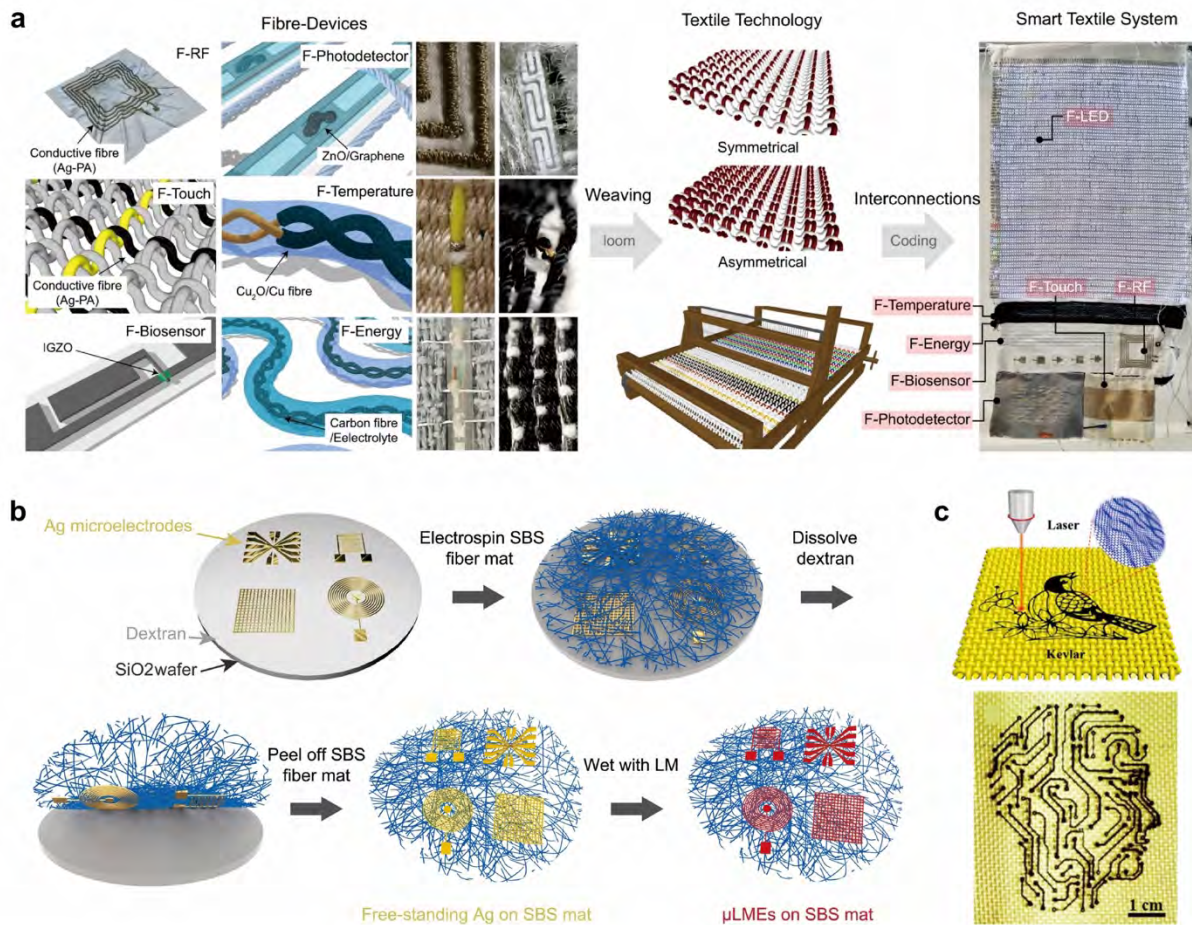


**Figure 15.** (a) Patterned metal yarns fabricated via embroidery for F-radio frequency antenna. Conductive metal fibers were embedded in asymmetrical weaving patterns. Reproduced with permission from ref <sup>240</sup>. Copyright 2022 Springer Nature. (b) Illustration of a transfer-printing process for microscale resolution LM patterns on SBS fiber mat. Reproduced with permission from ref <sup>244</sup>. Copyright 2023 American Association for the Advancement of Science. (c) Laser-induced carbonization for conductive patterns on Kevlar fabrics. Reproduced with permission from ref <sup>93</sup>. Copyright 2020 American Chemical Society.

## 2.4 Strategies to Endow Flexibility/Stretchability

Flexibility of textiles is essential for comfortability, durability, functionality, and aesthetics. Wearable electronics require flexibility, or even stretchability, to accommodate the motion of skins, reducing friction and discomfort.<sup>245</sup> The flexibility of textiles originates from both intrinsic characteristics of textile materials and their interlacing structures, and this section discusses the flexibility of PCTs from both aspects.

### 2.4.1 Stretchable Textile Structures

Twisting plays a vital role in determining the tensile strength, hairiness, stretchability, and wicking behavior of textile yarn.<sup>246</sup> **Figure 16a** shows the relationship between twist and yarn strength for yarns consisting of staple fibers.<sup>247</sup> Increasing yarn twist at low twist levels enhances fiber-fiber friction, thus bolstering yarn strength. However, at high twist levels, the obliquity effect of the fibers diminishes the influence of fiber strength on yarn strength. As a result, a moderate twist level usually yields the highest specific yarn strength. The untwisting of yarns results in changes in length and volume of yarns, enabling applications for stretchable electronics such as artificial muscle, mechanical energy harvester, and twistocaloric cooling.<sup>248-250</sup> **Figure 16b** shows the use of twist-spun CNT yarns as counter electrodes for rotary motors and torsional artificial muscle.<sup>251</sup> Once electronic charges are injected into the nanotubes, hydroelastic or quasi-hydroelastic pressure will be generated, causing volume expansion of the yarns.

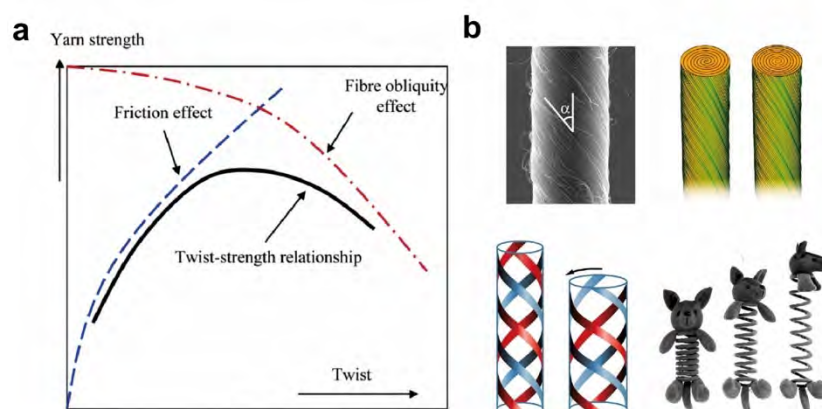


**Figure 16.** (a) Influence of yarn twisting on the strength of yarns. Reproduced with permission from ref <sup>247</sup>. Copyright 2016 Elsevier. (b) Application of yarn twisting for rotary motors and artificial muscle. Reproduced with permission from ref <sup>251</sup>. Copyright 2011 American Association for the Advancement of Science.

Researchers have been studying the behaviors of fabrics under strain via both experimental and theoretical approaches for decades.<sup>252</sup> For example, woven fabrics with double curvature or complex geometries will experience in-plane shear deformation under strains. This deformation, along with bending, is essential in determining the fabric's drape, which refers to its ability to conform to 3D objects. Studying shear deformation is critical to applications of flexible textiles, such as textile-reinforced composites for construction, automotive, and

aircraft.<sup>253, 254</sup> **Figure 17a** shows the schematic and experimental setup for the picture frame test, a method specifically designed to study the mechanical behavior of a woven fabric in response to shear forces.<sup>255</sup> In this method, a set of holes are drilled into every edge of the panel, the number of holes depends on the panel's strength and thickness, and the hole pattern corresponds to the four pairs of fixture rails. In classical biaxial woven fabrics, the warp and weft yarns are initially oriented perpendicular to each other at a 90° angle, while the angle decreases during the picture frame test. Since the shearing of the fabric comes from the rotation of yarns rather than the shearing of the yarn itself, the weaving structures show a significant influence on the shear force (**Figure 17b**).<sup>256</sup> The shear stiffness of a fabric is determined by the number of intersections in the weave: a higher number of intersections results in greater stiffness. Therefore, twill or satin weaves which have fewer intersections exhibit lower shearing resistance compared to plain weave. Multiple modeling approaches such as finite element analysis (FEA), hybrid element analysis (HEA), and boundary element analysis (BEA) are employed to simulate and predict the deformation behavior of textiles.<sup>257-259</sup> For example, multi-scale HEA is a typical model for analysis of plain weave-structured fabrics. In this model, four regions categorized as high (I), moderate (II), low (III), and minimal (IV) are divided based on the level of interactions between the projectile and fabric, as well as between the yarns, and their corresponding deformations.<sup>260</sup> Stress, strain, and modulus are the key parameters for evaluating the tensile behavior of textiles. The load-extension behavior of a woven fabric typically involves three regions: the initial region referring to the period where inter-fiber friction happens; the middle region indicating the crimp, where the shortening of yarn length in fabrics is reduced; and the final region corresponding to the extension of yarns.<sup>261</sup> The anisotropic feature of woven fabrics also affects the behavior of textiles under tension and compression. The stress-strain curve of the textile composites showed a significant dependence on the loading direction.<sup>262</sup>



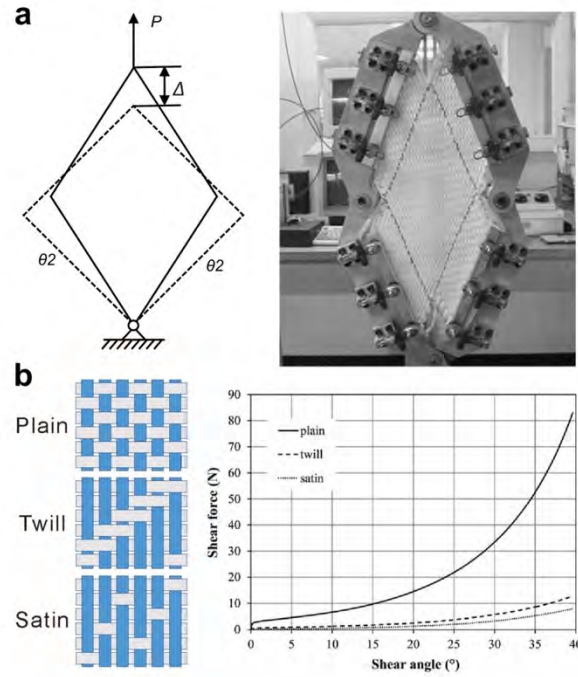


**Figure 17.** (a) Illustration of picture frame test for evaluating the mechanical behavior of textiles under shear force. Reproduced with permission from ref <sup>255</sup>. Copyright 2004 Elsevier. (b) The influence of weaving structure on the shear force of woven fabrics. Reproduced with permission from ref <sup>256</sup>. Copyright 2013 Elsevier.

In knitted fabrics, the meandering loops can provide additional stretchability. **Figure 18** compares the stress-strain curves of textile actuators with different textile structures. The loop elongation of knitted fabrics under strain resulted in a much lower fabric stiffness than that of woven fabrics.<sup>263</sup> Similar to woven fabrics, knitted fabrics also show an anisotropic response to the tensile load.<sup>264</sup> The high structural stretchability of knitted PCTs is a key feature for the development of stretchable electronics based on knitted PCTs. For example, Zhang *et al.*<sup>265</sup> fabricated wearable and stretchable heaters using carbonized weft-knitted fabrics, which showed a stable Joule heating performance under a high tensile strain of up to 70%. Dong *et al.*<sup>266</sup> presented stretchable and washable knitted power textiles consisting of yarn-based triboelectric nanogenerators (TENGs) and supercapacitors. Both the TENGs and supercapacitors can function normally under high strains and repeated stretch tests.

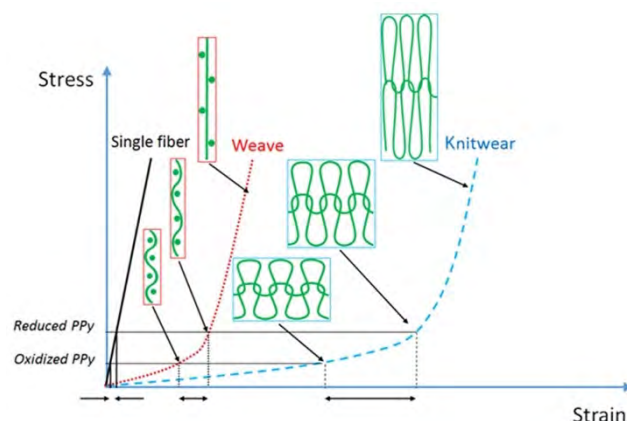


**Figure 18.** Different stress-strain curves of woven and knitted fabrics. Knitting structure provides extra stretchability because of meandering loops. Reproduced with permission from ref <sup>263</sup>. Copyright 2017 American Association for the Advancement of Science.

### 2.4.2 Intrinsically Stretchable Materials

Incorporating conductive materials with intrinsically stretchable textiles is another approach to obtaining stretchable PCTs. Spandex, also known as Lycra and Elastane, is a highly elastic synthetic polymer (polyurethane, PU) invented by DuPont in 1958.<sup>267</sup> The PU copolymer typically consists of soft and stretchable polyether segments and rigid segments (**Figure 19a**). The combination of soft and rigid segments enables both high strength and high stretchability of spandex fibers, increasing the pressure comfort of garments. As a result, such elastic fibers are mixed with cotton and polyester for soft and comfortable clothing such as sportswear, underwear, hosiery, and gloves.<sup>268</sup> For wearable electronics, researchers are interested in incorporating stretchable fibers into PCTs for highly stretchable textile conductors. **Figure 19b** illustrates a knitted PCT for wearable wireless strain sensing.<sup>269</sup> Conductive PU/PEDOT:PSS fibers were co-knitted with a Spandex yarn, showing a stable response in resistance to external load over a wide range of strain from 0 to 160%. Ding *et al.*<sup>270</sup> reported a simple approach to obtaining stretchable electrochromic textile via direct coating PEDOT:PSS on woven Spandex-based fabrics. The conductivity of the resulting PEDOT:PSS-coated fabrics was improved by multiple times. In addition, the percentage of Spandex in the fabric can affect the conductivity and stretchability of the textiles. Some elastomers show a higher stretchability than that of Spandex, and thus are also promising candidates for wearable stretchable electronics. For example, the polystyrene-block-poly(ethylene-ran-butylene)-block-polystyrene (SEBS) copolymer is a highly stretchable thermoplastic elastomer frequently used as a flexibilizer for rigid polymeric materials.<sup>271</sup> **Figure 19c** shows the preparation of stretchable and conductive

CNT-coated fibers with SEBS core fibers. The CNT sheets were coated on pre-stretched SEBS fibers, and hierarchical buckles were generated once the strain was released. The formation of reversible buckles resulted in a very small resistance change ( $< 5\%$ ) of the conductive fibers during stretching, even at a very high strain of 1000%.<sup>141</sup> Zhang *et al.*<sup>272</sup> reported a core-sheath stretchable conductive fiber based on a similar strategy, by coating conductive CNT and AgNW on a pre-stretched Lycra fiber. An additional SEBS coating was wrapped on conductive materials to serve as an encapsulation layer. In addition to the coating strategy, the conductive building blocks can be blended with elastic materials for stretchable PCTs. For example, Lan *et al.*<sup>273</sup> blended CNT and MXene with PU for making stretchable and conductive fibers via a wet-spinning process. The conductive fibers can reach a strain of  $\sim 140\%$  after coating active materials, showing a great potential for fiber-based wearable sensors. **Figure 19d** presents the two-step fabrication process of AgNW-reinforced stretchable conductive fibers.<sup>274</sup> The mixture of AgNW and SBS was wet-spun into a stretchable fiber, followed by repeated  $\text{Ag}^+$  absorption and reduction process. The doping of AgNW in SBS elastomer improved the conductivity of the stretchable fiber under high strains.

Hydrogels, 3D crosslinked hydrophilic polymers trapped with large content of water, can possess intrinsic stretchability and electrical conductivity at the same time.<sup>275</sup> Stretchable and conductive hydrogel fibers can be obtained via conventional spinning technologies such as microfluidic spinning, wet spinning, and electrospinning.<sup>276-278</sup> For example, PEDOT:PSS hydrogel microfibers fabricated via microfluidic spinning can function as strain-sensitive conductors.<sup>279</sup> Song *et al.*<sup>280</sup> reported the fabrication of anti-freezing, long-term stable, and conductive hydrogel fibers via a wet spinning approach, in which an ultraviolet (UV) curing process was employed to create chemical crosslinking for a high mechanical robustness. **Figure 19e** shows the synthesis of core-shell polymethyl acrylate-polyelectrolyte: sodium polyacrylate (PMA-PAAS) hydrogel via a simple gel spinning and dip-coating process.<sup>281</sup> The coating of hydrophobic PMA layer improved the water resistivity of the hydrogel while enhancing the tensile strength of the hydrogel against stretching.

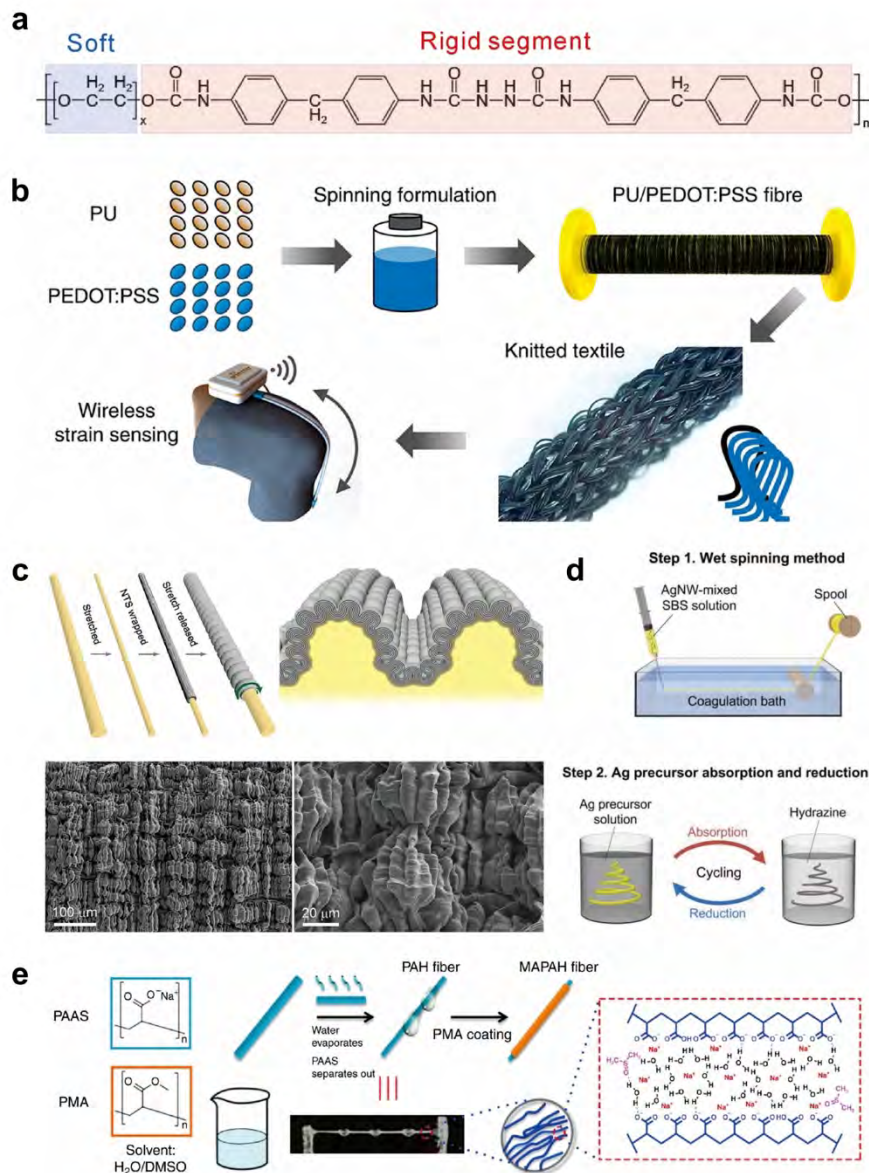


**Figure 19.** (a) Chemical structure of intrinsically stretchable copolymer Spandex. (b) Intrinsically stretchable PU/PEDOT:PSS composite fibers for strain sensing. Reproduced with permission from ref <sup>269</sup>. Copyright 2015 American Chemical Society. (c) Conductive CNT coated on pre-stretched SEBS fibers resulted in buckling of CNTs. Reproduced with permission from ref <sup>141</sup> Copyright 2015 American Association for the Advancement of Science. (d) Illustration of the fabrication process for wet-spun Ag-SBS composite stretchable fibers. Reproduced with permission from ref <sup>274</sup>. Copyright 2015 John Wiley and Sons. (e) Two-step synthesis of PMA-PAAS conductive hydrogels via gel spinning and dip coating. Reproduced with permission from ref <sup>281</sup>. Copyright 2018 Springer Nature.

## 2.5 Key Properties of PCTs

PCTs are designed to be indispensable components for the construction of wearable electronics, thanks to their unique combination of electrical conductivity and inherent softness originated from fibrous materials. For their applications in electronics that are designed to be worn on human bodies, the manufacture of PCTs has to take both electrical functions and physiological comfort into considerations. Key properties that PCTs needs to possess include: 1) suitable electrical conductivity for the electrical functionalization of PCT-based electronic devices; 2) promising mechanical properties to accommodate stress and strain induced by daily wear and skin deformation; and 3) good comfortability to ensure a healthy thermal and moisture microenvironment of skin/device interface so as to guarantee the biocompatibility of PCT-based wearable electronics (**Figure 20**). In this session, strategies to impart PCTs with high electrical conductivity, good mechanical properties, and good comfortability will be elaborated.

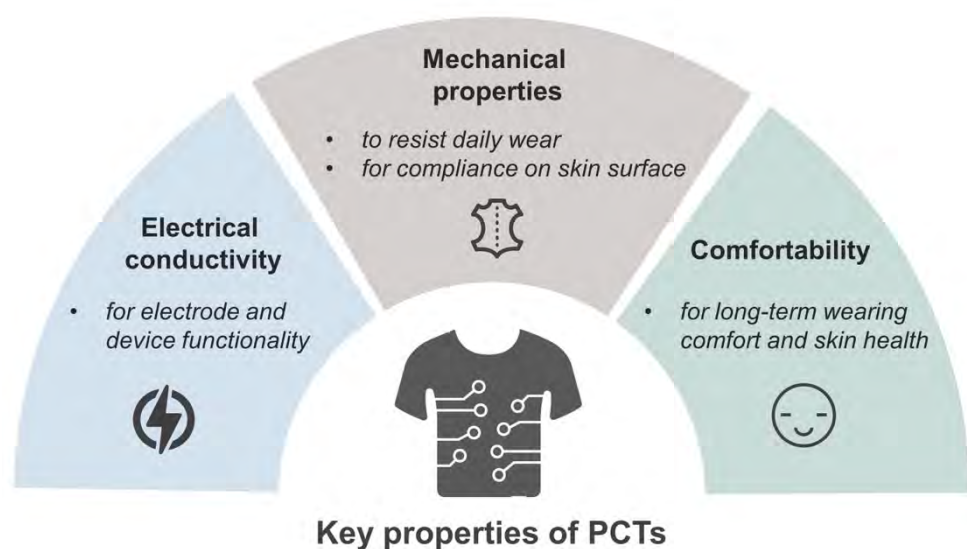


**Figure 20.** Key properties of PCTs: electrical conductivity, mechanical properties, and comfortability.

### 2.5.1 Conductivity

The electrical conductivity of PCTs is relevant to both the intrinsic conductivity of conductive materials and the way that conductive materials are assembled on PCTs. Among all conductive building blocks for PCTs, conducting polymers show relatively low conductivity ranging from  $10^{-5}$  to  $10^4$  S cm<sup>-1</sup>. As mentioned above, the conductivity of conducting polymers can be improved significantly from semiconductor level to a quasi-metallic level via oxidation and doping. Similarly, the conductivity of carbon materials also varies in a wide range from

semiconducting to metallic conducting. Single-layer graphene obtained via mechanical exfoliation can show a very high conductivity of  $\sim 10^6 \text{ S cm}^{-1}$  and a high intrinsic mobility limit of  $2 \times 10^5 \text{ cm}^2 \text{ V}^{-1} \text{ s}^{-1}$ .<sup>282, 283</sup> However, typical rGO sheets and composites for PCTs show a much lower conductivity due to the existence of defects such as vacancies and residual oxygen-containing groups.<sup>284</sup> A single CNT can be either metallic or semiconducting along the tubular axis depending on the rolling-up configuration of the CNT, and the conductivity value can be as high as  $\sim 10^5 \text{ S cm}^{-1}$  for an individual metallic CNT.<sup>285, 286</sup> Metals are good electrical conductor because of their electronic structure, and bulk metals show a high conductivity of  $10^4 \sim 10^5 \text{ S cm}^{-1}$ . Whereas metal-based PCTs obtained via solution approaches may be affected by impurities and defects, solution-processed metals can show a high conductivity that is  $\sim 1/6 \sim 1/2$  of bulk metals.<sup>287, 288</sup>

For NW/NP-based PCTs, the contact between nanomaterials plays an important role in electrical conductivity. For example, the experimental conductivity of CNT films is always much lower than that of a single CNT due to poor electronic tunneling at junctions. A first-principles study indicated that a strong hybridization between the  $d$  orbitals of the transition metal with the  $\pi$  orbitals of the nanotube can serve as an effective electrical bridge in nanotube-nanotube junctions.<sup>289</sup> Post-sintering and welding processes can reduce the junction resistance of nanowire-based conductors.<sup>290, 291</sup> For example, Garnett *et al.*<sup>292</sup> developed an optical approach for selective welding of AgNW at junction points. The light-induced plasmonic welding process generates local heat at junction points, which avoids thermal-induced damage of temperature-sensitive plastic substrates. Liu *et al.*<sup>293</sup> presented self-limited and room-temperature nano-welding of AgNW junctions by making use of the capillary force of water during evaporation. The moisture-treated AgNW films showed good stretchability and strong adhesion to the stretchable substrate.

Another way to obtain high electrical conductivity is by constructing composites from conductive building blocks. By making use of the  $\pi$ - $\pi$  interaction between graphene and conjugated polymers, high aspect ratio and large specific surface area graphene nanosheets can be embedded in the conducting polymer matrix for enhanced conductivity.<sup>294</sup> Cao *et al.*<sup>295</sup> discovered that embedding graphene in metals such as Al, Cu, and Ag can gain a maximum  $\sim 17\%$  enhancement in conductivity, even if the graphene volume fraction was only 0.008%. Strong  $\pi$ - $\pi$  interaction is also found in CNT and conducting polymer composites, which caused a significant blue shift of G band in CNTs. Such interaction facilitates the charge transport

between polymer and CNT, and thus improved the conductivity and performance of the thermoelectric material.<sup>296</sup> In addition, doping of non-conductive materials in conductive building blocks can improve the conductivity of nanowire composites. For instance, doping a small volume fraction of non-conductive Si nanoparticles (SiNPs) increased the conductivity of AgNW composites by up to 8 orders of magnitude.<sup>297</sup>

In general, PCTs exhibit lower electrical conductivity compared to their planar counterparts, such as metal films and solid polymer-supported conductive films, due to the porous nature of fibers and textiles. Despite this limitation, PCTs possess unique attributes such as lightweight, excellent flexibility and stretchability, and high permeability, rendering them well-suited for applications in wearable technology. Furthermore, recent research endeavors have significantly enhanced the electrical conductivity of PCTs to levels adequate for a wide range of flexible electronic devices, serving either as conductive electrodes or active components. Nevertheless, it is widely anticipated that ongoing efforts to further enhance the electrical conductivity of PCTs, especially when utilized as conductive interconnects and current collectors, will contribute to advancing the performance of flexible electronics. Besides augmenting electrical conductivity, ensuring long-term electrical stability in PCTs is crucial for their viability in wearable applications. Due to their porous nature, the electrical performance of PCTs can degrade easily during dynamic deformations like bending, twisting, and folding, as well as under wear-related conditions such as sweating, washing, and extended periods of use. Although considerable progress has been made in creating durable PCTs for wearable electronics, further endeavors are needed to enhance their stability for practical applications in wearables. Additional discussions pertaining to the electrical, chemical, and mechanical stability of PCTs are elaborated in Section 6.

### **2.5.2 Mechanical properties**

The ultimate tensile strength of materials for PCTs distributes in a great range from several MPa (hydrogels) to hundreds of GPa (graphene).<sup>298, 299</sup> For wearable electronics, most applications prefer a high tensile strength for PCTs to withstand tension during processing, and to resist wear and tear of clothing. For example, commercial weaving and knitting machines place a direct tensile stress of 2 ~ 4 MPa on yarns during operation, and the actual stress on yarns can be much larger due to frictions among yarns and machines.<sup>300</sup> One way to obtaining high tensile strength PCTs is incorporating mechanically strong carbon materials into PCTs. For example, wrapping of graphene nanosheets on nylon-6 yarns improved the tensile strength



of yarns from 138 MPa to 195 MPa.<sup>301</sup> Doping of graphene in carboxymethyl cellulose composites resulted in conductive textiles with high tensile strength of 613.9 MPa. Meanwhile, the incorporation of graphene improved the flame resistivity of textiles, which is critical for E-textiles and wearable energy storage devices.<sup>302, 303</sup>

Coating of metals on textile materials can affect the tensile strength of textiles significantly.<sup>304</sup> Depositing metals on textiles with several micrometer thick usually increases the tensile strength of textiles significantly because metals show a high strength of several hundreds MPa. However, continuous deposition of a thicker metal layer will cause a decrease in textile strength due to the delamination of metals at the interface caused by mechanical mismatch.<sup>305, 306</sup> Meanwhile, the surface treatment processes, which are usually necessary for efficient metal coating on textiles, can cause significant degradation in textile strength.<sup>307</sup> To avoid irreversible damage caused by harsh treatment, mild physical and chemical processes such as magnetron sputtering, mild small molecule modification, and PAMD are recommended for metal deposition on weak textile substrates.<sup>223, 308, 309</sup>

As discussed in **Section 2.4**, the structure of textiles endorses flexibility and stretchability for PCTs, and researchers have demonstrated the advantages of PCTs for stretchable and wearable sensors, actuators, solar cells, batteries, and supercapacitors. However, the abrasion resistance, which is a key factor for wearing durability of PCTs, is rarely noticed. Fortunately, researchers are paying more attention to the abrasion resistance of PCTs and wearable electronics in recent years. For example, Chen *et al.*<sup>310</sup> improved the abrasion resistance of wearable triboelectric yarns by introducing a nano-micro structure on the surface of yarns. Similarly, yarns with a Fermat spiral structure can withstand > 5000 cycles of Martindale standard abrasion test without a noticeable mass loss or a significant decrease in electrical performance.<sup>311</sup> In addition, E-textiles obtained by printing of metal inks on textile substrates can also show a high abrasion resistance thanks to the good adhesion between metal and substrate.<sup>312</sup>

### 2.5.3 Comfortability

Developing PCT-based electronics with good wearability is undoubtedly an urgent demand for wearable technologies.<sup>313</sup> Although state-of-the-art textile-based wearable devices have shown unique advantages in the field of E-textiles, further efforts should be made before achieving “wearable” due to the great challenge of achieving both promising electrical properties and comfortability in a single device. Therefore, for wearable applications, PCTs should possess



not only good conductivity but also excellent air permeability and wearing comfort comparable to conventional clothing, so that they can cover a large area of skin for a long time without causing discomfort.<sup>10</sup>

Recently, there has been considerable interest in the application of PCTs with good comfortability and air permeability for flexible and wearable electronics.<sup>314, 315</sup> Notably, permeable wearable electronics possess the ability of permeating gases, moisture, and liquids while still performing device functions when attached to the human body, which ensures a biocompatible interface between devices and human skin, benefiting long-term and real-time monitoring of human health in a noninvasive and imperceptible manner.<sup>316</sup> That is, PCTs should not prevent sweat (in the form of moisture or liquid water) from escaping from the skin surface to the external environment. From a materials structure perspective, the underlying mechanism for achieving permeability in PCTs is to introduce sufficient numbers of pores with appropriate pore sizes, thus allowing the diffusion of gas and moisture (molecules ~0.3 nm in diameter) and the transportation of liquid/sweat droplets (~100  $\mu\text{m}$  in diameter) throughout the textiles.<sup>317</sup> In recent years, significant efforts have been made on engineering conductive textiles into lightweight and porous fibrous structures with excellent air/moisture permeability while maintaining the versatility of wearable electronics.<sup>318, 319</sup> For example, a textile magnetoelastic generator (MEG) was developed by sewing a soft magnetoelastic film with a textile coil.<sup>320</sup> This porous textile MEG exhibited high air permeability and comfortability, and it can be seamlessly sewn onto clothes or chest straps, working as a self-powered sensor for long-term respiratory monitoring even under heavy perspiration. Recently, Ma *et al.* reported a highly permeable stretchable liquid-metal fiber mat (LMFM).<sup>24</sup> The LMFMs were used as a versatile and user-friendly platform to fabricate multifunctional monolithic stretchable electronics that can provide high air/moisture/liquid permeability for excellent wearing comfort. Such permeable, highly integrated, and versatile PCT-based electronics are envisioned to provide a comprehensive analysis of multiple bio-signals in a real-time, continuous, and non-interfering manner, enabling personalized healthcare monitoring.

With the rapid development of wearable electronics, higher requirements have been put on the comfortability of PCTs. In addition to air/moisture permeability, thermal and moisture management capabilities become important factors in evaluating the comfort level of PCTs.<sup>321</sup> The thermal and moisture management functions enable efficient sweat transport and thermal dissipation and cooling, thus improving human comfort.<sup>322</sup> Regarding personal moisture

management in wearable electronics, the sweat transport depends on the wettability and porosity of the material itself. PCTs can achieve directional sweat transport to keep the human skin dry and comfortable through a rational design of structures, such as incorporating hydrophilic/hydrophobic layers or multi-layered lamination.<sup>323, 324</sup> A bioinspired directional moisture-wicking electronic skin has been demonstrated through the design of distinct hydrophobic-hydrophilic difference by surface energy gradient and push-pull effect, which can spontaneously absorb sweat from the skin and achieve all-range healthcare sensing.<sup>325</sup>

Moreover, effective thermal dissipation has become a key issue in the emerging wearable electronics.<sup>326-328</sup> In wearable electronics, heat can be generated from internal electronic components, acquired from external sources like sunlight and hot air, or even emitted by the human body itself. In the field of personal thermal management, it has been proved that both the intrinsic properties of materials and structural photonic engineering design play a crucial role in improving thermal management performance.<sup>329, 330</sup> Electrospun micropylramid arrays (EMPAs) combined with gradient micropylramid geometry and gas-permeable structure were developed, endowing various imperceptible on-skin devices with superior performance.<sup>331</sup> In practice, the EMPA-based radiative cooling fabric reduced the temperature by  $\sim 4^\circ\text{C}$  under a solar intensity of  $1\text{ kW m}^{-2}$  and provided long-term comfort.<sup>328</sup> Flexible self-assembly of EMPAs has shown great potential for superb personal healthcare and excellent HMI in an interference-free and comfortable manner. Furthermore, multifunctional on-skin electronics with outstanding passive cooling capability ( $\sim 6^\circ\text{C}$  cooling effect) was developed by using multiscale porous SEBS as a supporting substrate. The porous SEBS substrates also show other desirable properties such as high breathability and outstanding waterproofing. In conclusion, significant progress has been made in the areas of moisture management and thermal management of PCTs. However, it is worth mentioning that these functions are often studied independently rather than in a cohesive manner, with few reports on the collaborative moisture and thermal management functions of PCTs. Therefore, there is still a long way to go in the study of thermal and moisture comfort in wearable electronics.

### 3. WEARABLE DEVICES BASED ON PCTs

PCTs that can serve as active sensing components, flexible electrodes, interconnects, *etc.*, offer a promising platform for the fabrication of flexible electronic devices. On one hand, the porous structure of PCTs allows them to exhibit electrical changes (*e.g.*, resistance, capacitance) when subjected to deformations such as compression and stretch, making them well-suited for use as active components in pressure and strain sensors. On the other hand, the good flexibility and porous nature of PCTs make them promising for use as electrodes (or current collectors) for a wide range of sensors, actuators, and energy devices. The high specific surface area provided by the porous structure offers ample active sites for loading active materials, transducing analytes, or promoting electrochemical processes. More importantly, the porous structure of PCTs facilitates the development of wearable devices with excellent permeability and wearing comfort. In this section, we introduce versatile PCT-based flexible textile devices including various sensors, actuators, therapeutic devices, energy harvesting/storage devices, and displays. In this context, the PCT-based textile devices encompass not only those directly employing PCTs as a functional unit, but also devices by integrating functionalized conductive fibers or multiple fiber devices into textiles. Consequently, PCT-based electronic devices can be formulated either in the form factor of 1D fiber shapes, 2D planar sheet structures, or integrated 3D monolithic configurations. **Table 1** provides an overview of the wearable devices, illustrating their typical device functions and working mechanisms, as well as emphasizing the functions/roles of PCTs within the devices.

**Table 1.** Wearable devices based on PCTs

Type of devices			Device functions in wearables	Working mechanism	Functions of PCTs in the devices
Sensors	Biophysical Sensors	Pressure Sensors	<ul style="list-style-type: none"> <li>• Detect externally applied compressing forces</li> <li>• Monitor body motions/gaits</li> <li>• Monitor blood pressure/pulse</li> </ul>	<ul style="list-style-type: none"> <li>• Piezoresistive</li> <li>• Capacitive</li> <li>• Electric (piezoelectric &amp; triboelectric)</li> </ul>	<ul style="list-style-type: none"> <li>• Active sensing components in piezoresistive sensors</li> <li>• Electrodes in capacitive and electric sensors</li> </ul>
		Strain Sensors	<ul style="list-style-type: none"> <li>• Detect applied strains</li> <li>• Monitor body motions</li> </ul>	<ul style="list-style-type: none"> <li>• Resistive</li> <li>• Capacitive</li> <li>• Electric (piezoelectric &amp; triboelectric)</li> </ul>	<ul style="list-style-type: none"> <li>• Active sensing components in resistive sensors</li> <li>• Electrodes in capacitive and electric sensors</li> </ul>
		Temperature Sensors	<ul style="list-style-type: none"> <li>• Sense environmental temperature</li> <li>• Sense body/skin temperature</li> </ul>	<ul style="list-style-type: none"> <li>• Thermo-resistive</li> <li>• Thermoelectric</li> </ul>	<ul style="list-style-type: none"> <li>• Temperature-sensitive / thermoelectric components</li> </ul>
		Photodetectors	<ul style="list-style-type: none"> <li>• Detect light intensity</li> </ul>	<ul style="list-style-type: none"> <li>• Photoelectric response</li> </ul>	<ul style="list-style-type: none"> <li>• Conductive electrodes</li> </ul>
	Chemical and Biological Sensors	Gas Sensors	<ul style="list-style-type: none"> <li>• Detect environmental gaseous substances</li> <li>• Detect human-emitted gaseous substances</li> </ul>	<ul style="list-style-type: none"> <li>• Resistive</li> <li>• Capacitive</li> </ul>	<ul style="list-style-type: none"> <li>• Conductive electrodes</li> <li>• Active components</li> </ul>
		Sweat Sensors	<ul style="list-style-type: none"> <li>• Monitor chemicals and biomolecules in sweat</li> </ul>	<ul style="list-style-type: none"> <li>• Potentiometric</li> <li>• Amperometric</li> <li>• Impedimetric</li> <li>• Transistor-based</li> </ul>	<ul style="list-style-type: none"> <li>• Conductive electrodes</li> <li>• Active components</li> </ul>
	Electrophysiological Sensors	ECG EMG EEG EOG	<ul style="list-style-type: none"> <li>• Monitor the bioelectric activity of biological cells or tissues to understand physiological behaviors</li> </ul>	<ul style="list-style-type: none"> <li>• Signal amplification of bioelectric signals</li> </ul>	<ul style="list-style-type: none"> <li>• Dry electrodes</li> </ul>
Actuators	Electrical Actuators		<ul style="list-style-type: none"> <li>• Undergo deformation under electrical stimuli</li> </ul>	<ul style="list-style-type: none"> <li>• Electromechanical actuation</li> <li>• Electrochemical actuation</li> </ul>	<ul style="list-style-type: none"> <li>• Conductive electrodes</li> </ul>
	Thermal Actuators		<ul style="list-style-type: none"> <li>• Undergo deformation under thermal stimuli</li> </ul>	<ul style="list-style-type: none"> <li>• Thermal-driven actuation</li> </ul>	<ul style="list-style-type: none"> <li>• Active components</li> </ul>
	Solvent Actuators		<ul style="list-style-type: none"> <li>• Undergo deformation under solvent.vapor stimuli</li> </ul>	<ul style="list-style-type: none"> <li>• Expand in volume upon solvent absorption</li> </ul>	<ul style="list-style-type: none"> <li>• Active components</li> </ul>

Therapeutic Devices	Thermotherapy		<ul style="list-style-type: none"> <li>Produce heat</li> </ul>	<ul style="list-style-type: none"> <li>Joule heating through applied voltage</li> </ul>	<ul style="list-style-type: none"> <li>Conductive electrodes</li> </ul>
	Electrical Stimulation		<ul style="list-style-type: none"> <li>Inject charges to stimulate muscles or nerves to alleviate pain</li> </ul>	<ul style="list-style-type: none"> <li>Electric charge delivery</li> </ul>	<ul style="list-style-type: none"> <li>Conductive electrodes</li> </ul>
	Drug Delivery		<ul style="list-style-type: none"> <li>Deliver drug</li> </ul>	<ul style="list-style-type: none"> <li>Iontophoresis</li> <li>Reverse iontophoresis</li> </ul>	<ul style="list-style-type: none"> <li>Conductive electrodes</li> <li>Drug-loading medium</li> </ul>
Energy Harvest and Storage Devices	Energy Harvest Devices	Solar Cells	<ul style="list-style-type: none"> <li>Convert light into electricity</li> </ul>	<ul style="list-style-type: none"> <li>Thin-film solar cells</li> <li>Dye-sensitized solar cells</li> <li>Perovskite solar cells</li> </ul>	<ul style="list-style-type: none"> <li>Conductive electrodes</li> </ul>
		Generators/ Nanogenerators	<ul style="list-style-type: none"> <li>Convert mechanical variations/temperature disparities into electricity</li> </ul>	<ul style="list-style-type: none"> <li>Piezoelectric</li> <li>Triboelectric</li> <li>Thermoelectric</li> </ul>	<ul style="list-style-type: none"> <li>Conductive electrodes</li> </ul>
		Wireless Energy Harvesting	<ul style="list-style-type: none"> <li>Use electromagnetic induction to provide electricity to portable devices</li> </ul>	<ul style="list-style-type: none"> <li>Inductive effect</li> </ul>	<ul style="list-style-type: none"> <li>Antenna</li> </ul>
		Biofuel Cells	<ul style="list-style-type: none"> <li>Convert chemical energy into electricity</li> </ul>	<ul style="list-style-type: none"> <li>Electrochemical reactions</li> </ul>	<ul style="list-style-type: none"> <li>Electrode/current collectors</li> </ul>
	Energy Storage Devices	Supercapacitors	<ul style="list-style-type: none"> <li>Convert chemical energy into electrical energy reversibly</li> </ul>	<ul style="list-style-type: none"> <li>Electric double-layer capacitive</li> <li>Pseudocapacitive</li> </ul>	<ul style="list-style-type: none"> <li>Current collectors</li> <li>Electrochemically active materials (<i>e.g.</i>, graphene PCTs)</li> </ul>
		Batteries	<ul style="list-style-type: none"> <li>Convert chemical energy into electrical energy reversibly</li> </ul>	<ul style="list-style-type: none"> <li>(De)Intercalation reaction</li> <li>Conversion reaction</li> <li>Alloy reaction</li> <li>Plating/stripping process</li> </ul>	<ul style="list-style-type: none"> <li>Current collectors</li> </ul>
Displays	Light-Emitting Devices		<ul style="list-style-type: none"> <li>Emit light upon applying electricity</li> </ul>	<ul style="list-style-type: none"> <li>Inorganic light-emitting diode</li> <li>Organic light-emitting diode</li> <li>Polymer light-emitting diode</li> <li>Light emitting electrochemical cell</li> <li>Alternating current electroluminescent</li> </ul>	<ul style="list-style-type: none"> <li>Conductive electrodes</li> </ul>
	Electrochromic Devices		<ul style="list-style-type: none"> <li>Change color upon applying electricity</li> </ul>	<ul style="list-style-type: none"> <li>Reversible oxidation–reduction</li> <li>Electrothermal</li> </ul>	<ul style="list-style-type: none"> <li>Conductive electrodes</li> <li>Active components</li> </ul>

### 3.1 Sensors

Wearable sensors have emerged as a promising technology in revolutionizing human life, especially for healthcare and wellness monitoring, as they can offer continuous, real-time, and non-invasive monitoring of various environmental and physiological parameters.<sup>10, 332-334</sup> While flexible and stretchable thin film materials have enabled the development of versatile wearable sensors, they lack permeability and comfortability due to their solid structures.<sup>316, 335</sup> In this regard, the PCTs provide an appealing platform for the fabrication of wearable sensors that can be highly permeable and comfortable, owing to their soft texture and porous structure. These textile-based wearable sensors can be fabricated by utilizing functional PCTs through weaving, knitting, or printing technologies. In this section, we summarize and classify a wealth of wearable PCT-based sensors, including biophysical sensors such as pressure, strain, temperature, and photo sensors for monitoring human motions and environmental conditions, chemical and biological sensors for detecting body healthcare-related indices, and bioelectrical sensors for real-time recording of physiological signals such as ECG, electromyography (EMG), electroencephalography (EEG), and electrooculography (EOG).

#### 3.1.1 Biophysical Sensors

##### 3.1.1.1 Pressure Sensors

Wearable pressure sensors, which can generate distinct signals in response to applied forces, are widely applied in various fields, including medical, human-computer interaction, and smart homes.<sup>336, 337</sup> Owing to their good conductivity, flexibility, durability, skin conformability, and permeability, PCTs have been widely used in the preparation of wearable pressure sensors for the monitoring of human motions.<sup>338, 339</sup> In terms of the working mechanisms, pressure sensors can be classified into piezoresistive, capacitive, and electric types.<sup>9, 340</sup> This section discusses the material selection and structural design of PCT-based pressure sensors according to these three types of sensing mechanisms.

***Piezoresistive Pressure Sensor.*** Typically, a piezoresistive pressure sensor functions based on the principle that the resistance of its conductive electrode changes with applied pressure, through which the pressure can be determined by correlating the change in resistance.<sup>341</sup> PCTs are excellent candidates as sensing layers for the assembly of piezoresistive pressure sensors due to their good flexibility and porous structure. The porous structure of PCTs allows ample space for resistance change, contributing to enhanced sensitivity for pressure sensors. To date, various conductive materials, such as CNTs, graphene, MXene, and metal, have been

incorporated into PCT formats for the preparation of textile-based pressure sensors. For example, Jiang *et al.*<sup>336</sup> used 3D porous rGO to prepare highly compressible and sensitive fabric pressure sensors through a filtration approach. Zheng *et al.*<sup>342</sup> designed a pressure sensor based on the conductive MXene/cotton fabric by taking advantage of the electrical conductivity of MXene nanosheets and the good softness and breathability of cotton fabric (**Figure 21a**). The pressure sensor showed high sensitivity and a wide sensing range, making it suitable for human motion detection and electronic skin applications. The coating of MXene on electrospun PU membranes could further endow stretchability to the flexible PCT-based pressure sensors (**Figure 21b**).<sup>343</sup> In addition to directly using PCT fabrics as the sensing layers, PCT-based pressure sensors can also be produced by integrating functional fibers/yarns into pressure-sensing textiles. For example, Luo *et al.*<sup>344</sup> prepared functional yarns using coaxial resistive fibers and automated coating technology, and then weaved the yarns into textiles with arbitrary 3D shapes (**Figure 21c**). The functional fiber was constructed in two parts: a conductive core and a piezoresistive sheath (**Figure 21d**). Conductive core is made of stainless-steel thread. Piezoresistive sheath is fabricated by mixing graphite NP, Cu nanoparticles (CuNPs) and polydimethylsiloxane (PDMS) elastomer.

Structural design plays an important role in the construction of PCT-based piezoresistive pressure sensors, which can significantly boost their sensing performance. For example, inspired by the structure of Merkel receptors, Song *et al.*<sup>345</sup> orthogonally weaved the high-modulus silver/nylon threads onto a piece of low-modulus micro-structured nonwoven fabric. Such a crossing-point structure could induce a high local stress concentration, leading to significant amplification of the pressure-sensing range and the enhancement of sensitivity (**Figure 21e**). Other structural design strategies, such as 3D structures,<sup>346</sup> porous spinous layer structures,<sup>347</sup> and array structures,<sup>348</sup> have also been developed to improve the sensing performance of PCT-based pressure sensors. Apart from improving sensitivity and detection range, stability is another critical issue of piezoresistive pressure sensors that needs to be taken into consideration, especially in practical applications. The stability issue mainly arises from two aspects. First, the resistance of most piezoresistive materials is susceptible to temperature changes, which pose difficulties for pressure sensing in varying temperature environments. Second, textile structures as the substrate of the pressure sensor can have an impact on the electrical and mechanical stability of the device, which may lead to signal deviation during the pressure sensing.

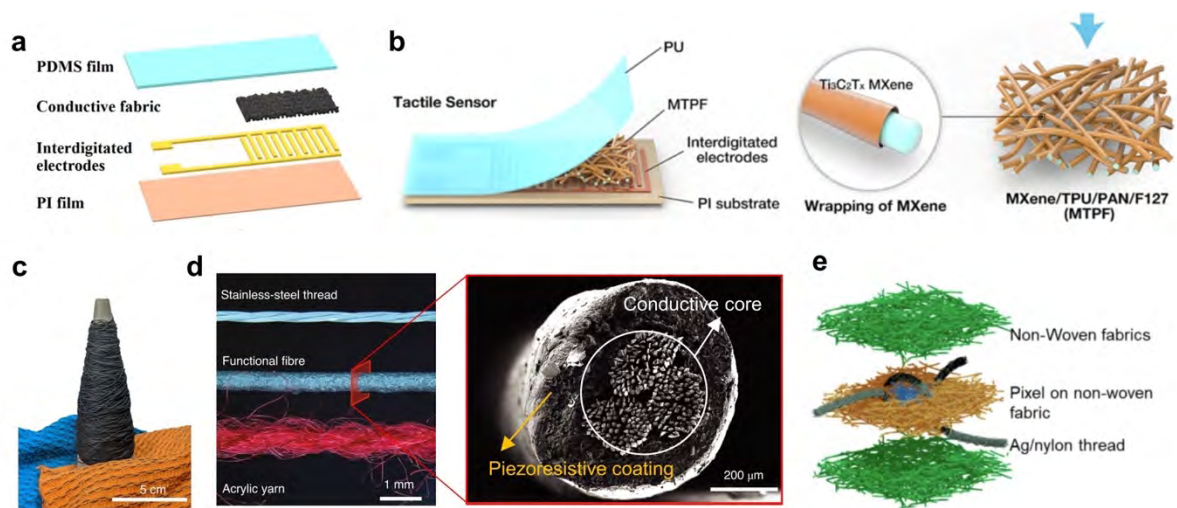


**Figure 21.** (a) Basic structure of piezoresistive pressure sensor. Reproduced with permission from ref <sup>342</sup>. Copyright 2021 Elsevier. (b) Structural design of MXene-based piezoresistive pressure sensor. Reproduced with permission from ref <sup>343</sup>. Copyright 2023 Elsevier. (c) Photograph of the piezoresistive functional fiber and sensing fabrics. (d) Optical image and SEM cross-sectional image of a stainless-steel thread, coaxial piezoresistive fiber, and acrylic knitting yarn. Reproduced with permission from ref <sup>344</sup>. Copyright 2021 Springer Nature. (e) Structural design of Merkel receptor-inspired piezoresistive pressure sensor. Reproduced with permission from ref <sup>345</sup>. Copyright 2022 Elsevier.

**Capacitive Pressure Sensor.** Currently, capacitive pressure sensor is one of the most mature types of commercial pressure sensors, which has the advantages of high accuracy, wide detection range, and high reliability. A capacitive pressure sensor usually consists of two conductive electrodes that are separated by a dielectric layer. The capacitance change of the sensor when subjected to external pressing force can be measured, which is then calculated to reflect the detected force and pressure.<sup>349</sup> Typically, conductive electrodes in the capacitive pressure sensors are required to maintain their stable conductivity upon stretching and bending. PCTs with good flexibility and stable conductivity are thus promising candidates. Compared to their planar film counterparts, the porous structure of PCTs can create airgaps between electrode and dielectric layer, thereby improving the sensitivity of sensors. Chen *et al.*<sup>350</sup> prepared a flexible textile electrode by electrospinning a Pd ion-doped PAN nanofiber membrane, followed by chemically plating Ag (**Figure 22a**). Such a PCT electrode showed excellent conductivity owing to the coral-like Ag coating on nanofibers. A fabric pressure sensor was then assembled using these PCT electrodes and a high-denier nylon mesh as the dielectric layer. In such a fabric pressure sensor, the porous structure of fabrics provided more



changes of contact area between PCT electrode and nylon dielectric layer, resulting in the excellent pressure sensing performance. To further improve the sensing performance of PCT-based capacitive pressure sensors, a reversible ion pump hybrid sensing layer triggered by hydrogen bonding was constructed by adding MXene and ionic salt to the sensing layer (**Figure 22b**).<sup>351</sup> During this process, ion pumping is initiated to form a thick electrical double layer (EDL) at the interface between electrode and electrolyte, thereby increasing the relative change in capacitance.

In addition to non-woven fabric electrodes, 1D conductive fibers, such as gel fibers, CNT fibers, graphene fibers, and PANI fibers, can also be used as electrodes for capacitive pressure sensors. Ding *et al.*<sup>352</sup> prepared a transparent, stretchable, and elastic capacitive pressure sensor using hydrogel fibers as electrodes (**Figure 22c**). They studied the influence of working distance on the capacitance change rate of the sensor, and results showed that the closer the working distance, the better the sensing performance. However, fiber-shaped electrode pairs can only detect the pressure changes at the intersection of the electrodes, limiting their application in large-area scenarios such as foot pressure, joint activity, and cardiovascular health monitoring. Therefore, different textile technologies, such as weaving and knitting, are employed to produce large-area sensor arrays. Wu *et al.*<sup>353</sup> made a large-area sensing array by weaving silver nanowire-treated elastic yarns (**Figure 22d**). The woven sensing fabrics showed good stability and excellent pressure-sensing performance (**Figure 22e**). As shown in **Figure 22f**, a basic sensing unit comprises two intersecting and overlapping conductive elastic yarns. Overall, for fabric-based capacitive pressure sensors, it is essential to ensure the stability between the fabric electrodes and the dielectric layer, as it determines the stability and lifespan of the sensor.

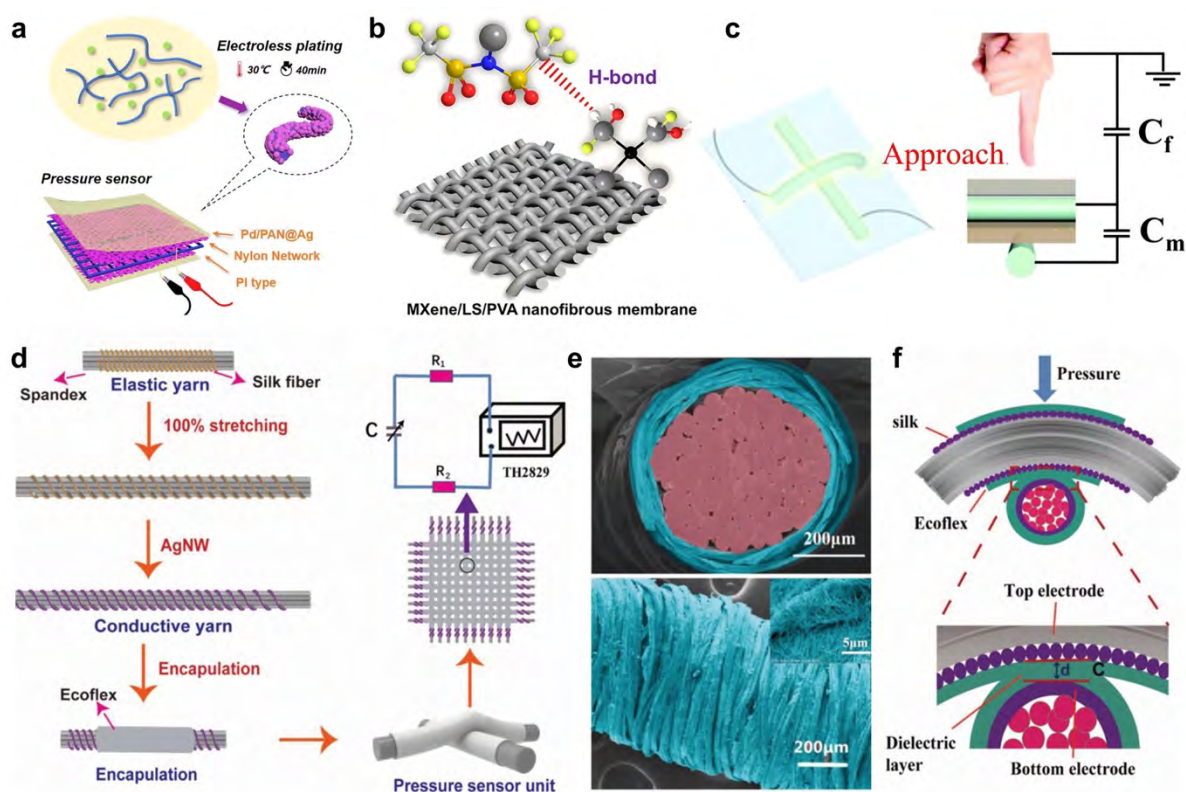


**Figure 22.** (a) Schematic illustration of assembled sandwich-structure capacitive pressure sensor. Reproduced with permission from ref <sup>350</sup>. Copyright 2021 Elsevier. (b) Schematic diagram of MXene/Li salt/PVA nanofiber membrane. Reproduced with permission from ref <sup>351</sup>. Copyright 2021 American Chemical Society. (c) Equivalent circuit of a cross-fiber shaped capacitive pressure sensor. Reproduced with permission from ref <sup>352</sup>. Copyright 2022 Royal Society of Chemistry. (d) Fabrication process and measurement setup of the pressure sensor. (e) SEM images of a conductive electrode of fibrous pressure sensors. (f) Basic sensing unit of the capacitance type of fibrous pressure sensors. Reproduced with permission from ref <sup>353</sup>. Copyright 2019 John Wiley and Sons.

**Electric Pressure Sensor.** Electric pressure sensor is a new type of sensor invented in recent years, which typically includes piezoelectric and triboelectric pressure sensors.<sup>354, 355</sup> The piezoelectric pressure sensors are assembled with piezoelectric materials, such as ZnO, BaTiO<sub>3</sub>, and polyvinylidene fluoride (PVDF). The application of pressure to a piezoelectric material induces a deformation in its crystal structure, causing a separation or displacement of charges and generating an electric field or voltage across the material, known as the piezoelectric effect. As a result, the piezoelectric material will produce equal positive and negative charges on the opposite surfaces of the material to maintain the original state, during which electrical pulses (voltage/current) are generated. A piezoelectric pressure sensor usually comprises conductive

electrodes and a piezoelectric sensing layer that is sandwiched between the electrodes. Fabric piezoelectric pressure sensors thus can be prepared by combining piezoelectric fabrics with PCTs electrodes.<sup>356</sup> Wang *et al.*<sup>357</sup> assembled a piezoelectric pressure sensor using PCT fabrics as the electrodes and PVDF nanofiber membrane as the piezoelectric sensing layer (**Figure 23a**). The use of PCT electrodes can form lots of air gaps at the interface between the electrode and the piezoelectric layer, which is beneficial to the induction and transfer of charges. To improve the contact degree and stability of the interface, Huang *et al.*<sup>358</sup> reported a phase separation method to produce a flexible piezoelectric sensor based on a PVDF/graphene composite coating on a commercial fabric.

Triboelectric pressure sensors are another type of electric sensor that emerged in recent years. Its working principle is based on the coupling effect of triboelectric electrification and electrostatic induction.<sup>359</sup> Unlike piezoelectric pressure sensors, triboelectric pressure sensors have more diverse device configurations and a wider selection of materials.<sup>315</sup> Since almost all polymers have the frictional electrification effect, two different polymers with opposite electrical polarities can be combined into a friction pair. Therefore, research on triboelectric pressure sensors surpasses that of piezoelectric pressure sensors. PCTs mainly play the role of inducing charges in friction voltage pressure sensors and sometimes also can serve as a positive friction layer. For example, a single-electrode triboelectric pressure sensor can be obtained by coating a layer of polymer on a conductive yarn, and pressure sensor fabrics can be then made by knitting the yarns (**Figure 23b**).<sup>360</sup> Larger internal gaps in the material contribute to reducing Young's modulus and increasing sensitivity, while reaching the maximum separation distance between the friction layers leads to the highest amount of charge transfer. This strategy has been proven and used to improve the sensing performance of triboelectric pressure sensors. The porous structure and high conductivity of PCTs are conducive to improving the performance of friction voltage pressure sensors. In addition to metallic wires, carbon yarns, conductive polymer yarns, and LM wires have also been used in triboelectric pressure sensors (**Figure 23c**).<sup>361</sup> The low modulus of LM further improves the sensitivity. In addition to woven and knitted fabrics, nonwoven fabrics can also be used to prepare fabric electrodes. Peng *et al.*<sup>362</sup> developed a contact-separation-type all-nanofiber electronic skin based on multilayer PAN and PA 66 nanofibers as triboelectric pairs, and gold as the electrode (**Figure 23d**). Overall, the main challenge faced by electric pressure sensors is the interference of sensing signals by humidity and externally charged objects. Therefore, a critical aspect in the advancement of electric pressure sensors lies in the design of encapsulation and shielding

structures.

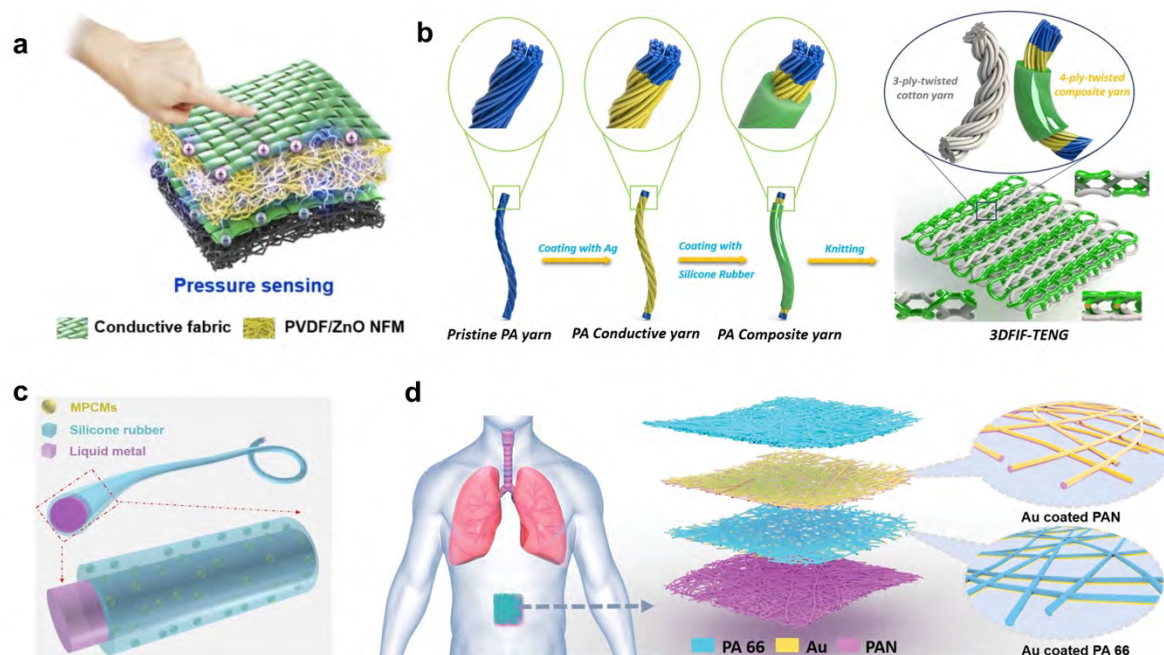


**Figure 23.** (a) Schematic illustration of piezoelectric pressure sensor fabric. Reproduced with permission from ref <sup>357</sup>. Copyright 2021 Elsevier. (b) Fabrication process of the core-sheath yarn and 3D structure-based triboelectric pressure sensor. Reproduced with permission from ref <sup>360</sup>. Copyright 2020 Elsevier. (c) Schematic structure diagram of LM-based multifunction fiber. Reproduced with permission from ref <sup>361</sup>. Copyright 2021 Elsevier. (d) Schematic illustration of the all-nanofiber triboelectric pressure sensor. Reproduced with permission from ref <sup>362</sup>. Copyright 2021 John Wiley and Sons.

### 3.1.1.2 Strain Sensors

A strain sensor detects strains caused by external forces and converts them into electrical signals.<sup>363</sup> Textile-based strain sensors find extensive applications in monitoring various aspects relating to body health.<sup>364</sup> For example, they can be used to monitor respiratory patterns for diagnosing and treating sleep apnea and other respiratory diseases. Additionally, they can track athletes' movement status and posture, aiding in training improvement and reducing the risk of injuries. Similar to pressure sensors, strain sensors can be mainly classified into three types: resistive, capacitive, and electric strain sensors. This section discusses the assembly of these three types of strain sensors based on PCTs.

**Resistive Strain Sensor.** The resistive strain sensor is widely used due to its simple device

structure and facile preparation process. Its working principle is based on the change of resistance under compression or tension to reflect the magnitude of strain.<sup>365</sup> PCTs with elasticity are often used as the sensing functional electrode, as they can offer good stretchability and easy control of conductivity. Regarding the diverse configurations of PCTs, strain sensors fabricated based on different PCT structures may have different equivalent circuits.

The equivalent circuit of a 1D piezoresistive strain sensor is determined by its device structure. Some 1D conductive fibers are created by blending conductive particles with non-conductive fibers, while others are formed by wrapping conductive fibers around non-conductive ones. For instance, Liu *et al.*<sup>366</sup> prepared a strain sensor based on multi-walled carbon nanotube (MWCNT) and silicone rubber composite conductive fibers prepared by thermal stretching. At the initial status, conduction paths are established between fibers through direct contact and tunneling effect between the interconnects and adjacent MWCNT (**Figure 24a**). Under stretching, the conductive percolation paths remained unchanged, while the contact and tunneling resistance between the segment lines expanded due to the tilt and separation of fibers. To improve the sensing performance of CNT-doped elastic fibers, Gao *et al.*<sup>367</sup> produced a composite spiral yarn composed of CNT and PU nanofibers (**Figure 24b**). Attributing to the twisting structure of CNT and the spring-like micro-geometry structure of PU, the spiral yarn showed excellent stretchability and conductivity. The equivalent circuit of this sensor is composed of numerous series resistors, with each resistor comprising multiple parallel carbon nanotubes. The resistance changes are caused by irreversible cracking. In addition to doping conductive particles in elastic fibers, intrinsic conductive polymer fibers such as gel fibers and PANI fibers can also be used for resistive strain sensors. Song *et al.*<sup>280</sup> transformed a wet-spun hydrogel fiber into an organohydrogel fiber through a mixed cross-linking strategy and simple solvent substitution, and the resulting strain sensor can accurately capture high-frequency and high-speed motion signals.

The conductive path as well as equivalent circuit become more complicated when it comes to 2D straining sensing fabrics. Liu *et al.*<sup>346</sup> create a 2D sensing fabric by embroidering elastic conductive yarns into a water-soluble substrate, followed by removing the substrate. The strain sensing network comprises conductive yarns in the x-direction. During stretching, the parallel circuit formed by continuous conductive wires gradually transforms into a mixed circuit due to the changes in connection between the threaded and continuous conductive wire parts (**Figure 24c**). The second method for fabricating 2D sensing fabrics is to cover a conductive material



on a 2D fabric substrate.<sup>368</sup> For instance, Li *et al.*<sup>369</sup> prepared a fabric strain sensor by combining electrospinning and ultrasound technology. By utilizing ultrasound, CNT was attached onto the surface of porous thermoplastic polyurethane (TPU) nanofibers to form a conductive fabric. This structure operates differently from that of a woven sensing cloth. As depicted in **Figure 24d**, CNTs form a dense network on the surface of TPU fibers, creating numerous contact points between CNTs. During stretching, microcracks occur in the CNTs network due to the long-distance slip of CNTs, resulting in a continuous increase in resistance. However, the influence of temperature on resistance-based strain sensors is still unavoidable, and there is a few research currently in this area.

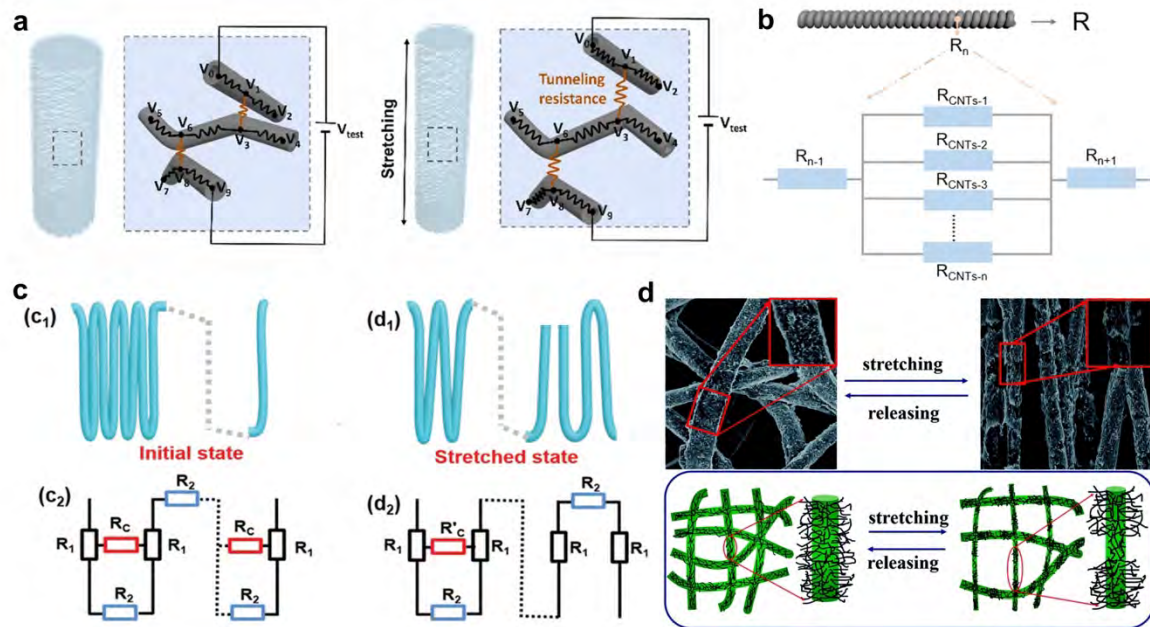


**Figure 24.** (a) The strain sensing mechanism enabled by tunneling effect in original and stretched state. Reproduced with permission from ref <sup>366</sup>. Copyright 2022 Elsevier. (b) The equivalent circuit of twisted resistive strain sensor. Reproduced with permission from ref <sup>367</sup>. Copyright 2020 American Chemistry Society. (c) The equivalent circuit of knitting strain sensor fabric. Reproduced with permission from ref <sup>346</sup>. Copyright 2021 John Wiley and Sons. (d) Strain sensing mechanism of TPU@CNTs fibrous mat. Reproduced with permission from ref <sup>369</sup>. Copyright 2021 Royal Society of Chemistry.

**Capacitive Strain Sensor.** The capacitive strain sensor responds to strain by changing its capacitance. The parallel-plate structure is a representative configuration for capacitive strain sensors. When an alternating-current voltage is applied, opposite charges accumulate on the



top and bottom electrodes. The capacitance then can change with the change in geometry under loading and unloading, regardless of the resistance of the fiber electrodes. When stretching, the capacitive strain sensor maintains the electrode area, while the thickness of the dielectric layer will change, resulting in a change in capacitance. When it comes to textile-based capacitive strain sensors, the classical parallel-plate structure is not suitable because it cannot adjust the area or thickness of the dielectric layer under stretching. Therefore, core-shell structure is usually adopted for manufacturing capacitive strain-sensing textiles. Frutiger *et al.*<sup>370</sup> adopted 3D printing technology to prepare a core-shell fiber consisting of alternating layers of ionically conductive fluid and silicone rubber, which can serve as conductive electrodes and dielectric/sealant layers, respectively. (**Figure 25a**). In addition to core-shell structure, double helix structure is also a viable option for creating capacitive strain-sensing fibers. Lee *et al.*<sup>371</sup> reported an all-fiber wireless capacitive strain sensing system, wherein the strain sensor consisted of two stretchable conductive fibers that formed a hollow double helix structure (**Figure 25b**). A PDMS coating was applied to ensure no short circuit between two fibers. The hollow section of the double helix structure served as the dielectric layer of the capacitor, while the two spiral conductive fibers served as the electrodes. When subjected to a strain, two double helix conductive fibers in the sensor gradually straightened and approached each other, leading to an increase in capacitance. When further stretched to a transition point, they became completely straightened and formed a twisted structure. Thereafter, the two twisted conductive fibers will naturally elongate and become thinner in accordance with the applied strain upon further stretching. Despite the progress in capacitive strain sensing textiles, the current device structure design primarily revolves at the fiber level. It is still challenging to produce capacitive strain-sensing fabrics, because how to make the fabric-shaped dielectric layer undergo area or thickness changes with strain under tension is yet to be addressed.

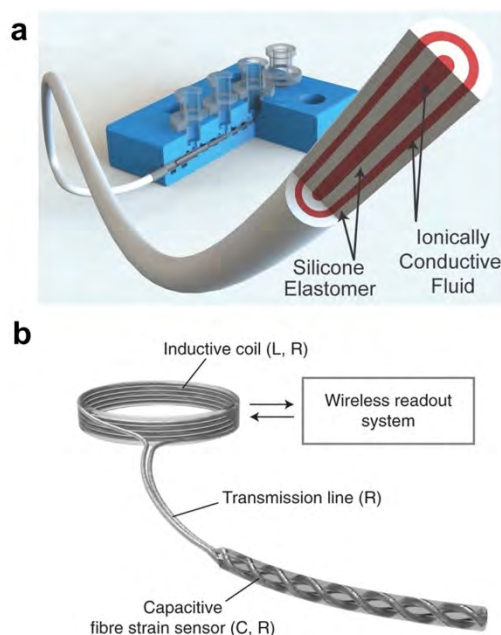


**Figure 25.** (a) Schematic illustration of multicore-shell printed capacitive strain sensor. Reproduced with permission from ref <sup>370</sup>. Copyright 2015 John Wiley and Sons. (d) Schematic illustration of a passive wireless strain-sensing system based on a fiber strain sensor. Reproduced with permission from ref <sup>371</sup>. Copyright 2021 Springer Nature.

**Electric Strain Sensor.** Similar to pressure sensors, electric strain sensors can also be classified into two types: piezoelectric strain sensors and triboelectric strain sensors. Piezoelectric strain sensors operate based on the piezoelectric effect of piezoelectric materials, which enables them to generate an electrical signal when subjected to stress. Since most piezoelectric materials are inorganic materials that exhibit poor tensile strain, the reported piezoelectric strain sensors usually have limited working strain ranges for practical use. Consequently, there are only a few research on piezoelectric strain sensors focusing solely on piezoelectric materials. PCTs such as carbon fibers, PANI fibers, and metal wires are mostly used as electrodes for making piezoelectric sensors. Liao *et al.*<sup>372</sup> manufactured a flexible piezoelectric strain sensor using a hybrid structure of carbon fiber-ZnO NW (**Figure 26a**). The ZnO NWs are grown on carbon fiber substrate by a hydrothermal method. However, due to the poor stretchability of carbon fibers and ZnO NWs, the strain detection range of the sensor is only 0.2~1.2%.

Triboelectric strain sensors operate through cyclic processes contact and separation between electrode and triboelectric layers. The charges are generated by electrification and transferred through PCT electrodes.<sup>373</sup> By selecting appropriate electrodes and triboelectric materials, the

detection strain range of triboelectric strain sensors can be effectively adjusted. Ning *et al.*<sup>374</sup> developed a helical fiber strain sensor that can respond to small tensile strains. Conductive fibers wrapped with nylon and polytetrafluoroethylene (PTFE) separated each other under tension, and regained contact once removal of the external force, during which a frictional electrical signal is generated. Increasing tension leads to a higher charge transfer between the two fiber electrodes, contributing to a greater output. The output voltage increases synchronously with the increase in strain, demonstrating its excellent strain-sensing performance. Recently, researchers have developed triboelectric strain sensors with single-electrode mode, which simplifies the sensor structure and improves its flexibility and convenience. Sheng *et al.*<sup>375</sup> created a helical strain sensor based on organogel and silicone rubber, where the conductive organogel fibers serve as the electrodes for inducing and transmitting charges (**Figure 26b**). In addition, stainless steel fibers have also been applied to the electrode for a single-electrode mode triboelectric strain sensor. Zhou *et al.*<sup>376</sup> reported a stainless-steel metal wire electrode with a winding structure, which has excellent conductivity. Thanks to the flexibility of the substrate and the stretchability of the winding structure, the sensor possesses good flexibility, which shows a detection strain range of up to 100%.

In recent years, electric strain sensors have attracted significant attention due to their active sensing capabilities and the ability to convert mechanical signals into electrical signals without the need for external power sources. In principle, these strain sensors can operate autonomously, eliminating the need for additional electrical power components and resulting in energy savings. However, further investigation is needed to evaluate the actual power consumption of these strain sensors. In addition, electric strain sensors require dynamic external forces to generate electrical signals, making it difficult to measure static strains. Finally, as the sensing principle relies on charge transfer, it is necessary to shield the sensor from the impact of charged objects in the environment using appropriate methods.

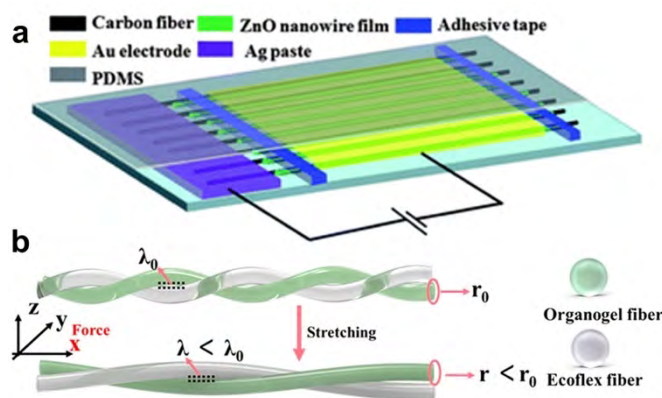


**Figure 26.** (a) The structure design of carbon fiber-based piezoresistive strain sensor. Reproduced with permission from ref <sup>372</sup>. Copyright 2013 Royal Society of Chemistry. (b) Two stretching states of organogel/silicone fiber-helical strain sensor. Reproduced with permission from ref <sup>375</sup>. Copyright 2022 American Chemistry Society.

### 3.1.1.3 Temperature Sensors

Monitoring body temperature is of paramount importance in understanding health conditions, serving as a critical tool for maintaining optimal well-being and effectively managing illnesses.<sup>377, 378</sup> Temperature-sensitive fabric, an intelligent textile with the capability to sense temperature, offers a valuable solution for wearable temperature monitoring applications. Temperature-sensitive fabrics usually employ two mechanisms for temperature sensing: thermo-resistive and thermoelectric.<sup>379, 380</sup> The resistance of a thermistor changes with temperature, and this change can be described by a temperature coefficient. Usually, as the temperature rises, the resistance of the material decreases, and *vice versa*. Hence, the most prevalent approach in designing and fabricating fabric temperature sensors is utilizing the thermo-resistive effect of conductive fabric. Materials such as CNTs, graphene, and PEDOT:PSS can be used to produce conductive fabrics for temperature sensing. Afroj *et al.*<sup>381</sup> prepared a graphene conductive yarn by coating graphene on a cotton thread by the dyeing method (**Figure 27a**). The graphene yarn was then made into temperature-sensitive fabric through knitting. In addition, metal wires can also produce changes in electrical signals at different temperatures. Similarly, Husain *et al.*<sup>382</sup> created a temperature-sensitive fabric by embedding temperature-responsive metal wires into a double-layered fabric using knitting technology (**Figure 27b**). Generally, knitting structures are better than weaving structures because they are comfortable and can fit according to body shape. Moreover, the double-layered structure of knitting can protect the sensing material and reduce wear and tear. As mentioned above, weaving conductive yarns into fabric and coating non-conductive fabric with

conductive materials are the two common methods for manufacturing conductive fabrics. Wang *et al.*<sup>383</sup> printed a mixture of PEDOT:PSS and PVA on TPU nanofiber membrane to fabricate temperature sensors (**Figure 27c**). By using the good thermo-resistive performance of PEDOT:PSS, the temperature sensing sensitivity can be significantly improved. PEDOT:PSS features a distinctive core-shell structure, where the core consists of a conductive but hydrophobic PEDOT-rich region, while the shell comprises an insulating but hydrophilic PSS-rich region. As temperature increases, the PSS shell tends to contract as the water molecules in the hydrophilic PSS layer are released into the surrounding environment. This leads to a decrease in the distance between adjacent PEDOT cores, which in turn enhances the electron hopping between them. Consequently, the resistance of PEDOT:PSS decreases with rising temperatures.

Another common sensing mechanism is thermoelectricity, which uses the thermoelectric effect of two different conductors to measure temperature. When one end of a thermocouple is exposed to a temperature environment, the potential difference between the two dissimilar conductors changes in response to the temperature variation. Jung *et al.*<sup>384</sup> prepared a textile-based temperature sensor using template printing technology. The sensing layers printed on the textile substrate consist of N-type and P-type thermoelectric materials, specifically PEDOT and AgNPs, with an overlapping area of 4 mm<sup>2</sup>. When the overlap between the P-type and N-type materials is heated, a temperature difference is generated, which causes charge exchange and transfer, thereby producing a potential difference. In addition to 2D structure, researchers have also reported a 3D temperature sensing fabric. In specific, it was assembled by combining a 3D spacer fabric coated with PEDOT and a silver paste electrode (**Figure 27d**).<sup>385</sup> Under a temperature difference, the conductive spacer fabric and silver paste electrode produce a voltage signal, which increases as the temperature rises (**Figure 27e**). In recent years, there has been significant progress in flexible temperature-sensing fabrics. However, the accuracy and stability of these sensors still need to be improved, especially for monitoring human body temperature during physical activity.

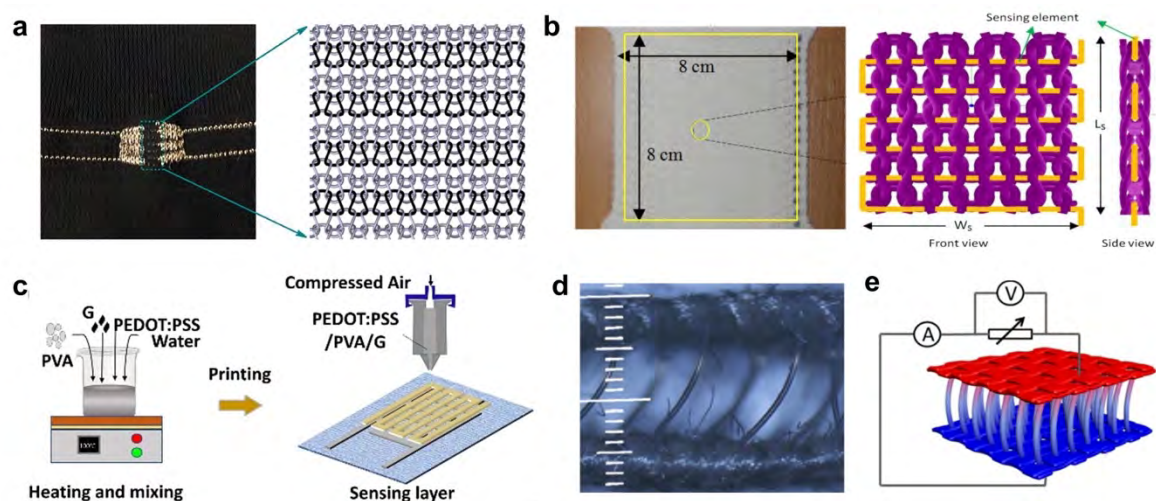


**Figure 27.** (a) A knitted temperature sensor with graphene-coated yarn. Reproduced with permission from ref <sup>381</sup>. Copyright 2019 American Chemistry Society. (b) Temperature sensing fabric where sensing wire inlaid in a double layer knitted structure. Reproduced with permission from ref <sup>382</sup>. Copyright 2013 MDPI. (c) Preparation process of PEDOT:PSS and PVA based temperature sensor. Reproduced with permission from ref <sup>383</sup>. Copyright 2023 Elsevier. (d) Images of 3D thermoelectric spacer fabric. (e) Physical model of the thermoelectric fabric. Reproduced with permission from ref <sup>385</sup>. Copyright 2020 American Chemistry Society.

### 3.1.1.4 Photodetectors

Human eye can only perceive light in the visible spectrum, which has wavelengths ( $\lambda$ ) in the range of approximately 380 to 780 nm. Wavelengths outside of this range, including UV light with  $\lambda=200\sim400$  nm and infrared (IR) light with  $\lambda>780$  nm, are invisible to the naked eye but are ubiquitous in our environment.<sup>386</sup> As a result, photodetectors play a crucial role in detecting and analyzing light beyond the visible spectrum, which is essential for various applications in daily life.<sup>387</sup> For example, excess UV exposure is a leading cause of skin cancers, thus a wearable UV sensor could alert us to the potential hazards of UV exposure in daily life. Conventional UV photodetectors are fabricated in planar metal-semiconductor-metal (MSM) configurations, using inorganic semiconductors such as ZnO, InGaAs, and GaN as active sensing materials.<sup>388, 389</sup> To fabricate textile-based flexible photodetectors, PCTs can indeed be used as the conductive electrodes,<sup>390</sup> whereas coating the bulky and rigid semiconductors on textiles is challenging. A commonly used strategy is the formation of inorganic nanostructures *in situ* on fibers/textiles *via* chemical synthesis such as hydrothermal growth.<sup>391</sup> For example, ZnO nanorod arrays (NRAs) can be grown uniformly on the surface of a Ni wire textile through



hydrothermal reaction.<sup>392</sup> The Ni textile coated with ZnO NRAs were further deposited with a layer of Ag nanowires (NWs) and graphene film, serving as another electrode (**Figure 28**). The sandwich-structured UV sensor exhibited a high photoresponsivity of  $0.27 \text{ A W}^{-1}$  under the bias of 1 V for the UV light with a wavelength of 365 nm, and the light-to-dark current ratio reached 100. Additionally, the textile UV sensor could endure severe bending conditions, the photocurrent even maintained 94% of the maximum value after bending 1000 times. Nonetheless, the modulus mismatch between the rigid ZnO NRAs and the flexible textile substrate can cause the ZnO NRAs to break or detach during long-term deformations, which will deteriorate the sensing performance of the device. To address this issue, a common approach is to enhance the interface between the ZnO NRAs and the flexible substrate by protecting it with a soft polymer cover.<sup>393</sup>

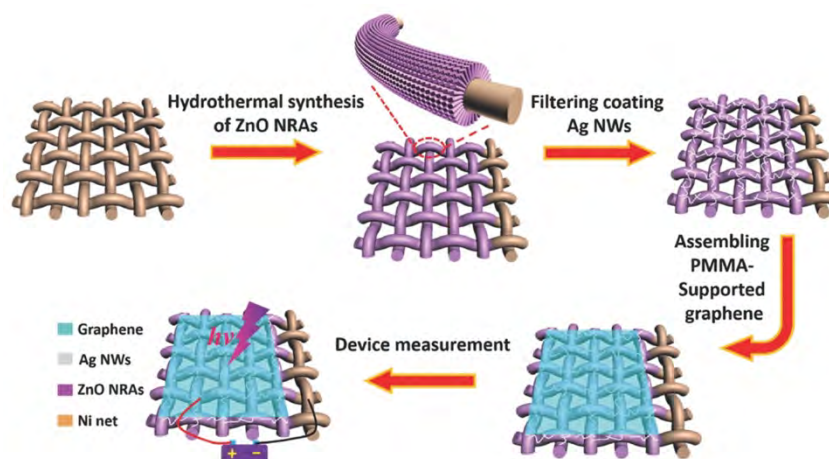


**Figure 28.** Schematic diagram of the device fabrication, illustrating the fabrication procedure of Ni/ZnO nanorod arrays/Ag NWs/graphene wearable photodetector textile. Reproduced with permission from ref <sup>392</sup>. Copyright 2017 John Wiley and Sons.

To fabricate textile photodetectors, an alternative approach is to make free-standing inorganic semiconductor fibrous mats using techniques such as electrospinning.<sup>394, 395</sup> The nanofibrous mats have a high aspect ratio, providing them a substantial surface area for light absorption. In addition, nanofibers with diameters in nanometer range generally possess excellent flexibility. Consequently, the resulting mechanically flexible/resilient nanofibrous mats can be used for assembling flexible photodetectors either as a self-supporting structure or conformally attached to various textile substrates. Polymer solutions containing inorganic semiconducting materials or their corresponding precursors can be used for electrospinning to fabricate free-standing inorganic semiconducting fiber mats directly or after additional post-processing such as

annealing. Inorganic semiconductor nanofibers like ZnO, TiO<sub>2</sub>, InZnO, and perovskite have been prepared by electrospinning for UV sensor applications.<sup>395-397</sup> For example, He *et al.*<sup>397</sup> synthesized InZnO nanowire by combining electrospinning and solution-processed combustion synthesis (CS) techniques, which involves annealing electrospun InZnO precursor nanofibers at a temperature of 375 °C. The resulting InZnO nanowire photodetector demonstrated remarkable photoelectric performance under the irradiation of 310 nm UV light, including a light-to-dark current ratio of  $1.2 \times 10^4$ , a photo responsivity of  $2.8 \times 10^3$  A W<sup>-1</sup>, and a high detectivity of  $2.4 \times 10^{16}$  Jones.

### 3.1.2 Chemical and Biological Sensors

#### 3.1.2.1 Gas Sensors

Human breath and skin respiration can release a large number of gaseous molecules involving inorganic gases (*e.g.*, H<sub>2</sub>O, CO<sub>2</sub>, CO, NO, NO<sub>2</sub>) and volatile organic compounds (VOCs) (*e.g.*, ketones, alcohols, hydrocarbons), which are byproducts of body metabolism.<sup>398, 399</sup> Wearable gas sensors are capable of detecting these gaseous substances in the vicinity of human body, making them an attractive means to analyze the biomolecules for point-of-care diagnosis.<sup>400</sup> Gas sensors usually work by absorbing gas molecules onto the electrode, where they interact or react with specific active sites on the electrode.<sup>401</sup> The interaction causes change in electrical properties such as resistance or capacitance. In general, the magnitude of the electrical signal change is proportional to the concentration of the gas of interest. Therefore, the sensing performance (*e.g.*, detection limit, response time) of a gas sensor is determined by the gas absorption/diffusion capability and reactivity of the sensing materials.<sup>402</sup> Consequently, active material for gas sensors typically requires a high specific surface area and/or an abundance of functional groups (*e.g.*, -OH, -COOH) which have good affinity to gaseous molecules.<sup>400</sup> Low-dimensional nanomaterials such as CNTs, rGO, MXene, metal oxides, and metal-organic frameworks (MOFs) are commonly used active components for gas sensors.<sup>403-405</sup>

PCTs with inherent flexibility and porosity are thus conducive to be used as the substrates for incorporating active materials for making wearable gas sensors. Gas sensors can be readily prepared through modification of ready-made fibers, yarns, and fabrics,<sup>406, 407</sup> and the resulting fiber-shaped sensors can be further woven or knitted into daily clothing at any location of interest on the human body.<sup>408</sup> For example, a fibrous NO<sub>2</sub> sensor was fabricated by coating GO (followed by reduction) and ZnO powders sequentially on a commercial cotton thread (CT) or elastic thread (ET) (**Figure 29a**).<sup>409</sup> The fibrous NO<sub>2</sub> sensor is capable of detecting NO<sub>2</sub> gas

with the concentration ranging from 0.2 to 15 ppm. Due to the good flexibility of the fibers and the intimate coating of rGO and ZnO, the fibrous NO<sub>2</sub> sensors can withstand cyclic washing and mechanical deformations including bending, twisting, and stretching. Moreover, this fibrous NO<sub>2</sub> sensor showed good scalability and wearability. For example, two broken fibrous sensors can be healed/connected through direct knotting (**Figure 29b**), and multiple sensor arrays can be easily prepared by weaving on a cloth (**Figure 29c-f**). The sensitivity of gas sensors based on conventional fibers/textiles is usually restricted by their large fiber diameter and smooth surface. Thus, constructing highly porous and heterogeneous structures is usually adopted to improve the sensitivity.<sup>410</sup> However, the mechanical properties of fibers/textiles may sacrifice during the activation process. Alternatively, decreasing fiber diameter is an effective way to increase the specific surface area. Hence, electrospun nanofibers with ultrafine diameters become a promising substrate to fabricate gas sensors.<sup>411</sup> For example, a PAN/PANI/rGO composite nanofiber, prepared by coating PAN nanofibers with rGO and PANI, showed high sensitivity (0-50 ppm) and fast response (70 s, 90% response) towards NH<sub>3</sub> gas.<sup>412</sup> By integrating this NH<sub>3</sub> sensor on a mask, it is capable of distinguishing healthy people and patients with chronic kidney disease (CKD).

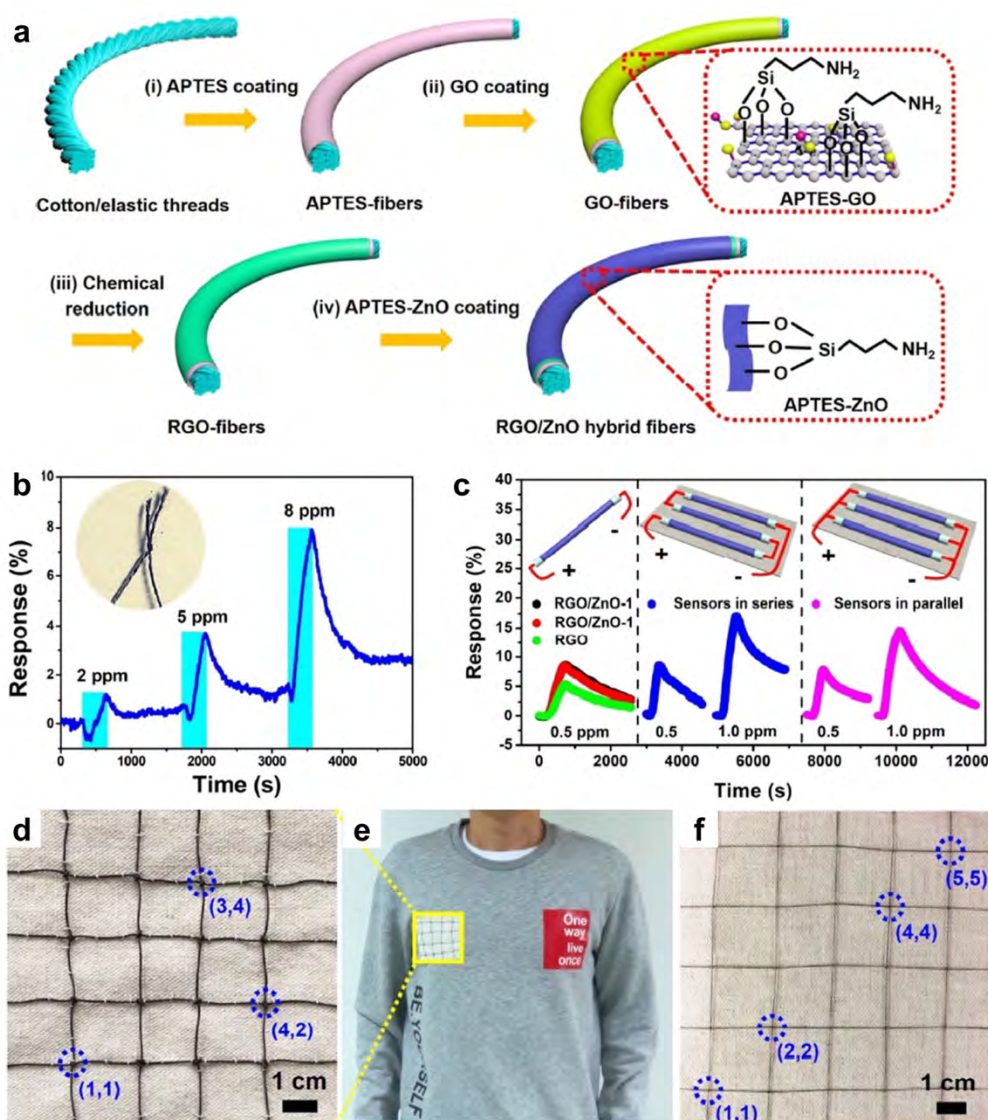


**Figure 29.** (a) Schematic diagram of the fabrication process for rGO/ZnO hybrid fibers, (b) gas-sensing properties of an integrated sensor by knotting the fractured CT sensors together. Inset shows the photograph of the knotted CT sensor. (c) Gas-sensing properties of CT sensors and the serial/parallel sensor incorporations. Insets are circuit schematics of the single sensor and serial/parallel sensors attached onto cotton cloth. Photographs of the weaved (d)  $4 \times 4$  ET sensor array networks, (e) sensor fabric stitched onto the dressings, and (e)  $5 \times 5$  CT sensor array networks. Reproduced with permission from ref <sup>409</sup>. Copyright 2019 American Chemical Society.

In addition to monitoring gas molecules emitted by human body, detection of environmental gases such as explosive and toxic gases (*e.g.*,  $H_2$ ,  $H_2S$ ,  $SO_2$ ) is also important, which can help people to prevent potential hazards. To detect  $H_2$ , noble metals such as Pt are usually employed

as the active material, where the absorbed H<sub>2</sub> can react with the metal to form metal hydrides, leading to resistance change.<sup>413</sup> Nair *et al.*<sup>414</sup> prepared a flexible H<sub>2</sub> sensor based on electrospun carbon nanofibers (CNFs) decorating with bimetallic Pt-Ni nanoparticles (average diameter of 2.8 nm). The sensor achieved the detection of hydrogen gas in a wide range (0.01-4%), and it showed negligible decrease in response during bending. The use of bimetals reduces the use of precious metals, which may lower costs. In another study, a highly flexible and sensitive SO<sub>2</sub> sensors is developed by incorporating a high-specific-surface-area material of MOFs (UiO-66-NH<sub>2</sub>) with PVDF nanofibers.<sup>415</sup> The SO<sub>2</sub> sensors exhibited a wide detection range of 1-150 ppm, and the response value maintained at 98.42% under bending 2000 times at the SO<sub>2</sub> concentration of 10 ppm.

The combination of porous textiles and novel functional nanomaterials paves the way for the development of wearable gas sensors, offering us the opportunity in real-time healthcare monitoring through noninvasive analysis of gas indicators. Although a variety of PCT-based gas sensors have been reported, their practical application deserves further optimization and improvement, because the performance of gas sensors is susceptible to environmental and body interferences such as variations of humidity and temperature, and mechanical deformations. Moreover, the sensitivity and selectivity of textile-based gas sensors towards wearable application need further improvement, since the gases emitted from human body are usually low in concentration and complex in component. Assembling sensor arrays on textiles and employing machine learning-based analysis would be a promising direction for developing wearable gas sensors for simultaneous detection of multiple gaseous substances.<sup>416, 417</sup>

### 3.1.2.2 Sweat Sensors

Currently, blood is regarded as the gold standard for clinic test of disease-related biomarkers. However, the extraction of blood is invasive, time-consuming, and may cause bacterial or virus infections. Alternatively, other biofluids (*e.g.*, sweat, interstitial fluid, tear, saliva) also contain a wealth of biomolecules including electrolyte ions (*e.g.*, Na<sup>+</sup>, Cl<sup>-</sup>, K<sup>+</sup>), metabolites (*e.g.*, glucose, lactate, urea), minerals (*e.g.*, Ca<sup>2+</sup>, Mg<sup>2+</sup>, Fe<sup>2+</sup>), nutrients, hormones, amino acid, and proteins, *etc.*<sup>332</sup> Wearable sweat biosensors emerge as a new platform for monitoring these biomolecules through a non-invasive, real-time, and continuous manner.<sup>380, 418-420</sup> Textiles are ideal substrate for fabrication of wearable biosensors due to their high flexibility and porosity, which are favorable for immobilizing active materials of biosensors such as bioreceptors (*e.g.*, enzyme, antibody).<sup>421, 422</sup> Moreover, textiles are conducive for absorption of sweat due to their

high surface capillary effect.<sup>423</sup> Currently, electrochemical principles are usually adopted for making biosensors, due to their high sensitivity and continuous monitoring ability comparing to others such as colorimetric ones. Specifically, electrochemical biosensors detect the target molecules by measuring the changes in electrical signals (*e.g.*, current, potential, impedance) caused by the inaction/reaction occurring on the electrode-analyte interface. Basically, there are four types of electrochemical biosensors including potentiometric, amperometric, impedimetric, and transistor-based.

**Potentiometric Sensors.** Potentiometric sensors are commonly used for the detection of electrolytic ions like  $H^+$ ,  $Na^+$ ,  $Cl^-$ , and  $K^+$ , and they are assembled with a working electrode and a reference electrode.<sup>424</sup> The working principle of potentiometric sensors is based on the measure of open circuit potential (OCP) between the two electrodes. The OCP is theoretically determined by the concentration difference between the two electrode surfaces, and it follows the Nernst equation, *i.e.*, the OCP is proportional to the analyte concentration. In practice, the performance of potentiometric sensors can be influenced by various factors such as electrode morphology, temperature, and interfering ions.<sup>425, 426</sup> A stable reference electrode and a highly selective working electrode are required for potentiometric sensors. The role of the reference electrode is to maintain a stable potential across different analytes, and Ag/AgCl reference electrodes are commonly employed. A flexible Ag/AgCl reference electrode can be fabricated on a textile by coating or printing Ag/AgCl ink on PCTs with predesigned patterns, or by coating a layer of Ag followed by chlorination, resulting in the formation of a thin layer of AgCl on the surface of Ag.<sup>427, 428</sup> The working electrode of potentiometric sensors is typically an ion-selective electrode (ISE), which is prepared by coating an ion-selective membrane (ISM) on the electrode.<sup>429</sup> The ISM selectively permits specific ions to pass through, thereby rendering the selectivity of potentiometric sensors.

Sweat pH is an important physiological parameter indicative of skin conditions, which is useful in dermatology, sport science, and healthcare monitoring.<sup>430, 431</sup> Conducting polymers such as PANI and PPy are commonly used transducers for making flexible potentiometric pH sensors due to their reversible doping/de-doping by  $H^+$  ions.<sup>432</sup> For example, Guinovart *et al.*<sup>433</sup> developed a wearable pH sensor by screen printing a carbon conductive layer on an adhesive bandage, followed by electropolymerizing PANI as the sensing electrode. The pH sensor exhibited a near Nernstian response ( $-58\text{ mV/pH}$ ) in the pH range of 4.35 to 8 with a response time of less than 20 s. This bandage pH sensor can be used to monitor wound pH.



In addition, electrolyte ions such as  $\text{Na}^+$ ,  $\text{Cl}^-$ ,  $\text{K}^+$ , and  $\text{Ca}^{2+}$  are essential in many physiological processes.<sup>434</sup> For instance,  $\text{Na}^+$  ions play a crucial role in maintaining electrolyte balance and preventing dehydration.<sup>435</sup> As such, monitoring the concentration of electrolytes in sweat may provide useful diagnostic and exercise-related information. For example, high concentration of  $\text{Cl}^-$  ions in sweat is a characteristic feature of cystic fibrosis (CF), a genetic disorder that affects the lungs, pancreas, and other organs. Moreover, excessive sweating during exercise can lead to dehydration and electrolyte imbalances, thus the monitoring of sweat electrolyte content would be useful for athletes training and daily exercise. ISE-based potentiometric sensors are effective for detection of the electrolyte ions in sweat.<sup>436,437</sup> For example, multiple fiber-shaped ion sensors including  $\text{Na}^+$ ,  $\text{K}^+$ ,  $\text{Ca}^{2+}$ , and pH are prepared by coating different active materials on a conductive CNT fiber.<sup>438</sup> To achieve a selective detection of ions, specific ion-selective ionophores are coated on the fibers. Meanwhile, the pH sensor is achieved by electrodeposition of PANI as the ion-to-electron transducer. These fibrous sensors were integrated into a fabric through weaving (**Figure 30**), and the resulting sensor array can perform real-time sensing of multiple electrolytes in sweat. Moreover, the sensors maintained their stability under repeated deformations, such as bending and twisting.

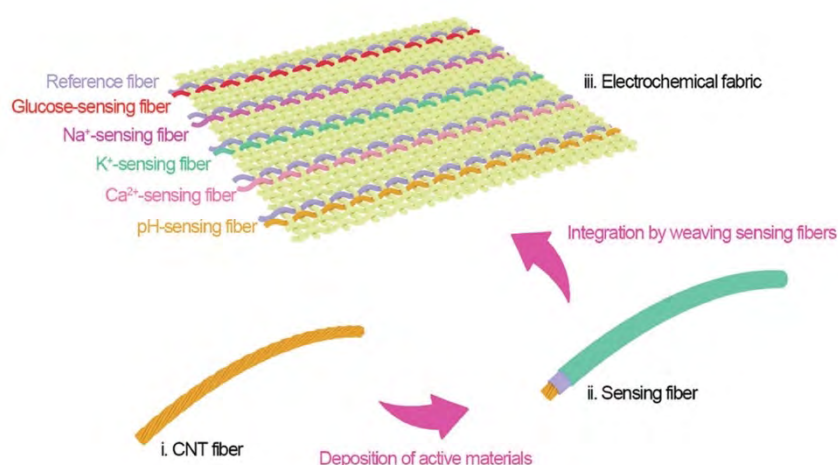


**Figure 30.** Schematic illustration for the fabrication of an electrochemical fabric sensor array by weaving multiple sensing fibers. Reproduced with permission from ref <sup>438</sup>. Copyright 2018 John Wiley and Sons.

**Amperometric Sensors.** In contrast to potentiometric sensors, amperometric sensors operate rely on the occurrence of a redox reaction on the electrode interface, and it measures the current

produced by the electrochemical reaction instead of the potential difference. Typically, an amperometric sensor comprises three electrodes: the working, counter, and reference electrode, and the analyte of interest is oxidized or reduced at the working electrode. The amperometric sensors directly associate the measured current with the concentration of the target analyte at a fixed oxidation or reduction potential. This characteristic makes the amperometric biosensors more accurate and sensitive for quantitative analysis. Biomolecules such as glucose, lactate, cholesterol, and uric acid are usually detected by amperometric sensors, due to their ability to undergo electrochemical oxidation.<sup>439</sup> Consequently, to selectively recognize the biomolecules, specific bioreceptors (*e.g.*, enzyme) that can target to the analyte of interest are required for biosensors, and thus amperometric sensors are commonly enzymatic sensors.<sup>440</sup> As such, the PCTs are advantageous for using as the electrode for enzymatic biosensors attributing to their high porous surface that can provide abundant loading sites for immobilizing the enzymes, which can potentially enhance the sensitivity and selectivity of biosensors.<sup>421</sup>

Fiber-shaped electrodes are commonly fabricated for textile amperometric biosensors, as they can be readily integrated into a textile to form the three-electrode configuration.<sup>441-443</sup> For example, Zhao *et al.*<sup>444</sup> developed a flexible glucose sensor by using elastic Au fibers as the substrate to fabricate electrodes. The Au fibers were fabricated by spinning of AuNPs/SEBS solution followed by electroless plating of Au film. The unmodified Au fiber was used as the counter electrode. The reference electrode was made by depositing a layer of Ag/AgCl on the elastic Au fiber, while the working electrode was fabricated by sequential functionalization of Prussian blue (PB), glucose oxidase (GOx), and chitosan solution (**Figure 31a**). These three electrodes were wound helically around an elastic fiber core and integrated into a fabric in parallel to form the textile glucose biosensor (**Figure 31b**). The as-fabricated textile glucose biosensor achieved a linear sensing range of 0-500  $\mu\text{M}$  and a sensitivity of  $11.7 \mu\text{A mM}^{-1} \text{cm}^{-2}$ . Remarkably, the sensing performance could be maintained even under a large strain of 200%. Textile-based biosensors can also be fabricated by directly patterning different electrodes onto a textile.<sup>445, 446</sup> In a typical process, conductive paths are first patterned on a non-conductive textile to serve the electrode, and then different active materials are functionalized on each electrode to form the counter, reference, and working electrodes. However, patterning the electrodes with high resolution is challenging due to the high porosity of textiles. One alternative method is to create conductive circuits on a conventional plastic thin film, while attaching textile-based active sensing layers onto the electrodes. By adopting such an approach, He *et al.*<sup>447</sup> prepared different electrodes by functionalizing a carbonized silk textile (denoted

as SilkNCT) with various biomarkers such as glucose, lactate, ascorbic acid, uric acid,  $\text{Na}^+$ , and  $\text{K}^+$ . The resulting SilkNCT patches were then clipped and transferred onto a conductive path that was previously fabricated on a flexible PET (**Figure 31c-g**). This enabled the creation of a multiplex sweat sensing patch, which could simultaneously detect multiple analytes in sweat. However, the use of solid film impedes the permeability of sensors; thus, directly developing multiple sensor arrays on textile with high resolution and pixel density is highly desired.

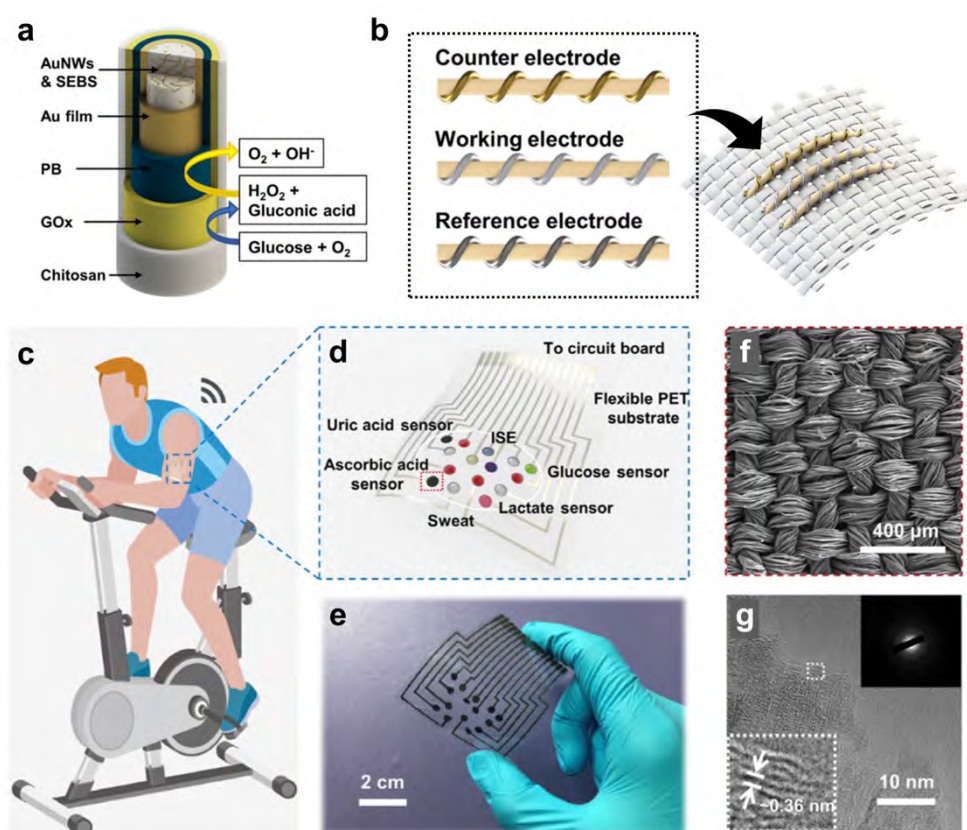


**Figure 31.** (a-b) Schematic illustrations of fabrication of a textile-based glucose biosensor (fabrication of working electrode (a), integration of the three electrodes into an elastic fabric (b)). Reproduced with permission from ref <sup>444</sup>. Copyright 2019 American Chemical Society. (c-d) Schematic illustration of wearable sweat analysis patch mounted on human skin (c) and the multiplex electrochemical sensor array integrated in the patch (d), (e) photograph of the wearable sweat sensing patch, SEM (f) and transmission electron microscope (TEM) (g) images of the carbonized silk fabric (SilkNCT). Reproduced with permission from ref <sup>447</sup>. Copyright 2019 The American Association for the Advancement of Science.

**Impedimetric Sensors.** Impedimetric sensors measure the changes in charge conductance and

capacitance at the electrode surface when it comes into contact with an analyte of interest.<sup>448</sup> Selective binding of the analyte to the electrode alters the surface charge density, which results in changes in impedance. The impedance change is typically measured using electrochemical impedance spectroscopy (EIS). PCTs with high surface are a good platform for immobilizing recognizers. For example, an impedimetric platform was developed using electrospun PA6/PPy conductive nanofibers decorating with ZnO nanoparticles for urea sensing.<sup>449</sup> Urease was immobilized on the surface of the composite nanofibers. This impedimetric biosensor exhibited high sensitivity, stability and selectivity towards urea. Despite the notable advantages such as high sensitivity, label-free characteristic, and low operating voltage, impedimetric biosensors have not been extensively studied.

**Transistor-based Sensors.** Recently, flexible field-effect transistors (FETs) have gained considerable attention for making wearable sensors due to their distinctive characteristics.<sup>450</sup> One advantage of FETs is their intrinsic amplification nature, which allows for high sensitive detection. Additionally, microfabrication techniques can be used to create micro-arrays of FET sensors on flexible substrates,<sup>451</sup> enabling the creation of flexible, lightweight, and comfortable wearable sensors that can be integrated into clothing or attached onto skin. There are generally two types of FETs-based biosensors: organic field-effective transistor (OFET) and OECT.<sup>452-454</sup> These two transistor-based biosensors have a similar configuration, which comprises three electrodes (*i.e.*, source, drain, and gate electrode), a semiconducting channel layer, and a gate dielectric layer. The difference between OFET and OECT is the dielectric layer, the former one usually uses a dielectric material such as metal oxide or polymer, while the later one adopts a liquid electrolyte. The operating principle of the transistors is that the conductance of the channel material (*i.e.*, the current between source and drain electrodes) can be modulated by the gate voltage.<sup>455, 456</sup> Compared to conventional thin film-based transistors, fiber-based transistors have emerged as an attractive option for biosensor development.<sup>457</sup> The integration of functional fibrous electrodes enables easy assembly without the need for complex microfabrication processes.<sup>458</sup> Additionally, the porous nature of fibers facilitates analyte penetration, thereby enhancing sensitivity and facilitating response time. For example, Qing *et al.*<sup>459</sup> developed a fiber-based OECT biosensor for highly sensitive monitoring of dopamine (DA). They first prepared a flexible conductive fiber (PPy/nanofibers/PA6) by coating PVA-co-PE and polymerizing PPy on a PA6 filament. Then, the conductive fibers were woven into a fabric with a cross-junction configuration, forming the fiber-based device (referred to as FEECTs). The fibers at the cross junction are separated by a certain volume of transparent gel

electrolyte (**Figure 32**). The FECTs demonstrated an on/off ratio of up to two orders of magnitude, and a rapid temporal recovery time between on and off states, as low as 0.34 s. Additionally, the sensor presented long-term sensitivity with a detection region from 1 nM to 1  $\mu$ M of DA.

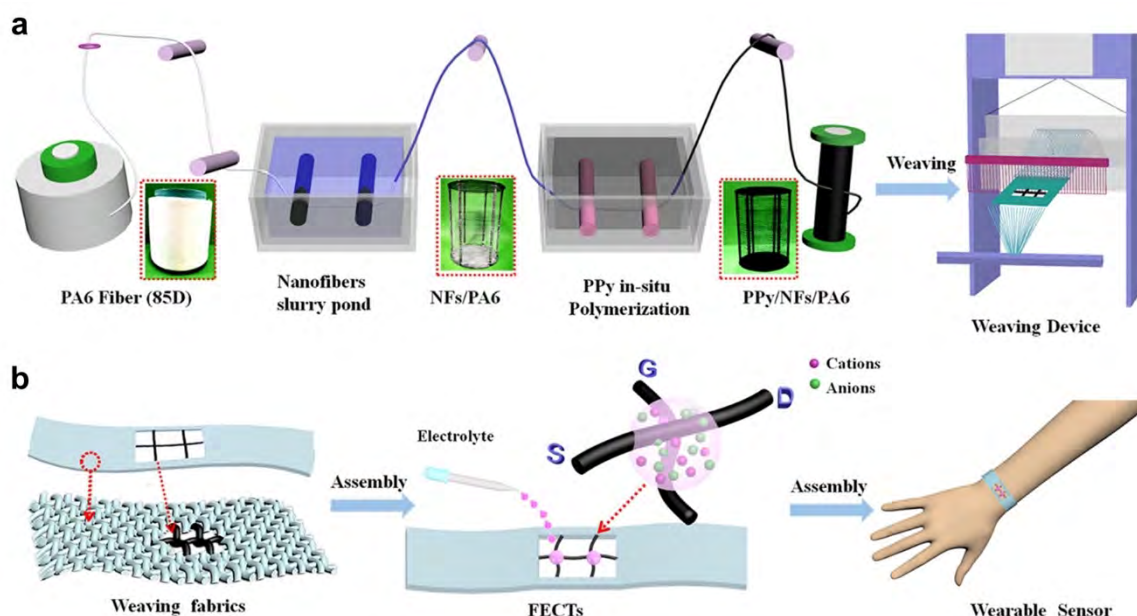


**Figure 32.** Schematic diagram of wearable DA sensors based on FECTs: (a) preparation process and weaving of coated fibers, (b) assembly of the woven FECTs and wearable DA sensors. Reproduced with permission from ref <sup>459</sup>. Copyright 2019 American Chemical Society.

To sum up, PCT-based biosensors are promising for wearable applications. While significant progress has been made in monitoring various biomarkers for point-of-care diagnosis, practical applications are still in the early stages. The sensitivity, selectivity, stability, and reproducibility of biosensors need further improvement, especially the stability, as the biomolecule-based recognizers (*i.e.*, enzymes and antibodies) are challenging to be immobilized on the electrodes and store for a long time. Further research opportunities exist in the development of artificial catalysts and recognizers, such as nanostructured catalysts and molecular imprint polymers (MIPs).<sup>460</sup> Additionally, continuous collection of sweat on human skin for sensing poses a critical issue,<sup>461</sup> as the production of sweat is intermittent and low under normal conditions without exercise. Furthermore, continuous monitoring requires a dynamic extraction of sweat, which is difficult due to sweat accumulation in the textile, leading to fouling of the continuous test. One possible solution to this challenge is to develop textiles with the ability to transport sweat directionally and dynamically.<sup>462</sup> Textiles with Janus



wettability and microfluidics-based textiles are promising options in this direction.<sup>463, 464</sup> For example, He *et al.*<sup>465</sup> developed a textile with Janus wettability that can unidirectionally and thoroughly transport sweat from skin to embedded electrode surface (**Figure 33**). Such a Janus textile is fabricated by electrospinning a hydrophobic PU nanofiber array onto a hydrophilic gauze.

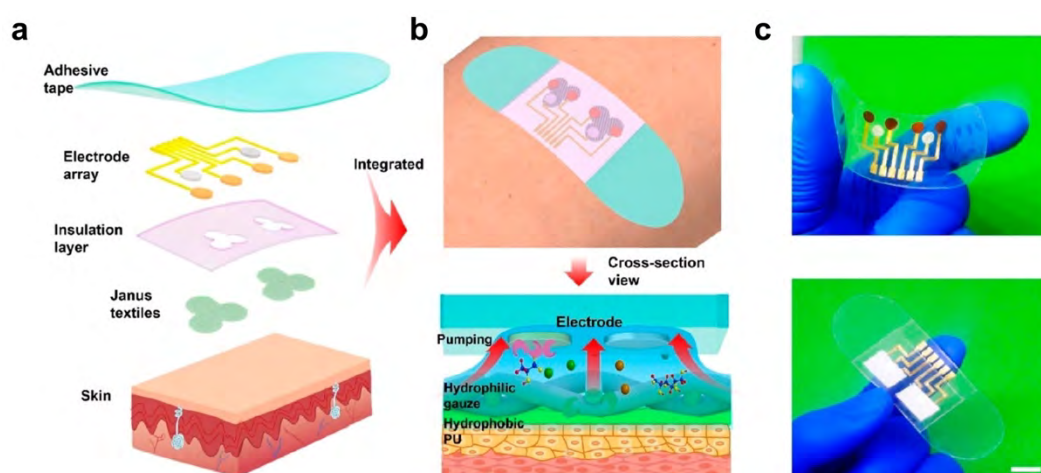


**Figure 33.** Design of an integrated smart band for self-pumping sweat sampling and electrochemical sensing. (a) 3D exploded view illustrating subsystems of the flexible hybrid sensor, (b) schematic of the band worn on a subject's arm and corresponding cross-section view of self-pumping and electrochemical detection process of sweat on the Janus textiles filled assay site. (c) actual photograph of the electrochemical band before (top) and after (bottom) Janus textile functionalization. Scale bar: 1 cm. Reproduced with permission from ref <sup>465</sup>. Copyright 2020 American Chemical Society.

### 3.1.3 Electrophysiological Sensors

Electrophysiological signals arise from the electrical activity of biological cells or tissues, such as neurons and muscles, and manifest as bioelectric potentials. These signals can be captured through a variety of techniques, such as ECG, EMG, EEG, and EOG, which correspond to the electrical activity of heart, muscles, brain, and eyes, respectively.<sup>466</sup> Monitoring these signals is crucial for diagnosis of humane health. For example, ECG are commonly utilized in clinical settings to diagnose cardiovascular pathologies and diseases. Skin-interfaced electrodes are essential components of electrophysiology sensors for acquiring signals from the skin surface.<sup>467</sup> The conventional ECG systems designed for clinical use adopt disposable gel-adhesive electrodes to establish a wet interface with the skin for signal acquisition.<sup>468</sup> These

gel electrodes consist of an Ag/AgCl ion-electron transducer and an ionic gel in contact with the skin, and they typically require adhesive tapes to secure them to the skin and hard-wired connections to external data acquisition instruments. However, the gel electrodes are incapable of long-term applications due to their susceptibility to dehydration, and their non-permeable nature may lead to skin irritation when attached to the skin for long durations. As a result, recent research efforts have been devoted to developing new types of electrodes, such as ultrathin skin-like electronic tattoos and dry electrodes.<sup>469</sup> PCT-based dry electrodes thus have gained attention due to their easy-manufacturing, flexibility, and breathability.<sup>470-472</sup>

A variety of conductive textiles have been created by incorporating conductive materials into traditional textiles through methods like electroless deposition, dip coating, screen printing, and electrospinning.<sup>223, 241, 473-476</sup> Electrophysiological signals, such as ECG, EMG, EEG, and EOG, can be collected by attaching the PCT-based electrodes to various sites on the human body (**Figure 34**).<sup>60, 477-479</sup> Skin-contact impedance is a key parameter for evaluating electrodes, as low contact impedance and low variations can contribute to stable and high-quality recordings of electrophysiological signals. However, despite the intrinsic conductivity of PCTs, their contact impedance is much higher than that of gel counterparts.<sup>480</sup> This is because both textiles and human skin are highly porous and rough, which creates numerous gaps between their contacts. Furthermore, due to the absence of adhesives, the contacts between textile electrodes and the skin are prone to movement, resulting in unstable contact impedance. The high contact impedance and variability can easily lead to motion artifacts. Consequently, existing PCT-based electrodes are usually designed with a tight fit or secured with an elastic band to maintain consistent skin contact,<sup>481, 482</sup> which may be uncomfortable for long-term use, despite the textiles' flexibility and breathability. To tackle this problem, developing ultra-soft textiles made of materials such as ionogel fibers and incorporating biocompatible adhesives could potentially improve signal quality and comfortability.<sup>483-485</sup> Nonetheless, PCT-based dry electrodes offer a significant advantage in terms of long-term stability, making them promising for continuous and long-term monitoring applications.



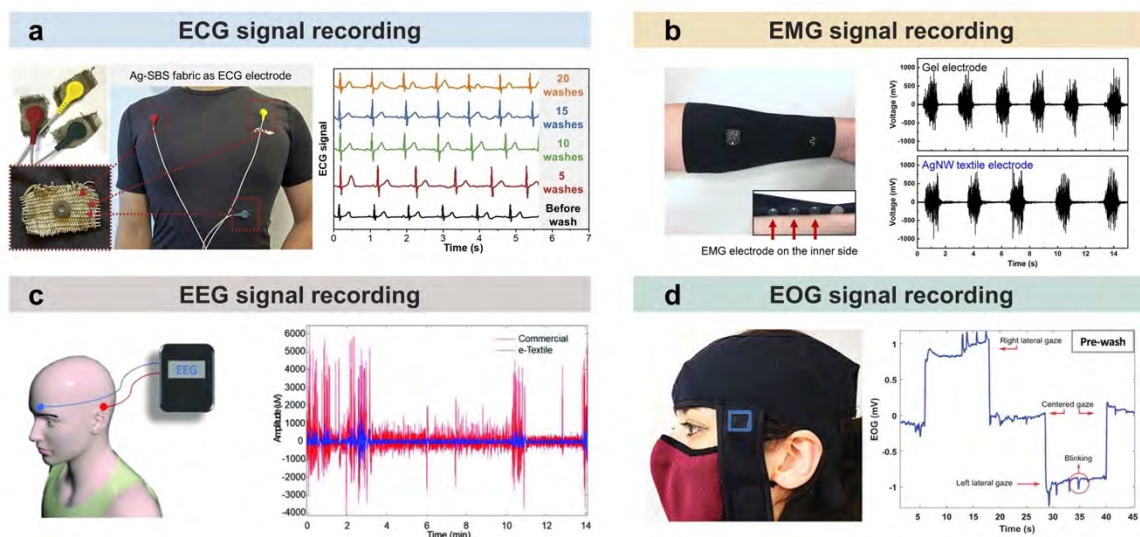


**Figure 34.** Applications of PCT-based electrodes for electrophysiological signal recording including (a) ECG, (b) EMG, (c) EEG, and (d) EOG. (a) Reproduced with permission from ref <sup>60</sup>. Copyright 2023 Cell Press. (b) Reproduced with permission from ref <sup>477</sup>. Copyright 2019 American Chemical Society. (c) Reproduced with permission from ref <sup>478</sup>. Copyright 2018 John Wiley and Sons. (d) Reproduced with permission from ref <sup>479</sup>. Copyright 2022 John Wiley and Sons.

### 3.2 Actuators

Actuating devices have garnered widespread attention with the development of flexible electronic devices.<sup>486, 487</sup> They can convert external stimuli like electricity, temperature, and moisture into physical changes in shape and size, which are valuable for various applications such as physical therapy, artificial muscle, and human-machine interaction.<sup>488</sup> PCTs are an ideal platform for manufacturing actuating devices due to their good flexibility, permeability, and conductivity.<sup>489</sup> With the help of conductive fibers, actuators can overcome their drawbacks of being hard, bulky, and noisy, and become soft and lightweight. Actuating textiles come in many different structural designs, with PCTs playing different roles based on the operating principles. In this section, we will classify actuating textiles into three categories: electrical actuation, thermal actuation, and solvent actuation, based on external stimuli. We will also discuss their working mechanisms and the roles of PCTs in each.

#### 3.2.1 Electrical Actuation

According to the reaction occurred during the working, electrical actuation can be classified into two types: electromechanical and electrochemical actuation. An electromechanical

actuator consists of an actuating material and a pair of electrodes. The actuating material is typically a dielectric elastomer or piezoelectric material, which can be combined with PCTs to obtain an electromechanical actuating fiber/textile. The dielectric actuating fiber works based on the Maxwell stress under a high bias voltage, and its basic structure consists of a sandwich structure with the dielectric elastomer enclosed by a pair of electrodes (**Figure 35a**).<sup>490</sup> This structure can be manufactured via various methods, such as thermal stretching, wet spinning, 3D printing, or winding. For example, Arora *et al.*<sup>490</sup> used silicone elastomer tubes as the dielectric, injected silver paste as the internal electrode, and wrapped a carbon black-doped silicone as the external electrode. The carbon black-doped silicone forms a uniform and thin electrode on the surface of the dielectric elastomer, which can maintain its conductivity under high strains, ensuring that the actuator has good stretchability. In addition, dielectric elastomer actuating fibers can also be prepared by winding. He *et al.*<sup>491</sup> manufactured anisotropic conductive poly(styrene-*b*-butyl acrylate-*b*-styrene) (SBAS) films into dielectric elastomer actuating fibers by rolling winding (**Figure 35b**). The SBAS achieved conductivity by transferring single-walled carbon nanotube (SWCNT) film to the SBAS. In contrast to these complicated methods, the 3D printing technique can be easier. Chortos *et al.*<sup>492</sup> prepared coaxial dielectric elastomer fibers by co-extruding dielectric elastomer and conductive electrodes (**Figure 35c**). The 3D printing method allows for better contact between the dielectric elastomer and fiber electrodes, resulting in significantly improved actuation performance. By controlling the ratio of the internal fiber electrode to the dielectric elastomer, the best actuation performance can be achieved. 2D conductive fabrics can also be used as the electrodes in dielectric elastomer actuators. For example, sandwiching a dielectric elastomer between two oriented carbon cloths can create a simple actuating fabric (**Figure 39d**).<sup>493</sup> Piezoelectric materials can also be applied for actuators, primarily utilizing the inverse piezoelectric effect. Piezoelectric materials such as BaTiO<sub>3</sub>, ZnO, and PVDF exhibit inverse piezoelectric effect. PVDF fiber produced via electrospinning or thermal stretching is suited for conductive fabrics. However, the combination of PVDF fiber and conductive fabric is mostly applied for sensing and energy harvesting applications, with limited exploration in the field of actuators. Nonetheless, electroactive fibers made either from dielectric elastomers or piezoelectric materials require very high operating voltages, typically around a kilovolt, posing a certain risk for wearables.

Electrochemical actuator is another type of electrical stimulus actuator, which operates at lower voltages, typically below 10 V. Its working mechanism is based on reversible ion migration at

the electrode/electrolyte interface and/or within the electrodes via electrochemical process such as formation of EDL, ion intercalation/deintercalation, and Faradic reaction. The device structure of electrochemical actuators is different from that of electromechanical actuators, since their working process requires an electrolyte to facilitate the migration of ions. Carbon-based PCTs, such as CNT fibers, graphene fibers, and PPy fibers, are the most commonly used electrode materials. For example, Mirfakhrai *et al.*<sup>494</sup> studied the electrochemical driving performance of twisted MWCNT yarns. The MWCNT yarn was prepared by dry spinning, which involved stretching and twisting CNTs from a CNT forest. When a voltage is applied, the CNT electrode attracts ions with opposite charges, causing a change in the C-C bond length and achieving actuation. The excess charges on the CNTs are compensated by ions (cations or anions) at the CNTs-electrolyte interface, and the CNTs act as double-layer capacitors, achieving charging and discharging during the driving cycles. Replacing the liquid electrolyte with a solid electrolyte can improve the convenience of the electrochemical actuator. Lu *et al.*<sup>495</sup> developed an electrochemical actuator with a unique hollow structure, where a solid PANI fiber was used as the internal electrode, a hollow PANI fiber was used as the external electrode, and the gel electrolyte was injected in the hollow fiber (**Figure 35e**). This structural design minimizes evaporation of electrolyte, extending the device's lifespan. Moreover, since the same material is used in solid and hollow fibers, the same oxidation-reduction process occurs on both electrodes. In addition to CNTs and PANI, graphene and PPy are also good choices for electrode materials in electrochemical actuators. Liu *et al.*<sup>496</sup> designed a bilayer actuator with an improved bending angle by combining graphene and PPy. The actuation mechanism of PPy involves a volume change caused by alternate oxidation/reduction processes, during which PPy gains or loses ionic species to maintain charge neutrality. The actuation mechanism of graphene is mainly achieved via a non-Faraday charging/discharging process. In summary, making electrochemical actuators all-solid-state is a crucial advancement to overcome the challenge of using them in wearable smart fibers, as it eliminates the need for an electrolyte and makes them more compatible with wearable applications.

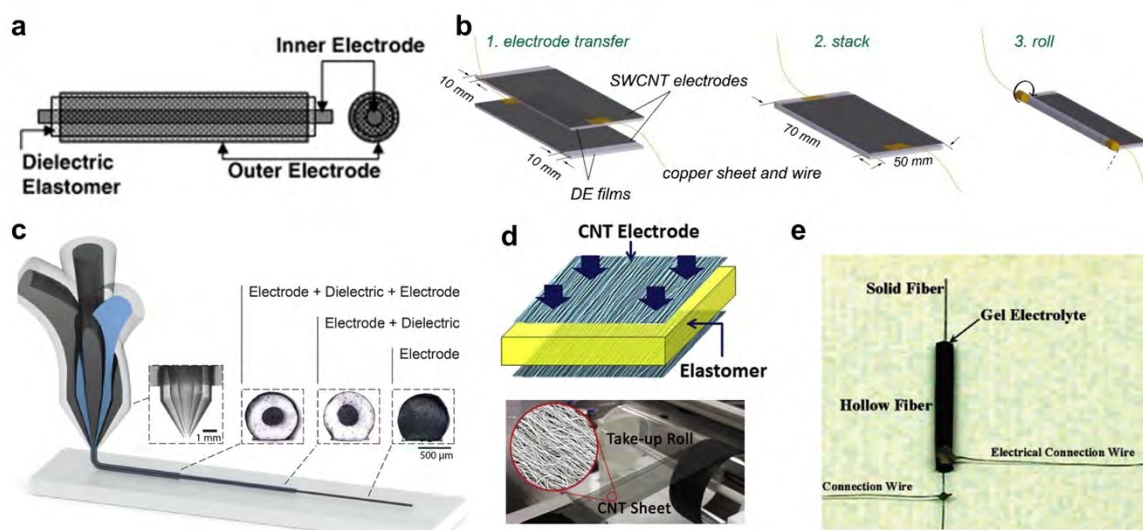


**Figure 35.** (a) Schematic diagram of dielectric elastomer actuating fiber. Reproduced with permission from ref <sup>490</sup>. Copyright 2007 Elsevier. (b) Fabrication method of a rolled dielectric elastomer actuating fiber. Reproduced with permission from ref <sup>491</sup>. Copyright 2022 American Chemical Society. (c) Schematic illustration of 3D printing core-shell dielectric elastomer actuating fiber. Reproduced with permission from ref <sup>492</sup>. Copyright 2021 John Wiley and Sons. (d) Schematic diagram of CNT sheet based dielectric elastomer actuating fiber and photograph of CNT sheet. Reproduced with permission from ref <sup>493</sup>. Copyright 2015 Elsevier. (e) Photograph of solid-in-hollow fiber linear actuator. Reproduced with permission from ref <sup>495</sup>. Copyright 2004 American Chemical Society.

### 3.2.2 Thermal Actuation

Thermally responsive actuators employ materials capable of undergoing deformation under thermal stimuli. Prominent examples of such materials include thermal expansion polymers, liquid crystal polymers, shape memory polymers, and shape memory alloys. PCTs are one of the primary raw materials can be used to prepare thermal-driven actuators, and further incorporation of guest materials can enhance their driving performance. For instance, CNT yarns not only possess high conductivity but also high thermal conductivity, enabling them to conduct more heat per unit area in a given time. The prevalent method for making thermally responsive actuators based on CNT yarns is to introduce guest materials such as elastomers or paraffin. It has been found that appropriate twisting of CNT yarns can significantly enhance their actuation performance. Lima *et al.*<sup>497</sup> designed and produced twisted CNT yarns filled with paraffin by different twisting methods and compared their effect (**Figure 36a**). **Figure 36b** illustrates CNT yarns with different twist structures. Paraffin is material with high thermal

stability and good wettability on CNT yarns, and it has a significant volume change during phase transition. When heated, the CNT yarns transfer heat to the paraffin in their nanopores, causing the expansion of paraffin. The authors found that adding paraffin can significantly improve the sensitivity of the actuation performance of CNY yarn.

In addition to actuating in the stretching direction, thermally responsive actuators can also achieve actuation in the twisting direction. Yuan *et al.*<sup>498</sup> achieve twisting actuation by designing composite yarns of coiled graphene and PVA (**Figure 36c**). Results showed that twisting force of the fibers can be increased by twisting, and adding CNTs and graphene can further improve the mechanical properties of the actuating fibers. By comparing their recovery torque, it was found that the composite conductive fibers perform better actuation performance. The combination of graphene and PVA shows the best performance. Shape memory alloy wires can be woven or knitted into various fabrics, and they have extensive applications across many industries, including medical, robotics, and textiles. In medicine, shape memory alloy wires can be used to create medical devices like stents, sutures, implants, and equipment. Owing to the shape memory effect, shape memory alloy wires can also be employed as thermal actuators. For instance, by Joule heating the gold-coated half length of a NiTi twisted wire, it is possible to achieve fully reversible torsional driving at a speed of up to 16 degrees per minute and a peak speed of 10,500 rpm.<sup>499</sup> Compared to CNT yarns, shape memory alloy wires offer superior driving performance without the need for introducing guest materials, along with simpler device structure and manufacturing processes.

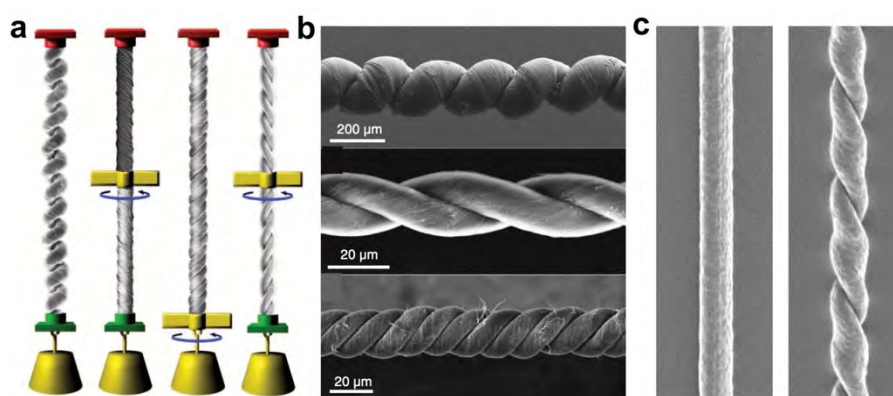


**Figure 36.** (a) Schematic diagram of comparison between different twisting methods. (b) SEM photographs of twisted CNT yarn. Reproduced with permission from ref <sup>497</sup>. Copyright 2012 American Association for the Advancement of Science. (c) SEM photographs of PVA fiber (left) and coiled PVA fiber (right). Reproduced with permission from ref <sup>498</sup>. Copyright 2019

### 3.2.3 Solvent Actuation

In general, conductive fibers composed of metals like copper and silver exhibit good hydrophilicity, whereas most carbon fibers materials exhibit hydrophobicity and tend to expand in volume upon absorbing organic solvents. The volume expansion of some carbon fiber materials can exceed 30% when absorbing solvent, and even approach 400% in some cases, largely surpassing the volume expansion of paraffin under heat absorption. Consequently, carbon-based conductive fiber shows potential in manufacturing solvent-driven actuators. In 2013, Qu *et al.*<sup>500</sup> fabricated an asymmetric graphene/oxidized graphene fiber actuator through laser reduction positioning. This actuator quickly bends towards the G-side upon exposure to humidity and returns to its initial state once return to the original environment. Twisting is effective to optimize the strength, flexibility, and other characteristics of fiber structures. By reasonably designing the rotation of graphene through twisting, Cheng *et al.*<sup>501</sup> reconstructed the configuration of graphene in the fiber and prepared a new type of humidity-driven actuator. Although twisting can improve the actuator's performance, it was insufficient to meet the practical application. Subsequently, Fang *et al.*<sup>502</sup> manufactured graphene fiber actuators with good flexibility and high mechanical strength through wet spinning and industrial twist stretching technology (**Figure 37a**). The prepared graphene actuator can operate in polar solvents, achieving a high rotation speed of 6050 rpm, a large starting torque of  $2.7 \times 10^{-7}$  N·m, and a peak power output of 89.3 W kg<sup>-1</sup> under the drive of 0.05 mL acetone. In their study, they further examined the graphene fiber actuator in a double-unit system. Results showed that the actuation effect of the double-unit system is counteracted when the spiral direction of the two fibers is opposite (**Figure 37b**), while it was enhanced when the spiral direction of the two fibers is the same (**Figure 37c**).

Carbon-based fibers, including graphene fibers, exhibit volumetric responses to solvents, especially organic solvents. Nonetheless, caution must be exercised when utilizing organic solvents due to their potential toxicity. Therefore, it is preferable to replace the organic solvent by water or moisture. Plasma treatment of CNT fibers can induce a transition from hydrophobic into hydrophilic, by introducing hydrophilic groups on the surface. He and colleagues designed layered spiral channels with hydrophilic surfaces in aligned CNT fibers, enabling rapid and large contraction and rotation.<sup>503</sup> They employed plasma treatment for the preparation of the



hydrophilic multilayered spiral CNT fibers. By oxygen plasma treatment at 100 W for 15 min, the CNT fibers become hydrophilic (**Figure 37d**). To enhance the actuation performance of CNT fibers, Chen and colleagues developed MWCNT into multilayered primary fibers using a spiral assembly strategy. These fibers were subsequently twisted together to obtain a CNT fiber actuator (**Figure 37e**).<sup>504</sup> The resulting layered spiral fiber actuator can contract and recover reversibly underwater driving. The actuator exhibited a large stress response and a short response time of less than 2 s. The volume expansion of the fiber is due to the infiltration of the gap driven by capillary force of the solvent. The layered spiral fiber contains nano- and micro-scale gap structures, which promote the penetration of solvent into the fiber.

In recent years, with continuously exploring new driving mechanisms and striving to improve the performance, remarkable progress has been made in fiber actuators. However, several issues still need to be addressed. First, it is crucial to ensure that the actuators can generate sufficient force/stress, particularly using for artificial muscles or tendons, which necessitate the production of forces equivalent to those by human muscles. Second, the reversibility and stability of actuators need to be enhanced. Moreover, despite the availability of various stimuli that can drive the actuators, their stability may be compromised when multiple stimuli occur simultaneously. Thus, it is imperative to develop a simple and minimally environmentally influenced driving mechanism.

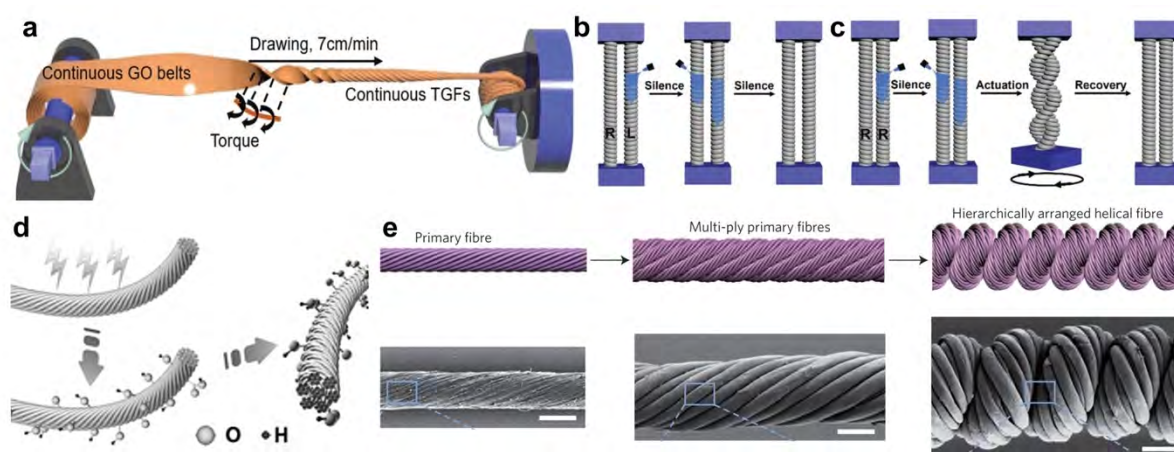


**Figure 37.** (a) Schematic illustration of a continuous drawing–twisting process of twisted graphene oxide fibers. (b) The response scheme of homochiral graphene oxide fibers suffering the wetting of acetone. (c) The response scheme of heterochiral graphene oxide fibers suffering the wetting of acetone. Reproduced with permission from ref<sup>502</sup>. Copyright 2019 Royal Society of Chemistry. (d) Schematic illustration of oxygen plasma process. Reproduced with



permission from ref <sup>503</sup>. Copyright 2015 John Wiley and Sons. (e) Fabrication method of the hierarchically arranged helical fiber. Reproduced with permission from ref <sup>504</sup>. Copyright 2015 Springer Nature.

### 3.3 Therapeutic Devices

Apart from wearable sensors that can monitor diverse physiological signals and offer instantaneous access to body conditions and disease diagnosis, textile electronics can also provide on-body therapeutics. This includes devices such as thermotherapy and transcutaneous electrical nerve stimulation (TENS) for pain relief, as well as iontophoresis devices for transcutaneous drug delivery. In this section, we will discuss several therapeutic devices that utilize PCTs for targeted therapeutics.

#### 3.3.1 Thermotherapy

Thermotherapy is a therapeutic technique that involves the use of heat to alleviate various conditions such as muscle pain, inflammation, and stiffness.<sup>505</sup> For instance, thermotherapy is effective in enhancing the local blood flow in joint osteoarthritis, which can lead to increased supply of oxygen and nutrients to the muscles, lubrication of the joints, and relief for joint stiffness and pain.<sup>506</sup> Radiofrequency ablation (RFA) and microwave thermosphere ablation (MTA) are two main heating techniques clinically used in thermotherapy,<sup>505, 507</sup> while they are bulky, inflexible, and require professional guidance, making them unsuitable for everyday patient use. With the advancement of technology, several new heating techniques such as ultrasound heating, plasmonic photothermal heating, and electric Joule heating have emerged.<sup>507</sup> Among these techniques, Joule heating is the simplest, most straightforward, and non-invasive, as it can be achieved by applying a voltage across a resistor.<sup>508</sup> In the context of textile electronics, thermotherapy can be implemented through wearable garments embedded with Joule heating elements (*i.e.*, PCTs).<sup>509</sup> Metals are excellent conductors and are broadly used for making Joule heating devices,<sup>510</sup> for example, the commercially available electric blankets are generally made of metals wires, while they are relatively rigid and heavy. Making metallic textiles by mixing or coating a thin layer of metal on fibers/textile is a promising alternative.<sup>511, 512</sup> For example, Wang *et al.*<sup>513</sup> fabricated a unidirectional Ag nanofibers (AgNFs) network by sputtering a layer of Ag on electrospun PVA nanofibers. The AgNFs exhibited excellent conductivity, making them suitable for constructing a hyperthermia patch (HTP) for thermotherapy. To prevent the AgNFs from oxidizing due to prolonged exposure to air and to ensure compliance with the skin, the metalized layer was enveloped by a soft PDMS

layer. This allowed the HTP to be conveniently and conformally attached to various joints on the human body (**Figure 38a**). In addition to these conventional metals, LMs with inherent fluidity have garnered significant interest for producing flexible and stretchable PCTs.<sup>514, 515</sup> For instance, by coating eutectic-gallium-indium (EGaIn) liquid metal onto an electrospun elastic SBS fibrous mat,<sup>24, 227</sup> the resulting conductive fibers not only show remarkable stretchability and conductivity but also outstanding permeability. Such fibers are well-suited for wearable heaters.

Various conductive nanomaterials such as metal nanowires, CNTs, graphene, and MXene can be assembled into free-standing networks or coated onto textiles for making flexible electric heaters.<sup>516-518</sup> Vacuum filtration is commonly used to assemble free-standing networks of the conductive nanomaterials, during which a suspension of nanomaterials is filtered through a porous membrane using vacuum pressure. The nanomaterials are deposited onto the membrane, resulting in a randomly overlaid network structure due to the interweaving and entanglement of the low-dimensional nanomaterials. Dip-coating and spray-coating are common techniques for coating conductive materials onto textiles.<sup>519, 520</sup> Adhesives may be incorporated into inks to improve the adhesion of conductive nanomaterials to the surface of textiles. Conductive polymers can also be used for coating textiles to achieve strong adhesion due to their good flexibility and affinity to polymeric fibers.<sup>519</sup> Another method to make freestanding PCTs is to carbonize textiles, forming carbon textiles.<sup>521</sup> For example, Zhang's group has developed a range of carbon textiles by carbonizing various fabrics, such as silk and cotton.<sup>265, 522, 523</sup> Due to the weft-knitted structure, the carbonized textiles not only show good flexibility but also a certain stretchability. As shown **Figure 38b**, the carbon textiles can be applied for Joule heating device by connecting with electrodes.<sup>522</sup> Due to their low resistance, the heating device only requires a low voltage of a few volts to rapidly heat to over 100 °C. The temperature increases with applied voltage, and it can reach a temperature of approximately 150 °C under a voltage of 3.5 V (**Figure 38c**). Moreover, the heating performance would not deteriorate even under tensile strain up to 70% (**Figure 38d**), thus it can be applied on human joints for wearable thermotherapy applications (**Figure 38e**). Overall, PCT-based Joule heating devices are suitable for body thermoregulation and wearable thermotherapy. However, for practical applications, it is advisable to integrate them with temperature sensors and a control system to prevent overheating and potential burning issues.

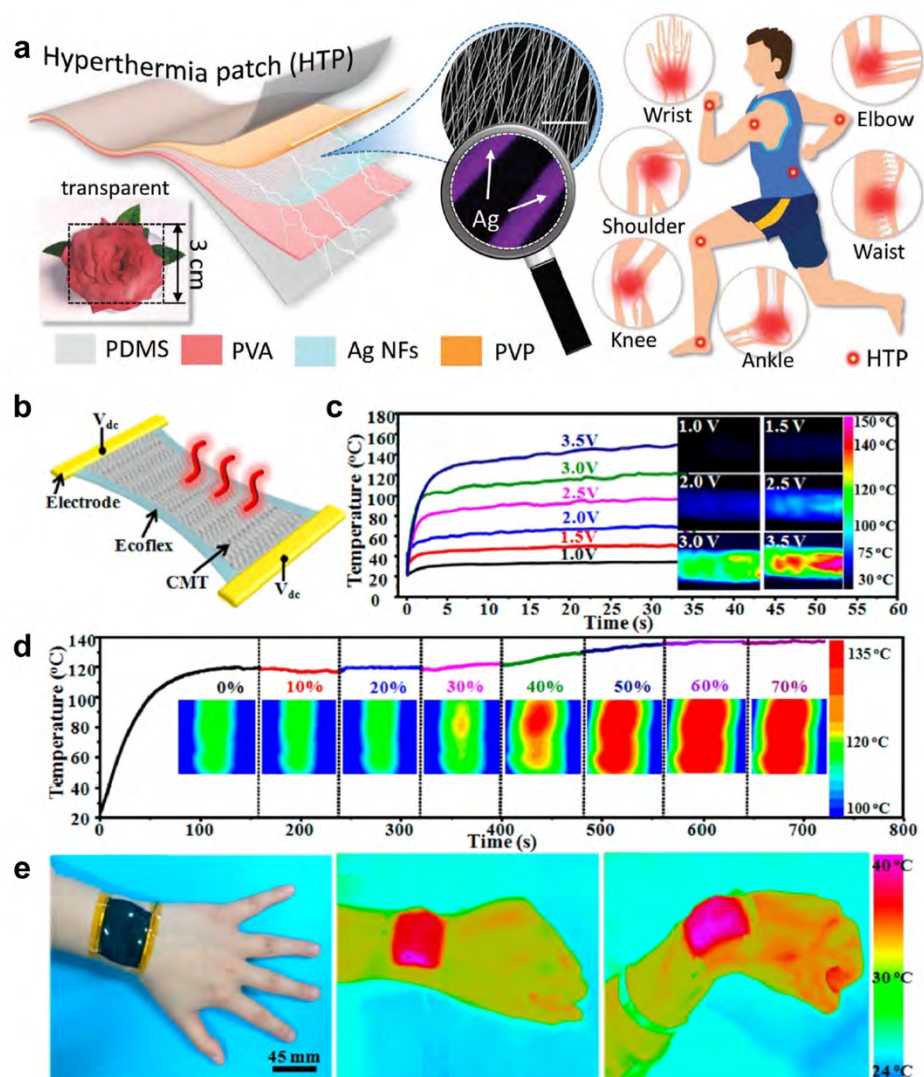


**Figure 38.** (a) Schematic illustration of a HTP including a heating layer of metalized AgNFs network, PVA and PVP supporting layer, and PDMS elastomer encapsulation layers. Reproduced with permission from ref <sup>513</sup>. Copyright 2022 John Wiley and Sons. (b-e) Performance of a wearable heater based on the intrinsically stretchable and conductive textile: (b) Schematic illustration showing a stretchable carbonized Modal textile (CMT) heater, (c) evolution of the maximum temperature of a bare CMT under DC voltages from 1.0 to 3.5 V, (d) evolution of the temperature of an Ecoflex-encapsulated CMT heater under stepwise strains of 0-70% at a constant DC voltage of 4.0 V, (e) photograph showing a wearable CMT heater affixed on a wrist and IR images showing the temperature profiles of the CMT heater with the wrist under relax and bending conditions at a constant DC voltage of 5.0 V after about 120 s. Reproduced with permission from ref <sup>522</sup>. Copyright 2017 American Chemical Society.

### 3.3.2 Electrical Stimulation

Transcutaneous electrical nerve stimulation (TENS) is a non-invasive physical therapy that involves applying mild electrical pulses (0~100 mA, 2~150 Hz) to specific areas on the skin.<sup>524</sup> It can stimulate the sensory nerves and interfere the pain signal transmission, thereby it is often used to treat chronic pain conditions, such as arthritis and back pain.<sup>525, 526</sup> Gel electrodes are commonly used for TENS, while they may suffer from drying out and skin irritation problems during long-term applications. Therefore, various types of dry electrodes such as PCTs have been developed for the long-term wearable purpose.<sup>527-530</sup> For example, Li *et al.*<sup>531</sup> designed a smart garment with TENS capabilities using the intarsia knitting technique. In their study, an elastic fabric was used, and the size of the garment was intentionally designed to be smaller than typical clothing to ensure that the electrodes maintained tight contact with the skin, thereby providing effective therapy. The confining pressure was kept within the comfortable range of clothing pressure (1.96-3.92 kPa). Silver conductive yarn was knitted into knitwear to serve as electrodes and conducting wires. The electrodes demonstrated stable resistance thanks to the turning routing design and intarsia knitting technique. Ultimately, a prototype of the garment with TENS capabilities was successfully produced. Despite the stability of conductive textile-based dry electrodes, they often have poor contact with the skin, resulting in high impedance. To overcome this challenge, researchers have explored ultra-thin and conformable electrodes such as conductive thin films and microneedles. Additionally, a portable or wearable power source is necessary for wearable TENS devices, which can be a hurdle for comfortable design as conventional batteries are bulky and heavy. To this end, the recently emerged TENG devices themselves can generate electrical pulses, therefore they can provide electrical stimulation in a battery-free mode for TENS electrotherapy.<sup>532</sup>

### 3.3.3 Drug Delivery

Transdermal drug delivery is a convenient method to deliver drugs locally through the skin, which can avoid the drawbacks of oral administration, such as low targeting efficiency, possible decomposition, and side effects. However, transdermal drug patches usually have slow delivery rate and uncontrollable efficiency, since many drugs are hydrophilic that are difficult to pass through the thick stratum corneum. To facilitate the delivery of drugs, iontophoresis technique has been developed recently for transdermal drug delivery.<sup>533</sup> The mechanism of iontophoresis is based on the principle of electro-repulsion, that the movement of ions (ionized drug molecules) can be facilitated by an applied electrical potential. During iontophoresis, two electrodes are placed on the skin, one with the drug to be delivered and the other with a

countercharge. The electrodes are connected to a power source, which generates an electric current. The current facilitates the drug molecules to move towards the skin, where they are absorbed by the underlying tissues and blood vessels. Moreover, the delivery rate, amount, and area can be readily controlled by adjusting drug loading concentration, applied potential, and electrode size. Apart from drug delivery for therapeutic purposes, iontophoresis can also be applied in combination with wearable sweat biosensors to achieve on-demand sweat extraction.<sup>534-536</sup> This is achieved by delivering certain pharmaceuticals, such as pilocarpine, into the skin to stimulate sweating (**Figure 39**).<sup>537</sup> Another method to extract sweat is through reverse iontophoresis,<sup>538</sup> which involves directly extracting interstitial fluid (ISF) from the tissue, without the need for delivering a stimulant to induce sweating. The main difference between iontophoresis and reverse iontophoresis is that iontophoresis is used for transdermal drug delivery, whereas reverse iontophoresis is used to extract ISF through the skin, relying on the force of an electric field.

The iontophoresis devices currently reported are mostly made from hydrogel materials, wet patches, or microneedles, since they are suitable for drug loading.<sup>539-541</sup> Although conductive textiles have not been widely used for iontophoresis drug delivery, it is believed they would be a promising electrode for loading drugs. For instance, the drugs can be loaded into fibers *via* techniques such as electrospinning,<sup>542</sup> and by incorporating them into everyday wearables, a controllable and on-demand drug delivery can be realized. Furthermore, by integrating iontophoresis devices with textile-based biosensors and power supply devices,<sup>543, 544</sup> a closed-loop drug administration system with simultaneous drug delivery, sweat extraction, and drug metabolite monitoring can be realized.<sup>545</sup>

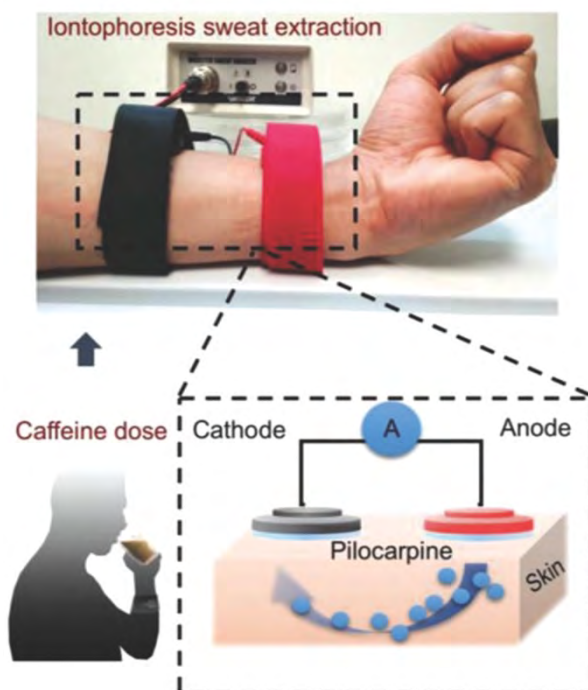


**Figure 39.** Schematic of iontophoresis-based sweat extraction. Reproduced with permission from ref <sup>537</sup>. Copyright 2018 John Wiley and Sons.

### 3.4 Energy Harvest and Storage Devices

The demand for flexible energy harvesting and storage devices, encompassing solar cells, nanogenerators, bio-fuel cells, supercapacitors, and batteries, has become increasingly pressing to power wearable electronics. However, the existing commercial energy devices, such as lithium-ion batteries (LIBs), lack acceptable deformation capability as they are rigid. The primary bottleneck lies in the low yield strain of substrates (such as current collectors in batteries), rather than the active materials themselves.<sup>47, 546</sup> Accordingly, the use of PCTs with high flexibility and conductivity as a new kind of substrate shows great potential for flexible energy devices.

#### 3.4.1 Solar Cells

Solar cells, or photovoltaics, are energy harvesting devices that convert light to electricity. Three generations of solar cells have been developed since the first Si-based solar cell appeared in 1946: 1<sup>st</sup> generation wafer-based solar cells, 2<sup>nd</sup> generation thin-film solar cells, and 3<sup>rd</sup> generation emerging thin-film solar cells.<sup>547, 548</sup> The thin-film solar cells are more competitive than bulk wafer solar cells for wearable electronics because of their advantages in power-per-weight, flexibility, and cost efficiency.<sup>549</sup> Nevertheless, thin-film solar cells on dense polymeric

flexible substrates still show disadvantages of poor breathability and moisture permeability. As a result, researchers are interested in developing porous textile-based solar cells with good flexibility and permeability. There are two strategies in realizing a solar cell fabric for wearable electronics: one is fabricating fiber solar cells, and then weaving the fiber solar cells to a solar cell fabric; the other is fabricating solar cells on textile fabrics directly via thin-film coating technologies.<sup>550</sup>

As the building block for fabric-based solar cells, realizing high efficiency and flexible fiber solar cells is critical. **Figure 40** shows three typical configurations for fiber solar cells, namely coaxial, twisting, and interlaced.<sup>551</sup> For a coaxial device, the solar cell consists of a single fiber, and the outer electrode is coated on surface of the device uniformly. For twisting and interlaced configurations, the outer electrodes are standalone conductive fibers that physically contact with solar cell fibers.

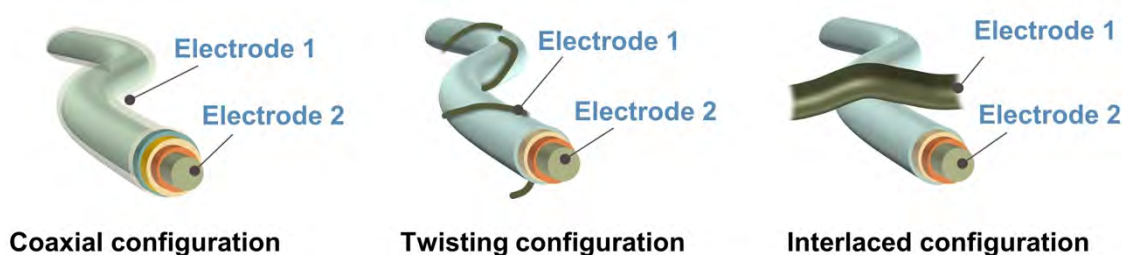


**Figure 40.** Three typical configurations for fiber-based solar cells.

Coaxial fiber solar cells require uniform coating of each layer on the surface of core fibers. If light comes through the inner side, the core fiber should be an optical fiber (*e.g.*, silica fiber) to allow light pass through the transparent electrode and the active layer.<sup>552</sup> Since optical fibers are electrically non-conductive, a layer of transparent electrode, indium tin oxide (ITO) in most cases, should be deposited on the surface of the optical fiber. For example, Weintraub *et al.*<sup>553</sup> reported optical fiber-based dye-sensitized solar cells (DSSCs) using ITO as the working electrode. ZnO nanowire arrays were deposited on ITO via a chemical approach to increase the light absorbing surface area of the DSSC (**Figure 41a**). On the other hand, conductive fibers made of metals, carbon materials, conducting polymers, or their composites can serve as core fibers for outer-illuminated fiber solar cells. Zhang *et al.*<sup>554</sup> reported a fiber organic solar cell (OSC) with a Ti wire as the core fiber and the inner electrode. Meanwhile, the same Ti wire also served as the current collector for a supercapacitor, which can be charged by the fiber OSC



(**Figure 41b**). As the surface smoothness of the core fiber is critical for successful fabrication of coaxial fiber solar cells, stainless steel wires are good choice for fiber thin-film solar cells such as OSCs and perovskite solar cells (PSCs).<sup>115, 555</sup>

Whereas coaxial fiber solar cells usually show higher efficiency than that of twisting and interlaced devices because of the high utilization of surface area, twisting and interlaced configurations have advantages in manufacturing and flexibility.<sup>555</sup> **Figure 41c** shows schematics of a double-twisted fiber PSC with CNT fibers as electrodes.<sup>556</sup> AgNW network was employed to increase the effective contact area between the CNT fiber electrode and the hole transport layer. The double-twisted fiber PSC showed a maximum power conversion efficiency (PCE) of 3.03%, and a negligible degradation after 1000 cycles of bending cycles. Dong *et al.*<sup>557</sup> reported a record-breaking fiber PSC with high quality perovskite active layer obtained via a vapor-assisted deposition technology (**Figure 41d**). The gas phase reaction improved the grain size of perovskite crystals, and thus eliminated grain boundaries along the longitudinal direction. As a result, the fiber PSC showed a high maximum PCE of 10.79%. The high surface area of PCTs is favorable for photoelectrochemical devices such as DSSCs.<sup>558</sup> Fu *et al.*<sup>559</sup> designed and fabricated fiber DSSCs based on hydrophobic core/hydrophilic sheath CNT fibers (**Figure 41e**). The solar cells showed a high maximum PCE of 10% because of the high electrochemical activity of Pt modified on the hydrophilic sheath of CNT fibers. Zhang *et al.*<sup>560</sup> reported Pt-free fiber DSSCs with  $\text{Co}_{0.85}\text{Se}$  on CNT fibers as counter electrode, which further improved the catalytic activity for the redox process of the electrolyte (**Figure 41f**). Such high activity enabled a high short-circuit density of  $16.47 \text{ mA cm}^{-2}$  and a high PCE of 10.28%. In addition, the power output of the devices was almost independent to different bending angles. To enhance the ion diffusion and charge transfer in the fiber counter electrode, Kang *et al.*<sup>561</sup> designed a hierarchically assembled carbon nanotube (HCNT) fiber through twisting multiple CNT fiber bundles. The HCNT showed hierarchically aligned channels with large sizes of micrometers and small sizes of tens of nanometers, which can offer high-flux pathways for rapid ion diffusion and abundant active area for charge transport. When applied as a counter electrode twisted with Ti wire-based photoanode, the fiber DSC achieved PCE of 11.94%. Although CNT fibers demonstrated decent conductivity, they remain inferior to metallic counterparts. To improve the conductivity, Zhu *et al.*<sup>562</sup> integrated metal fibers with CNT by preparing a core-sheath Ti/CNT fiber counter electrode. Axially aligned CNT sheet was closely attached to the Ti wire in the core-sheath fiber, significantly boosting the counter electrode's electrical conductivity to facilitate charge collection and transport at the interface.

A fiber DSC assembled using the core-sheath Ti/CNT fiber counter electrode showed PCE of 25.53% under 1500 lux illuminance, demonstrating the potential application in indoor dim light conditions. To increase the light absorbing efficiency, they further designed a reflective hybrid counter electrode based on CNT fibers.<sup>563</sup> The reflective hybrid counter electrode consists of a metal current collector (stainless-steel wires twisted around a nylon fiber), aligned CNT sheet, and porous TiO<sub>2</sub>/P(VDF-HFP) film. The CNT sheet is closely affixed to the highly conductive metal fiber to enhance charge collection and transport, while the outer porous TiO<sub>2</sub>/P(VDF-HFP) film ensures robust diffuse reflection within the 400-750 nm wavelength range (average reflectance of 93.37%). The resulting fiber DSC achieved a record PCE of 12.52%.

Fiber solar cells can be woven into solar cell fabrics for wearable electronics. **Figure 41g** shows the schematics of a woven DSSC fabric with nylon warp filaments as spacers.<sup>564</sup> Dye-loaded porous metal ribbons and Pt-coated carbon yarns served as photoanodes and counter electrodes, respectively. Fiber solar cells can be woven to a fabric with other fiber-based electronics as an energy harvesting system. For example, Chen *et al.*<sup>565</sup> demonstrated a micro-cable structured textile system that integrated DSSCs and TENGs (**Figure 41h**). Interlaced Cu-coated polymer fibers were employed as both counter electrodes for DSSCs and electrodes for TENGs. The weaving process was done by an industrial weaving machine, showing great potential for the large-scale fabrication of wearable energy harvesting textiles in the future.

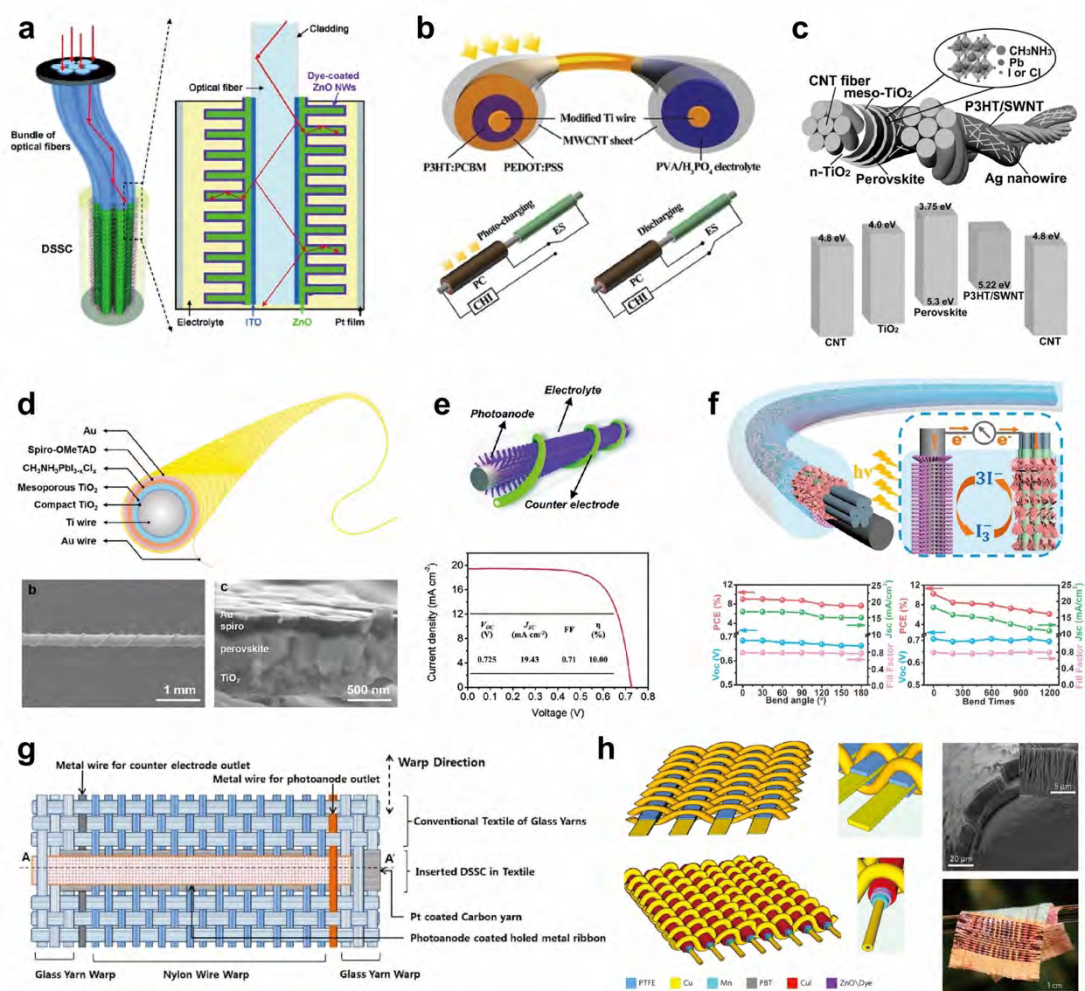


**Figure 41.** (a) Schematical illustration of fiber-shaped DSSC based on optical fiber. Reproduced with permission from ref <sup>553</sup>. Copyright 2009 John Wiley and Sons. (b) Illustration of OSC and supercapacitor integrated on a single Ti wire. Reproduced with permission from ref <sup>554</sup>. Copyright 2014 John Wiley and Sons. (c) Double-twisted fiber-shaped PSC with CNT yarn electrodes. Reproduced with permission from ref <sup>556</sup>. Copyright 2015 John Wiley and Sons. (d) High quality perovskite active material on fiber core obtained via vapor-assisted deposition. Reproduced with permission from ref <sup>557</sup>. Copyright 2019 John Wiley and Sons. (e) Illustration of hydrophobic core/hydrophilic sheath CNT fibers for fiber-shaped DSSCs. Reproduced with permission from ref <sup>559</sup>. Copyright 2018 Royal Society of Chemistry. (f) Pt-free fiber-shaped DSSC with good stability of power output under bending. Reproduced with permission from ref <sup>560</sup>. Copyright 2019 American Chemical Society. (g) A woven DSSC fabrics design with nylon warp filaments spacers to avoid short-circuit. Reproduced with permission from ref <sup>564</sup>. Copyright 2016 Springer Nature. (h) An integrated system of DSSC and TENG based on Cu-coated polymer fibers. Reproduced with permission from ref <sup>565</sup>. Copyright 2016 Springer Nature.

In addition to weaving from fiber solar cells, another strategy to obtaining fabric-based solar cells is using conductive fabrics as electrodes directly. As a substitute to planar metal film or foil electrodes, PCTs show advantages in high flexibility and high surface area. In 2007, Fan *et al.*<sup>566</sup> reported transparent conducting oxide (TCO)-free DSSCs with stainless steel mesh electrodes, which can be regarded as metal-based woven PCTs. **Figure 42a** shows a woven carbon cloth and its application in DSSCs. The carbon cloth was modified with a composite of MOF and sulfonated polythiophene, which showed a large surface area and a high catalytic activity. The DSSCs showed a high efficiency of 9.75% under dim light, which is promising for wearable applications in indoor scenarios.<sup>567</sup> Chemically stable carbon cloth is also a competitive candidate for PSCs, which suffer from stability issues due to metal migration and the chemical reaction between halide perovskites and metal electrodes.<sup>568</sup> **Figure 42b** shows the fabrication process of a carbon cloth-based PSC with commercially available carbon fibers as back contact.<sup>569</sup> The PSCs with carbon cloth electrodes showed a significantly higher efficiency stability than that of control devices with Au electrodes. Liu *et al.*<sup>570</sup> reported *p-i-n* type solar cells with carbon cloth anodes, showing a maximum PCE of 17.02%. The device also exhibited a good thermal stability at 85 °C, which is critical for the stable operation of PSCs in high intensity sunlight. In addition to carbon cloth, other PCTs such as metal fabrics, metal-coated fabrics, and polymer-coated fabrics are ideal electrodes for flexible and wearable solar cells. For example, AgNW-coated polyester cotton fabric was applied as the substrate and the bottom electrode for wearable OSCs. The electrodes and functional layers of the OSC was deposited via low-cost spray coating processes. Whereas the maximum PCE of the OSC was only 0.02%, this work enabled possibilities for fully solution-based fabrication of wearable solar cells on textiles directly.<sup>571</sup> Zhen *et al.*<sup>572</sup> developed another fully solution-based strategy for textile-based OSCs with metal-coated fabric electrodes (**Figure 42c**). Ag was coated on polyester fabric via aforementioned PAMD technology. The rest of solar cell components were transfer-printed on the Ag-coated fabric in water, and then bind together with an additional ultrathin polyethyleneimine (PEI) layer. Such method produced 2.90% efficiency OSCs that can maintain photovoltaic performance after repeated folding.

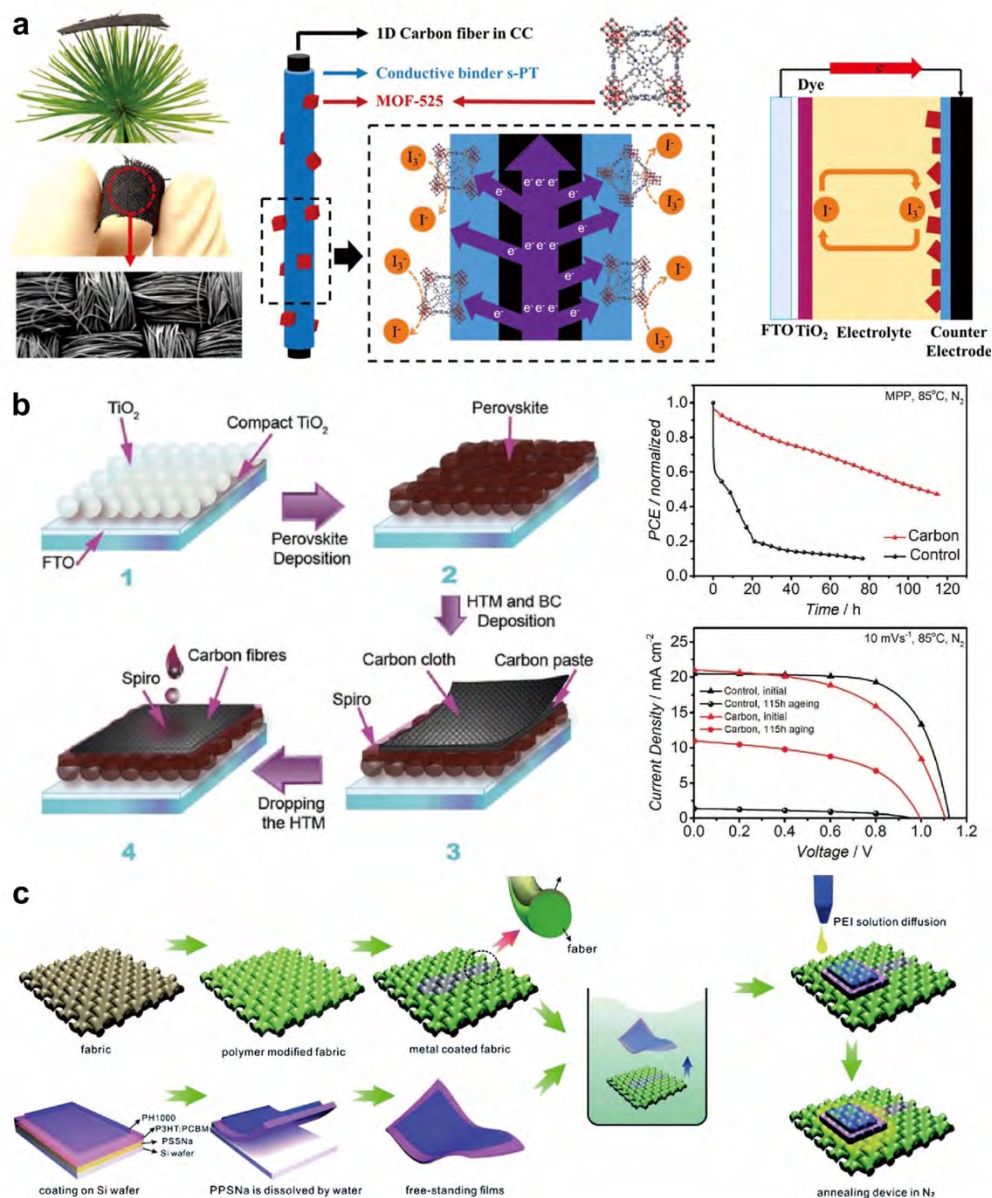


**Figure 42.** (a) Application of MOF-modified carbon cloth as the counter electrode for DSSCs. Reproduced with permission from ref <sup>567</sup>. Copyright 2017 Elsevier. (b) Fabrication process of thin-film PSCs with carbon cloth top electrodes. The devices with carbon cloth electrodes showed a good thermal stability. Reproduced with permission from ref <sup>569</sup>. Copyright 2016 John Wiley and Sons. (c) Illustration of the fabrication of water-borne OSCs by transfer-printing thin-film OSCs onto Ag-coated fabrics. Reproduced with permission from ref <sup>572</sup>. Copyright 2018 Royal Society of Chemistry.

### 3.4.2 Generators

Generator, which is known as energy scavenger, is a device that can capture and convert energy from various sources such as human bodies and natural environment. Unlike solar cells,

generators primarily harvest and convert mechanical or thermal energy into electricity. Generators play a vital role in diverse applications where the use of conventional energy storage devices (*e.g.*, batteries) is impractical. They provide a sustainable and efficient method of powering various systems, including IoT devices and health monitoring systems.<sup>573</sup>

**Piezoelectric Nanogenerator.** The emergence of piezoelectric nanogenerators (PENGs) provides a promising and novel avenue for harvesting mechanical energy.<sup>574, 575</sup> Researchers have developed piezoelectric textiles for harvesting mechanical energy generated by human activity.<sup>358</sup> Piezoelectric textiles are mainly composed of PCTs and piezoelectric materials, such as ZnO, ZnS, PbTiO<sub>3</sub>, BaTiO<sub>3</sub>, and PVDF. Among them, PVDF is an organic polymer that can be processed into fibers, while the others are powdery inorganics that require coating or in-situ growth to be coated on conductive fabrics. The structure of PCTs can determine the configuration of PENG, and the reported textile-based PENGs can be divided into two types: 1D fiber type and 2D fabric type. The 1D fiber-type PENG usually employs conductive fibers as the core electrode. The piezoelectric materials are usually coated on the core fiber, and covered with another layer of conductive material on the outer layer, forming a co-axial fiber-shaped PENG. For example, Du *et al.*<sup>576</sup> grew ZnO nanowires on a carbon fiber electrode, between which an insulating layer was wrapped to establish an interface barrier, and an ITO film was coated on the outer layer serving as another electrode (**Figure 43a**). In another study, a similar structure of ZnO nanowires grown on carbon fiber was reported, while the outer electrode employs the plating of gold (**Figure 43b**).<sup>577</sup> In addition, PVDF nanofibers were produced for making flexible PENG. For example, Sim *et al.*<sup>578</sup> prepared a PENG by winding PVDF nanofibers on a silver-plated nylon yarn electrode, and wrapping CNT film on the PVDF nanofibers for another electrode (**Figure 43c**). The obtained piezoelectric fiber generated a positive voltage when compressed and a negative voltage when released, and the final potential difference can reach ~3 V. While mass production of piezoelectric fibers poses challenges, the application of heat stretching method utilizing carboxylated polycarbonate as the electrode layer and polyvinylidene fluoride-trifluoroethylene (PVDF-TrFE) as the piezoelectric layer has proven successful in achieving mass production of these fibers (**Figure 43d**).<sup>579</sup>

2D fabric-type PENG can be produced through two methods: weaving piezoelectric threads into a fabric through a weaving or knitting process, or assembling PCTs and piezoelectric material films into a sandwich structure. Kim *et al.*<sup>580</sup> developed a non-toxic breathable piezoelectric fabric by utilizing a low-temperature hydrothermal method to grow ZnO nanorods



on the surface of PVDF nanofibers and incorporating a conductive silver cloth as the electrode (**Figure 43e**). The incorporation of PCTs ensures a sufficient interface contact between the electrodes and piezoelectric material. Song *et al.*<sup>581</sup> created a textile PENG by manually weaving warp and weft yarns with PVDF strips embedded with Ni/Cu alloy deposition. Electrospinning represents another approach to produce PVDF nanofiber films with improved piezoelectric effect.<sup>582</sup> To strengthen the bonding between piezoelectric layer and PCTs, piezoelectric material can be grown directly on the conductive fabric. Zhang *et al.*<sup>583</sup> fabricated a fabric electrode by screen printing silver paste on a fabric, followed by growing ZnO nanorod array on surface of the silver paste using a hydrothermal method. The obtained piezoelectric fabric displayed a stable working state and excellent piezoelectric performance (output voltage of up to 4 V).

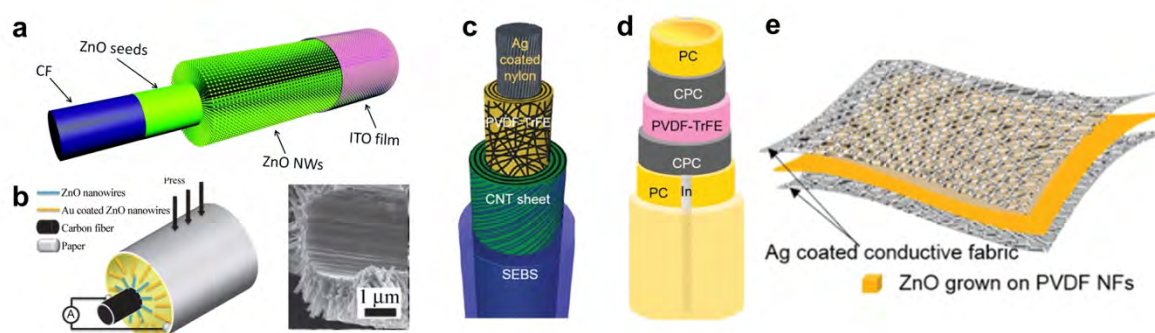


**Figure 43.** (a) Schematic diagram of single fiber-based PENG. Reproduced with permission from ref <sup>576</sup>. Copyright 2017 Royal Society of Chemistry. (b) Schematic diagram of single-fiber base PENG with outer foldable Au-coated ZnO nanowires on paper. Reproduced with permission from ref <sup>577</sup>. Copyright 2014 Springer Nature. (c) Schematic diagram of Ag coated nylon based piezoelectric fiber. Reproduced with permission from ref <sup>578</sup>. Copyright 2015 John Wiley and Sons. (d) Schematic diagram of cylindrical piezoelectric fiber. Reproduced with permission from ref <sup>579</sup>. Copyright 2010 Springer Nature. (e) Ag-coated conductive fabric-based piezoelectric fabric. Reproduced with permission from ref <sup>580</sup>. Copyright 2018 MDPI.

**Triboelectric Nanogenerator.** Triboelectric nanogenerator (TENG) is another energy harvesting technology that emerged in recent years. Similar to PENG, it can also convert mechanical energy to electricity.<sup>584, 585</sup> Due to the superior electrical output of TENG, researchers have increasingly turned their attention to TENG and various TENG textiles have been developed for electricity generation.<sup>586</sup> TENG works based on contact electrification and electrostatic induction, and there are four working modes: vertical contact-separation mode,



lateral-sliding mode, single-electrode mode, and freestanding triboelectric layer mode.<sup>585, 587-589</sup> The vertical contact-separation mode and single-electrode mode are commonly adopted in TENG textiles because they are easier to implement and have simpler device structures. TENG fabrics with vertical contact-separation mode typically consist of two electrodes and two friction layers with opposite electrical properties. In certain special cases, it can also work with two electrodes and one friction material with negative electrical properties. Wen *et al.*<sup>590</sup> developed a contact-separation mode TENG fiber by coating copper foil on silicone fibers, and wrapping a layer of silicone friction material on one of the electrodes (**Figure 44a**). During its operation, a potential difference can be generated from the contact electrification between the copper foil and silicone, as well as the electrostatic induction between the electrodes during the separation process. The single-electrode mode TENG has a simpler device structure compared to the contact-separation mode, requiring only one frictional layer wrapped around a fiber electrode. Therefore, it has a wide range of electrode material choices, such as copper, nickel, silver, or carbon-based materials. Yang *et al.*<sup>591</sup> prepared single-electrode triboelectric fibers by injecting LM into hollow silicone fibers, which is a simple and low-cost process (**Figure 44b**). However, the output of a 1D fiber-shaped TENG is low due to the limited frictional area, resulting in low mechanical energy collection efficiency.

1D fiber-shaped TENG can be woven into 2D fabrics by knitting or weaving, or directly designing using conductive and insulating yarns. Zhao *et al.*<sup>210</sup> manufactured metal yarns by coating Cu on PET yarns through the PAMD method, and a vertical contact-separation mode TENG fabric was assembled by weaving Cu-PET yarns and PI-Cu-PET yarns. To simplify the device structure and preparation process, Fan *et al.*<sup>61</sup> utilized fully open-knit stitches to intertwine conductive yarns and non-conductive yarns, forming a loop unit configuration in both the horizontal and vertical orientations. The conductive yarns employ stainless steel metal wire wrapped in nylon, while non-conductive yarns employ raw nylon yarns (**Figure 44c**). When two yarns contact with each other, contact electrification occurs on the surfaces of the conductive yarn and nylon yarn, and equal amounts of positive and negative charges are generated on the surfaces of the two yarns. Once the two yarns separate, positive charges are induced in the stainless steel due to the electrostatic induction effect. This TENG fabric can generate output voltages up to 12 V and currents up to 8 nA.

Furthermore, researchers have designed 3D TENG fabrics to further improve energy harvesting performance. With multiple layers of electrodes and triboelectric layers, the 3D structure can

effectively increase the contact area of the device during the friction process per unit area. Dong *et al.*<sup>592</sup> fabricated a 3D TENG fabric using three-strand twisting of stainless steel/polyester fiber blended yarns (warp), PDMS-coated energy collection yarns (weft), and thickness-directional binding yarns (Z-yarn). The output voltage of the 3D fabric can reach 45 V, with a current of 0.35  $\mu\text{A}$ . However, the device only had two layers of electrodes, so the output improvement was limited. Therefore, they further developed a 3D five-directional weaving structure TENG using multi-axis winding yarns as the axis yarns and PDMS-coated energy yarns as the weaving yarns, by a four-step weaving technology. **Figure 44d** shows the preparation process of multi-axis winding conductive yarns, where conductive fibers obtained by winding are used as the core.<sup>593</sup> With this structural design, the output voltage of the TENG fabric can reach 90 V, with a current of 1  $\mu\text{A}$  (**Figure 44e**).

Although the output and energy harvesting efficiency of TENG fabrics can be notably improved by designing fiber and/or fabric structures from 1D to 2D to 3D,<sup>594</sup> the output of TENG fabrics operating in the contact-separation and single-electrode modes remains low. It has been demonstrated that the freestanding triboelectric layer mode can further improve the output of TENG fabrics. Huang *et al.*<sup>595</sup> developed a TENG with the freestanding triboelectric layer mode by connecting two conductive fabrics with a non-conductive fabric, and rubbing an insulating fabric on top of the entire fabric. The output voltage and current of the TENG reached 1600 V and 15  $\mu\text{A}$ , respectively. In addition, Jung *et al.*<sup>596</sup> further improved the energy harvesting performance by integrating supercapacitors and TENG fabrics with a freestanding triboelectric layer mode (**Figure 44f**). Sheng *et al.*<sup>597</sup> also integrated fiber-shaped TENG with fiber-shaped supercapacitors for constructing a on-body self-charging power systems. In recent years, significant progress has been made in TENG textiles, with the output voltage levels reaching over 1000 V. However, the current generated by fabrics is still small and can hardly reach the mA level required for practical applications.<sup>598</sup> Therefore, increasing the current is a crucial need to improve energy collection performance.<sup>599</sup>

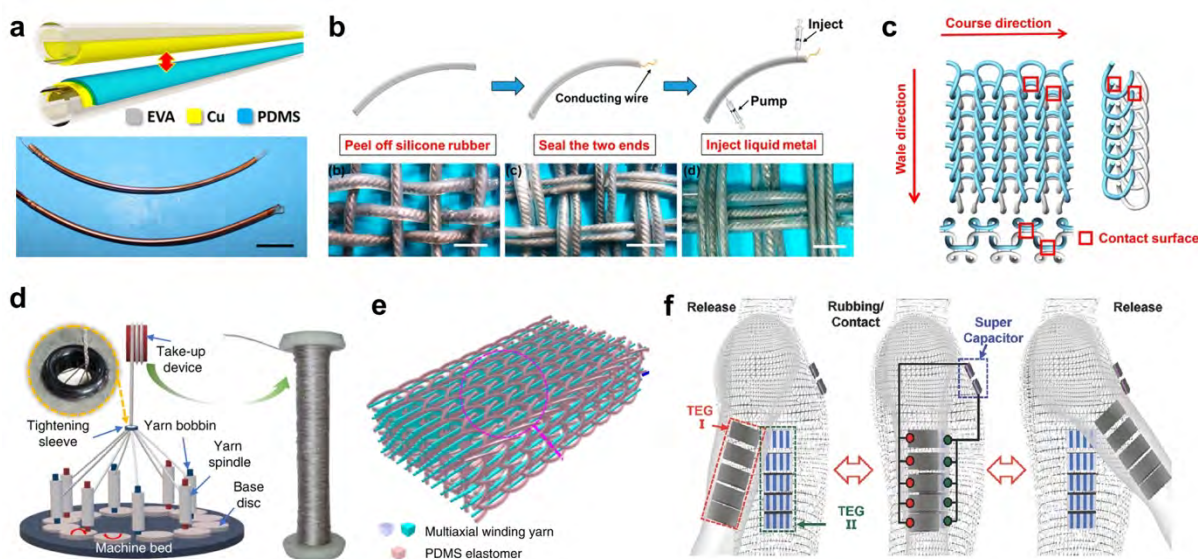


**Figure 44.** (a) Structure design of PDMS fiber-shaped TENG. Reproduced with permission from ref <sup>590</sup>. Copyright 2016 American Association for the Advancement of Science. (b) Fabrication method and images of LM fiber-based TENG. Reproduced with permission from ref <sup>591</sup>. Copyright 2018 American Chemistry Science. (c) Structure of knitted fabric TENG. Reproduced with permission from ref <sup>61</sup>. Copyright 2020 American Association for the Advancement of Science. (d) Schematic illustration of the multiaxial yarn winding machine. (e) Schematic illustration of 3D five-directional braided structure based TENG. Reproduced with permission from ref <sup>593</sup>. Copyright 2020 Springer Nature. (f) Schematic illustration of arm swings with TENG and supercapacitor equipped. Reproduced with permission from ref <sup>596</sup>. Copyright 2014 John Wiley and Sons.

**Thermoelectric Generator.** Thermoelectric generators can convert heat energy into electrical energy based on the thermoelectric effect, while thermoelectric textiles enable direct heat collection from the human body for continuous power supply.<sup>600</sup> Selecting suitable thermoelectric materials is the basis for designing thermoelectric textiles.<sup>601, 602</sup> Commonly used semiconductor materials for thermoelectric textiles include Si, Ge, and  $\text{Bi}_2\text{Te}_3$ . In addition, oxide materials such as  $\text{TiO}_2$  and  $\text{Fe}_2\text{O}_3$ , as well as organic conductive materials such as PANI and CNTs, can also be utilized in the preparation of thermoelectric textiles. Compared with inorganic thermoelectric materials, carbon materials are easier to be fabricated into fibers and are conducive to mass production, thus they are the most widely used in thermoelectric textiles. In addition, the Seebeck coefficient of most CNTs and graphene is positive due to oxygen doping. Therefore, the main focus of research on carbon thermoelectric fibers lies in reducing thermal conductivity and preparing n-type materials with stable chemical properties.

Chemical doping is an effective method to coordinate thermoelectric parameters and regulate the carrier type of CNTs, which can increase the carrier concentration in CNTs. Researchers have explored various dopants, including acids, molten salts, organic small molecules, ionic liquids, and polymers. Lee *et al.*<sup>603</sup> prepared wet-spun CNT fibers with high thermoelectric performance by controlling the longitudinal carrier mobility while maintaining the carrier concentration (**Figure 45a**). By optimizing the carrier migration rate within CNTs, the conductivity was increased without reducing the thermoelectric potential, resulting in an improvement in the power factor. In addition, doping of ionic liquid can also improve the thermoelectric performance of CNT fibers.<sup>604</sup> For example, the smaller volume  $\text{BF}_4^-$  anion can preferentially adsorb to the bent CNT surface. With an increase in the number of anions in direct contact with the surface of CNT, the CNT undergoes n-type doping. In addition to directly doping carbon fibers, carbon materials can be coated on a substrate before doping. Jin *et al.*<sup>605</sup> produced CNT conductive fibers by electrostatic spraying CNTs on PAN fibers for thermoelectric applications (**Figure 45b**).

Generally, thermoelectric textiles can be divided into two categories: 1D thermoelectric fibers and 2D thermoelectric fabrics. Sun *et al.*<sup>606</sup> fabricated thermoelectric loops by bending doped thermoelectric fibers with a certain repeated length, and they studied the mechanical stability of thermoelectric loops. To further improve the thermoelectric performance of thermoelectric fibers, Wang *et al.*<sup>607</sup> developed a thermoelectric fiber with radial heterojunction interlayers (**Figure 45c**). By rolling patterned CNT thin films and cellulose nanofiber membranes, the device forms a high-density p-n junction, and the final output voltage density can reach 65.4 mV/cm<sup>2</sup>. Under the same temperature difference, 2D thermoelectric fabrics can have a larger heating area and produce a larger output voltage. Allison *et al.*<sup>608</sup> printed p-doped PEDOT on a piece of commercial cotton fabric to prepare thermoelectric fabrics and designed a wearable wristband to collect heat energy generated by the wrist (**Figure 45d**). Additionally, the option of attaching Ag foil to the fabric substrate for connecting thermoelectric materials is advantageous, particularly for the production of thermoelectric fabrics with a linear structure (**Figure 45e**).<sup>609</sup> Embroidery techniques can weave yarns into various patterns on fabrics. Therefore, Kim *et al.*<sup>610</sup> created thermoelectric textiles by sewing silver-plated nylon and PEDOT:PSS wires in the form of p-n junctions on a fabric substrate (**Figure 45f**). In addition to embroidery, knitting and weaving methods can also be used to prepare 2D thermoelectric fabrics. For example, Ding *et al.*<sup>602</sup> prepared p/n-type thermoelectric fibers by alternately

doping SWCNT and PEI during the gel extrusion process, which was successfully woven into 2D thermoelectric fabrics by weaving. Furthermore, knitting can also assemble single thermoelectric fibers into 2D thermoelectric fabrics.<sup>606</sup> Unlike weaving, the fabric obtained by knitting has better elasticity, which is conducive to long-term wearing comfort. However, the energy conversion efficiency of current thermoelectric generators is still relatively low, typically between 5% and 8%, which cannot meet the energy needs of high-energy applications.

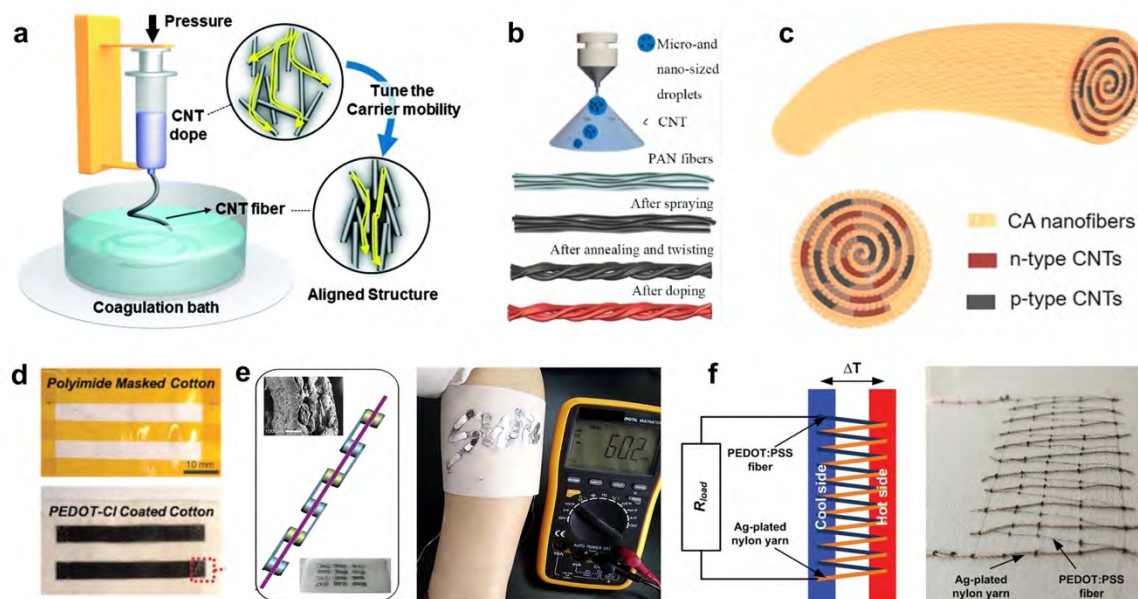


**Figure 45.** (a) Wet-spinning process for CNT fiber. Reproduced with permission from ref <sup>603</sup>. Copyright 2019 Royal Society of Chemistry. (b) Schematic diagram for preparing CNT fibers. Reproduced with permission from ref <sup>605</sup>. Copyright 2021 Elsevier. (c) Schematic diagram of the structure of the scrolled thermoelectric device. Reproduced with permission from ref <sup>607</sup>. Copyright 2022 Elsevier. (d) Standard cotton patterned with polyimide tape before and after coating with PEDOT-Cl. Reproduced with permission from ref <sup>608</sup>. Copyright 2019 John Wiley and Sons. (e) Images of silk fabric-based thermoelectric device. Reproduced with permission from ref <sup>609</sup>. Copyright 2016 Elsevier. (f) Schematic and photograph of PEDOT:PSS-fiber embroidered thermoelectric module consisting of ten elements. Reproduced with permission from ref <sup>610</sup>. Copyright 2020 John Wiley and Sons.

### 3.4.3 Wireless Energy Harvesting

Wireless energy transmission offers a promising solution to power wearable sensors, as they eliminate the need for bulky batteries and simplify the design and integration of wearable systems. Radio Frequency Identification (RFID) technology is a widely used method for

wireless energy transmission,<sup>611</sup> which works by harvesting electromagnetic energy through wireless inductive coupling between two conducting coils. In specific, a RFID tag (also known as an antenna) can acquire power from an RFID source, such as a cellphone or any other compatible reader.<sup>24</sup> When the RFID source emits a signal, it generates a magnetic field that induces an electric current in the antenna of the RFID tag, enabling it to power up and transmit information back to the RFID source. Near-field communication (NFC), one type of RFID that operates exclusively at a frequency of 13.56 MHz, is a popular choice for wearable applications due to their good stability and security.<sup>612, 613</sup> To ensure reliable communication and efficient energy transfer, NFC devices need to maintain a stable impedance match between the tag and reader, which requires the antenna that not only has low but also stable impedance. Therefore, it is crucial to design the NFC tag with low and stable impedance. If patterning conductive paths on textiles using conventional coating and printing technologies with conductive inks, the resulting conductive patterns are likely to encounter resistance variations during deformations. Therefore, the majority of textile-based NFC tags are created by embroidering conductive threads such as metal wires into a fabric.<sup>612, 614, 615</sup>

A deformation-resilient NFC coil with low resistivity and high stretchability was created by embroidering a conductive thread into a textile with spiral coil structures.<sup>612</sup> The conductive thread is composed of twisted copper fibers and coated with stretchable nylon yarns. Traditional embroidery techniques typically employ interlocking stitches to form the geometry, which can exert high tensions on the substrate fabric and limit its stretchability. To address this issue, the authors utilized a new embroidery design that utilizes zigzag stitches to secure the conductive thread, as shown in **Figure 46a**. This design enables the NFC coil to withstand extreme stretching of up to 50% strain. In a proof-of-concept study, the authors demonstrated a complete energy-harvesting NFC wearable body sensor system for breast cancer monitoring using the embroidered NFC coil antenna (**Figure 46b**). Compared to metal wires, LMs have greater potential for achieving high conductivity and stretchability due to their fluid nature. Lin *et al.*<sup>213</sup> developed an electronic textile system with NFC power and communication capabilities by digitally embroidering LM fibers onto clothing. The LM fibers are prepared by infiltrating galinstan ( $\text{Ga}_{68.5}/\text{In}_{21.5}/\text{Sn}_{10}$ ) into perfluoroalkoxy alkane (PFA) tubing. Textiles embroidered with LM fibers exhibited robust electrical resistance with less than 1% variation during stretching 20% strain. The researchers then designed a wireless and washable thermal monitoring shirt by connecting a sensor node and a smartphone reader through NFC relay (**Figure 46c**). Despite advancements in textile-based NFC devices, challenges remain in



achieving NFC tags with stable impedance under stretching, washability, miniaturization, and seamless integration, *etc.* Additionally, the NFC tags usually require a short operation distance (typically less than 10 cm),<sup>616</sup> which limits its applications.

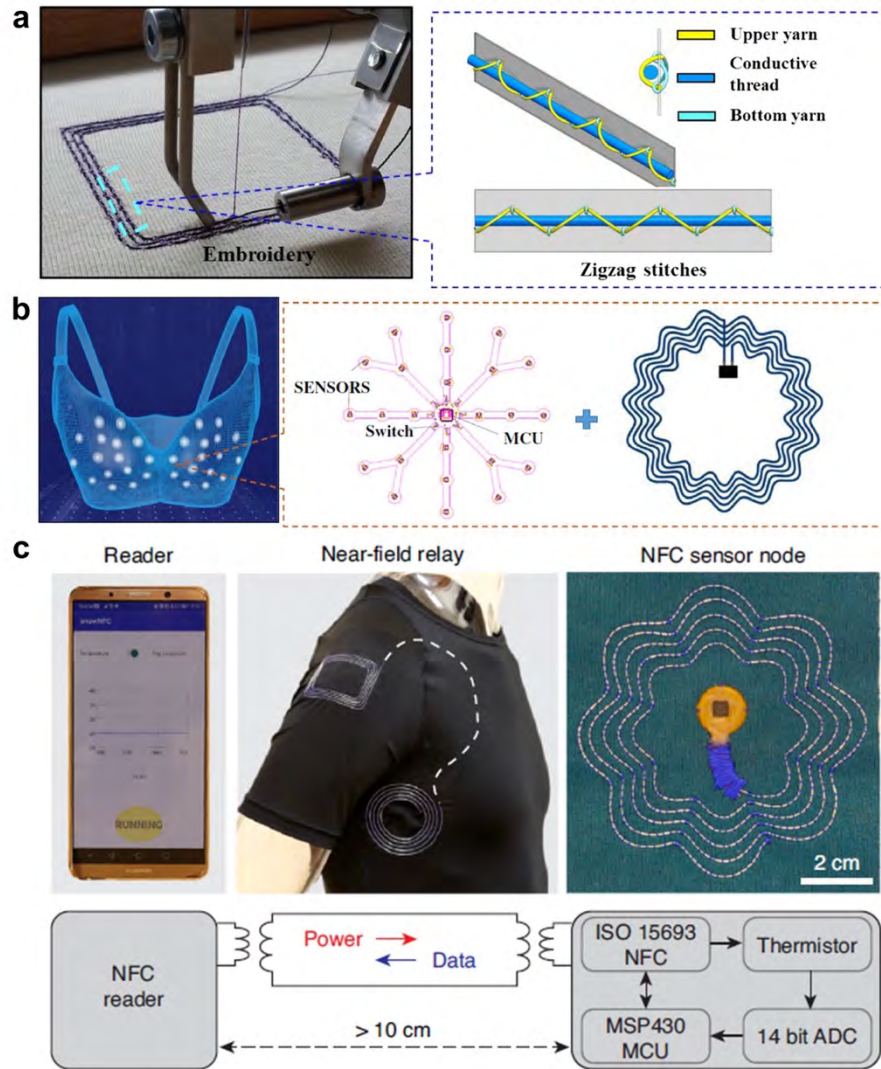


**Figure 46.** (a-b) Proposed embroidery processes of NFC coils: (a) Conductive threads fastened by the zigzag stitches; (b) NFC-based battery-free body sensing of temperature by integrating the NFC coil into a bra. Reproduced with permission from ref <sup>612</sup>. Copyright 2019 John Wiley and Sons. (c) Textile thermal monitoring system comprising a sensor node connected with a smartphone reader *via* a near-field relay integrated on a shirt. The top row shows images of the system components while the bottom row shows the block diagram. The distance between the reader and sensor node is more than 10 cm apart. Reproduced with permission from ref <sup>213</sup>. Copyright 2022 Springer Nature.



### 3.4.4 Biofuel Cells

Fuel cells are a class of electrochemical devices that can convert chemical energy into electricity *via* electrochemically oxidizing and reducing fuels on the electrodes.<sup>617</sup> A fuel cell typically comprises two electrodes (*i.e.*, cathode and anode) and an electrolyte, where oxidation and reduction reactions are taken place on the anode and cathode, respectively. Biofuel cells belong to a class of fuel cells, the difference with the traditional fuel cells is that they use biocatalysts such as enzymes and microorganisms instead of metallic inorganic catalysts (*e.g.*, Pt).<sup>618</sup> In addition, biofuel cells employ the biochemicals rather than small molecules (*e.g.*, H<sub>2</sub>, methane) as the fuels.<sup>619</sup> Specifically, wearable on-body biofuel cells make use of the chemicals contained in sweat, such as glucose, lactate, and urea, as fuel sources.<sup>620, 621</sup> As an illustration, a wearable biofuel cell that uses glucose as the fuel source operates by oxidizing glucose on the anode and reducing oxygen on the cathode.<sup>622, 623</sup> To promote these reactions under ambient conditions, the anode is usually immobilized with GOx enzyme to facilitate glucose oxidation, while the cathode is immobilized with bilirubin oxidase (BOx) enzyme to promote the reduction of oxygen to water.

Due to their good biocompatibility and on-body energy-harvesting behavior, biofuel cells have been widely explored as a power source to integrate with biosensors for making self-powered wearable devices.<sup>624, 625</sup> PCTs are a promising platform for assembling biofuel cells due to their good conductivity and large geometric area, which are beneficial for immobilizing biocatalysts and reserving sweat. When assembling biofuel cells with textile electrodes, the sandwich structure is the most straightforward configuration.<sup>626</sup> For example, Wang *et al.*<sup>627</sup> assembled a glucose biofuel cell using carbon fabrics as the substrate of electrodes. In specific, the anode was fabricated by immobilizing GOx on a carbon fabric, while the cathode was fabricated by immobilizing PB on a carbon fabric. In addition, the electrolyte layer employs a moisture management fabric (MMF), which can quickly absorb and wick sweat (**Figure 47a**). During operation, glucose was oxidized to hydrogen peroxide, which then served as the fuel for the cathode. The PB on the cathode was able to reduce the hydrogen peroxide, and the resulting reduced PB was subsequently re-oxidized by oxygen, which entered through the waterproofed cathode from the ambient air. However, the carbon fabric used in the biofuel cell assembly has limitations in terms of flexibility and durability, making it less suitable for use in wearable devices that may undergo large deformations during strenuous exercise. Therefore, PCTs prepared from coating conductive materials on stretchable fabrics would be more promising options for wearable applications. Hereof, Ogawa *et al.*<sup>628</sup> demonstrated a stretchable fructose-

based biofuel cell using stretchable conductive textile as electrodes. The stretchable conductive textile was prepared by coating CNTs on a commercial pantyhose textile, and the resulting textile electrodes can withstand 30 cycles of 50% stretching strain (**Figure 47b-d**). Another approach to creating textile-based biofuel cells involves making fibrous electrodes and weaving them into fabrics. As illustrated in **Figure 47e**, a textile lactate biofuel cell was assembled by weaving fibrous anode and cathode, followed by immersion of an ionic gel serving as the electrolyte.<sup>629</sup>

Although textile-based biofuel cells have shown promise as on-body power sources, some issues need to be addressed for practical applications. These include limitations in energy density and stability, since human sweating is limited and intermittent, which makes continuous operation of the biofuel cells challenging. While adding external fuels to the electrolyte and stimulating sweating can help to some extent, they can still be inadequate and make the device more complicated. Moreover, enzymes, which are used as catalysts in biofuel cells, may not be stable under harsh conditions, such as temperature and pH variations. To address these challenges, it may be worth considering the exploration of conventional inorganic catalysts that can function under sweat physiological conditions.<sup>630</sup> Recent research in the field of electrochemistry has been thriving in this direction.<sup>631, 632</sup>

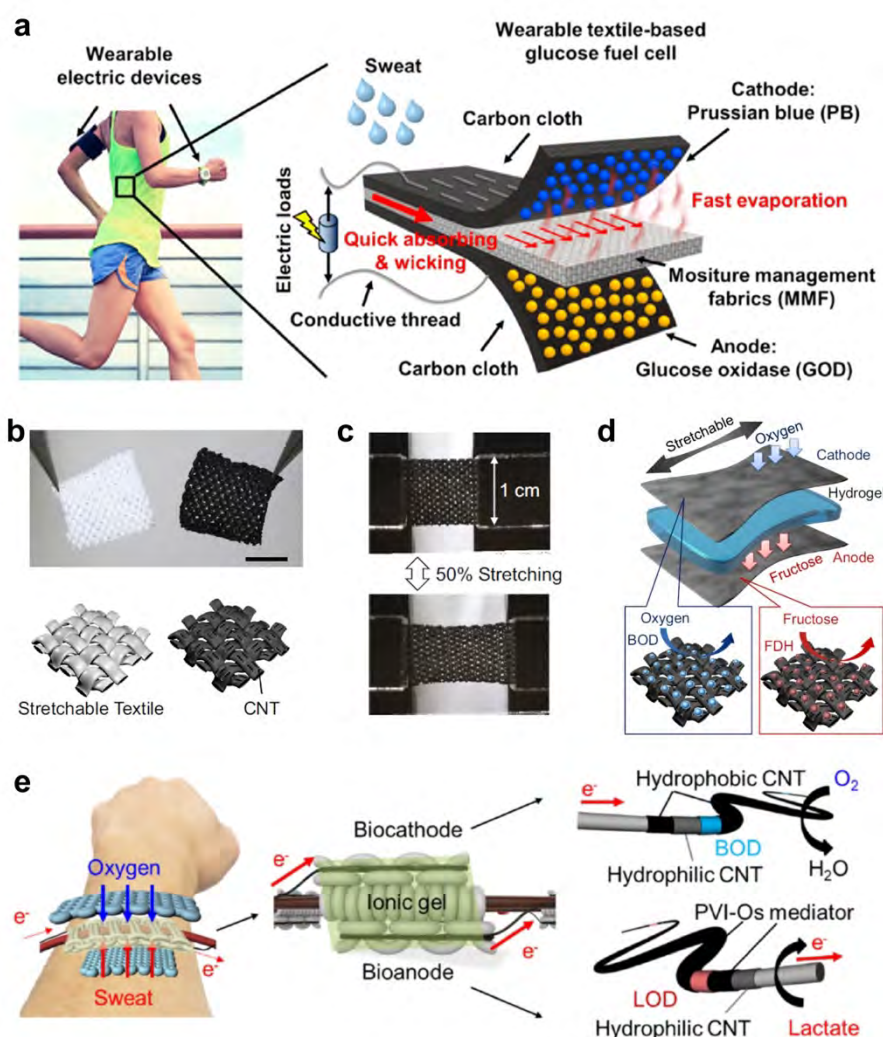


**Figure 47.** (a) Schematic of the assembly of a glucose-based biofuel cell using carbon cloth as electrodes. Reproduced with permission from ref <sup>627</sup>. Copyright 2020 Elsevier. (b-d) Assembly of a fructose-based biofuel cell using stretchable conductive textile as electrodes: (b) photographs and illustrations of virgin and CNT-modified stretchable pantyhose textile (ST) strips, (c) photographs showing 50% stretching of a CNT-modified ST strip, (d) a schematic of a stretchable biofuel cell constructed by laminating enzyme-modified conductive textiles with a hydrogel film that retains electrolyte solution and fructose fuel. Reproduced with permission from ref <sup>628</sup>. Copyright 2015 Elsevier. (e) Schematic figure of fiber-crafted lactate-based biofuel cell bracelet using a lactate oxidase/polyvinylimidazole-[Os(bipyridine)<sub>2</sub>Cl] mediator/CNT anode fiber, a BOx/CNT cathode fiber, and an ion gel formed textile. Reproduced with permission from ref <sup>629</sup>. Copyright 2021 Elsevier.

### 3.4.5 Supercapacitors

Supercapacitors with high power density, long cycle life, and low cost are desirable

supplements to LIBs.<sup>633</sup> PCTs have been widely used in supercapacitors serving as conductive substrates (*e.g.*, carbon cloth) or even active materials (*e.g.*, active carbon fibers), endowing high flexibility and fast kinetics of supercapacitors.<sup>46, 47, 633</sup> In this part, three main kinds of electrode materials in PCT-based supercapacitors, including carbon materials (*e.g.*, active carbon (AC), CNTs, and Graphene), metal compounds (*e.g.*, metal oxides, metal hydroxides, and MXene), and conductive polymers (*e.g.*, PANI and PPy), are introduced in detail. Of note, capacitance of supercapacitors is basically in direct proportion to the specific surface area of active materials owing to their surface charge storage mechanisms, including EDL and pseudo-capacitance reactions, and thus the corresponding material and electrode preparation methods are the key points in this section.

**Carbon Materials.** Active carbon (AC) materials have been widely used in commercial supercapacitors, owing to their high surface area, tunable pore structure, and low cost.<sup>634-636</sup> Nevertheless, the pure EDL mechanism causes their relatively low capacitance (normally 50~260 F/g). Micropores and mesopores in AC have been demonstrated to effectively enhance specific surface area and ion diffusion, and thus the pore configuration design such as AC with hierarchical structure is one of the most important modification strategies.<sup>637</sup> Moreover, heteroatom doping such as N, O, B, and S can also improve the capacitance of AC due to the extra active position for ion adsorption. For example, N/S-co-doped AC materials were prepared through a facile pyrolysis method with urea and lignosulfonate as mixed precursors and then incorporated into interface-activated cellulose fabrics, generating a pomegranate-like structure (**Figure 48a**).<sup>638</sup> The obtained self-supported electrode with a high mass loading of 19.5 mg cm<sup>-2</sup> exhibited remarkable capacitance (335.1 F g<sup>-1</sup>). Moreover, supercapacitor fiber gained popular attention in recent years since it can maximize mechanical flexibility and is easy to integrate into various application devices. For instance, a 100-m long supercapacitor fiber was fabricated by a thermally drawn strategy with AC and PVDF as active material and gel framework respectively (**Figure 48b**).<sup>36</sup> This fiber exhibits high energy density (306  $\mu$ Wh cm<sup>-2</sup>), long cycle life (no capacity decay over 13 000 cycles), desirable moisture resistance (100 washing cycles), and high mechanical strength (68 MPa).

CNTs with ultrahigh conductivity and special 1D structure have been drawing wide attention in the energy storage area. Nevertheless, pure CNTs usually display very low capacitance (20~80 F g<sup>-1</sup>) due to their limited micropore volume.<sup>639</sup> Instead, it is commonly served as

conductive additives rather than active materials in supercapacitor or batteries.<sup>640</sup> Graphene with ultrahigh specific surface area and tunable functional groups is another kind of novel carbon material for supercapacitors. Further, Graphene with high activity supported by PCTs with desirable adaptability has been widely used in wearable supercapacitors.<sup>641</sup> For example, a rGO/Ni-cotton composite electrode was prepared by first electroless deposition of Ni on cotton yarns, and then electrochemical deposition of rGO (**Figure 48c**).<sup>173</sup> The obtained electrode displayed greatly enhanced conductivity and mechanical strength, endowing high energy and power density ( $6.1 \text{ mWh cm}^{-3}$  and  $1,400 \text{ mW cm}^{-3}$ ) in the 1D flexible supercapacitors. Furthermore, the combination of 1D CNTs and 2D Graphene is a desirable method to assemble 3D porous hybrids for high-performance supercapacitors owing to the synergistic effect of these two types of materials. Such materials would be achieved by alternative filtration of CNTs and rGO on metallic textiles (**Figure 48d**), exhibiting high areal capacitance ( $>6.2 \text{ F cm}^{-2}$  at  $20 \text{ mA cm}^{-2}$ ), long cycling stability ( $3.2 \text{ F cm}^{-2}$  after 10,000 cycles), and excellent flexibility (no capacitance decay after 10,000 bending cycles).<sup>113</sup>

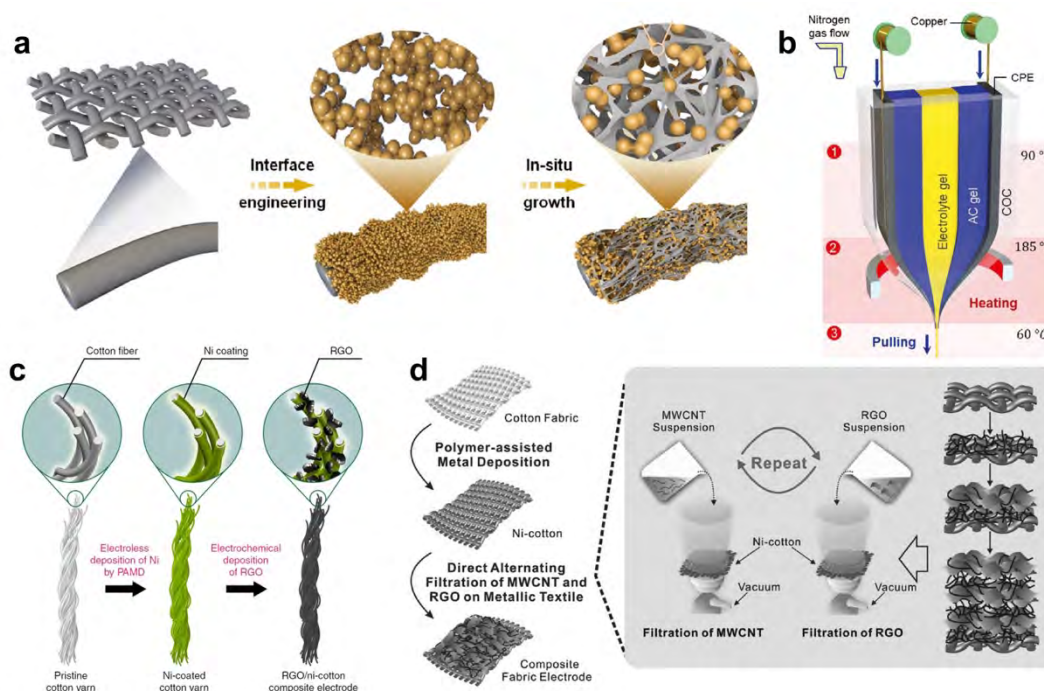


**Figure 48.** (a) Schematic of the preparation of N/S-co-doped AC materials. Reproduced with permission from ref <sup>638</sup>. Copyright 2023 John Wiley and Sons. (b) Schematic of supercapacitor fiber drawing process. Reproduced with permission from ref <sup>36</sup>. Copyright 2020 John Wiley and Sons. (c) Schematic of the fabrication of rGO/Ni cotton yarn composite electrodes. Reproduced with permission from ref <sup>173</sup>. Copyright 2015 Springer Nature. (d) Schematic of

the preparation of composite fabric electrodes. Reproduced with permission from ref <sup>113</sup>. Copyright 2017 John Wiley and Sons.

**Metal Compounds.** Metal-based materials for supercapacitors mainly include metal oxides, sulfides, hydroxides, and MXene, possessing the pseudo-capacitance mechanism with high capacitance. Although RuO<sub>2</sub> shows the best performance among metal oxides for supercapacitors regarding capacitance (theoretical value: 768 F g<sup>-1</sup>) and kinetics, its high cost renders it only used in a few special scenarios such as military and aerospace projects.<sup>642</sup> Potential substitutes mainly include Mn, Ni, Co, Fe-based oxides, sulfides, and hydroxides,<sup>643-647</sup> because of their low cost, environmental friendliness, and wide electrochemical window (> 1 V in aqueous electrolytes).

There are three key points when preparing PCTs and metal-based composite electrodes. Firstly, surface modification of PCTs, as this can supply growth position for metal compounds and sometimes also increase conductivity of PCTs such as metal coating. Secondly, morphology control of metal compounds, including specific surface area and pore size distribution. Thirdly, constructing 3D conductive networks, which would enable the fast charging/discharging of thick electrodes, bypassing the trade-off between energy density and power density in supercapacitors. For example, an alternating pseudocapacitive material (MnO cathode or Fe<sub>3</sub>O<sub>4</sub> anode)/Au nanoparticles (AuNPs) electrode was prepared by a ligand-mediated layer-by-layer method (**Figure 49a**), and the corresponding supercapacitors exhibited greatly enhanced energy (267.3 μWh cm<sup>-2</sup>) and power density (15.1 mW cm<sup>-2</sup>).<sup>648</sup> The AuNPs coating layer can convert insulating paper textiles into metallic current collectors, and the alternating strategy would help maintain high conductivity, despite the increased thickness of pseudocapacitive active materials with poor kinetics. Fabricating 3D carbon materials as frameworks for active metal compound deposition is another effective method to achieve the rapid operation of thick electrodes. A soft hybrid scaffold method was designed by using CNTs and reduced holey graphene oxides (rHGO) as substrates for pseudo material growth and conductive nodes, respectively (**Figure 49b**).<sup>649</sup> Of note, the CNTs here can not only help form the 3D conductive networks, but also block the agglomeration of nano pseudo materials (MnO cathode and FeOOH anode). These materials were then vacuum filtrated on carbon cloth to generate a 3D self-supported electrode, possessing the highest energy density (1.05 mWh·cm<sup>-2</sup>, 9.93 Wh·L<sup>-1</sup>) reported in aqueous wearable supercapacitors. Moreover, an inverse opaline metallic membrane served as another novel kind of 3D conductive networks was also fabricated through



a template and metallization (for the growth of active Ni(OH)<sub>2</sub> materials) strategy (**Figure 49c**), and the corresponding binder-free supercapacitors exhibit remarkable volumetric capacitance of 1,500 F cm<sup>-3</sup> over 18,000 cycles.

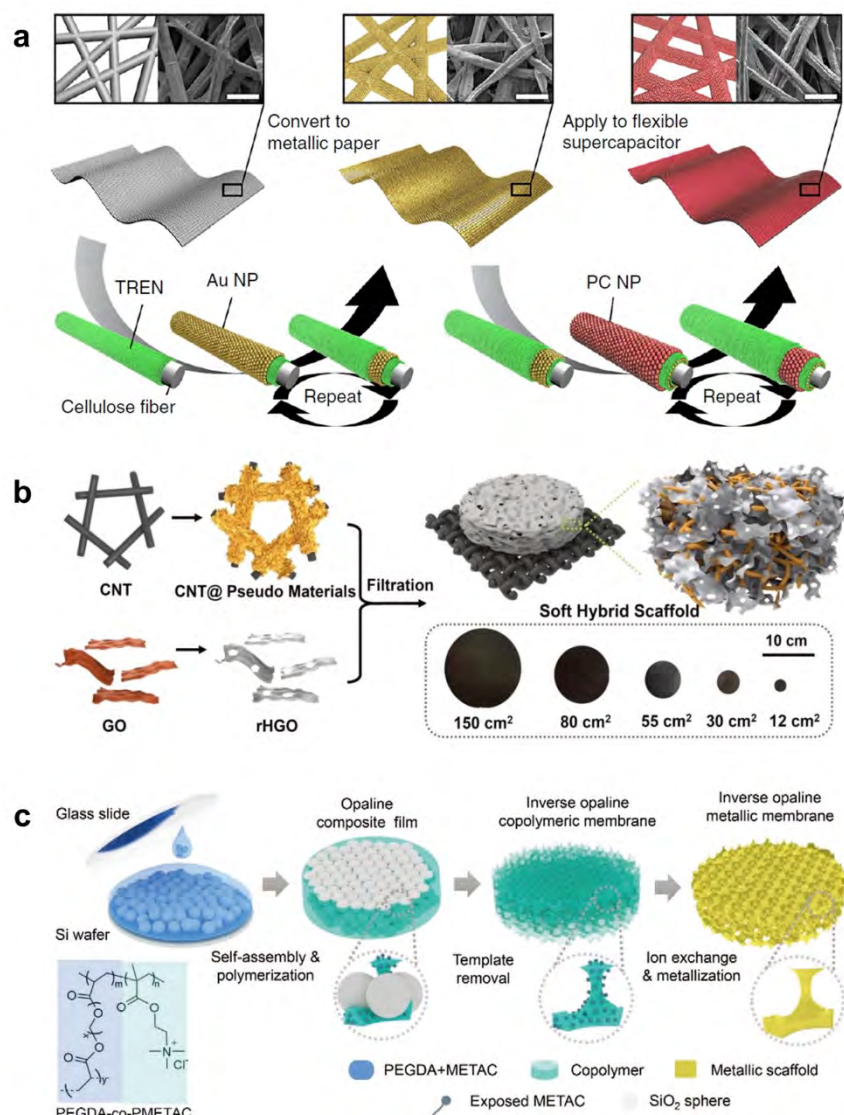


**Figure 49.** (a) Schematic for the preparation of the metallic paper-based supercapacitor electrodes. Reproduced with permission from ref <sup>648</sup>. Copyright 2017 Springer Nature. (b) Schematic for the fabrication of SHS@MnO<sub>2</sub> and SHS@FeOOH electrodes (SHS: soft hybrid scaffold). Reproduced with permission from ref <sup>649</sup>. Copyright 2017 John Wiley and Sons. (c) Schematic of the fabrication process of inverse opaline metallic membrane. Reproduced with permission from ref <sup>645</sup>. Copyright 2022 John Wiley and Sons.

**Conducting Polymers.** Though conducting polymers possess the advantages of low cost and environmental friendliness, their stability in supercapacitors remains challenging because of



their volume expansion issues during the charging/discharging process. Accordingly, designing high-capacitance conducting polymers and their composites with high conductivity and stability is the critical research direction. Conducting polymers used in supercapacitors mainly include PANI, PPy, PEDOT:PSS, and polyindole.<sup>650-653</sup> They are usually incorporated with carbon and metal materials in the fabrication of PCT-based supercapacitors. For instance, a lignosulfonate/polyaniline/functionalized graphene hydrogel/functionalized carbon cloth (Lig/PANI/FGH/FCC) electrode was fabricated by first chemical oxidation of carbon cloth, then hydrothermal assembly of FGH on FCC, and finally polymerization of aniline (ANI) in the presence of Lig.<sup>654</sup> The Lig/PANI/FGH/FCC electrode exhibits high energy density ( $160.6 \text{ mWh cm}^{-2}$  at  $1000 \text{ mW cm}^{-2}$ ) and excellent flexibility, originating from 3D conductive scaffolds constructed by FGH and extra capacitance coming from the oxidated Lig (**Figure 50a-b**). Yarn-shaped PCTs have also been demonstrated as current collectors for the assembly of supercapacitors through the incorporation of conducting polymer composites. A novel kind of PCTs, PPy@MnO<sub>2</sub>@rGO-deposited conductive yarns, was designed by firstly continuously producing soft conductive yarns with a twist-bundle-drawing technique and thereafter coating rGO, MnO<sub>2</sub>, and PPy on the yarns in turn (**Figure 50c**). The obtained PPy@MnO<sub>2</sub>@rGO-deposited conductive yarn electrode exhibited competitive specific areal capacitance ( $486 \text{ mF}\cdot\text{cm}^{-2}$ ) and energy density ( $1.1 \text{ mWh}\cdot\text{cm}^{-2}$ ), and the corresponding woven textiles with desirable flexibility can light 30 light-emitting diodes (LEDs) (**Figure 50d**).<sup>300</sup>

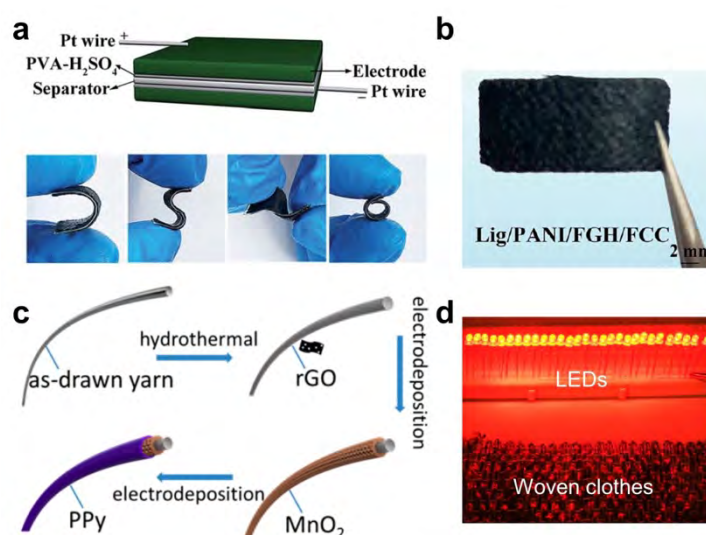


**Figure 50.** (a) Schematic illustration and optical images of the flexibility of the Lig/PANI/FGH/FCC supercapacitors. (b) Optical images of the Lig/PANI/FGH/FCC electrode. Reproduced with permission from ref <sup>654</sup>. Copyright 2019 Royal Society of Chemistry. (c)

Illustration of the preparation of PPy@MnO<sub>2</sub>@rGO composites. (d) Photographs of the supercapacitors textiles can light 30 LEDs. Reproduced with permission from ref<sup>300</sup>. Copyright 2015, American Chemical Society.

### 3.4.6 Batteries

Although the energy density of the state-of-the-art commercial LIBs can be as high as 300 Wh kg<sup>-1</sup>, they are normally rigid without satisfactory flexibility.<sup>655-657</sup> Despite the low yield strain of active materials, the porosity and binders in electrodes endow the acceptable deformation ability of batteries.<sup>658</sup> Accordingly, current collectors with relatively low yield strain (Al, 0.9%; Cu, 1.2%) are the main bottleneck for flexible batteries.<sup>546</sup> PCTs such as carbon cloth and metallic textiles can serve as ideal current collectors applied in flexible batteries.<sup>659, 660</sup> They can offer outstanding flexibility with yield strain typically over 5%, rendering the as-made battery flexible. Firstly, the high yield strain of PCTs (normally more than 5%) can endow the ideal flexibility of batteries.<sup>546</sup> More importantly, the desired porosity and conductivity of PCTs can not only largely improve the kinetics of electrodes but also enable an ultrahigh active material loading. The formation of a textile composite electrode, which is an interconnected fibrous matrix composited with active materials, can ensure rapid charge transfer (**Figure 51**).<sup>46</sup> This means both the energy and power density would be enhanced simultaneously by using the PCT-based current collectors. Of note, though PCTs themselves normally would increase the volume of current collectors, they are still potential candidates for flexible batteries considering both energy density and flexibility, according to a figure of merit (FOM) suggested by Zheng's group.<sup>546</sup> The key point in this section is how to integrate active materials into PCTs. Typical methods to prepare alkali metal anodes, conversion anodes or cathodes, and intercalation anodes or cathodes, are introduced in detail.

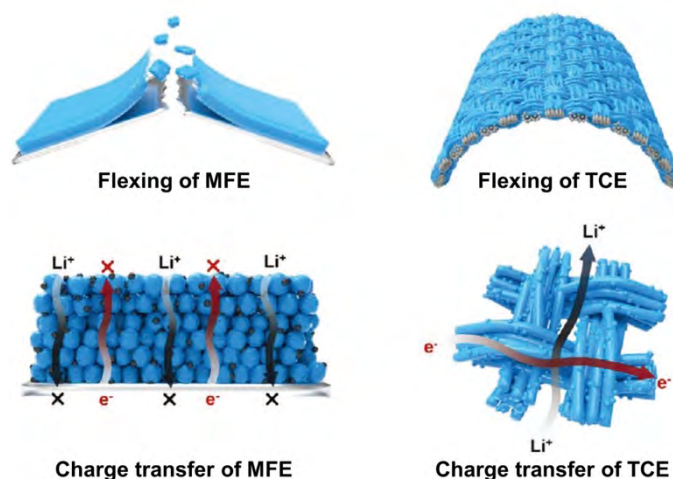


**Figure 51.** Schematic of rapid kinetics of thick electrode by using PCTs. The MFE and TCE represent metal-foil-supported electrodes (MFEs) and textile composite electrodes (TCEs) respectively. Reproduced with permission from ref <sup>46</sup>. Copyright 2021 John Wiley and Sons.

**Alkali Metal Anodes.** Metal anodes such as Li metal with very high capacity ( $3860 \text{ mAh g}^{-1}$ ) and low potential ( $0 \text{ V vs. Li/Li}^+$ ) can be used to largely enhance the energy density of batteries, whereas their dendrite formation and low Coulombic efficiency cause the severe safety issues and poor cycling stability of metal batteries.<sup>661</sup> The combination of metal anodes and PCTs by melting infusion or electrochemical deposition method is one popular strategy due to the 3D host and lithiophilic positions of PCTs for metal nucleation and growth. Nevertheless, pure carbon-based PCTs such as carbon fabrics normally exhibit poor affinity to metal anodes.<sup>662</sup> Further deposition of a metallic layer onto carbon-based PCTs has been proven to promote the affinity to metal anodes, while exhibiting greatly enhanced mechanical property and conductivity.<sup>165</sup> For instance, the first example of flexible Li-S battery based on metallic carbon-based PCTs with only 100% oversized lithium was reported, exhibiting high energy density ( $288 \text{ Wh kg}^{-1}$  and  $360 \text{ Wh L}^{-1}$ ), excellent cycling stability (260 cycles), and desirable flexibility.<sup>663</sup> Cu-coated and Ni-coated carbon cloth were prepared by the PAMD method and were used as hosts for lithium anode and sulfur cathode, respectively (**Figure 52a**). The Cu coating layer can improve the lithiophilic property of carbon cloth, enabling the nanosheet nucleation behavior without the formation of lithium dendrites. On the cathode side, the Ni layer would catalyze the conversion between S and  $\text{Li}_2\text{S}$ , endowing largely improved kinetics and rate capacity. Actually, the controllable alkali metal electrochemical plating is also valuable for metal batteries. An inverted anode structure with metal coating layer on only one side of current collectors far away from separator was designed, enabling the bottom-up lithium

deposition mode, which would reduce the short-circuit risk of the battery (**Figure 52b**).<sup>664</sup> Moreover, the metal in the coating layer which can alloy with alkali metal would further enhance the plating/stripping efficiency of metal anodes. For instance, the NiSb-coated carbon cloth was developed by PAMD and galvanic displacement method, where the generation of Na-Sb alloy can facilitate the smooth deposition of sodium metal (**Figure 52c**).<sup>664, 665</sup>

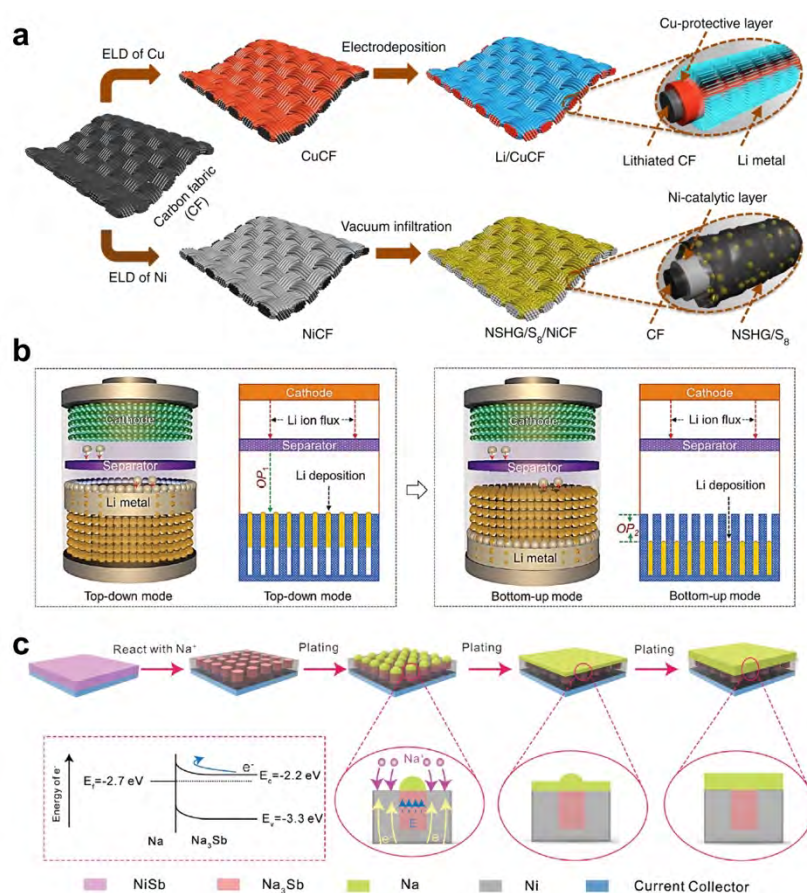


**Figure 52.** (a) Schematic of the fabrication process for the Li metal anode and S cathode. Reproduced with permission from ref <sup>663</sup>. Copyright 2018 Springer Nature. (b) Schematic of the fabrication process of the inverted Li metal anode. Reproduced with permission from ref <sup>664</sup>. Copyright 2022 John Wiley and Sons. (c) Schematic of the self-regulating mechanism of Na metal. Reproduced with permission from ref <sup>665</sup>. Copyright 2021 John Wiley and Sons.

**Conversion Anodes and Cathodes.** Common conversion anodes mainly include metal oxides (*e.g.*, Fe<sub>2</sub>O<sub>3</sub>, SnO<sub>2</sub>) and sulfides (*e.g.*, SnS, VS<sub>2</sub>),<sup>666-669</sup> whereas cathodes include metal fluorides (*e.g.*, FeF<sub>3</sub>, FeF<sub>2</sub>) and V<sub>2</sub>O<sub>5</sub>.<sup>670-674</sup> Although conversion materials with relatively high capacity (normally 500~1500 mAh g<sup>-1</sup> for anode, 300~1000 mAh g<sup>-1</sup> for cathode) and suitable working voltage (0.5~1.5 V for anode, 2~4 V for cathode) are hot topics in the battery area,

large volume expansion and unstable solid electrolyte interphase (SEI) during cycling remain challenging. Morphology and size control by wet chemical methods are the main strategies, for example, the utilization of nanomaterials or hollow structures can be able to buffer the strain caused by charge-discharge cycles. For instance, cotton textiles embedded with  $\text{NiS}_2$  nanobowls were fabricated through a two-step heat treatment method, which was used as self-supported electrodes in flexibility LIBs.<sup>675</sup> The cell exhibited excellent cycling performance ( $\sim 1016 \text{ mAh g}^{-1}$  at  $0.1 \text{ C}$  after 400 cycles) and acceptable flexibility, originating from the flexible carbon cloth substrates and special nanostructure of active materials, enabling the rapid ion diffusion and high electrode stability (**Figure 53a**). Furthermore, defective hydrated vanadium oxide grown on porous carbon textiles (d-VOH@CT) was fabricated by a sequential pyrolysis and natural oxidation approach, which was used as cathode for flexible Zinc-ion battery (ZIB) (**Figure 53b**).<sup>671</sup> The obtained cell exhibited a desirable reversible capacity ( $416 \text{ mAh g}^{-1}$  at  $0.1 \text{ A g}^{-1}$ ), high energy density ( $293 \text{ Wh kg}^{-1}$ ), and long cycle life with excellent mechanical robustness (**Figure 53c-d**), resulting from the enlarged interlayer spacing and reduced crystal size, which can effectively accelerate Zn-ion diffusion.

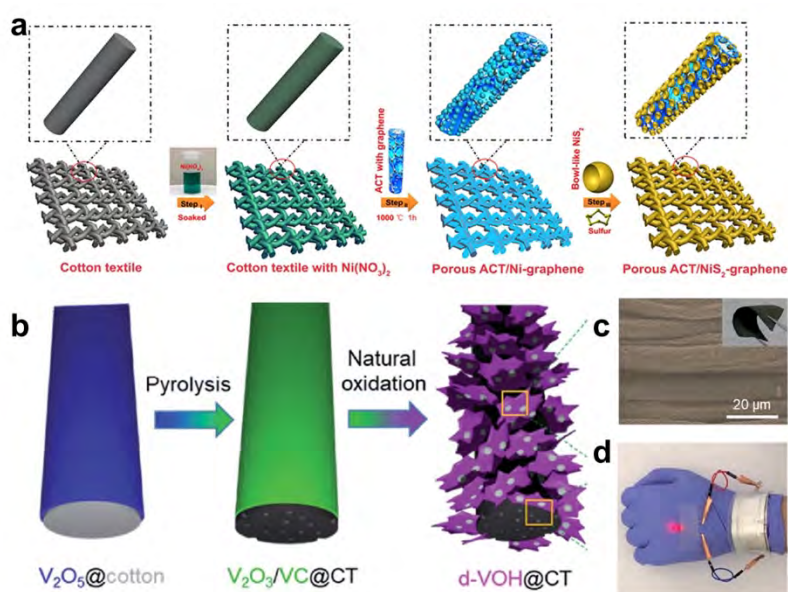


**Figure 53.** (a) Schematic illustration of the preparation of ACT/NiS<sub>2</sub>-graphene composite (ACT: active carbon textile). Reproduced with permission from ref <sup>675</sup>. Copyright 2015, American Chemical Society. (b) Schematic illustration of the preparation of d-VOH@CT heterostructure. (c) SEM images of the d-VOH@CT. (d) Wearable application of the flexible ZIBs. Reproduced with permission from ref <sup>671</sup>. Copyright 2022 Royal Society of Chemistry.

**Intercalation Anodes and Cathodes.** Intercalation anodes (graphite and  $\text{Li}_4\text{Ti}_5\text{O}_{12}$ ) and cathodes (layer-typed  $\text{LiCoO}_2$ , spinel-typed  $\text{LiMn}_2\text{O}_4$ , and olivine-typed  $\text{LiFePO}_4$ ) with remarkable stability, are main materials for commercial LIBs. Therefore, the integration of these materials on PCTs is one of the most significant strategies for the commercialization of flexible batteries. Fiber LIBs are attractive as flexible power supply since they can be woven into textiles, which offers a convenient way to power wearable electronics. However, popular methods used in commercial batteries through layer-by-layer coating processes will render fiber batteries with low production rates. Hence, scalable methods including continuous fabrication and solution-extrusion were developed, accelerating the practical progress of fiber batteries. For instance, meters of fiber-typed lithium-ion full batteries with  $\text{LiCoO}_2$  cathode and graphite anode were produced by a scalable process (**Figure 54a-b**), displaying high energy density ( $86 \text{ Wh kg}^{-1}$ ), remarkable cycling stability (capacity retention: 90.5% after 500 cycles), and excellent flexibility (capacity retention: 80% after 100,000 bending cycles).<sup>80</sup> The fiber batteries woven into textiles can wirelessly charge a cell phone or power a health management jacket integrated with fiber sensors and a textile display (**Figure 54c**). Moreover, aqueous LIBs were designed by a continuous solution-extrusion method with three channels simultaneously extruding and combining electrodes and electrolyte (**Figure 54d-e**) at the industrial scale (length: 1,500 km).<sup>35</sup> The obtained battery delivers high energy density ( $550 \text{ mWh m}^{-2}$ ) and excellent flexibility (**Figure 54f**), originating from the stable electrode structure and excellent mechanical deformation ability. These two scaling preparation strategies make fiber batteries one of the most promising schemes for commercializing flexible batteries.



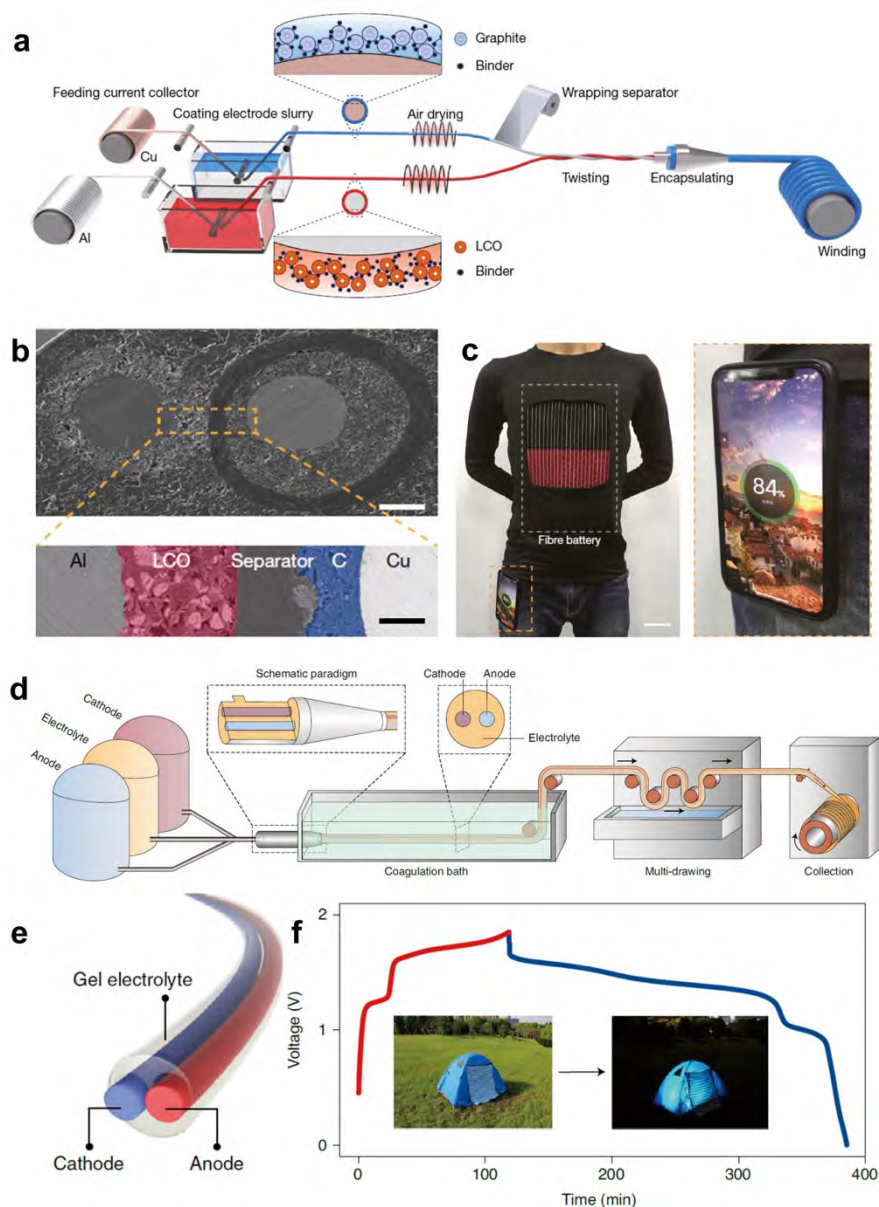


**Figure 54.** (a) Schematic of the set-up used to prepare fiber batteries. (b) Cross-sectional SEM image of the fiber batteries (scale bar, 100  $\mu\text{m}$ ). (c) Photograph of a shirt integrated with a fiber battery (scale bar, 15 cm). Reproduced with permission from ref <sup>80</sup>. Copyright 2021 Springer Nature. (d) Schematic showing the preparation of fiber batteries. (e) Schematic of a fiber battery. (f) Photo-charging (red line) by textile solar cells and discharging curves (blue line) of the textile batteries. Reproduced with permission from ref <sup>35</sup>. Copyright 2022 Springer Nature.

### 3.5 Displays

Flexible displays play a crucial role in wearable electronics for the real-time presentation of information, including notifications, health data, and navigation instructions. Electroluminescent and electrochromic devices are common optoelectronics that are capable



of emitting light or changing color, thus can serving as wearable displays.<sup>110, 676, 677</sup> In addition, these textiles with light-emitting or color-changing capabilities can also enhance aesthetics in smart clothing and find utility in camouflage.

### 3.5.1 Light-Emitting Devices

Textile-based displays can provide new opportunities for the fashion industry by integrating electronic displays into fabrics, creating new forms of wearable technology. These wearable displays can also revolutionize the way we interact and communicate by seamlessly integrating into our daily routines, allowing us to access information and communicate with others more easily and conveniently. Flexible displays rely on light-emitting devices, which emit lights upon applying a voltage on the electroluminescent devices.<sup>678</sup> According to the active luminescent materials and working mechanisms, there are several types of electroluminescent devices including inorganic light-emitting diode (ILED), organic light-emitting diode (OLED), polymer light-emitting diode (PLED), light emitting electrochemical cell (LEC), and alternating current electroluminescent (ACEL) devices.<sup>678-681</sup>

The ILEDs, OLEDs, and PLEDs have similar working principle and device configuration, but differ in their core materials. The ILEDs uses inorganic semiconductors (*e.g.*, GaAs and GaN), while the OLEDs use conjugated small molecules and the PLEDs use conjugated polymers as the active luminescent materials.<sup>676</sup> The typical structure of these devices involves a series of layers, including cathode, electron injection, emissive, hole injection, and anode layer. When a DC voltage is applied to the active luminescent material, electrons and holes are injected into the material and recombine to produce excitons. These excitons then relax to the ground state, releasing energy in the form of light.<sup>682</sup> The OLEDs and PLEDs that employ organic and polymeric luminescent materials are more easily fabricated into fiber-based devices and demonstrate better flexibility.<sup>683</sup> The active materials can be readily coated onto the fibers using simple solution processes like dip-coating. Additionally, the OLEDs and PLEDs require much lower operating voltages while exhibiting higher brightness than the ILEDs. Textile-based electroluminescent devices can be generally fabricated in two architectures: 1) planar multilayer architecture, where the PCTs serves as the substrate and/or bottom electrode,<sup>684</sup> and 2) fiber-shaped coaxial architecture (**Figure 55**).<sup>685</sup> However, while the planar structure is easy to process, its multilayer structure with a relatively large thickness can result in the loss of inherent properties of textile such as porosity and flexibility. On the other hand, the electroluminescent fiber can be further weaved or knitted to form a large-scale light-emitting

textile.

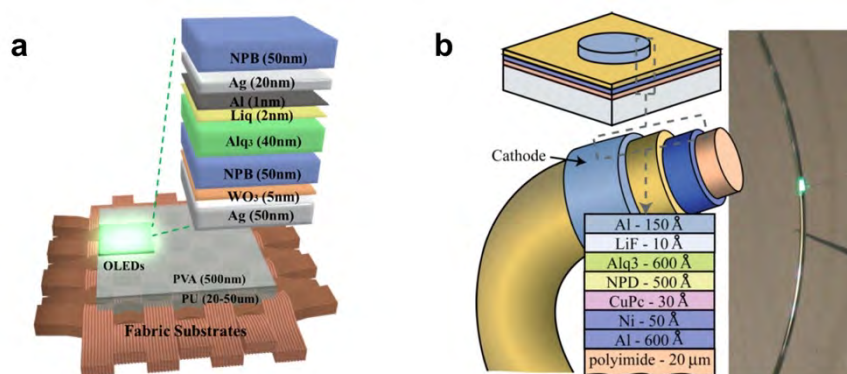


**Figure 55.** (a) Schematic diagram of a planar fabric OLED using a textile as the substrate, Reproduced with permission from ref <sup>684</sup>. Copyright 2013 Elsevier. (b) Schematic diagram of the structure of a coaxial fiber-shaped OLED. Reproduced with permission from ref <sup>685</sup>. Copyright 2007 John Wiley and Sons.

The LECs have a similar structure to OLEDs, but they incorporate additional ionic materials such as ionic salts and transition metal complexes.<sup>686</sup> Due to the unique ion mobility mechanism, LECs typically operate at a low voltage, exhibit high electron-to-light conversion efficiency, and have high power utilization. Recently, Zhang *et al.*<sup>687</sup> reported a novel fiber-shaped polymer-based LEC (PLEC), which has a coaxial structure including a modified metal wire cathode, a conducting aligned CNT sheet anode, and an electroluminescent polymer layer sandwiched between them (**Figure 56a-c**). The electroluminescent polymer layer is composed of a blend of a blue light emitting polymer (PF-B), ethoxylated trimethylpropane triacrylate (ETT-15) and lithium trifluoromethane sulphonate (LiTf), and it was deposited on the modified steel wire using the dip-coating method. The resulting fiber-shaped PLEC is lightweight, flexible and soft, and can be woven into light-emitting textiles for large-scale applications.

Unlike the electroluminescent devices described above, ACELs are another type of LED device that operates on alternating current (AC) voltage.<sup>688</sup> ACEL devices employ a simple sandwiched configuration, in which a luminescent layer is sandwiched between two transparent conductive electrodes.<sup>689</sup> The luminescent layer is typically composed of doped zinc sulfide (ZnS) phosphor dispersed in a dielectric elastomer.<sup>690</sup> Therefore, the simple configuration enables the design of ACEL arrays with high pixels through inter-weaving fiber electrodes and luminescent fibers.<sup>691</sup> By employing this strategy, Shi *et al.*<sup>81</sup> developed a large-area display

textile. As illustrated in **Figure 56d**, the electroluminescent unit is constructed at the fiber crossover point of luminescent warp and transparent conductive weft. The conductive weft fibers are produced by melt-spinning ionic-liquid-doped polyurethane gel, while luminescent warp fibers are produced by coating commercially available ZnS phosphor on a silver-plated conductive yarn. The electric fields at the contact points or crossover points are stable and uniform, enabling the textile to display stably. A 6 m-long and 25 cm-wide textile display containing  $5 \times 10^5$  electroluminescent units was realized, demonstrating its large-scale fabrication with decent resolution (**Figure 56e-h**). The textile display is flexible, breathable, and can withstand repeated machine washings, making it suitable for practical applications in navigation or healthcare displays. This endeavor represents a significant leap forward in the scalable fabrication of textile displays, which is highly promising to open avenues for practical applications and shape the next generation of wearable electronics.

Despite significant advancements in light-emitting fibers and textiles, the optical performance of interwoven textile displays still lags behind modern display technology, especially in terms of brightness and resolution. However, textile-based displays have the potential to seamlessly integrate wearable electronics into our daily lives, creating new opportunities for fashion and technology.<sup>692</sup> Through the development of new luminescent materials, innovative weaving microstructures, and promising integration methods, high-performance textile displays may become the next-generation display technology for everyday use.

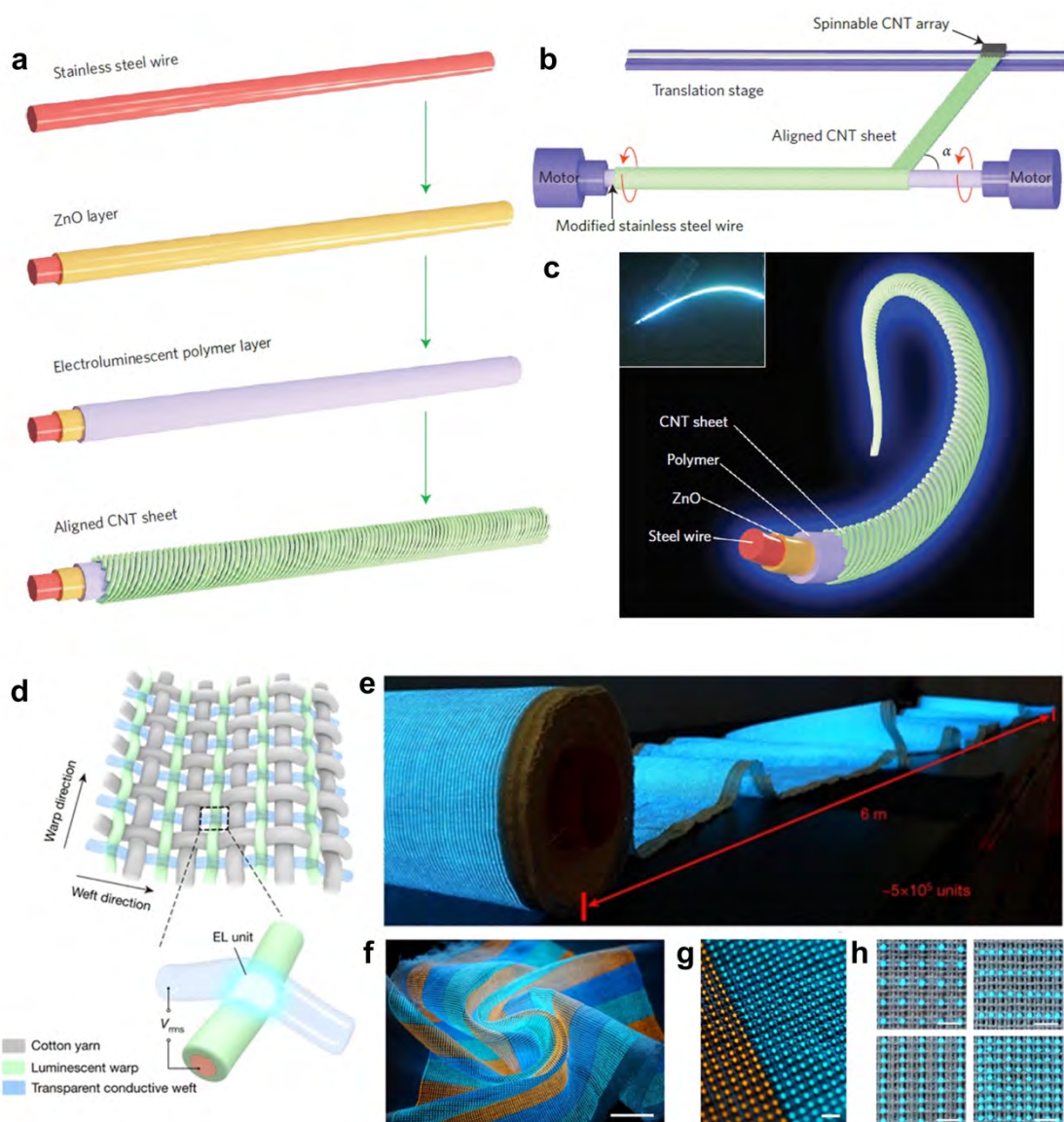


**Figure 56.** (a) Schematic of fabrication of a fiber-shaped PLEC, (b) schematic of wrapping an aligned CNT sheet around a modified stainless-steel wire, (c) schematic of the structure of a flexible fiber-shaped PLEC. Inset: photograph of a fiber-shaped PLEC biased at 10 V. Reprinted with permission from ref <sup>687</sup>. Copyright 2015 Springer Nature. (d) Schematic showing the weave diagram of a display textile. Each contacting luminescent warp and transparent conductive weft forms an EL unit (inset). An applied alternating voltage turns on the EL units. (e) Photograph of a 6-m-long display textile consisting of approximately  $5 \times 10^5$  EL units. (f) Photograph of a functional multi-color display textile under complex deformations, including bending and twisting. Blue and orange are achieved by doping ZnS with copper and manganese, respectively. Scale bar, 2 cm. (g) Magnified photograph of the multi-color display textile shows that the EL units are uniformly spaced at a distance of  $\sim 800 \mu\text{m}$ . Scale bar, 2 mm. (h) Photographs of EL units spaced at different distances, obtained by changing the weave

parameters. Scale bars, 2 mm. Reprinted with permission from ref <sup>81</sup>. Copyright 2021 Springer Nature.

### 3.5.2 Electrochromic Devices

Electrochromism refers to a phenomenon where a material's optical properties, such as color or transparency, are altered by an applied electric charge.<sup>677</sup> Electrochromic textiles have diverse applications, including smart windows, displays, eyewear, and camouflage.<sup>693, 694</sup> These devices usually consist of several layers, including an electrochromic electrode layer, a counter electrode layer, an electrolyte layer, a transparent conductive layer, and a support substrate. Applying a voltage to the electrochromic layer induces its oxidation or reduction, leading to a change in the material's optical properties. By applying a reversible voltage, the electrochromic layer can return to its original state and color. Transition metal oxides (*e.g.*, WO<sub>3</sub>, NiO, and V<sub>2</sub>O<sub>5</sub>) and conducting polymers (*e.g.*, PANI, PEDOT:PSS) are commonly used electrochromic materials.<sup>270, 695, 696</sup> Sinha *et al.*<sup>697</sup> demonstrated a single layer printed electrochromic textile by using a PCT substrate, which is prepared by screen printing PEDOT:PSS on a textile. The electrochromic polymer, a copolymer of 3,4-bis(2-ethylhexyloxy) thiophene and 3,4-dimethoxythiophene, was then spray-coated onto the PEDOT:PSS-based PCT. The resulting device was able to switch between red and blue colors at -1 and 2 V, respectively (**Figure 57a**), the switch occurred quickly and was cyclically reversible (**Figure 57b**). In addition, the authors also demonstrated the use of a wireless power system to control the electrochromic textile (**Figure 57c-e**).

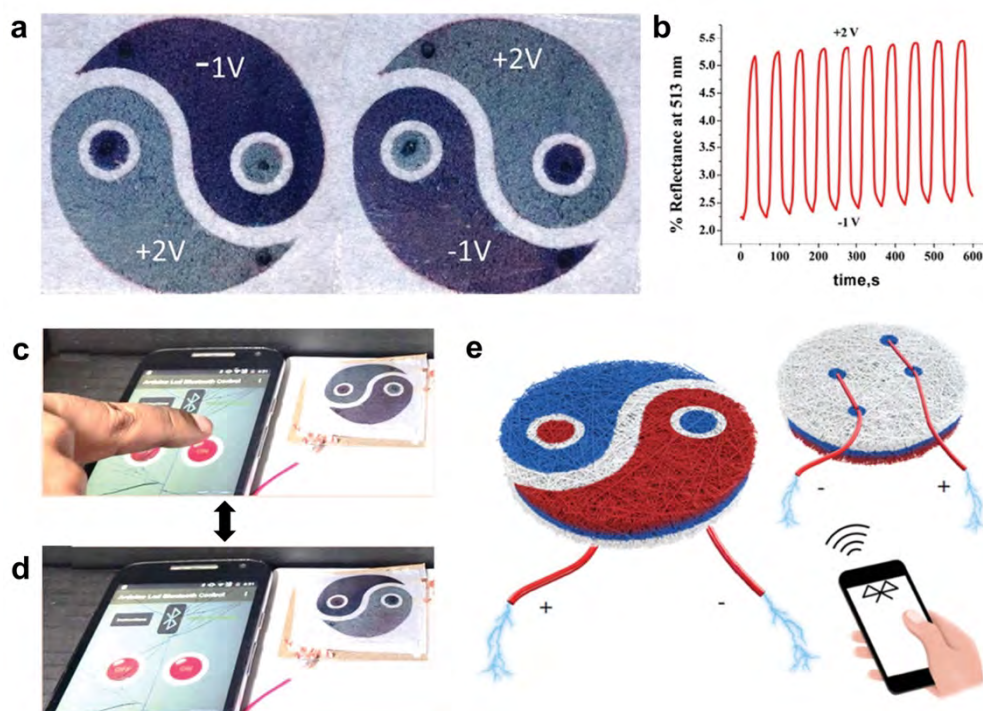


**Figure 57.** (a) Electrochromic Yin-Yang design with back connections. (b) Kinetic stability of device over 10 cycles of switching monitored at 513 nm. (c, d) Switching of Yin-Yang device from a Bluetooth-enabled phone app. (e) Cartoon illustration of wireless device depicting front of device and back connections. Reproduced with permission from ref<sup>697</sup>. Copyright 2022 John Wiley and Sons.



#### 4 INTEGRATED WEARABLE SYSTEMS BASED ON PCTS

The integration of electronic components onto textiles can be categorized into three levels (**Figure 58**).<sup>316</sup> At the 1<sup>st</sup> level, conventional off-the-shelf electronic components are simply attached to a garment. The first example can date back to the use of electric light headband with battery concealed in the dancing clothing that debuted in the ballet *La Farandole* in 1883.<sup>7</sup> Later, smart textiles were developed in this way. For example, fiber-optic lights and a microprocessor were embedded into a sweatshirt to control the pattern of lights on the garment. However, garments created using this level of integration are relatively bulky, limiting comfortability and durability. While at the 2<sup>nd</sup> level of integration, commercial microelectronics are integrated onto textiles. This involves the integration of miniaturized silicon-based electronic components such as sensors, microcontrollers, and communication modules into the textile system using flexible and stretchable conductive interconnects. However, the mechanical durability of hybrid electronics at this level is yet to be mature and relies on the material and structural design. On the other hand, the 3<sup>rd</sup> level involves the integration of electronic fibers and yarns to incorporate multiple functions into a wearable system. This can be achieved through techniques like braiding, stitching, weaving, or knitting these fibers and yarns. Functional materials or devices can also be integrated into textile substrates using printing methods. In comparison to the hybrid wearable systems at the 2<sup>nd</sup> level, the approaches at the 3<sup>rd</sup> level enable a seamless integration of all stretchable and conformable components into the textile, preserving its porous and permeable nature. As the integration level increases, wearing comfort significantly improves, while compatibility with standard microfabrication processes decreases. Although fiber-based electronic textiles offer the highest conformability and wearing comfort, their fabrication processes are often tedious and incompatible with microfabrication techniques. However, fabric-based integration with commercially available microelectronics facilitates standard scale-up production. Additionally, to ensure the durability of fiber-based electronic textiles, it is necessary to develop new strategies that refine the material and structural design.

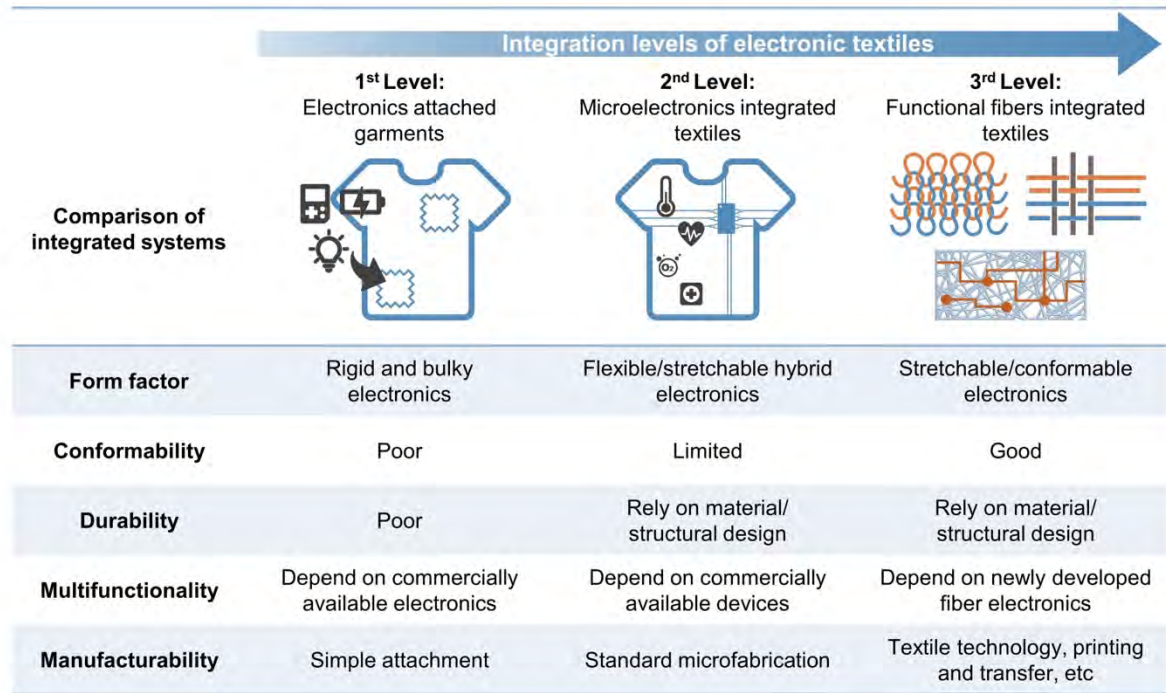


**Figure 58.** Three integration levels of electronic textiles.

#### 4.1 Hybridizing Microelectronics with PCTs

Besides developing intrinsically flexible/stretchable materials and/or structures, integrating existing off-the-shelf electronic components onto flexible textiles represents another promising way to achieve high flexibility and stretchability. Wearable hybrid electronic systems, integrating various rigid functional units on porous, flexible, stretchable, and conformable substrates via stretchable interconnects, have the capacity of sensing, actuating, powering, communicating, *etc.* Compared with the components with intrinsic softness and stretchability that are researched in recent years, rigid semiconductor-based electronic components have been well developed and can be fabricated in large scale, meanwhile showing much better performance than the soft ones. Therefore, the fabrication of PCTs electronic systems by using rigid electronics and unique structural designs are of great interest.

##### 4.1.1 Microelectronics Integrated Hybrid Systems

In general, it is possible to integrate commercial functional electronic components including integrated circuits (ICs), electrodes, and printed circuits onto fabric substrates to form a hybrid textile electronic system via electrical bonding. Such kind of hybrid electronic circuits are composed of discrete functional parts with small dimensions, which could reduce the mechanical stiffness on specific areas of the fabric and improve the imperceptibility of the

device on humans when compared to the conventional bulky devices. In addition, the soft, compliant, and porous nature of textile circuits endows the stretchable hybrid electronics with non-destructiveness and wearing comfort.

However, due to the loose nature and rough surface of the textiles manufactured by traditional processes, high-resolution integration of rigid electronic components is difficult to be achieved. To fabricate hybrid electronic circuits with high resolution, one approach is to integrate the electronic components on conventional thin-film-based substrates, followed by integrating the thin-film circuits onto textiles. In this strategy, microelectronics are integrated into flexible thin-film substrates using a process closer to standard microfabrication. Commonly used flexible substrates include PI, PET, and polyethylene naphthalate (PEN) films. Among them, PIs are most extensively used because of their high thermal stability and stable mechanical properties. Cherenack *et al.*<sup>698</sup> developed a smart textile band by combining textiles with thin-film-based electronic fibers. The smart textile band developed was integrated into a tablecloth, where the LED electronic fibers can indicate the temperature or humidity sensor signals within the textile (**Figure 59a**). The electronic fibers were fabricated by cutting flexible PI (50- $\mu\text{m}$  thick) substrates into 5-cm-long and <2-mm-wide fibers. Then, interconnect lines, contact pads for loading integrated circuits, thin-film sensors, and transistors were integrated onto the surface of individual PI fibers by standard microfabrication techniques (**Figure 59b**). The electronic fibers were inserted into the textile along the weft direction using a commercial weaving machine and the smart electronic textile was formed (**Figure 59c**). An encapsulation layer of PI or PE for the electronic fibers was developed. Bending tests showed that the interconnect lines encapsulated ruptured at a radius below 100  $\mu\text{m}$  and the flexible thin-film transistors (TFT) loaded strip with encapsulation can be bent to a radius of 0.25 cm before electrical failure (**Figure 59d**). This suggested that the fabricated fibers can withstand friction during weaving and mechanical stress when worn as clothing.

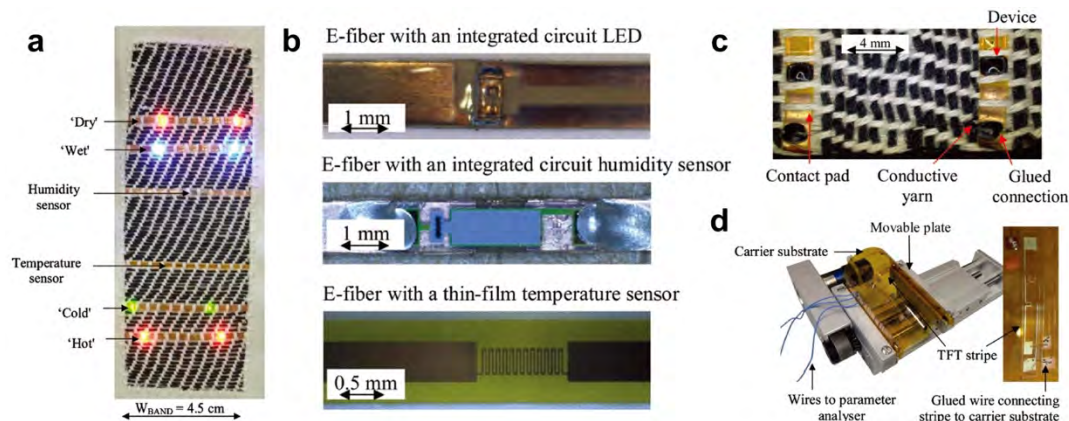


**Figure 59.** Flexible electronics integrated woven smart textile for sensing and display. (a) A smart textile band containing LED electronic fibers, temperature sensors, and humidity sensors was integrated into a table cloth. (b) Close-up views of sensors and LED chips on electronic fibers. (c) Photograph of the textile containing woven electronic fibers with sensor integrated circuits. (d) The TFT bending set-up showing a loaded TFT stripe for bending tests. Reproduced with permission from ref <sup>698</sup>. Copyright 2010 John Wiley and Sons.

Wicaksonol *et al.*<sup>699</sup> developed an electronic textile integrated with multimodal physiological (temperature, heart rate, and respiration) sensing system by using standard, accessible and high-throughput textile manufacturing and garment patterning techniques (**Figure 60a**). Flexible-stretchable electronic strips consisting of sensor ICs soldered on PI substrate and interconnected by serpentine-shape Cu traces were embedded in the textile channels by weaving technique. Then entire sensing module was encapsulated by a commercial TPU shell on both sides for washing stability (**Figures 60b-d**). Moreover, a commercial main hub for powering, processing, and wireless communication through I<sup>2</sup>C bus interface was used to connect all sensor modules with four thin copper wires (VDD, SCL, SDA, GND) (**Figure 60e**). The main hub is pluggable and can be connected to the textile through conductive snap button, which endowed the electronic textile with full circuitry performance while maintaining the reliability to machine washing.

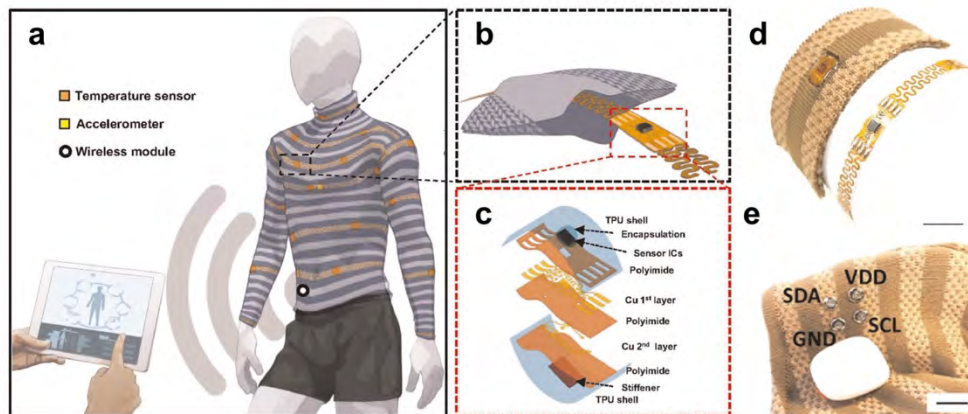


**Figure 60.** An integrated electronic textile system for distributed sensing wirelessly. (a) Illustration of concept of an electronic textile that monitors the human skin surface temperature distribution, heart rate, and respiration. (b) Illustration of a textile channel for embedding flexible-stretchable electronic strips. (c) Exploded diagram of a sensor island. (d) Photograph of a bare flexible-stretchable electronic strip (right) and a woven electronic strip in a knit textile (left) (scale bar: 1 cm). (e) Exploded view of the pluggable main processing and communication module (scale bar: 2 cm). Reproduced with permission from ref <sup>699</sup>. Copyright 2020 Springer Nature.

Though the flexible hybrid electronics can be integrated into textiles for promising applications such as environment monitoring and personalized health monitoring, they still face the issue of unconformable to human skin since they could hardly comply to the complex 3D curvatures of the body. As such, stretchable hybrid electronics by using stretchable substrates are desired for the integration of electronic wearables. An “island-bridge” design is developed to achieve flexible and stretchable hybrid electronics by integrating rigid microelectronics onto soft and stretchable substrates.<sup>700</sup> The “island” refers to flexible but non-stretchable positions hosting rigid electronic components distributed on the substrate, such as electrodes, sensors, actuators, displays, antennas, power supply and storage, flexible circuit boards, *etc.* The “bridge” refers to flexible and stretchable conductive tracks embedded in the fabrics. These conductive interconnects can be fabricated by traditional textile manufacturing processes such as weaving, knitting, embroidery, and stitching. Drawbacks of these processes include the limited designs of the circuit since the fiber/yarn could only follow the warp or weft directions in weaving/knitting, and the circuit resolution using embroidery and stitching is limited as well. Another way to add circuit interconnects in a textile is the patterning of conductive materials such as conductive inks or pastes by stencil printing, screen printing, inkjet printing, and direct

writing. Well-designed patterns with high patterning resolution can be achieved in this way. However, the strain applied on the textile substrate will be transmitted to the interconnects and cause mechanical failures. Structural designs for the interconnects such as wave, serpentine, 3D helix, origami and Kirigami have been reported.<sup>701-704</sup> The device integration for stretchable hybrid electronics is through bonding the rigid electronics islands onto the flexible and stretchable interconnects bridges on the soft fabric substrates.

Most of the soft and thin stretchable substrates applied in previous work are silicone elastomers, such as PDMS and Ecoflex, while they are impermeable that may lead to uncomfortable sensations and skin irritations. To create electronic textile systems that are both permeable and comfortable, new substrate materials have been employed. One of such materials is micro/nanofiber-based fibrous membranes fabricated by electrospinning. These membranes have been developed and used as stretchable and permeable platforms to integrate electrical interconnects, electrodes, and electronic components.<sup>705, 706</sup> For example, a permeable and stretchable electrode was prepared by printing and pre-stretching LM onto an electrospun fiber mat.<sup>24</sup> The resulting LM fiber mat showed excellent air and moisture permeability, superelasticity, and ultrahigh conductivity, addressing the trade-off between permeability and fabrication resolution of electronic textiles.

An integrated hybrid wearable system mainly contains three parts, *i.e.*, PCTs as substrates, flexible and stretchable interconnects, and rigid microelectronics. It is critical yet challenging to integrate the rigid electronic components onto PCTs for efficient and scalable manufacturing of integrated systems. Approaches for bonding rigid electronics and strategies for enhancing the bonding strength of rigid components on PCTs will be discussed.

#### **4.1.2 Connection of Rigid Electronics on Textiles**

Generally, the integration of commercial off-the-shelf ICs or miniaturized electronics on textile substrates can be achieved by soldering, welding, mechanical gripping, and adhesives bonding.<sup>707</sup>

**Soldering.** Soldering has been widely used to join different types of electronic components on textiles substrates including fabrics with printed conductive patterns, metallic threads and wires.<sup>708-710</sup> Since most textile materials will melt or deform at temperatures even lower than 250 °C, low-temperature soldering materials are needed for electronic bonding in PCTs.<sup>708</sup> Sn-



and In-based alloys are commonly used solders with low melting point ( $T_m$ ). For example,  $\text{Sn}_{42}\text{Bi}_{58}$  is a representative low-temperature solder for textiles owing to its low melting point of 138-139 °C and low cost.<sup>711,712</sup> However, the brittleness and poor wettability of Sn-Bi solder hinders its application. In contrast, In-based alloys have lower melting point ( $T_m$  of  $\text{In}_{52}\text{Sn}_{48}$  is 118 °C), higher ductility, and wettability.<sup>713</sup> Besides, by adding trace amounts of other elements such as Ag, Sb, Zn and rare-earth elements (Ce, La) into the eutectic Sn-Bi alloy, the melting temperature can be reduced, and the ductility and wettability can be improved.<sup>711</sup> A study was conducted to select low-temperature solder pastes for the integration of a circuit on textile substrate.<sup>708</sup> It was found that the Sn-Bi-Ag alloy ( $\text{Sn}_{42}\text{Bi}_{57}\text{Ag}_1$ ) showed better results than the other three commercially available solders of  $\text{Sn}_{48}\text{In}_{52}$ ,  $\text{Sn}_{42}\text{Bi}_{58}$  and  $\text{Sn}_{42}\text{Bi}_{57.6}\text{Ag}_{0.4}$ .

The reliability of the soldering relies on the bonding interaction between the solder and the textiles and the conductive interconnects. Molla *et al.*<sup>714</sup> integrated surface-mounted device (SMD) LED into textiles by soldering conductive threads stitched on a fabric using reflow process. Two circuits consisting of 5 LEDs, were created in “parallel” and “perpendicular” layouts, respectively. The perpendicular traces showed better performance and durability than the parallel ones (**Figure 61a**). They found the electrical failure occurred in several parts, including the connections between the solder joint and LED lead, between the solder joint and thread trace, within the solder joint, and within the LED package (**Figure 61b**). It was also found that bigger LED package size, thicker conductive traces and larger LED pad size helped to reduce the failure rate. However, these could lead to the limited flexibility and resolution of the circuit in the textile. To improve the performance of the soldered connection, several techniques besides direct soldering have been reported, such as infrared soldering, laser soldering, and ultrasonic soldering.<sup>715-717</sup>

EGaIn, which is a kind of room-temperature LM, can be used as both the solder and conductive interconnect to integrate microelectronics into textile substrates without a heating process. For example, EGaIn was printed on the permeable and stretchable electrospun fiber mat and LED arrays were mounted on the EGaIn pattern.<sup>24</sup> Due to the high conductivity and stretchability of LM, the LED array performed stably underwater in both released and stretched states. With patterning techniques such as stencil printing, direct writing and spray coating using pre-designed masks, and transfer printing, LM connections with higher resolution can be achieved.<sup>718-720</sup>

**Mechanical Gripping.** Mechanical gripping is a physical approach to make bonding between electronic components and PCTs at room temperature. Detachable connectors such as snap fasteners are usually integrated into the electronic textiles by mechanical gripping methods such as crimping, stapling, and embroidery.<sup>721</sup> Crimping is a process of deforming a metal with force to hold and connect to another piece of deformable conductor. Crimp terminals instead of standard lead wires were connected to textiles for the integration of electronics.<sup>721, 722</sup> This method is useful for the integration in large-area textiles, though it is not a good approach to integrate miniaturized electronics. Moreover, the connections are rigid and difficult to be compatible with the flexible and stretchable PCTs substrate.

Sewing and embroidery performed by hand or machine are common ways to join conductive yarns on fabrics with electronics. Electronic through-hole components can be sewn into the conductive yarns directly.<sup>723</sup> For some cases the through-hole size of electronics is not suitable for needlework, a metallized flexible contact pad with pierced holes will be useful.<sup>724</sup> The commercial product “LilyPad” is a sewable microcontroller board that can provide connections between textiles and various electrical components.<sup>725</sup> To make SMD components sewable, metallic crimping beads were attached to the SMD LED by soldering (**Figure 61c**). The resulting LED sequins could then be stitched on fabrics easily.<sup>726</sup> To facilitate the connection of pluggable devices such as microcontroller to textiles, socket buttons with through holes were sewn on the fabrics with conductive thread (**Figure 61d**).<sup>726</sup> Further, computer-aid design (CAD) is a useful tool for embroidery to improve the integration productivity and quality control, which makes the production of commercial wearable electronics by machine embroidery possible.<sup>723, 727</sup>

**Adhesives.** Adhesives can form strong adhesion to various substrates including metal, plastics, and textiles. The flexible adhesives can be applied quickly in high volumes by automated pick and place machines, and thus are suitable choice for fixing SMDs on flexible substrates and PCBs. Several types of adhesives can be used in bonding of components on PCTs, including non-conductive adhesives (NCA), isotropic electrically conductive adhesives (ICA), and anisotropic conductive adhesives (ACA).

NCA is used in flip-chip bonding process in electronics. Linz *et al.*<sup>728</sup> adopted NCA technique for contacting rigid electronic modules to textiles. TPU film was used as the bonding adhesive placed between the PCB module and fabric circuit, and the insulator on the textile conductor.

Under applying load and heat, the TPU adhesive melted, then the PCB contact pad and the conductive yarn was brought into contact (**Figure 61e**). LEDs can be integrated onto textiles by NCA bonding with two different implementations, as shown in **Figure 61f**. The implementation on the right is a packaged RGB LED electronics module with contact pads at the bottom, while the implementation on the left is a LED cut from the wafer without housing and bonded with the conductive fabric using NCA as adhesive and insulation. UV-curable NCA with fast curing was used to integrate SMD chip resistors onto conductive and stretchable textile ribbons.<sup>729</sup> The stable electrical resistance of the sample after 30 cycles of washing and drying indicated the reliability of the NCA glued joints.

Conductive adhesives are extensively applied in electronic connections as they can provide both sufficient binding strength and electrically conductive pathways. ICAs are composed of conductive filler and adhesive material, of which Ag nanoflakes and epoxy adhesive are used representatively.<sup>730, 731</sup> ICAs can conduct electricity in all directions (**Figure 61g**). In contrast, ACAs, containing spherical fillers at relatively low concentration, only conduct at the Z-direction while restricting the electrical contact at X- and Y-axis (**Figure 61h**).<sup>732</sup> The use of ACA prevents short circuits. However, the assembly process requires high temperature and pressure, and high contact resistance is resulted when using this technique. A commercial ACA (ZTACH® ACE, SunRay Scientific) was applied as a bonding material to provide mechanically robust electrical connections E-textile to E-textile, E-textile to SMD resistor, and E-textile to electronic module board.<sup>733</sup> The adhesive can be cured at low temperature (140 °C for 15 s) or UV light in the presence of a magnetic field, which makes it require less pressure during assembly and enables the potential for large-scale manufacturing. Besides epoxy-based adhesives, PU-based and silicone-based conductive adhesives with lower modulus have been developed to endow the adhesive with better flexibility and stretchability.<sup>734, 735</sup>

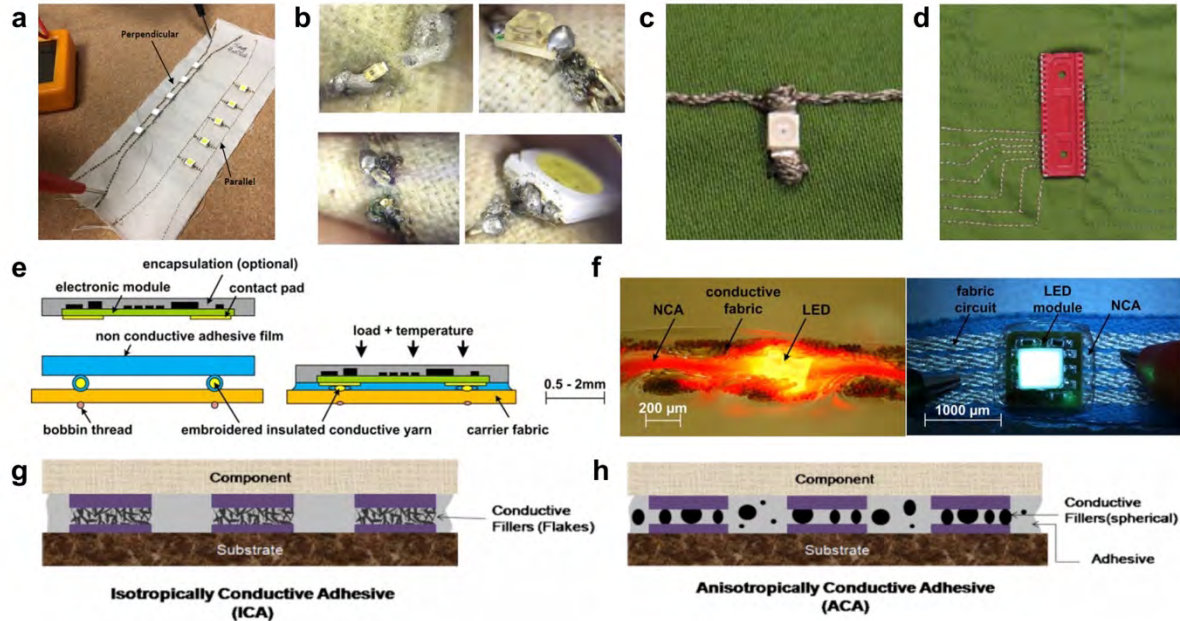


**Figure 61.** Bonding of rigid electronics on textiles. (a) Two 5-LED parallel circuits created in parallel layout and perpendicular layout, respectively. (b) Types of joint failure for soldering LED on the conductive threads and LED display implementation. Reproduced with permission from ref <sup>714</sup>. Copyright 2017 Association for Computing Machinery. (c) A LED sequin stitched to fabric, (d) A stitched socket button on fabric. Reproduced with permission from ref <sup>726</sup>. Copyright 2009 Springer. (e) Illustration of the flip-chip bonding process with NCA for electronic textiles. (f) LED integrated into textiles by NCA bonded contacts with two different implementations. Reproduced with permission from ref <sup>728</sup>. Copyright 2012 Taylor & Francis Group. Illustrations of (g) ICA and (h) ACA. Reproduced with permission from ref <sup>732</sup>. Copyright 2020 Elsevier.

Though electrically conductive adhesives can be used to replace solder pastes due to their lower processing temperature and simpler manufacturing method, they tend to exhibit higher contact resistance and lower mechanical strength than soldering. As mentioned above, LM could be applied as a room-temperature solder with high electrical conductivity. Since LM could not provide binding strength, the combination of adhesive and LM solder could be a choice for joining electrical components and PCTs. For example, Wang *et al.*<sup>736</sup> fabricated a stretchable electronic textile-based device by printing LM circuits on an electrospun substrate, and mounted rigid ICs on the LM patterns for electrical interconnection using PVA as the adhesive. The bonding provided by PVA remained a reliable connection even during stretching the device at a large tensile strain of 900%.

## 4.2 Integrating Fibrous Devices Made of PCTs

The 3<sup>rd</sup> generation of electronic textiles, which integrate fibrous devices made of PCTs, are promising alternatives to the traditional wearable electronics composed of rigid off-the-shelf electronic components. Fibrous devices are becoming increasingly popular due to their 1D structure with small diameters, lightweight, air and moisture permeability, high strength, and ability to conform to the curved skin of the human body. With proper material and structural designs, multifunctional fiber-based integration can be achieved, enabling a broad range of wearable applications.

### 4.2.1 Functional Fibrous Devices Integrated Systems

Fibrous devices with the functions of energy harvesting and storage, sensing, and display have been developed extensively.<sup>80, 81, 346, 438, 554, 621, 737-739</sup> The fabricated fibrous devices can be integrated into textiles to create wearable electronic systems with a wide range of functions. Integration of multiple fibrous devices with single functions can be achieved by various textile techniques, such as weaving, knitting, embroidery, and braiding. For example, Lee *et al.*<sup>63</sup> demonstrated an integrated textile electronic system composed of multiple single-function fiber-based electronic components, including fiber photodetectors, fiber supercapacitors, fiber field-effect transistors, and fiber quantum dot LEDs (**Figure 62a**). The functional fibrous devices were inserted into the textile by automated weaving and interconnected via conductive threads by laser soldering (**Figure 62b**). An integrated textile system was designed as a prototype to modulate light emission corresponding to the intensity of incident sunlight (**Figure 62c**). As illustrated in **Figure 62d**, the designed textile system exhibited multiple functions with the successive operations of the fiber photodetectors as an input device, fiber supercapacitors as an energy storage, fiber FETs as an electrical driving device, and fiber quantum dot light-emitting diodes as an output device. Their work shows the capability of achieving specific and scalable functionalities in an integrated textile system through the design of system architecture with multifunctional fiber devices.

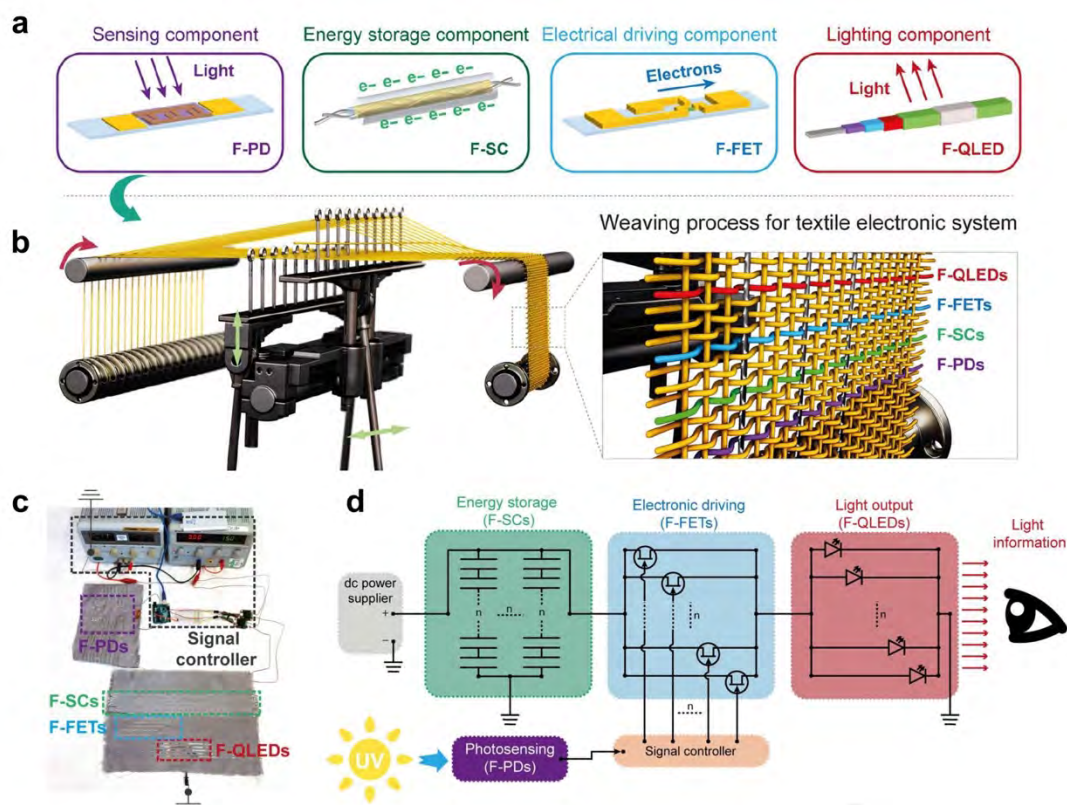


**Figure 62.** Wearable textile system integrated by single-function fibrous devices. (a) Schematic illustration of the single-function fiber-based electronic devices, which are fiber photodetectors, fiber supercapacitors, fiber field-effect transistors, and fiber quantum dot light-emitting diodes. (b) Schematic illustration of the automated weaving process to integrate the fiber-based components into the textile. (c) Photograph of the integrated textile electronic system designed to modulate light emission corresponding to the intensity of incident sunlight (scale bar: 10 cm). (d) Schematic of the integrated textile system for generating environmental information by light modulation. Reproduced with permission from ref <sup>63</sup>. Copyright 2023 American Association for the Advancement of Science.

In addition to integrating single-function fibrous devices, the development of multifunctional fiber devices is another strategy for achieving textile electronic system integration. For example, TENG has been widely studied as the power source and self-powered sensors for health monitoring. It is also desirable to integrate energy storage devices with TENG to form a self-charging power system. Han *et al.*<sup>740</sup> developed a multifunctional coaxial energy fiber for energy harvesting, energy storage, and energy utilization. The fabricated energy fiber consisted an all-fiber-shaped TENG, SC, and pressure sensor, which were integrated in a coaxial geometry (**Figure 63a**). The inner core is a fiber supercapacitor for energy storage, the outer



sheath is a fibrous TENG in single-electrode mode for energy harvesting, and the outer PDMS friction layer and inner PMDS layer covered with Ag constitute a self-powered pressure sensor. The assembled soft energy fiber showed stable electrochemical and mechanical performances under different mechanical deformations, exhibiting promising potential in wearable electronic devices (**Figure 63b**). The prepared fibrous TENG can utilize the harvested electricity from the fiber supercapacitor and correlate it with external pressure to work as a self-powered pressure sensor, which can be readily used to monitor the real-time finger motions and work as a tactile interface for a fibrous electronic piano (**Figures 63c, d**).

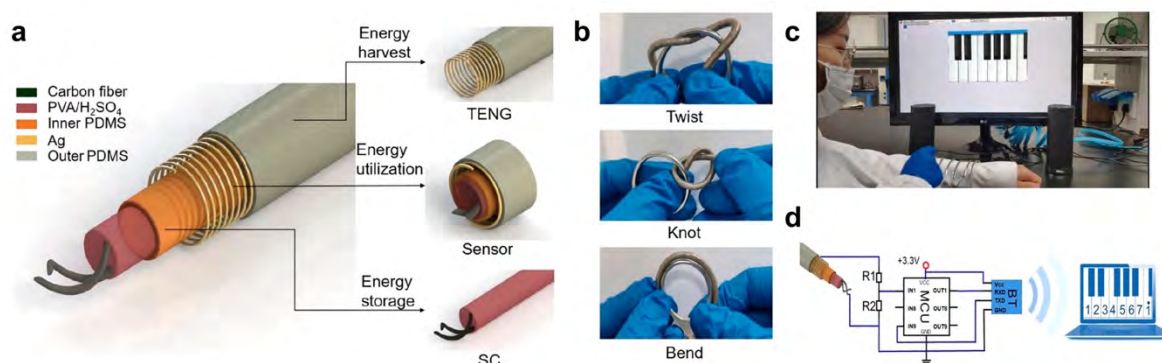


**Figure 63.** Integration of multiple electronic functions on a coaxial fiber. (a) Schematic structure diagrams of the energy fiber for energy harvesting, utilization, and storage (including TENG, sensor, and supercapacitor). (b) Photographs of the energy fiber subjected to different mechanical deformations, including twisting, knotting, and bending. (c) Photograph of the energy fiber as the tactile interface for playing an electronic piano. (d) Circuit diagram of the fibrous tactile interface and processing circuit. Reproduced with permission from ref <sup>740</sup>. Copyright 2021 American Chemical Society.

Significant advancements have been made in the field of fiber-integrated wearable electronic systems. These advancements include the development of fabrication methods of electronic fiber devices, the assembly of the fibrous devices into textiles, and the interconnection of fibrous devices for the integration of wearable systems. These topics will be discussed in the following sections.

#### 4.2.2 Fabrication Methods of Fibrous Devices

Several fabrication methods have been developed to create fibrous devices with multiple functionalities. These methods include spinning, electrospinning, thermal drawing, coating, printing, and nanofabrication.

Spinning is a simple and cost-effective method for electronic fiber fabrication, which can be performed using different techniques, such as melting spinning, wet spinning, and dry spinning. This method involves extruding a polymer melt or solution through a spinneret to create fibers. The properties of the fabricated fiber devices can be controlled by tuning the composition of the polymer melt/solution, the spinning conditions, and the design of the spinneret. Kou *et al.*<sup>741</sup> developed a continuous fabrication method for polyelectrolyte-wrapped graphene/carbon nanotube core-sheath fibers using a coaxial wet-spinning assembly approach. The fibers were then applied directly as safe electrodes to assemble two-ply wearable yarn supercapacitors. For more complex structures of fibrous devices, the spinning method can be combined with other fabrication methods, such as electrospinning and thermal drawing.

Electrospinning is another type of spinning process, which can generate highly stretchable fiber mats with fibers with diameters in the nano- to micrometer scale. The electrospun fibers have unique large specific surface area and high porosity, making them suitable to be used in soft and stretchable electronic applications such as conductors, sensors, nanogenerators, supercapacitors, batteries, and transistors.<sup>24, 742-746</sup> In addition to electrospun fiber mat, yarn devices can be fabricated by collecting the electrospun fibers on a metal wire, or by cutting and twisting the electrospun mats. He *et al.*<sup>747</sup> fabricated a stretchable fiber conductor by dip-coating Ag nanowires on electrospinning-derived porous SBS yarn. A stainless steel wire was used as the collector to collect electrospun SBS microfibers. The porous structure of the yarn endowed the fiber electrode with high permeability and enhanced electrical properties. As another approach, Kim *et al.*<sup>748</sup> cut an electrospun fiber mat into strips and twisted them to fabricate barium titanate-doped-poly(vinylidene fluoride-trifluoroethylene) (BTO-P(VDF-TrFE)) yarns. Then a piezoelectric yarn device was prepared by weaving the yarns into the cotton sport shorts. This device exhibited high structural robustness and mechanical flexibility, as well as piezoelectric performance, enabling the capability of body signal monitoring when subjected to repetitive physical damage.

Thermal drawing of fibers is an industrial method for optical fibers in kilometer-scale length. The process involves heating and drawing a thermoplastic material perform above the softening temperature to produce fibers. Thermally drawn multifunctional electronic fibers have been extensively studied to explore their potential use in sensing, energy, healthcare, robotics, and so on. Compared with other fiber fabrication strategies, thermal drawing exhibits the

advantages of continuous and large-scale manufacturing, producing fibers with high mechanical strength and stable electrical properties, and easy to combine with other technologies. Ma *et al.*<sup>60</sup> developed a continuous and high-throughput thermal drawing and chemical deposition process to fabricate highly stretchable and conductive monofilament and multifilament yarns. The fabricated electronic fibers and yarns were strong and robust enough to be integrated into various textiles through conventional textile manufacturing processes such as weaving, knitting, and braiding. The integrated wearable devices can undergo standard machine washing. Despite the promising potential of this strategy, the available materials compatible with the thermal drawing process are limited. The rheology properties of the elastomer materials should be identified and modified to meet the requirement for manufacturing.

Coating is a scalable fabrication technique used for fiber devices, involving immersing or passing the fiber core through a solution containing functional materials.<sup>80, 81</sup> This process produces a core-sheath structure, with a conductive layer formed on the surface of the fiber. Coating process can be applied to a wide range of fiber materials. The selection of solution composition depends on the desired electrical properties of the resulting devices and the compatibility with the fiber material. However, this technique may have limitations in terms of conductivity due to non-uniform thickness and weak adhesion of the conductive layer formed on the fibers. Additionally, the potential environmental impact of the coating solution should be taken into consideration.

Printing methods are widely used for the fabrication of fibrous devices due to their ability to create complex patterns and structures in a cost-effective manner. The commonly used printing methods include screen printing, inkjet printing, and 3D printing.<sup>212, 749, 750</sup> Screen printing is a well-established method for depositing large amounts of inks onto fibrous substrates at high throughput, though the resolution is relatively low compared to other printing techniques. On the other hand, inkjet printing allows for a higher printing resolution with minimized material waste. 3D printing can be used to fabricate and integrate stretchable conductive fibers into a textile system with complex geometries, offering a rapid prototyping approach for wearable electronic devices.

Nanofabrication techniques are used to create highly complex and precise structures at the submicron scale. Examples of nanofabrication techniques include physical vapor deposition

(PVD), atomic layer deposition (ALD), electron-beam lithography (EBL), and nanoimprint lithography (NIL). In contrast, microfabrication techniques such as photolithography and micro-electromechanical system (MEMS) fabrication are typically used to fabricate structures and devices at the micrometer scale. As an example, Hwang *et al.*<sup>751</sup> utilized ALD to deposit Al<sub>2</sub>O<sub>3</sub> for the gate dielectric and encapsulation layers on a fiber substrate. Nanofabrication techniques offer several advantages, including high precision and miniaturization, which enable the development of fibrous devices with specific properties and the integration of multiple functions into a single fiber. However, several challenges and limitations must be considered. For instance, the cost of nanofabrication can be high due to the need for specialized equipment, materials, and expertise. In addition, some materials may not be suitable for use at the nanoscale. Furthermore, scaling up the fabrication process can be challenging due to the complexity of structures being fabricated and the sensitivity of the tools used. Addressing these challenges is crucial for the continued development and advancement of nanofabrication techniques and their applications in wearable electronics.

#### **4.2.3 Assembly and Connection of Fibrous Devices**

The design of an integrated wearable system involves the assembly of electronic fibers, yarns, or fabrics containing functional electronic components into a textile system. The fibrous devices can be assembled into textiles by various techniques, such as weaving, knitting, embroidery, printing, and adhesion. The selection of the assembly technique depends on the specific application of the integrated device. For example, weaving and knitting are ideal for creating durable fabrics, while embroidery and printing can be used to create designed patterns. Adhesion techniques, such as lamination or heat bonding, can be used to attach as-fabricated electronic devices onto the fabric. After assembling fibrous electronic devices into a textile system, interconnections between the individual devices are to be established to create electrical pathways among the electronic modules in the system. Typical methods for interconnecting fibrous electronic devices include thread/wire bonding, soldering, and conductive adhesives. These methods allow for the formation of a network of functional components that can communicate with each other and achieve the desired properties and functions of the integrated wearable system.

Weaving is a technique to produce woven fabrics by interlacing two orthogonal sets of yarns, *i.e.*, weft and warp, in a uniform structure with high stability and durability. To fabricate an electronic textile, conductive yarns and the functional fibers can be incorporated into the

weft/warp threads to create an interconnected network. Woven fabrics are widely researched in wearable electronic devices due to their ability to withstand wear and tear while remaining stable electrical properties. For example, Zhang *et al.*<sup>752</sup> demonstrated the fabrication of photo-rechargeable fabric using a scalable shuttle-flying weaving process (**Figure 64a**). The fabric was woven with various types of functional fibers, including colored cotton yarns, metal-coated polymer fibers, photoanode wires, and battery wires. The interconnections between energy-storage and conversion components were achieved using Cu wires. The resulting energy textile exhibited an excellent mechanical robustness and was capable of working normally without observable performance degradation under mechanical twisting and heavy rainfall conditions (**Figures 64b, c**). Zhao *et al.*<sup>210</sup> developed a machine-washable textile TENG for effective human respiratory monitoring through loom weaving of Cu-PET and PI-Cu-PET yarns. The weaving process for the textile TENG is fully compatible with high-throughput textile processing. The as-prepared textile TENG showed remarkable washing durability in repeated standard machine-wash cycles.

Knitting is a process for creating interlocked loops of yarns to form fabrics that have a high degree of stretchability and conformability, making them ideal for wearable electronic devices, especially in scenarios involving large deformation. Luo *et al.*<sup>344</sup> created full-body tactile textiles using digital machine knitting of coaxial piezoresistive fibers (**Figure 64d**). The textiles fabricated in a scalable manner can conform to arbitrary 3D geometries (**Figure 64e**). The interlocked loops of yarn used in knitting create a soft and stretchy fabric that is comfortable and compatible with natural human motions, making it ideal for studying human activities.

Embroidery is a versatile technique for assembling fibrous electronic devices into a textile system. It can be applied to create flexible and stretchable interconnection circuits and customized patterns on textile substrates. For example, NFC tags or antennas made of conductive fibers can be integrated into textile systems, making smart and wirelessly connected electronic devices.<sup>213, 240</sup> Besides, embroidery can be used to assemble fibrous devices into fabrics, such as supercapacitors,<sup>641</sup> memory arrays,<sup>753</sup> and transistor arrays.<sup>754</sup> The circuit lines and patterned devices integrated by embroidery exhibit strong connections to the textile substrates and individual devices, resulting in a durable integrated system with good flexibility. Compared to embroidery, printing can create more smooth and uniform patterns on textiles, which is useful for creating conductive circuits and patterned devices with high precision and resolution. In addition to traditional printing methods such as screen printing and inkjet printing,

transfer printing combined with high-precision photolithography can create micropatterns on fibrous textile substrates.<sup>244, 755</sup>

Similar to the connection of rigid electronic components on textiles, soldering, and conductive adhesives are common methods to assemble and interconnect fibrous devices onto a textile system. Both methods can create a conductive pathway between the fibrous devices and the textile substrate or other integrated devices, enabling the multiple functionalities of the wearable electronic system. However, soldering typically requires higher temperature and creates additional soft-rigid interfaces in the fiber-integrated systems, which can cause unstable electronic stability of the fibrous devices and the textile system.

As an alternative, conductive adhesives are promising. They can create a strong and reliable connect without requiring high temperatures and minimize mechanical mismatch in the systems. Thermoplastic hot melt resin is a commonly used adhesive in the assembly and interconnection of fibrous devices. These adhesives are softened or melted when heated, to create a tough bonding between the fibrous devices and other components. Strategies have been proposed to reduce the heat stress from the adhesive bonding process in order to minimize any potential damage to heat-sensitive textiles. For example, Dils *et al.*<sup>756</sup> employed ultrasonic spot welding for the electrical interconnection of embroidered conductive yarns with each other at defined cross-points. A welding tool was used to transfer the vibration energy from the welding machine and apply the pressing force of the machine to the crossing contact area. In the study, Lee *et al.*<sup>63</sup> woven fibrous devices were interconnected via conductive threads using laser soldering. It is a contactless and rapid process, in which silver adhesives can be solidified at a temperature below 150 °C within 1 s by using a 980-nm infrared laser (**Figure 64f**). The durability of the soldered connection was confirmed by an abrasion test, which demonstrated a mechanically stable integrated system.



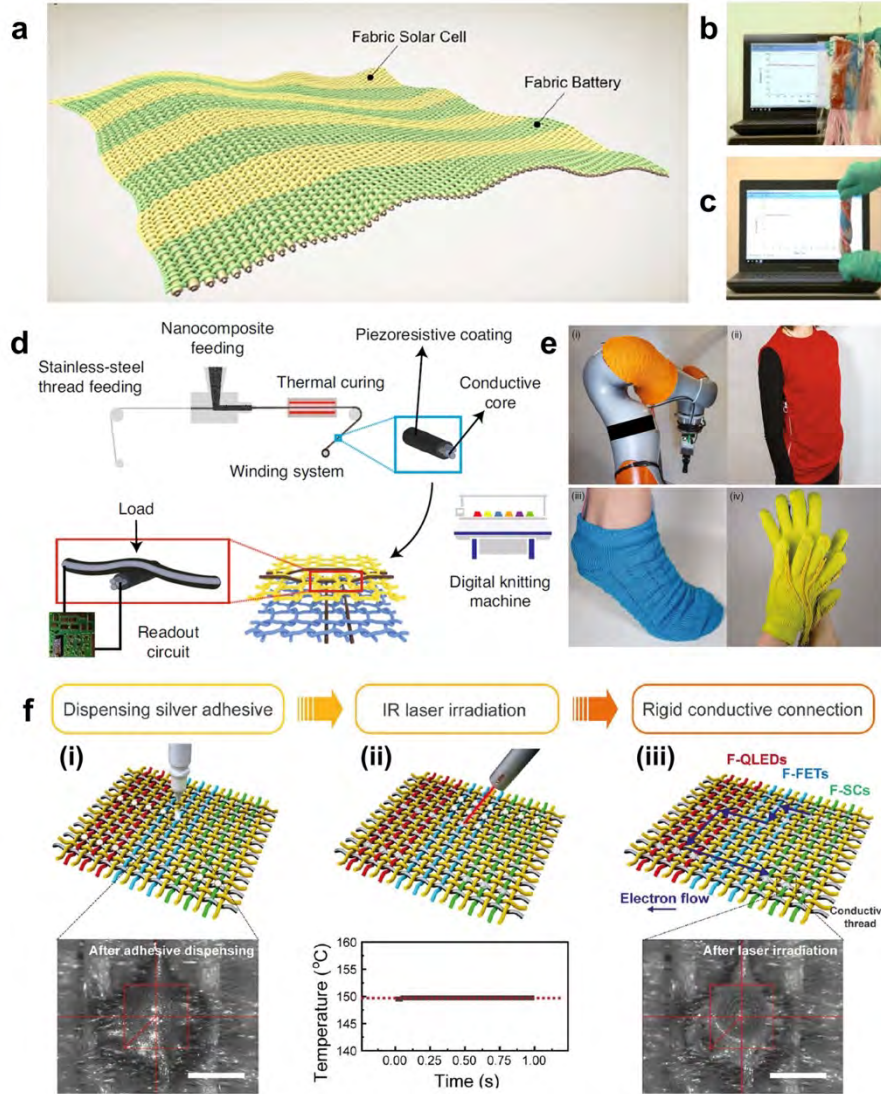


**Figure 64.** Assembly and interconnection of fibrous devices into textile systems. (a) Schematic illustration of a woven photo-rechargeable Fabric. Demonstration of the photo-rechargeable fabric working under (b) heavily twisting and (c) water pouring down. Reproduced with permission from ref <sup>752</sup>. Copyright 2020 Elsevier. (d) Schematic of the scalable manufacturing of tactile sensing textiles using coaxial piezoresistive fibers and digital machine knitting. (e) Photographs of knitted full-sized tactile sensing wearables: artificial robot skin, vest, sock, and glove. Reproduced with permission from ref <sup>344</sup>. Copyright 2021 Springer Nature. (f) Illustration of the contactless automated interconnection process involving the dispensing and solidification of conductive adhesive by laser. Reproduced with permission from ref <sup>63</sup>. Copyright 2023 American Association for the Advancement of Science.

### 4.3 Optimizing Wearable Durability and Performance

The integration of versatile components, including rigid microelectronics and fibrous

electronic devices onto textiles, is the crucial step in developing wearable electronic systems with complex functions for use in multidisciplinary areas. The key challenge in integrating wearable electronic systems is ensuring the seamless combination and reliable performance of different components. Wearable electronics are subject to harsh external environments containing chemical and mechanical stresses. Conversely, some of the electronic components may pose potential hazards to the wearers. In addition, to endow wearable devices with higher durability and user experience, it is necessary to achieve a higher level of functionality in a small form factor. Advanced techniques, including bonding strength enhancement, strain engineering at the integration interface, encapsulation, and multilayer structure, can help address these challenges.

#### **4.3.1 Bonding Strength Enhancement**

Integrating various units into PCTs substrates can result in low bonding strength and mechanical mismatch at the connection interfaces, leading to interfacial failures. To achieve mechanical reliability of the electronic interconnects and bonding sites on PCTs, approaches have been developed to enhance the interfacial bonding strength. These approaches include interlocking structures at molecular, nano, micro and macro scales, chemical treatments, and physical treatments.

***Interlocking Structures.*** Interlocking structures can enhance the interfacial strength through interactions such as molecular interdiffusion and mechanical interlocking at multiple scales. The adhesion between substrate and polymer involves two stages: absorption and diffusion. Natural fibers contain a large number of functional groups, such as hydroxyl groups, that could form hydrogen bonds with polar molecules like water. Water or water-based liquids can be absorbed on the surface and transported to the inner part of the fiber by diffusion or capillary force.<sup>757</sup> Adhesives or coating materials with reactive molecules can be attracted by the functional groups on the fibers, and interactions such as van der Waal's, electrostatic, and covalent bond are formed for strong interfacial bonding. The degree and extent of the interdiffusion are mainly determined by the chemical compatibility of the two materials and the penetrability of the substrate.<sup>758</sup> Polymeric synthetic fibers, such as polyester, PA, PE, contain abundant polymer chains, which could provide molecule interdiffusion across the interface as well as polymer chain entanglement. A high molecular weight polymer with good mechanical properties could enhance the interfacial strength.<sup>759</sup> And the interfacial adhesion between different components in the electronics could be enhanced by using two components

sharing similar chemical composition.<sup>760, 761</sup>

Mechanical interlocking is an easy way to improve the interfacial strength by enhancing the contact area and provides additional friction force and mechanical force. The porous structure and rough surface of textile materials are advantageous for mechanical interlocking between the textiles and adhesives or coatings. The surface roughness can be enhanced by chemical etching or particle grafting. Nanoparticles can be introduced to textiles to endow multiple characteristics without altering the bulk properties of textiles. Various nanoparticles such as nano clays, silica, TiO<sub>2</sub>, ZnO, nanocarbon materials have been used to reinforce the textile-matrix interface by providing nano-scale interactions.<sup>762-766</sup> Interlocking structures at multiple scales can be achieved in one system for interfacial enhancement. For example, the bonding strength between the cement-based matrix (concrete) and the fabric was enhanced by applying hydrophilic micron-size particles (cement or silica) or nanocarbons (functionalized carbon nanotubes or graphene oxide) into the epoxy polymer coating of the carbon fabric.<sup>767</sup> The bonding strength characterized by pull-off test was increased by 25% by the cement powder decoration and the mechanical properties of the composite was improved by 30%. At the micron scale, the particle decoration resulted in a formation of 100-μm thick interlayer between the fabric and the matrix. Further, it was found that a NaCl environment exposure of the sample resulted in an enhanced bonding strength due to the formation of salt crystals at the fabric-matrix interface.

**Chemical Treatments.** Common adhesives provide non-covalent interactions with low bonding strength, such as hydrogen bonding, van der Waals, and electrostatic interactions, between different components. Covalent interactions formed by chemical reactions have much higher interfacial strength than the non-covalent ones. Adhesives containing reactive groups such as hydroxyl, carboxyl, carbonyl, sulfonation, amide, or amine groups are capable of adhering to the surfaces containing similar functional groups. For example, polyacrylate (PAA), PU-based polymer adhesives are often used in textiles.<sup>768</sup> Surface chemical treatment of fibers including dewaxing, delignification, silane, acetylation, benzylation and grafting of monomers can promote the interfacial adhesion.<sup>769, 770</sup> As an example, date palm fibers (DPFs) were treated by alkali aqueous solution and silane coupling agents with various concentrations and the interfacial properties with PU and epoxy were improved.<sup>771</sup> In situ polymerization of monomers to graft polymers (*e.g.*, PAA, PU) and copolymers (*e.g.*, butadiene, vinyl acetate) onto fibers could create firm interaction between textiles and polymeric matrix.<sup>768, 769</sup> Since

butadiene and vinyl acetate copolymers show poor light resistance and adhesion, a better adhesion performance can be obtained by combining other monomers.<sup>772, 773</sup> A reactive Ag ink was reduced in situ on the chemically etched PET fabric and uniformly deposited on the microfibers of the fabric.<sup>774</sup> The resulted fabric exhibited a better electrical conductance and Ag adhesion than the fabrics coated with nanoparticles and nanowires. Though such chemical modification approaches could provide tough interfacial bonding strength between textiles and other components, the reactive chemicals have potential biotoxicity to human when applying in wearable electronics, careful attention should be paid to the material design.

**Physical Treatments.** Physical treatments of textiles can change their structure and surface characteristics to modify their interactions with external components. For example, plasma technology has been employed to alter the surface properties of textile materials. Plasma treatment can be categorized into thermal and non-thermal plasmas, in which non-thermal plasma is more suitable for heat-sensitive textiles. The treatment results are dependent on the type of working gas, excitation frequency, power, treatment time, and the type of substrate used. Low-pressure plasma operated under vacuum has been commonly used in the microelectronic industry and applied for the surface treatment of textiles.<sup>775, 776</sup> However, the low-pressure condition is not compatible with the continuous processing of textiles. Therefore, atmospheric plasma has been investigated for textile industry. There are mainly four types of atmospheric plasma techniques applied in textiles, including corona discharge (CD), dielectric-barrier discharge (DBD), atmospheric-pressure glow discharge (APGD) and atmospheric-pressure plasma jet (APPJ).<sup>777</sup> Surface modifications such as the wettability and adhesion of textiles can be improved by introducing functional groups to the textile surface by atmospheric plasma treatment.<sup>778, 779</sup> Kim *et al.*<sup>780</sup> used silicone polymers to improve the dimensional properties of wool fabrics. Oxygen plasma treatment was applied to modify the cuticle surface of wool fabric and enhance the surface reactivity of the fabric towards silicone polymers, increasing the dimensional stability, wrinkle resistance and performance of the wool fabrics. In Bozaci's work, flax fibers were treated by argon and air atmospheric pressure plasma to improve the interfacial adhesion between the flax fibers and high-density polyethylene (HDPE) and unsaturated polyester.<sup>781</sup> It was found that the argon-treated flax fiber showed a superior interfacial adhesion to HDPE than the air-treated and untreated flax fibers. While the air-treated flax fiber showed a better adhesion to polyester than the argon-treated one. The greater plasma power resulted in greater interfacial adhesion. The results can be explained by the changes on the surface chemical composition and functional groups and the increased surface roughness

induced by different plasma treatment conditions. Felix *et al.*<sup>782</sup> adopted oxygen plasma treatment to enhance the interfacial adhesion between regenerated cellulose fiber (rayon) and PE considerably. The enhanced adhesion was attributed to the covalent bonds formed between the fibers and the PE matrix. It was also proved that the longer plasma treatment duration improved the adhesion. The adhesion promotion of synthetic fibers was extensively studied as well. For example, atmospheric-pressure nitrogen plasma was used to enhance the adhesion of PET monofilament surface to epoxy resin matrix due to the polar group interactions.<sup>783</sup> Argon plasma induced the surface modification of ultra-high molecular weight polyethylene (UHMWPE) textile and increased the peel strength of the UHMWPE textile/adhesive (PU\_T01) composite.<sup>784</sup>

Generally, for integrating various units onto textiles, the interfacial strength between the textiles and adhesive materials can be enhanced through molecular interdiffusion, mechanical interlocking structures, chemical treatments, and physical treatments. These approaches can be sometimes applied simultaneously and have influence on each other for better interfacial bonding strength.

#### **4.3.2 Strain Engineering**

While fibrous devices made of PCTs provide wearing comfort for near-body applications, conventional silicon-based microelectronic components with high electrical performance are compatible with standard microfabrication processes. However, since microelectronics are rigid with limited flexibility and stretchability, integrating them onto soft PCT substrates can cause mechanical mismatch and stress concentration at the rigid-soft interface, leading to mechanical and electrical failures. To address this, strain engineering strategies are needed to reduce strain concentration at the interface under large mechanical deformation and ensure the reliability of wearable electronic systems.

**Interposer Technology.** Interposer technology has been proposed to route circuits on textiles.<sup>785</sup> The interposer is design to adapt both the pitch mismatch and mechanical mismatch between electronic components and textile fabrics. Stanley *et al.*<sup>786</sup> demonstrated two interposers enabling the detachable connection between fabric and flexible electronics, using two types of connectors, *i.e.*, the smaller mezzanine connector and the larger zero insertion force (ZIF) connector. The flexible interposers consisted of copper traces plated on PI film, which was supported by a bottom PI stiffener. The mezzanine connector was soldered on the

interposer, while the ZIF connector was inserted into the interposer. The interposers with encapsulation layer can be integrated onto the fabrics via the connections to conductive threads. Both interposers showed good stability in preliminary mechanical and electrical testing, though further modification for better robustness and washability is required. The ZIF interposers were found to be less susceptible to failure and easier to handle because of their larger size. Takamatsu *et al.*<sup>787</sup> described a thin-film stress-concentration-relocating interposer that can withstand a 36% expansion of electronic textile devices. The interposer consisted of thin and soft TPU film perforated via holes worked as the adhesive and was inserted between the rigid electronic components and the fabric circuit to shift the stress-concentration area from the stretchable Ag paste wiring to the soft film in the interposer (**Figure 65a**). The optimal interposer with 100- $\mu$ m thick film enabled the incorporation of LEDs and MEMS sensors into electronic textile devices.

**Rigid Island Strategy.** Rigid island strategy is based on modulus engineering for strain isolation. Stretchable hybrid electronics can be constructed by fixing stiff electronic components on high-modulus materials connected by stretchable interconnects on soft substrates. Such strategy has been applied in the integration of electronics in textiles by preparing rigid and flexible circuit boards.<sup>699, 788</sup> For example, Vervust *et al.*<sup>788</sup> used PI as the flexible substrate to support SMD for making non-stretchable functional islands based on standard PCB manufacturing technologies. The non-stretchable islands were interconnected by stretchable copper tracks, resulting in flexible and stretchable modules (**Figure 65b**). Subsequently, the stretchable modules were embedded in PDMS by liquid injection molding for the bonding on fabrics and encapsulation of the module. No observed delamination during washing showed sufficient adhesion strength between the fabric and the module and a good reliability of the integrating method.

For a better compliance to textiles and mechanical stability of the hybrid devices, miniaturized electronic components instead of flexible PCBs were integrated into textiles. To ensure the miniaturization at a higher solution, rather than woven or knitted fabric structures, electrospun fiber mat can be used as the substrate for the fabrication of stretchable hybrid electronics. Wang *et al.*<sup>736</sup> used stiff and flexible PVA glue as both the adhesive and rigid island to integrate ICs on electrospun TPU nanofiber membrane (**Figure 65c**). It was shown from electrical and mechanical testing that the PVA glue could isolate the regional strain, enhancing the joint stability and reliability at the interface between the rigid IC chip and the stretchable TPU



membrane. FEA results verified almost no deformation of the chip and PVA glue under 40% strain (**Figure 65d**). This strategy demonstrated good performance and reliability in the applications including stretchable sensors, human-computer interaction devices and displays.

**Gradient Structure.** Even though the rigid island strategy could isolate regional strains and prevent stress concentration of the electronics under deformations, the large Young's modulus difference may lead to the easy delamination of the electronics and the rigid island. Thus, gradient structures were created to reduce the abrupt change in modulus at the border of the rigid island. Vanfleteren *et al.*<sup>789</sup> found that the mechanical reliability of the structure can be improved by creating a smooth transition in the width of the copper interconnects, and the thickness of encapsulant between the rigid solder assembled standard components and the soft and stretchable interconnects (**Figure 65e**). Cotton *et al.*<sup>790</sup> adjusted the tensile modulus of PDMS film in the range of 0.65-2.9 MPa by decreasing the UV exposure dose for cross-linking from 24000 to 0 mJ cm<sup>-2</sup>. By using a patterned UV mask, a PDMS rubber film with graded and localized mechanical properties was prepared. A stretchable electronic structure was then formed by integrating the mechanically graded PDMS substrate, a rigid PI island, and an Cr/Au thin film interconnect (**Figure 65f**). The stretching cycling test showed that the PDMS film with modulus gradient could provide strain relief near the island interfacial and reliability to the stretchable electronics. Libanori *et al.*<sup>761</sup> created a stacked patch with an elastic modulus gradient spanning over five orders of magnitude by solvent-welding individual PU films with different levels of reinforcement. The modular patch can be solvent-welded on the surface of a stretchable PU substrate to form a 3D composite with elastic modulus profiles in the in-plane and out-of-plane directions (**Figure 65g**). The elastic moduli of the multilayers of films were controlled by tuning the amount of inorganic nanoplatelets and microplatelets in PU. Experimental results and FEA analysis revealed the entangled polymeric PU matrix and the elastic modulus gradient were effective to reduce the stress concentration at the patch-substrate interface, and the composite could withstand tensile strain up to 350%. Gu *et al.*<sup>791</sup> fabricated a stretchable conductor by multilayer stacking of PU-Au nanoparticles composite with a concentration gradient of Au (**Figure 65h**). The high gradient conductive layer and low gradient stretchable layer were stacked alternatively to provide both mechanical and charge transport properties of the composite. Nevertheless, few of the previous methods have addressed the strain concentration issue on textile substrates. When applying rigid electronic components on PCTs at high resolution, more appropriate designs of the interfacial contacts are required.

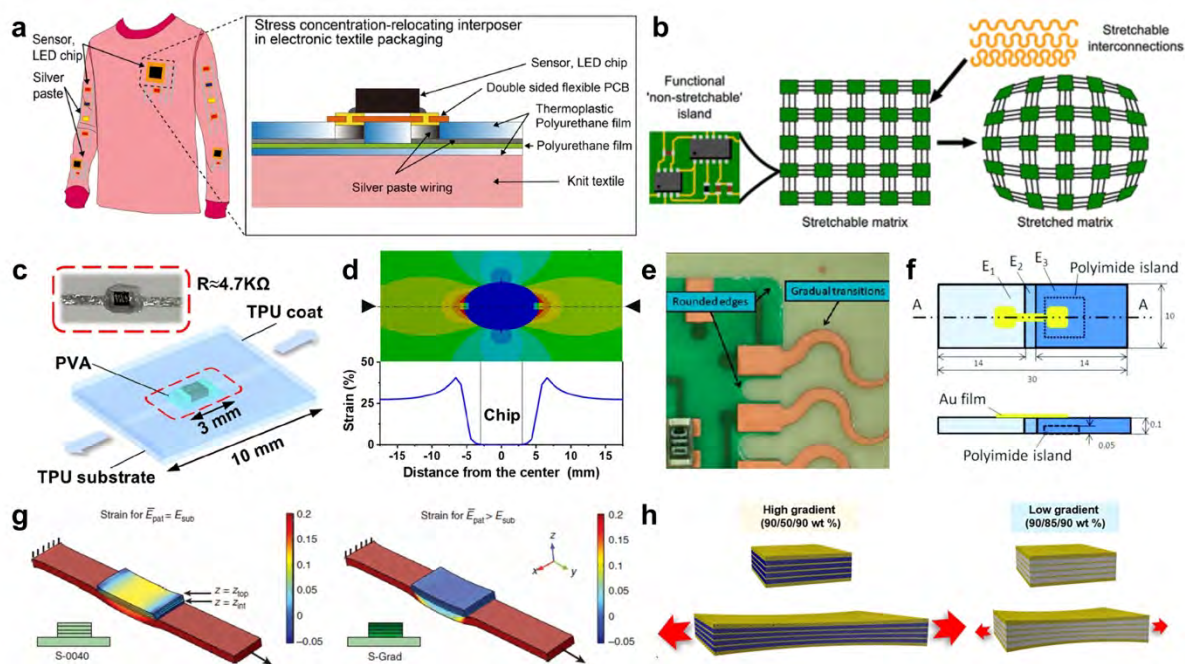


**Figure 65.** Strain engineering for stretchable hybrid electronics. (a) Illustration of the stress-concentration-relocating electronic textile packaging structure with TPU film as interposer. Reproduced with permission from ref <sup>787</sup>. Copyright 2022 Springer Nature. (b) Design of functional “non-stretchable” islands interconnected via stretchable copper connections. Reproduced with permission from ref <sup>788</sup>. Copyright 2012 Taylor & Francis Group. (c) Schematics of a simplified device with a resistor chip bonded by PVA glue. (d) Finite element analysis and relevant strain vs. position curve of the substrate. Reproduced with permission from ref <sup>736</sup> Copyright 2022 American Chemical Society. (e) Gradual transition in the width of the copper tracks to avoid the local stress concentrations in the transition area. Reproduced with permission from ref <sup>789</sup>. Copyright 2012 Springer. (f) Diagram of a stretchable Au thin-film fabricated on a graded photopatternable-PDMS stripe. Reproduced with permission from ref <sup>790</sup>. Copyright 2011 AIP. (g) Distribution of strains for the non-graded (left) and graded (right) patches after applying a longitudinal global strain of 25% in the y-direction. Reproduced with permission from ref <sup>761</sup>. Copyright 2012 Springer Nature. (h) A stretchable conductor made from multilayer stacking of gradient-assembled polyurethane comprising gold nanoparticles. Reproduced with permission from ref <sup>791</sup>. Copyright 2019 American Association for the Advancement of Science.

### 4.3.3 Encapsulation

Effective encapsulation materials and strategies are crucial for insulating wearable electronics

from mechanical stress, chemical corrosion, and potential hazards to the wearers. In addition, the loose nature of textiles can cause fiber movement, making proper insulation of electronic components are important for enhancing integration density and resolution. A variety of encapsulation materials, such as PU, silicones and epoxies, have been used. The common encapsulation processes employed in the manufacture of electronic textiles include printing, glob top, underfill, and transfer molding.

Due to the porous structure of textiles, conductive inks can penetrate deeply into the textile. To protect the conductive interconnects on textiles, encapsulation layers can be applied through printing hydrophobic elastomers on them. For example, both sides of a textile printed with silver wires were protected by a commercial TPU layer encapsulation (50  $\mu\text{m}$ ) to improve the machine washing stability.<sup>792</sup> The fabricated device remained conductive after 40 washing cycles in 40 °C warm water and hang-dried between cycles. Yang *et al.*<sup>793</sup> used UV-curable waterproof PU to encapsulate printed Ag tracks on fabrics by screen printing. A dual-material four-layer structure was proposed in their work, which was composed of a waterproof interface layer and adhesion interface layer to smooth the fabric surface for good conductivity of the printed Ag tracks, and an adhesion encapsulation layer and waterproof encapsulation layer as the protective layers and electrical insulators. This structure combines the advantages of the waterproofness of hydrophobic PU and adhesion property of hydrophilic PU. The conductive Ag tracks prepared with this design showed excellent waterproofing property and flexibility.

Glob top is a flexible and non-stretchable encapsulation technique, which commonly applies epoxy to protect individual small chips in the microfabrication processes of PCBs. The epoxies for glob top are thixotropic so that they can be dispensed freely but become viscous and encapsulate a small area without spreading. For the fabrication of fiber-based electronic devices, Kunigunde *et al.*<sup>698</sup> used a two-step method to protect the electronic fibers from weaving friction and mechanical stress during wearing and washing. The electronic fibers fabricated using flexible Kapton substrates were first covered with a spray-on layer of silicone before insertion into the weaving machine, then the fibers were encapsulated by another Kapton layer with the glob top technique. The Kapton layer encapsulation also shifted the sensitive device layers close to the neutral bending axis of the system. This neutral plane shifting strategy via an encapsulation layer has been widely applied in the field of TFT, allowing a higher deformation of device without failure.<sup>794</sup>

Kallmayer *et al.*<sup>795</sup> developed a two-step glob top encapsulation for a single chip module of a textile transponder. The textile transponder IC chip was assembled to a fabric pocket by a flexible interposer, and the encapsulation from both sides protected the interposer with IC against high mechanical stress. The encapsulation was achieved in a two-step process. In the first step, a conventional underfill material with a low viscosity was dispersed inside the fabric pocket to cover the interposer and wet the fabric. In the second step, an encapsulation material was screen printed on the fabric from the outside. The overall thickness of the circuit became ~1 mm with the thin chip thickness of 150  $\mu\text{m}$ . To achieve higher tolerance to mechanical stress, the thickness could be further reduced by using an ultrathin mold. For a much larger module, molding has been applied for encapsulation.<sup>723</sup> Encapsulation by molding made the protection more reliable and the flexible fabric module was washable up to 5 washing cycles. However, the molding method requires the fabric to be flat and the process should be neat otherwise the mold compound will be pressed outside the module site. Moreover, the high curing temperature (~160 – 180 °C) will pose heat stress on most heat-sensitive textiles.

To fabricate a mechanically reliable, foldable, and washable textile-based OLED, Jeong *et al.*<sup>796</sup> developed a multi-functional near-room-temperature encapsulation layer. The encapsulation has a double-layer structure, composing an impermeable  $\text{Al}_2\text{O}_3/\text{TiO}_2$  nanolaminate layer and a flexible and waterproof 1,3,5-trivinyl-1,3,5-trimethyl cyclotrisiloxane (pV3D3) polymer film. The bilayer encapsulation was applied on both the top and bottom sides of the OLED to realize a wearable OLED on conventional T-shirts (**Figure 66a**). The OLED emitted red light normally when folded under water during hand-washing, exhibiting the practical applicability of the wearable OLED (**Figure 66b**).

For next-to-skin wearable applications, the encapsulants for textile electronics are required to be soft, stretchable, and biocompatible. Biocompatible water-resistant elastomers with high stretchability have been extensively applied as encapsulants for wearable electronics, such as PU, TPU, PDMS, and Ecoflex. These protective materials can also be used as an adhesion layer to integrate functional components onto textiles. PU is a common protective layer for textile finishing. Hydrophobic PU can be modified in their structure to improve the water dispersion property. By adding hydrophilic monomers into PU prepolymers, environmentally friendly waterborne PU (WBPU) emulsion can be synthesized, which can be used as waterproof and breathable textile encapsulants. For example, Wu *et al.*<sup>797</sup> developed a water-processable thermoelectric composite made of WBPU, MWCNT, and PEDOT:PSS. The composite was

coated on commercial cotton and polyester yarns for potential wearable thermoelectric textiles application. Huang *et al.*<sup>641</sup> fabricated wearable and washable textile-based supercapacitors by encapsulating the textile with Ecoflex (**Figure 66c**). To further enhance the mechanical robustness and washing fastness of the device, a waterproof TPU fabric was laminated over the Ecoflex encapsulated substrate. The fabricated textile-based supercapacitor showed good flexibility and softness, and the capacitance of the textile-based supercapacitor remained well under flat, rolling, twisting, and even underwater conditions (**Figure 66d**). It was also demonstrated that the textile-based supercapacitor can be machine washed for 20 cycles with a standard AATCC laundry process. Encapsulating fiber-shaped devices can be easily achieved using encapsulation tubes, offering a straightforward and scalable method. For instance, He *et al.*<sup>80</sup> demonstrated this method for continuously producing meter-long fiber LIBs. These fiber LIBs were created by twisting fiber-based electrodes and encasing them within a polypropylene tube wrapped with aluminum-plastic tape, which has a low water-vapour transmission rate of  $<0.005 \text{ g m}^{-2} \text{ d}^{-1}$ . The electrolyte was injected into the tube before sealing at both ends. Utilizing thermal-shrink encapsulation tubes for encapsulation presents a versatile strategy, especially for devices employing liquid electrolytes, enabling efficient encapsulation of fiber-shaped devices like batteries and solar cells.

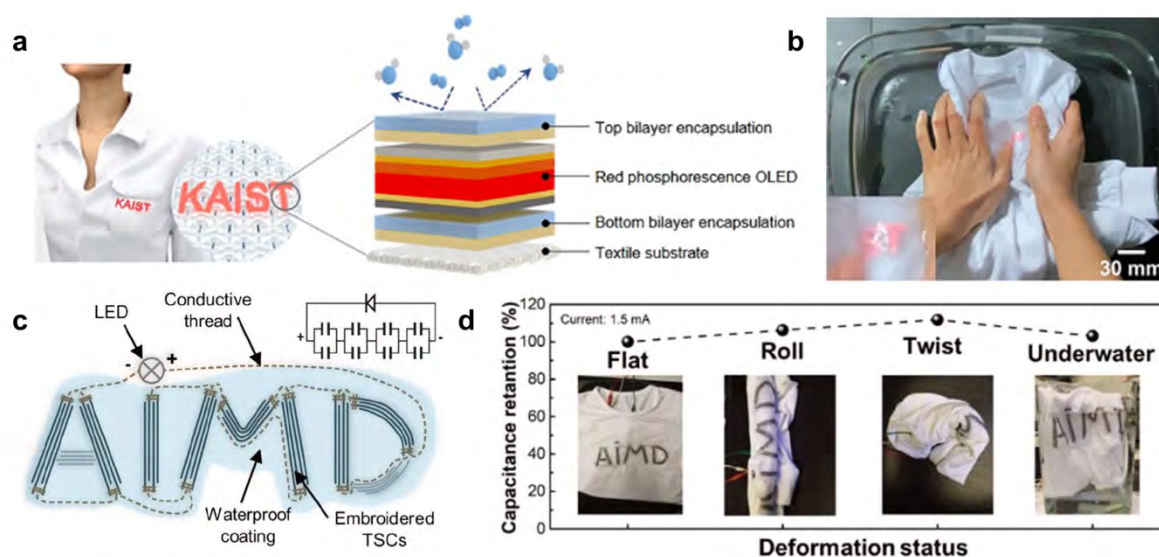


**Figure 66.** Encapsulation of electronic textiles. (a) Illustration of the textile-based OLED and encapsulation layer. (b) Photograph of the OLED textile being folded by hand in water. Reproduced with permission from ref <sup>796</sup>. Copyright 2021 Springer Nature. (c) Schematic illustration of the T-shirt embroidered with textile-based supercapacitors with waterproof coating. (d) Capacitance retention of the textile-based supercapacitors on T-shirt under flat, rolling, twisting, and underwater conditions. Reproduced with permission from ref <sup>641</sup>.

#### **4.3.4 Multilayer Electronics on PCTs**

PCT-based hybrid/integrated wearable systems are designed with sophisticated functions of sensing, actuation, power supplies, data communications, and processing. To achieve these functions, it is necessary to consider the processes for textile seaming and rational designs for electrical interconnects of various electrical components. Though single-layer flexible and stretchable electronics can offer multifunctional applications, they have limited space for electronics integration. Multilayer stretchable devices with high levels of integration, function density, and spatial resolution are crucial for miniaturized multifunctional systems.

Multilayer flexible electronics can be manufactured using various methods, such as flexible printed circuit board (FPCB) fabrication, transfer printing, and screen printing on flexible substrates. These methods provide interlayer interconnects and multilayer functional circuits. For multilayer textile devices, they can be fabricated in a way that is similar to that for FPCBs. Layers of conductive traces can be printed on fabrics and separated by layers of iron-on insulating fabric.<sup>726</sup> The iron-on method is simple to be applied by using adhesive and iron. This method provides the insulation of conductive trace, protection of circuit from wearing and corrosion, and decorative purpose, without interfering the conductivity. However, the stiffness of adhesive and high processing temperature will hinder its applications. Roh developed a one-stop fabrication method for all-fabric multilayer electronic textile sensors.<sup>58</sup> The components of the multilayer structured fabrics included precise circuit patterns formed on fabric layers, intra-layer or inter-layer conductive materials electrically connected, and individual fabric layers fixed to the base layer one by one, which were realized all through embroidery on a commercial computer numeric control embroidery machine. The interconnections between individual layers, and the interconnections between the textile sensor unit and the external control devices for signal transmission were achieved through the textile vertical interconnect access (VIA). A mesh fabric and an ultra-thin and tightly woven nylon fabric were inserted between the resistive sensing patterns and conductive fabrics in order to make space and prevent electrical contact outside of the touch sensing area, as shown in. This method provided the fabricated device with high electrical conductivity, mechanical durability and reliability, with the simple fabrication process, low cost, and easy for mass production.

The multilayer structural design is especially effective for fabricating fabric-based TENGs by

simply stacking alternative conductive fabric and dielectric fabric layer-by-layer. The multilayer stacking structure also provides more contact-separation space to enhance the performance of TENG. For example, Lin *et al.*<sup>798</sup> developed a pressure-sensitive, large-scale and washable textile-based TENG array as bedsheet for sleep monitoring. The TENG consisted three layers, in which wavy-structured PET films were sandwiched by top and bottom layers of Ag-coated conductive fabrics to generate an electrical potential difference between them (**Figure 67a**). The uniform distribution of Ag coating on the fiber surface rendered good electrical conductivity and promoted surface triboelectrification (**Figure 67b**). The fabrication process of the smart textile-based bedsheet was straightforward and compatible with large-scale manufacturing (**Figure 67c**). Moreover, the smart textile was washable, and no resistance change was detected throughout the washing test in tap water. Cao *et al.*<sup>314</sup> fabricated a washable electronic textile by screen printing CNT ink on a fabric, which was used as a self-powered touch/gesture sensor based on TENG (**Figure 67d**). The electronic textile can be manufactured at large scale, which showed a high sensitivity and fast response, high air permeability, and washing durability (**Figures 67e, f**).

However, the multilayer stacking structure may face problems of weak interfacial bonding strength between adjacent layers, which are prone to delaminate during usage. Electrospinning, as an additive manufacturing technique, could solve this problem by continuous fabrication of multilayer nanofiber membranes with multiple functions. Patterning LM as the electrode onto electrospun elastomeric membranes has been proposed for the preparation of stretchable and permeable multilayer electronic devices.<sup>24, 799</sup> For example, Ma *et al.*<sup>24</sup> reported the fabrication of a new type of highly permeable and superelastic conductor by stencil-printing EGaIn on an electrospun SBS fiber mat. By repeating the electrospinning and printing processes, the vertically stacked multilayer stretchable electrodes were formed (**Figure 67g**). The 3D interconnects of the components on different layers in electrical circuit was achieved by simple punching and injection of EGaIn to form the VIA. The monolithic multilayer elastic mat maintained a high permeability with a thickness up to ~2 mm, which enabled the wearing comfort. An additional SBS fiber mat was electrospun on top to serve as the encapsulation layer to enhance the stability of the electrode. A three-layer (thickness of ~1 mm) EGaIn-SBS electrode comprising an ECG sensor, a sweat sensor and an electrothermal heater was prepared, revealing the multilayer electronics could provide high integration density, multifunctionality, and long-term wearability (**Figures 67h, i**).



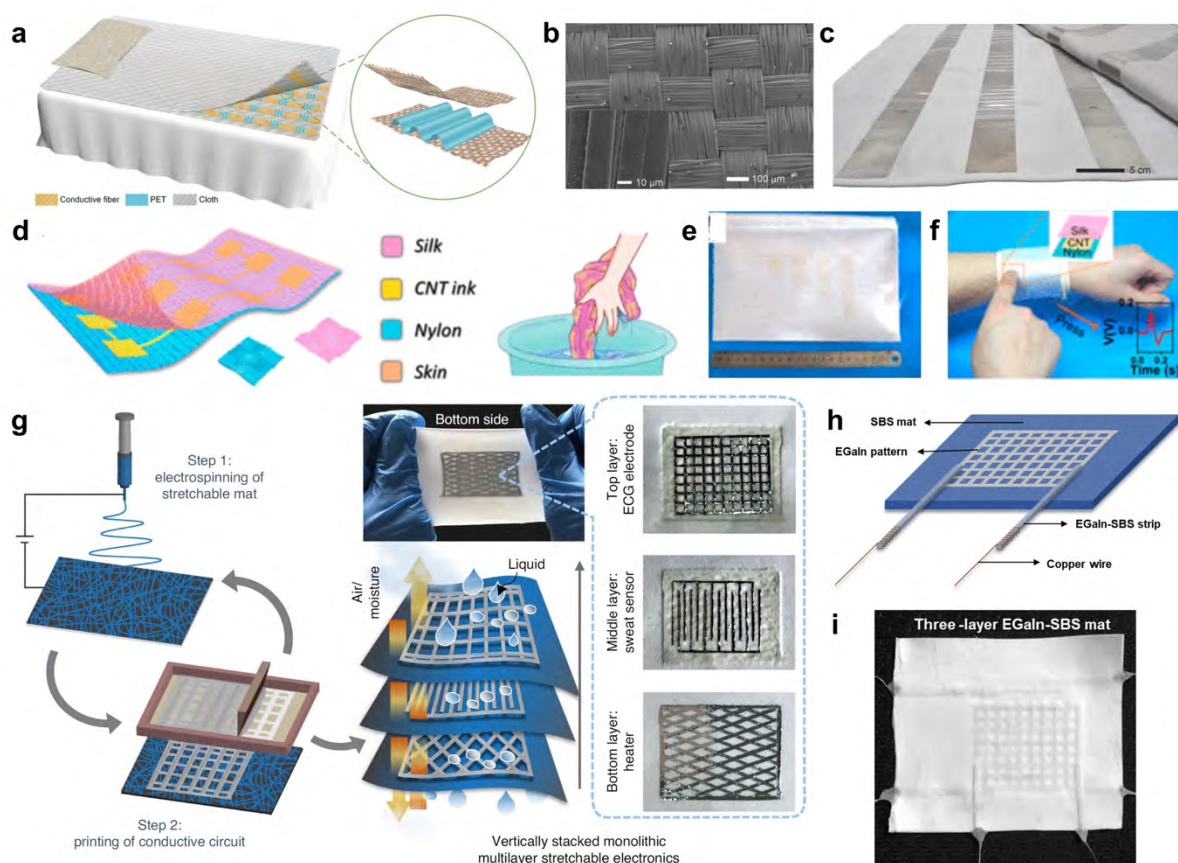


**Figure 67.** Multilayer structures in electronic textiles. (a) Illustration of the TENG-based self-powered smart textile. (b) SEM image of the conductive fiber on the surface of the smart textile and (c) digital photograph of the smart textile bedsheet. Reproduced with permission from ref <sup>798</sup>. Copyright 2018 John Wiley and Sons. (d) Illustration of the structural design of a washable electronic textile (WET). (e) Digital photograph of a large-scale WET. (f) Schematic diagram of the process to produce a signal of the WET. Reproduced with permission from ref <sup>314</sup>. Copyright 2018 American Chemical Society. (g) Schematic illustration of the fabrication of the vertically stacked monolithic stretchable electrodes by alternative electrospinning of SBS fiber mat and stencil printing of EGaIn. (h) Schematic diagram and (i) digital photograph showing the connection of EGaIn-SBS electrodes. Reproduced with permission from ref <sup>24</sup>. Copyright 2021 Springer Nature.

#### 4.4 System Integration

PCTs are used to integrate functional electronic components for various wearable applications. In comparison to conventional rigid PCBs, PCT-based integrated electronic systems containing discrete electronic components can avoid the attachment of large and stiff circuits on the body, effectively improving the imperceptibility of the devices. Additionally, assembling dispersed

components onto textiles at a higher-level of integration provides the conformal and intimate contact between the integrated electronics with the body, ensuring precise sensing data with minimal noise or drift. A typical hybrid wearable electronic system on PCTs comprises several main components for full functionality, including a textile substrate with conductive interconnects, sensors, actuators, energy supply, data processing unit, transmission and communication units, and data analysis, *etc.*

#### **4.4.1 Integrated Circuits**

Traditional silicon-based IC chips, which offer higher performance over the flexible thin-film or stretchable fiber-based counterparts, are suitable for the integration into textile electronic systems. The package types of IC chips can be divided into two categories based on their mounting style, *i.e.*, through-hole technology (THT) and surface mount technology (SMT). SMT is more commonly used than THT because SMDs components are relatively smaller and lighter, making them ideal for miniaturized devices. SMDs are also less expensive and can be directly mounted on either side of PCBs using pick-and-place processes without drilling a hole, favoring the automated microfabrication process. In addition, the assembly of SMD onto fabrics is compatible with the textile industry due to the simple manufacturing and wearing comfort of the SMD-integrated textiles. To achieve conformability on body and mechanical reliability, it is necessary to further miniaturize IC chips. However, for the integration of miniature electronics on textiles, a higher resolution of interconnects and bonding points is required due to the narrow pin distances.

Transmission and communication of the data is a crucial technology in wearable electronics. Data collected by sensing units is transmitted to a microcontroller unit (MCU) for processing. Analog-to-digital converters (ADC) are needed to translate analog signals from the electronics to digital form, enabling the microcontroller to read and process the data. Besides, energy for powering the sensing units and the MCU can be supplied by various kinds of energy harvesters or energy storage devices. This allows for a data acquisition-processing-transmission cycle to be performed under power supply within the electronic system.

Traditional wired connections for powering, processing, and communication units in wearable systems may cause safety and maintenance issues, as well as limiting wearing comfort and portability. Therefore, wireless transmission technologies are highly desirable for compact wearable electronic systems. As illustrated in **Figure 68**, the sensing units can be connected to

wireless energy supply, processor, and communication units via electrically conductive interconnects, such as conducting threads and printed patterns. Then the data can be wirelessly transmitted to portable devices or uploaded to the cloud for data analysis and storage. These individual functional units can be assembled independently as part of the smart electronic textile system, which can be attached directly to the skin or integrated into clothing. The wireless communication technology for textiles will be discussed in the following section.

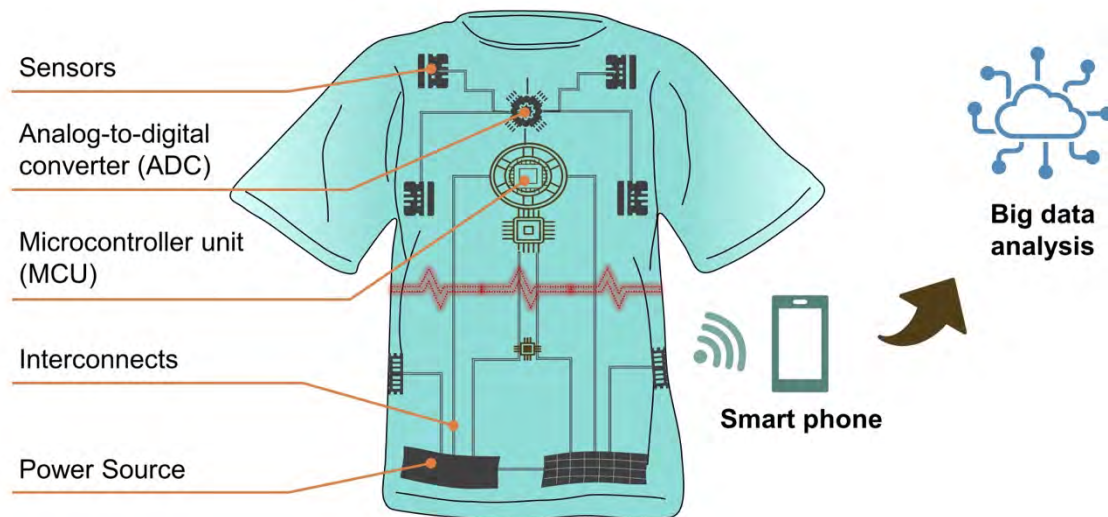


**Figure 68.** Illustration of an integrated textile system.

#### 4.4.2 Wireless Communications

Wireless communication systems such as NFC, Bluetooth, Wi-Fi, and ZigBee have been well developed and frequently used in electronic devices. In comparison, Wi-Fi could provide a high-speed and high-bandwidth data transmission to the cloud, though it requires to consume the most energy. ZigBee is a mesh network protocol for sharing information among multiple devices at the same time. However, it is not suitable for portable applications since it is prone to network interference. NFC and Bluetooth are the most commonly used protocols for wireless communications in wearable electronics. NFC is based on RFID technology. Since it uses a lower frequency, it consumes lower power usage for communication compared with Bluetooth. On the other hand, NFC has a much shorter operating range (up to 4 cm) than Bluetooth (up to 10 m), making it much more secure for data transfer and widely used for access control and payments.

Antenna is an essential component for wireless communications. When the antenna of an NFC

tag enters the electromagnetic field generated by an NFC reader, wireless interconnection is achieved through inductive coupling. Antenna can be printed on fabrics by using conductive inks or embroidery of conductive threads. The porous nature of textiles could promote the tough adhesion of the antenna and allows the antenna to be thin and flexible. However, the deformability of textiles will cause the unstable performance of the antenna. Therefore, efforts have been made for the structural design of antennas on textiles. For example, Jiang *et al.*<sup>800</sup> presented an antenna embroidered on textile that could be operated under significant bending and human body effects, which was attributed to the operating bandwidth of the antenna was considerably broader than the commercial ones (**Figure 69a**). As the antenna working frequency shifts under mechanical bending of garments, the reflected power from the NFC tag gradually decreases and the consequent reader range is shorten. With a broader bandwidth, the NFC tag could be read when it was bended with 120° bend angle (**Figure 69b**). To further reduce the influence of bending and stretching on textile antenna, the authors proposed to reduce the circuit size and select a relatively less influential body location to place the device.<sup>615</sup> A textile NFC enabled temperature and sweat sensing device was fabricated, and the sensors can be powered by the reader. The relatively small size of NFC prototype showed a more stable performance and the NFC antenna performed properly under bending up to 150°. The miniaturization design of antenna is important since antenna normally occupies a large area for NFC communications. Ashyap *et al.*<sup>801</sup> developed a compact wearable antenna with dimensions of 46×46×2.4 mm<sup>3</sup>. Electromagnetic bandgap (EBG) structures at 2.4 GHz were used to eliminate the mismatch and frequency shifting caused by the human body, as well as to reduce the unwanted radiation toward the human body. The dimension of the antenna for wearable textiles was further reduced to 30×20×0.7 mm<sup>3</sup> by the same research group, which was 75% smaller than a conventional antenna.<sup>802</sup> The sustainable performance of the constructed antenna was proved under bending condition, showing its promising application in wearable medical electronics.

Different from the NFC requiring an electromagnetic radio field for the communication between the sender and receiver antennas, Bluetooth uses direct radio transmissions and allows the transmission over longer distance between paired devices. Bluetooth is a more preferable wireless technology for health monitoring, since it allows continuous data flow exchange with a gateway device, such as a smartphone. However, with the high capability of streaming data, Bluetooth Classic consumes power quickly. Bluetooth Low Energy (BLE) is an energy-efficient wireless protocol introduced in 2010, which was designed to address the trade-off

between operation range and power consumption. BLE is compatible with most of the smart phones, tablets, and computers on the market. It is ideal for application in wireless wearable sensor networks that requires small data rate transmission and long power life. There are examples of electronic textiles adopting BLE for wireless transmission. Plant *et al.*<sup>803</sup> fabricated an electronic textile glove to measure the motor disorders of Parkinson's disease (PD) and used a wireless microprocessor and a flexible sensor to transmit the motion data to a personal, patient-oriented app. A BLE Nano board was applied for the data processing and wireless transmission of data, which was programmed with Arduino software and powered by a 3 V battery. Tao *et al.*<sup>804</sup> integrated a washable textile electronic system to sportswear (**Figure 69c**). The electronic module was fabricated on a flexible PCB to facilitate the integration and was encapsulated by PDMS for washability. The collected data including ECG signals, skin temperature, breathing rate and acceleration outputs was received by a smart phone via a Simblee BLE smart module, then transmitted into a remote database server via 4G or Wi-Fi for internet remote monitoring.

Besides integrating antennas into textiles or attaching flexible wireless communication modules directly on textiles, wireless body sensor networks have been built by researchers. To enable the continuous physiological monitoring using NFC technology, Lin *et al.*<sup>613</sup> demonstrated a near-field-enabled clothing capable of establishing wireless power and data connectivity around the human body (**Figure 69d**). Electromagnetically responsive patterns were integrated on the clothing by computer-controlled embroidery between physically separated sensors, extending the connectivity of near-field technologies from a range of few centimeters to meter-scale networks of power-free sensors in proximity to these patterns on clothing (**Figures 69e-g**). Tian *et al.*<sup>616</sup> constructed the energy-efficient and secure wireless sensor networks by confining radio-waves emitted by standard wireless devices onto metamaterial textiles (**Figure 69h**). The metamaterials textiles are clothing made from conductive textiles, which can achieve the interconnections of discrete wireless devices through the propagation of radio-waves when the devices are in the proximity of the textiles. Results demonstrated that the wireless Bluetooth transmission efficiency can be enhanced compared to conventional radiative networks without metamaterial textiles, and the transmission of personal health data can be localized to within 10 cm of the body (**Figures 69i, j**). Both the near-field-enabled clothing and metamaterial textiles enabled high-efficiency and secure wireless communications without the incorporation of PCB modules or narrow operation range limitation, proposing the ways of fabricating light-weight and robust electronic



textiles as personal data networks for health monitoring.

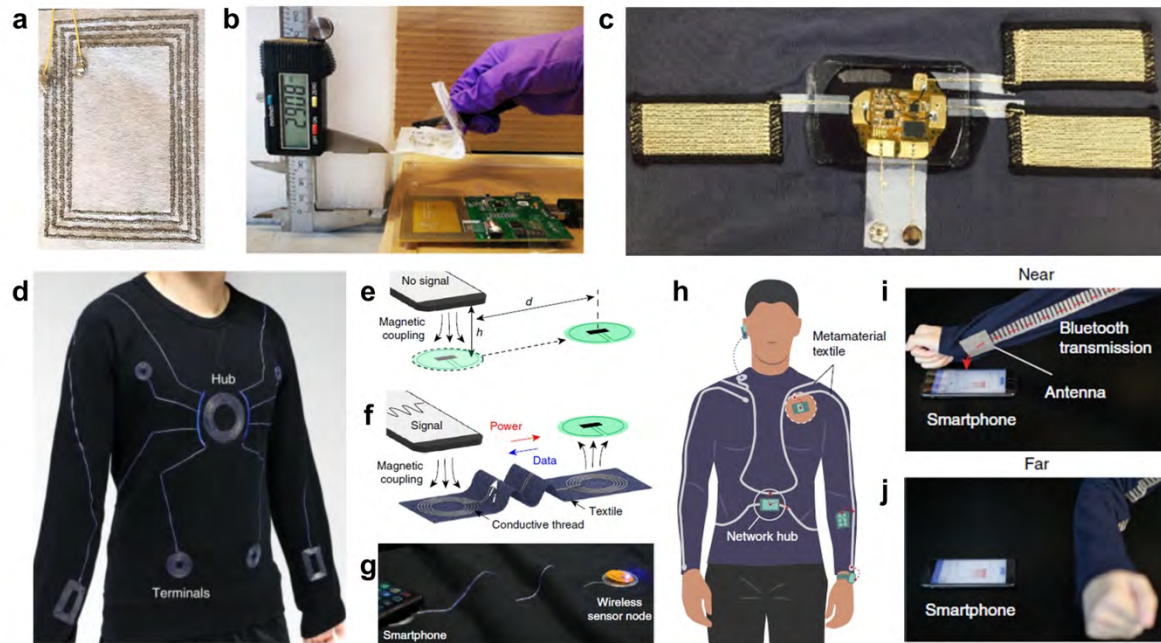


**Figure 69.** Wireless communications in wearable systems. (a) A fabricated electronic textile wearable NFC RFID tag. (b) Bending test applied on the NFC tag with 120° bend angle. Reproduced with permission from ref<sup>800</sup>. Copyright 2019 John Wiley and Sons. (c) Photograph of the electronic textile system with an integrated electronic system on the flexible printed circuit board (PCB). Reproduced with permission from ref<sup>804</sup>. Copyright 2018 John Wiley and Sons. (d) Photograph of near-field-enabled shirt comprised of a network with a single hub and eight terminals. Schematics of (e) conventional near-field communication and (f) the near-field relays connected communication. (g) Photograph of a smartphone wirelessly powering a sensor node over a 40-cm-length relay. Reproduced with permission from ref<sup>613</sup>. Copyright 2020 Springer Nature. (h) Illustration of a wireless sensor network with metamaterial textile. (i) and (j) Secure Bluetooth data transmission of ECG data along a sleeve integrated with an antenna near the wrist. Reproduced with permission from ref<sup>616</sup>. Copyright 2019 Springer Nature.

#### 4.4.3 Machine Learning

Wearable IoT devices generate tremendous amounts of data from wearable sensors, which demand high-quality big data analysis and drive the development of artificial intelligence (AI) based on machine learning algorithms. Machine learning is promising for healthcare applications, such as medical diagnosis, health state assessment, risk prediction, remote monitoring, and fitness tracking. For example, machine learning can be used in electronic

textiles to monitor vital signs such as body temperature, heart rate and respiration, providing early warning of potential health problems. It can also be applied to develop electronic textiles that can interact or adapt to the surrounding environmental factors such as temperature, humidity and UV lights, providing comfort and tailored performance to wearer.

Machine learning can be used to analyze the data collected by textile sensors to monitor the health status of the wearer, which could be especially useful for monitoring chronic conditions such as cardiovascular disease and diabetes. For example, Fang *et al.*<sup>805</sup> developed a machine-learning-assisted wireless textile system for high-fidelity and continuous pulse waveform monitoring. A low-cost, lightweight, and mechanically durable textile triboelectric sensor was fabricated to convert subtle skin deformation caused by arterial pulse into electricity. With the assistance of machine learning algorithms, the textile sensor can continuously and precisely perform pulse monitoring and cardiovascular condition assessment in an ambulatory and humid environment. The accuracy of the measured systolic and diastolic pressure was validated via a commercial blood pressure cuff at the hospital. The textile sensor was also integrated with a wearable signal processing unit, a Bluetooth transmission module, and a customized cellphone application (APP) to enable one-click health data sharing and data-driven cardiovascular diagnosis.

The integration of machine learning with wearable sensors to recognize human gestures has significant potential for developing applications in healthcare and robotics. Zhou *et al.*<sup>376</sup> demonstrated the value of this approach with a wearable real-time sign-to-speech translation system assisted by machine learning. The system consisted of yarn-based stretchable sensor arrays and a wireless PCB. Hand gesture movements were detected by the sensor arrays, and the processed signal was wirelessly transmitted to a customized APP that embedded with a machine-learning algorithm for robust translation of the hand gestures into speech. A total of 660 sign language hand gestures of American Sign Language were recognized, achieving a high recognition rate of 98.63% and a short recognition time less than 1 s.

Moreover, the use of machine learning is increasingly popular in the recognition of full-body motions, which can be valuable for motion tracking, activity recognition, health monitoring, rehabilitation, athlete performance analysis, human-environment interaction, and virtual reality (VR). For example, Zhu *et al.*<sup>806</sup> developed a self-powered and self-functional sock that can



harvest energy and sense various physiological signals. Through a machine learning process, the textile TENG can achieve walking pattern recognition and Parkinson's disease detection. As another example, Luo *et al.*<sup>344</sup> reported a textile-based tactile learning platform that records, models, and understands human-environment interactions. In this work, a full-body tactile sensing textile based on piezo-resistive fibers was prepared for the study of human activities. Machine learning techniques was applied for sensing correction and calibration to normalize the sensor responses and correct malfunctioning sensors in the array. This AI-assisted sensing textile system can classify humans' sitting poses and motions, with potential applications in biomechanics, cognitive sciences, and intelligent robotics.

Despite the great progress of machine learning in textile sensing systems, the large amount of raw sensor data collected must be transmitted and stored in external computing units or the cloud. In-sensor machine learning can largely reduce energy consumption, improve data latency and security. However, the integration of machine learning algorithms into the textile systems remains challenging, which requires advanced design strategies and architectures.<sup>807,</sup>

808

## 5. APPLICATION SCENARIOS

The integration of flexible electronics into textiles has paved the way for a plethora of wearable applications. The flexible and permeable nature of textile electronics makes them comfortable to wear and allows for seamless integration into daily clothing. Recent advancements in the fabrication of PCTs have improved the performance of textile electronics. By adopting PCTs, textile electronics are created to be permeable, flexible, sensitive, stable, and multifunctional. In addition to the advances in the fabrication of PCTs, the rapid evolution of microfabrication technologies, advanced nanomaterials, and AI have paved the way for practical applications of PCT-based wearable electronics. By combining these state-of-the-art technologies, textile electronics with enhanced functionality and performance are applied for a wide range of application scenarios, including health monitoring, disease diagnosis and therapeutics, exercise and sports, VR/AR, human-machine interaction, IoT, *etc.* (**Figure 70**).

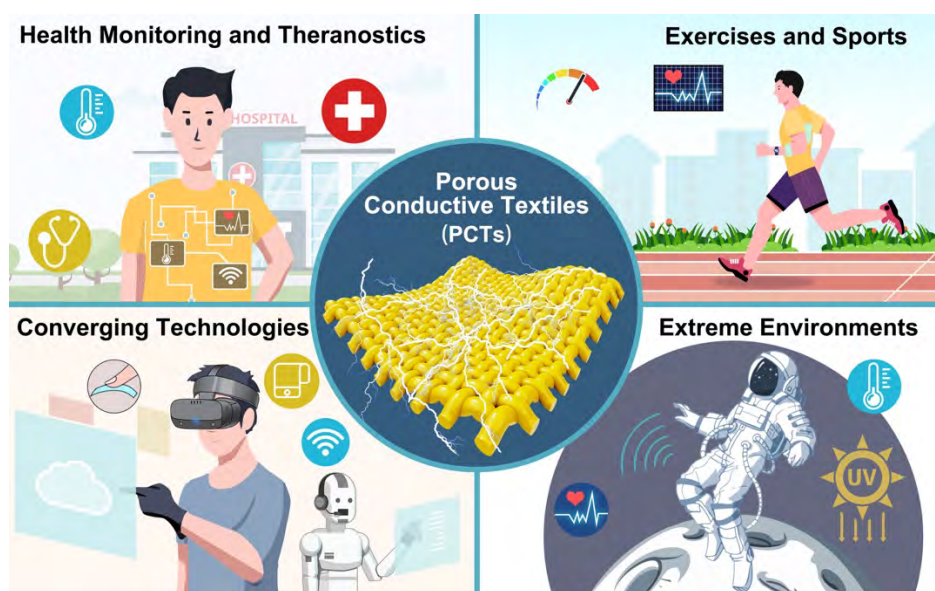


**Figure 70.** Representative application scenarios of PCT-based wearable electronics.

### 5.1 Health Monitoring and Theranostics

Health monitoring is one of the most promising applications of wearable electronics and current research is indeed dedicated to this field. PCT-based sensors that can comfortably worn on human body are capable of collecting a variety of health-related data, including activity levels, physiological status, biomarker concentrations, medication metabolites, sleep patterns, *etc.*<sup>809-</sup>  
<sup>813</sup> By enabling continuous and timely monitoring of these metrics, wearable sensors can assist in health monitoring, disease diagnosis, and therapeutic interventions. Consequently, such a point-of-care and personalized health monitoring system would revolutionize the traditional

diagnostic process that typically requires going to a hospital. This could alleviate issues such as high expenses, time constraints, and the need of professional medical personnel. The various types of PCT-based sensors and therapeutic devices are detailed in the Sections 3.1 & 3.3 in terms of their working mechanism, fabrication process, and performance. In this section, we further outline the implications for specific applications in health monitoring and theranostics, including the monitoring of biophysical, biochemical, and electrophysiological signals, as well as therapeutics (**Figure 71**).

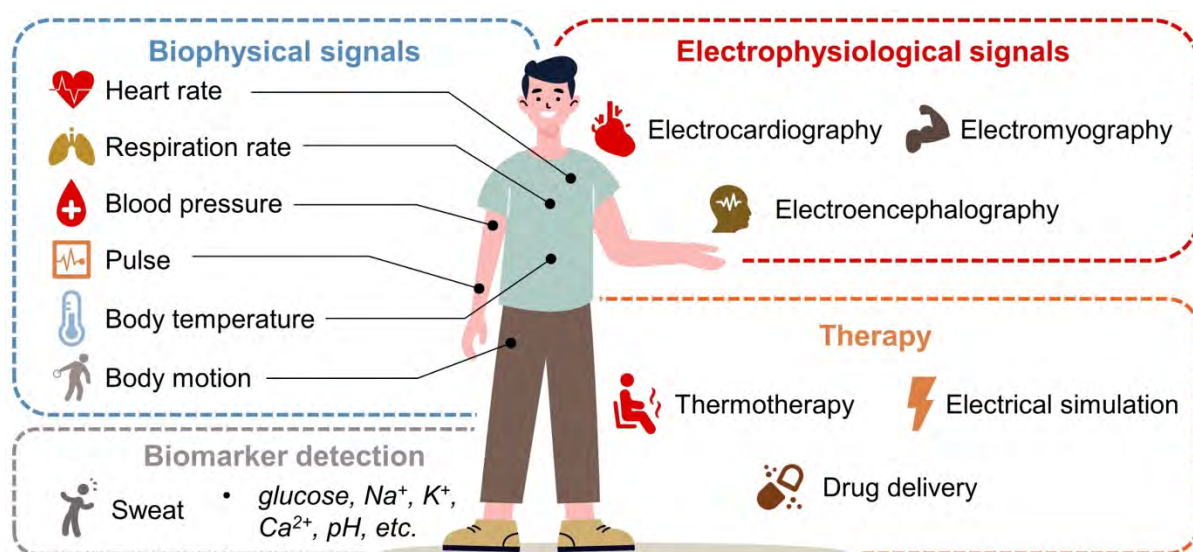


**Figure 71.** Schematic of representative health-monitoring signals and therapeutics that can be achieved by PCT-based wearable electronics.

Biophysical signals such as body temperature, respiration rate, blood pressure, pulse, heart rate, and body motions are essential indicators in evaluating an individual's health and physical conditions.<sup>61</sup> For example, continuous temperature monitoring is crucial in detecting fever for people who may lack self-awareness, such as infants, as well as in special scenarios like during the COVID-19 pandemic.<sup>357</sup> Additionally, localized temperature detection around a wound can function as a vital factor for monitoring inflammation conditions.<sup>814</sup> Strain and pressure sensors have the ability to detect a range of human body movements, including large motions such as joint bending, as well as vital motions such as pulse, speech vibrations, facial expressions, and heartbeats, among others. As a result, by attaching strain and/or pressure sensors around human joints, it becomes feasible to monitor the joint kinematics, mechanical loadings, and pressure distribution,<sup>815, 816</sup> allowing for the detection of motion abnormalities such as those found in arthritis and Parkinson's disease. Similarly, when mounted on socks or insoles, the sensors can

monitor and analyze plantar pressure and gait,<sup>817, 818</sup> facilitating the detection of motion abnormalities for disease pre-diagnosis, prevention, or rehabilitation purposes. In particular, the combination of machine learning-based recognition in recent research has significantly improved the accuracy of the aforementioned motion detections.<sup>819</sup> Moreover, strain and pressure sensors can also be used to detect vital signals such as respiration rate, pulse, and heartbeats, which can be utilized in various applications such as field search and rescue, sleep monitoring,<sup>820</sup> and disease diagnosis based on the in-depth analysis of these vital signals. An intriguing application is disease diagnosis and recognition of pregnancy by monitoring the pulse using pressure sensors mounted on the wrist, based on the pulse-taking procedure in traditional Chinese medicine.<sup>821, 822</sup> Li *et al.*<sup>823</sup> developed a wearable intelligent health monitoring system by combining a strain sensor array and a deep learning-assisted algorithm for monitoring blood pressure and cardiac function. In specific, a sensor array comprising six strain sensors constructed from carbonized silk georgette was placed near the artery on the wrist, which achieved the acquisition of high-precise and feature-rich pulse waves. The integration of deep learning assistance into the sensor array system eliminated the need for precise positioning and professional knowledge, making it accessible and convenient for users. In conclusion, by incorporating textile physical sensors into everyday clothing, human activity levels and biophysical signals can be continuously collected and analyzed, allowing for the creation of a significant personal database for long-term health monitoring and lifestyle improvement.

Detecting the concentration of specific biomolecules in blood is the common diagnostic method for diseases, yet it is labor-intensive and has limited effectiveness. Therefore, there is a growing demand for portable and wearable devices that individuals can use to monitor the biological indicators themselves, particularly for chronic diseases such as diabetes that require frequent glucose concentration measurement.<sup>824</sup> Although some portable glucose sensors are available, they still rely on the invasive process of extracting blood from the fingers, which carries the risk of infection. Thus, there is a need for non-invasive alternatives that can provide accurate and reliable measurements of biomolecules in biofluids.<sup>825</sup> Consequently, the biosensors that can measure the concentration of biomolecules present in sweat become a promising alternative. Recently, the application of textile-based biosensors for monitoring biomolecules containing in sweat has made considerable advancements. Compared to conventional film-based flexible biosensors, the textile platforms offer significant advantages such as the ease of integrating multiple sensors through textile engineering, improved sweat

extraction, and good permeability due to their porous structure. For example, Wang *et al.*<sup>438</sup> integrated five biosensors including glucose, Na<sup>+</sup>, K<sup>+</sup>, Ca<sup>2+</sup>, and pH in a textile through weaving individual functional fibers, and He *et al.*<sup>447</sup> developed an integrated textile sensor patch with six biosensors including glucose, lactate, ascorbic acid, uric acid, Na<sup>+</sup>, and K<sup>+</sup> by using carbon textile electrodes. These integrated textile biosensors can simultaneously detect the biomolecules in sweat, and they can remain their performances under deformations, demonstrating the potential for real-time noninvasive monitoring of human body biomarkers. Apart from detecting sweat biomolecules, the detection of gas molecules exhaled during human respiration and skin odors presents another intriguing avenue for disease indicator detection, which has been relatively understudied. A trial of this can be the integration of sensors into a facemask for real-time detection of gaseous molecules.<sup>826, 827</sup> In conclusion, the use of textile biosensors for disease diagnosis and health monitoring through sweat and expiration is a promising approach, although current research primarily demonstrates prototypes.<sup>828</sup>

The acquisition of electrophysiological signals is crucial for understanding the behavior and function of several physiological systems, such as the cardiovascular, nervous, and muscular systems, and can provide valuable insights into human health. Bioelectrical signals such as ECG, EMG, and EEG are commonly used to diagnose various health conditions, including heart arrhythmias, epilepsy, and sleep disorders.<sup>829</sup> For instance, ECG can be detected to identify heart abnormalities that may result in a heart attack or stroke if not diagnosed and treated in a timely manner. The utilization of EMG in analyzing specific muscle abilities is useful in post-stroke rehabilitation and prosthesis applications.<sup>830</sup> EMG enables the assessment of muscle function and activation patterns, which can guide the development of targeted rehabilitation protocols and prosthesis control strategies. PCTs have several benefits when utilized as the electrodes for recording the electrophysiological signals. One of the advantages is their excellent stability, which eliminates the concern of dehydration that commonly arises with conventional gel electrodes. Consequently, PCTs allow for long-term applications without experiencing any degradation in performance. At present, garments with integrated functions for detecting electrophysiological signals have seen extensive development, but the majority of them rely on the weaving of metal wires into clothing, which can be relatively inflexible and prone to oxidation or corrosion due to sweat exposure. As a result, there is a need to develop more flexible and stable textile electrodes capable of withstanding harsh sweating conditions and even washing, without compromising their performance.

In addition, PCT-based wearable electronics have been implemented to aid in the therapy of diseases. Thermotherapy, a simple and effective therapeutic technique that involves applying heat to specific areas to alleviate muscle pain and discomfort, has demonstrated significant effects in treating conditions such as rheumatoid arthritis, inflammation, joint stiffness, and improving blood circulation. PCT-based Joule heating devices, due to their excellent flexibility and conductivity, can conveniently provide heating to the human body by applying relatively low voltages. For example, Chen *et al.*<sup>831</sup> prepared a conductive yarn by continuous capillary dip-coating of CNTs, and stitched the conductive yarn into a knee brace, which achieved joint motion monitoring and Joule heating thermotherapy (**Figure 72**). Besides, electrical stimulation through the direct delivery of electrical pulses is also an effective method for pain management, muscle rehabilitation, and neurological disorders. Numerous studies have explored the integration of conductive fibers into clothing for TENS applications.<sup>530</sup> In addition to physical therapy, textile electronics can also facilitate therapy through the delivery of drugs. Iontophoresis devices have proven to be effective tools for transdermal drug delivery to achieve localized drug delivery through the skin, avoiding the adverse effects of oral administration. Drugs can be loaded into the fibers, and their delivery can be controlled by adjusting the applied current and duration. Furthermore, real-time monitoring of drug metabolism is important as it can provide valuable information on drug efficacy and potential adverse effects. Sweat is a promising matrix for drug metabolite monitoring due to its non-invasive and continuous collection capability. Versatile biosensors can be integrated into wearable devices to detect drug metabolites in sweat, allowing for real-time monitoring of drug metabolism. Therefore, the integration of versatile biosensors in textile for drug metabolite monitoring in sweat is a promising area of research with potential applications in personalized medicine and drug development.



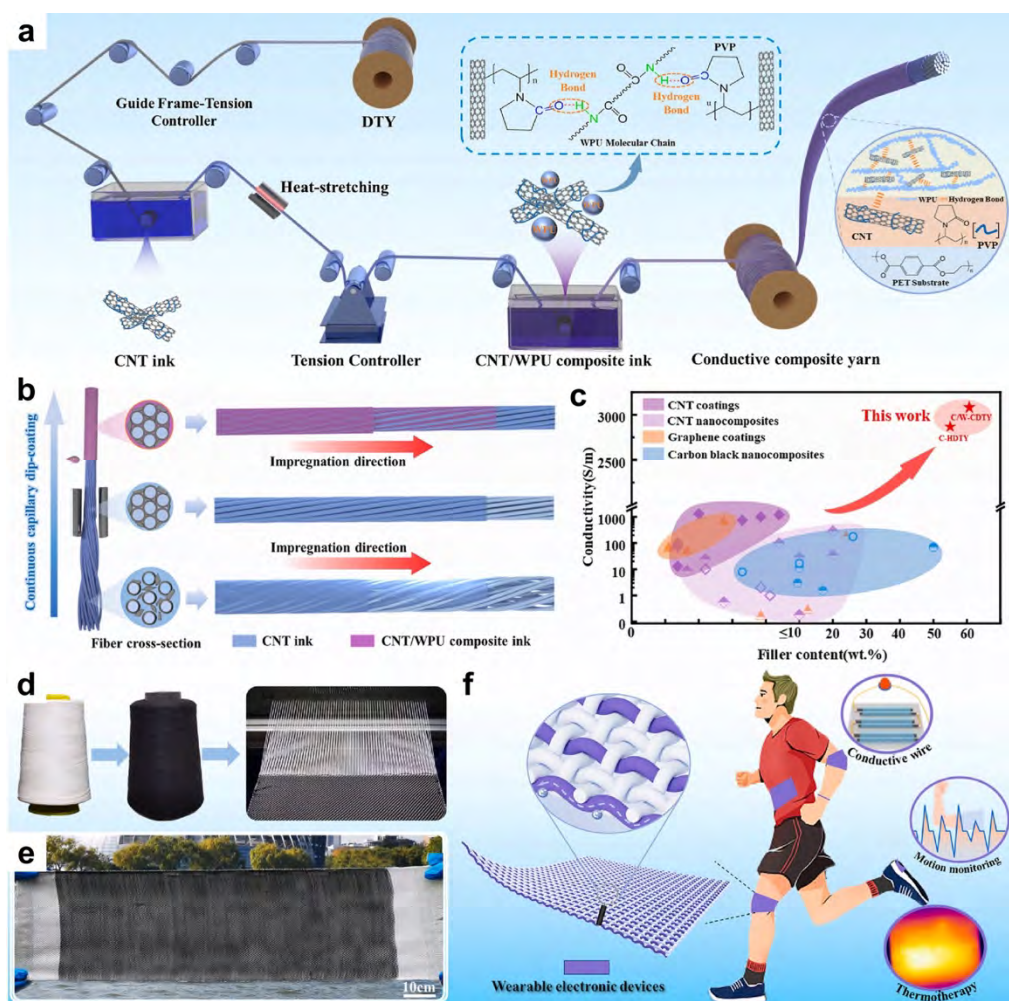


**Figure 72.** Schematic of the manufacture of a conductive yarn (CNT/WPU) and the application for motion sensors and thermotherapy: (a) Schematic illustration of the manufacture procedure of conductive yarn; (b) schematic illustration of yarn structure in continuous capillary dip-coating process; (c) overview of conductivity and conductive filler content with other yarns; (d, e) optical image from yarn to fabric through commercial braiding machine; (f) the applications of the yarn-based wearable electronic devices. Reproduced with permission from ref <sup>831</sup>. Copyright 2023 Elsevier.

## 5.2 Exercises and Sports

Wearable electronics offer great potential in exercise and sports for evaluating activity levels and tracking the physical condition of athletes and sports enthusiasts.<sup>832</sup> By monitoring an individual's physical and physiological state during exercise or competition, valuable information can be obtained, such as hydration levels, muscle fatigue, and injury risk. This data can be used by coaches and trainers to customize training programs and make real-time adjustments during competitions to optimize performance and minimize the likelihood of



injury. Although there are currently various wearable devices, including fitness trackers and smartwatches, that can gather data on metrics such as heart rate, calorie burn, steps taken, and distance covered, they are generally fabricated by bulky, thick, and non-permeable materials, which can make wearing them unpleasant for the user. In addition, the present athlete training monitoring systems are mostly based on video technology, which can only perform motion analysis but cannot collect any biosignals. Thus, there is a significant need for highly flexible, comfortable, and multifunctional wearable electronics specifically designed for exercise and sports. Textile electronics are an excellent choice due to their good flexibility, lightweight, and permeable qualities, which allow them to be seamlessly integrated into sportswear without hampering the athletes' performance.

Monitoring biomechanical, electrophysiological, biochemical, and tissue dynamic signals are essential in exercise and sports. The biomechanical signals encompass motion, force, speed, posture, and other kinematic factors that can be used to assess the performance and technique of athletes.<sup>833</sup> In the case of a runner, step frequency, step length, range of motion, and joint angle are essential parameters to consider. Therefore, by mounting textile-based strain and pressure sensors around the joints and foot, dynamic information could be accurately harvested. In addition, real-time detection of body contact and/or contact force (*e.g.*, punching speed and force) is useful in athletic contests for assisting judgment or guiding training. For example, Liang *et al.*<sup>834</sup> developed a helical fiber-based pressure sensor, which is capable of detecting contact pressure and realizing noncontact proximity detection during playing basketball and Taekwondo display (**Figure 73**). Ye *et al.*<sup>835</sup> demonstrated an all-textile pressure sensor capable of precisely monitor the punching speed and pressure during physical combat sports such as sparring and boxing. This all-textile sensor was assembled by sandwiching a 3D spacer-fabric dielectric layer between two conductive woven electrodes, and it was integrated into a training suit. Furthermore, textile motion sensors may also be utilized for monitoring underwater sports such as swimming. However, this poses a significant challenge as ensuring the waterproofing of materials and devices is difficult due to the high porosity of textile materials. While some highly hydrophobic textile devices have been demonstrated, it is unlikely that they will be suitable for long-term practical applications, as most electronic components are sensitive to water and it is challenging to completely prevent water from penetrating the textile. Thus, a specific package is required, which entails a trade-off between sensing functionality and permeability.

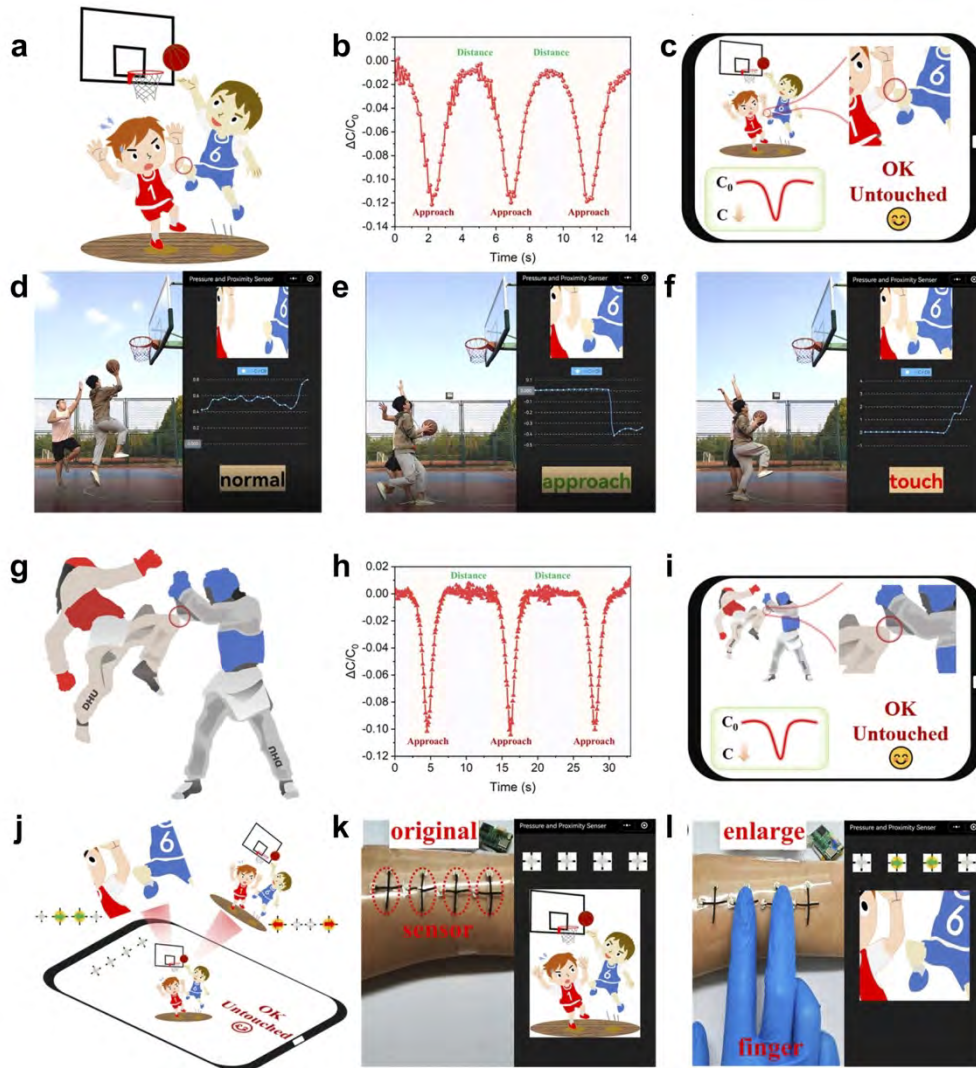


**Figure 73.** (a-f) Schematic diagram of applying pressure sensors for contact monitoring during playing basketball. (g-i) Schematic diagram of applying pressure sensors for contact monitoring during Taekwondo athlete noncontact display. (j) Results displayed after processing. (k-l) The noncontact gesture operation sensor at the original (k) and enlarge (l) states. Reproduced with permission from ref<sup>834</sup>. Copyright 2023 Elsevier.

Electrophysiological signals play an important role in understanding the physical and mental states of athletes. First, EMG signals that measure the muscle activity can be used to assess muscle fatigue, identify muscle imbalances, and guide exercise optimization and rehabilitation. For example, an athlete's EMG signals can be analyzed to determine whether they are using proper technique during a particular exercise or whether they need to adjust their training. Second, ECG signals that measure the electrical activity of the heart can detect abnormalities that may indicate an increased risk of sudden cardiac death. Additionally, EEG signals can provide beneficial insights into an athlete's mental and emotional state, allowing them to

optimize their performance and reduce the risk of injury or burnout. Monitoring electrophysiological signals during exercise and training is of great challenge due to their weak nature and susceptibility to motion artifacts. A crucial requirement for gathering these signals is a tight and stable contact between the electrodes and the skin. However, large body movements and sweating during exercise can cause the electrodes to become displaced or detached from the skin, leading to contact impedance variations and signal loss. The commonly used gel sticky electrodes have limitations such as loss of adhesion under sweating, and cause skin irritation and dehydration during prolonged application. The stretchable and permeable PCT-based dry electrodes hold great promise in addressing the dehydration and irritation issues for long-term applications,<sup>836</sup> while they may still be susceptible to motion artifact caused by movements due to their poor adhesion performance. Nonetheless, significant efforts have been devoted to the development of soft and elastic textile electrodes that can tightly wrap around the human body, potentially overcoming these challenges. Despite to the advancements in textile-based bioelectrodes for measuring electrophysiological signals, the most crucial challenge in wearable applications is the absence of small and flexible data collection devices that are necessary for signal amplification and data processing. Consequently, future efforts should be directed towards developing a closed-loop system that integrates both the electrodes and hardware onto textiles for wearable applications.

Biochemical signals such as the concentration of  $\text{Na}^+$  and  $\text{K}^+$  ions, glucose, and lactate are crucial indicators of human body's functions during exercise. For example, lactate is produced during intense physical activities, due to anaerobic metabolism in the absence of sufficient oxygen.<sup>837</sup> Therefore, the concentration of lactate can be an indicator in evaluating muscle fatigue and pain.<sup>838</sup> Wearable sweat biosensors are thus promising in detecting these chemicals during exercise,<sup>839</sup> given that sweating is a natural occurrence during exercise. Zhao *et al.*<sup>840</sup> designed a fully integrated wearable sweat sensor platform by integrating lactate and  $\text{Na}^+$  sensors, signal readout and data communication circuits in a wearable headband. The lactate and  $\text{Na}^+$  sensors are made by using conductive threads decorated with ZnO nanowires as electrodes. These sensors achieved the detection of lactate and  $\text{Na}^+$  in linear ranges of 0-25 mM and 0.1-100 mM, respectively. Moreover, real-time on-body sweat collection and analysis were validated during intense exercise. In addition to biomolecules that can indicate athletes' competitive state, detecting other chemicals such as banned substances (*e.g.*, alcohols, stimulants) can also be valuable.<sup>841</sup> Doping control is crucial both before and after competitions, but the current invasive blood test method can be painful for athletes. Therefore, utilizing

wearable textile biosensors to detect sweat metabolites could serve as a useful prescreening tool, enabling non-invasive and convenient monitoring of athletes for doping control purposes.

Tissue dynamic signals refer to the physiological changes that occur in various tissues during and after exercise. For example, during exercise, blood vessels in skeletal muscles undergo vasodilation, which leads to an increase in blood flow to the muscles. This increase in blood flow helps to supply the muscles with oxygen and nutrients needed for energy production. Additionally, during exercise, the heart rate increases to pump more blood to the working muscles and other organs. Therefore, monitoring tissue dynamic signals is also critical to assess individual's health conditions during exercise. Wearable strain or pressure sensors are capable of measuring tiny changes in pulse and heartbeat, making them suitable for monitoring these signals during exercise. In particular, wearable textile-based PENG and TENG sensors are advantageous because they work in a self-powered manner and are comfortable to wear.<sup>61</sup> Additionally, ECG signals can provide heart rate information through arithmetic calculations.

In conclusion, textile-based wearable sensors have a wide range of applications in monitoring both physical and physiological signals during exercise.<sup>842</sup> These sensors have the potential to not only improve athletic performance but also safeguard human health during exercise. With the increase in popularity of outdoor and extreme sports nowadays, wearable sensors, despite the monitoring of health conditions, can also provide valuable information such as environmental temperature, humidity, and UV index, enabling users to take adequate precautions for healthy exercise.<sup>843</sup> Additionally, in unforeseen circumstances, wearable sensors can provide emergency rescue information through IoT. Furthermore, other wearable devices can also be useful during exercise, such as wearable displays, can provide lighting, warnings and communications in dark environments.<sup>844</sup> It is envisioned that PCT-based wearable electronics will make fitness safer, smarter, and more enjoyable in the future.

### **5.3 Converging Technologies**

The swift progress of the internet, information technology, and AI has resulted in a significant expansion in the application scope of wearable electronics. The convergence of these technologies with wearable devices has triggered a plethora of advanced functionalities in areas such as HMI, extended reality (XR), and the IoT, which are revolutionizing human life in various aspects including personalized healthcare, smart homes, smart cities, education, and entertainment, *etc.* In general, these smart application scenarios require devices that can interact

seamlessly between the human body and external environments, encompassing perceptions of both the human body and surroundings, as well as the ability to provide feedback to the outside world. However, the majority of the devices and/or systems currently developed rely on bulky and rigid components, which significantly affect wearing comfort. Therefore, utilizing textiles as a platform for designing wearable systems tailored to these smart applications becomes highly applicable. Given that versatile textile-based flexible electronics including sensors, actuators, and power supply devices are matured in recent years, the fusion of textile electronics with the emerging converging technologies can be readily realized. In this section, we will introduce several proof-of-concept examples highlighting the potential of textile-based devices for applications in HMI, XR, and IoT.

### 5.3.1 Human-Machine Interaction

An HMI system is designed to facilitate communication between humans and machines, such as computers or robots, which has broad applications in industries, healthcare, and entertainment.<sup>845, 846</sup> Commercial mechanical arms are typical examples of HMI devices that can carry out routine commands. However, these devices can only perform predefined and repetitive tasks with limited intelligence. Wearable HMI systems that can execute real-time, rapid, and precise manipulation is still of great challenges and remains an area of great interest.<sup>847</sup> To achieve this objective, conformably integrating flexible and sensitive sensors on human body is crucial for accurately transducing the physical signals and stimuli.<sup>848</sup> Strain and pressure sensors are often used in human-oriented HMI, as they are capable of detecting human motions and applied force. Attaching stretchable strain sensors to finger joints is a simple way to create motion-controlled HMI. In specific, a strain sensor is capable of perceiving the finger bending motions and converting them into electrical signals, which are subsequently transmitted to a processing unit. Once the information is received, a machine (*e.g.*, robot hand) will carry out corresponding actions as commanded. By performing appropriate motions, various actions can be achieved, such as controlling the bending degree and/or frequency of a robot hand.<sup>849</sup> Moreover, the utilization of a sensor array with multiple pixels allows for the execution of intricate actions, such as grasping a robot hand with different gestures.<sup>850</sup> For example, a glove platform was developed by knitting conductive fibers-based strain sensors into a glove, and integrating a FPCB as the processing and wirelessly transmitting unit (**Figure 74a-c**).<sup>851</sup> Assisted by machine learning, this system-level glove platform realized underwater finger-controlled piano playing and real-time remote control of a robotic hand in water *via* hand gestures (**Figure 74d**).

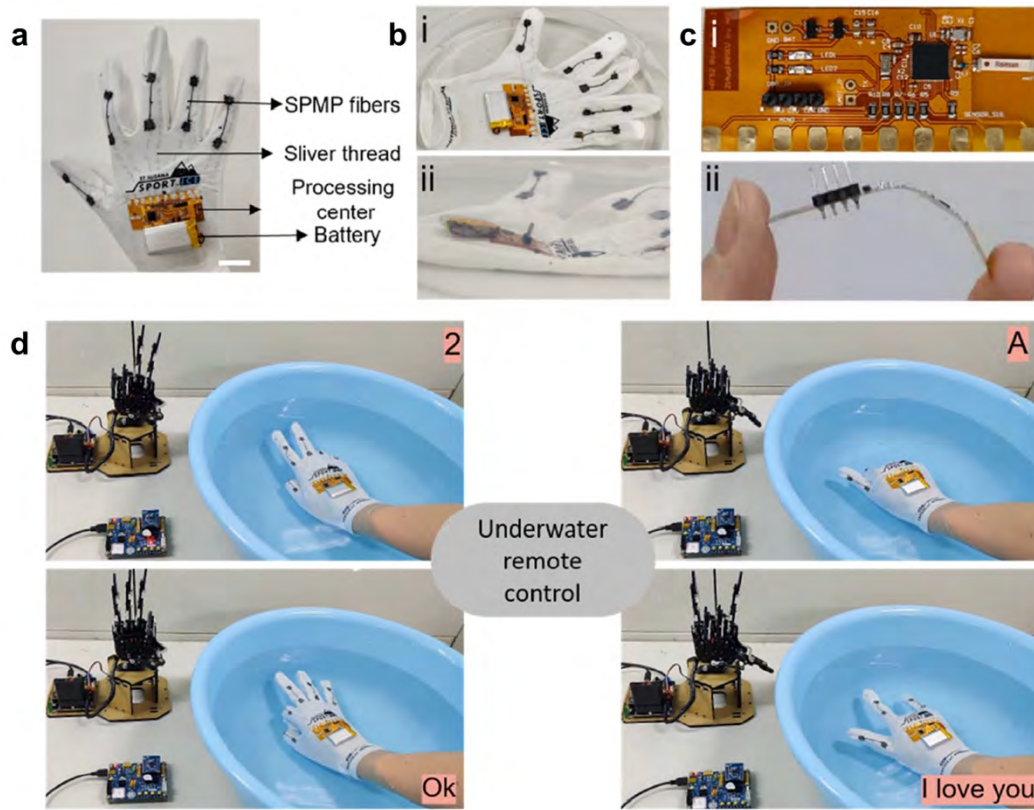


**Figure 74.** (a) Picture depicting the hybrid intelligent system involving SPMP fibers, conductive sliver threads, micro-controller and battery. (b) Anterior and lateral pictures of the hybrid intelligent system in water. (c) Pictures of the FPCB (i), and it is bendable (ii). (d) The corresponding screens for remote control of a robot hand in water. Reproduced with permission from ref <sup>851</sup>. Copyright 2022 Elsevier.

In addition to attaching strain sensors around joints for controlling machines, pressure sensors can be readily integrated into a textile and worn on human body.<sup>852</sup> For instance, a wearable HMI device with sound feedback was developed by stitching multiple fiber-based tactile sensors into a textile and integrating them onto sportswear around the wrist.<sup>853</sup> The signal input for this device involved finger tapping on the tactile sensors, which have an impressive sensitivity of  $0.84 \text{ kPa}^{-1}$  and a rapid response time of under 4 ms. Apart from capturing large motions, even subtle motions like facial muscle activity can also be utilized to provide control instructions for HMI applications. Furthermore, pressure sensors based on PENG and TENG are excellent choices for wearable HMI applications,<sup>854-856</sup> as they operate in a self-powering manner.

Except for mechanical motion sensors, other sensors such as electrophysiological sensors can also be designed for HMI. For example, by mounting multi-channel electrodes on human skin (*e.g.*, around the arm), the EMG signals can be acquired for real-time manipulating a robot hand.<sup>857</sup> This application holds great promise for controlling prosthetic devices. In contrast to conventional HMI that necessitate direct contact with human body or proximity to transmission signals, non-contact mode HMI presents a more promising outlook. This is particularly useful in specific scenarios like hospitals and during the COVID-19 pandemic, as it can eliminate the risk of cross-infection of bacteria or viruses. Recently, Lu *et al.*<sup>858</sup> demonstrated such a non-contact HMI application scenario. They fabricated a facial mask integrated with a humidity sensor made from electrospun conductive nanofibers, which is capable of detecting infant asthma *via* monitoring the respiration rate. The noncontact mode detection of asthma further enabled remote alarm and noncontact controlling HMI (*i.e.*, noncontact interfaces for medicine delivery). It is envisioned that this type of applications would have great prospects in the field of medical and healthcare.

### 5.3.2 Extended Reality

The recently emerged extended reality (XR) technologies, including VR and AR, has revolutionized the way we experience and interact with digital environments by providing immersive and realistic experiences. These technologies have seen widespread applications in the fields such as entertainment, medical training, navigation, tourism, and education. Currently, the VR/AR experiences are primarily delivered through the use of a headset or goggles, enabling the users to explore digital environments enriched with visual and auditory signals created by computers. However, this approach has certain limitations. First, the headsets and goggles are often rigid, heavy, and bulky, which will cause discomfort for users, especially during extended period of wearing. Second, the exclusive reliance on visual and auditory signals largely limits the immersion experience. Therefore, the development of flexible, lightweight, and thin interactive devices would be crucial to improve wearing comfort. In addition, other sensory inputs such as touch (haptic), smell (olfactory), and temperature (thermal) play essential roles in our perception and understanding of the real world.<sup>859-862</sup> Thus, the incorporation of these additional sensory elements into XR devices would enhance the level of immersion and make the experiences more realistic.<sup>863</sup> As a result, extensive research endeavors have been dedicated to exploring the potential applications of flexible and wearable electronics in VR/AR devices.<sup>859-861, 863, 864</sup>



In VR and AR systems, there are two essential components: input devices and output devices. The input devices are responsible for gathering information from the physical environment and the user, while the output devices generate signals or feedback from the processor to stimulate the user's sensory system through appropriate signal transduction. In this regard, textile electronics are an excellent platform for capturing the physical signals and generating feedback that can replicate realistic sensations. Notably, wearable sensors with versatile capabilities enable the real-time monitoring of body and environmental conditions.<sup>865</sup> For instance, textile strain sensors and pressure sensors embedded in fabrics can accurately detect body motions, moving postures, and external touch, *etc.*<sup>866, 867</sup> Zhang *et al.*<sup>868</sup> integrated triboelectric textile sensors into socks for the gait analysis, and a VR fitness game with the smart sock as control interface was demonstrated (**Figure 75**). Combining with deep learning data processing, the smart sock can be used as a functional part in both smart home and smart classroom applications by creating a virtual figure with replicated motions of the user. Furthermore, versatile textile actuators can generate appropriate feedback to users, providing a realistic motion or haptic experience. While lots of studies have demonstrated the utilization of textile electronics for VR/AR applications, most of them have focused on developing prototypes that serve a specific function. However, the development of truly multifunctional devices or closed-loop systems that can perceive physical signals and provide feedback is still relatively limited, particularly in the context of textile electronics. Nevertheless, textiles possess inherent advantages in terms of wearing comfort and ease of functionalization, making them an ideal platform for the integration of VR/AR functionalities.<sup>61</sup> This opens up exciting possibilities for the future development of smart clothing that combines VR/AR capabilities, similar to the concept depicted in the movie "*Ready Player One*".

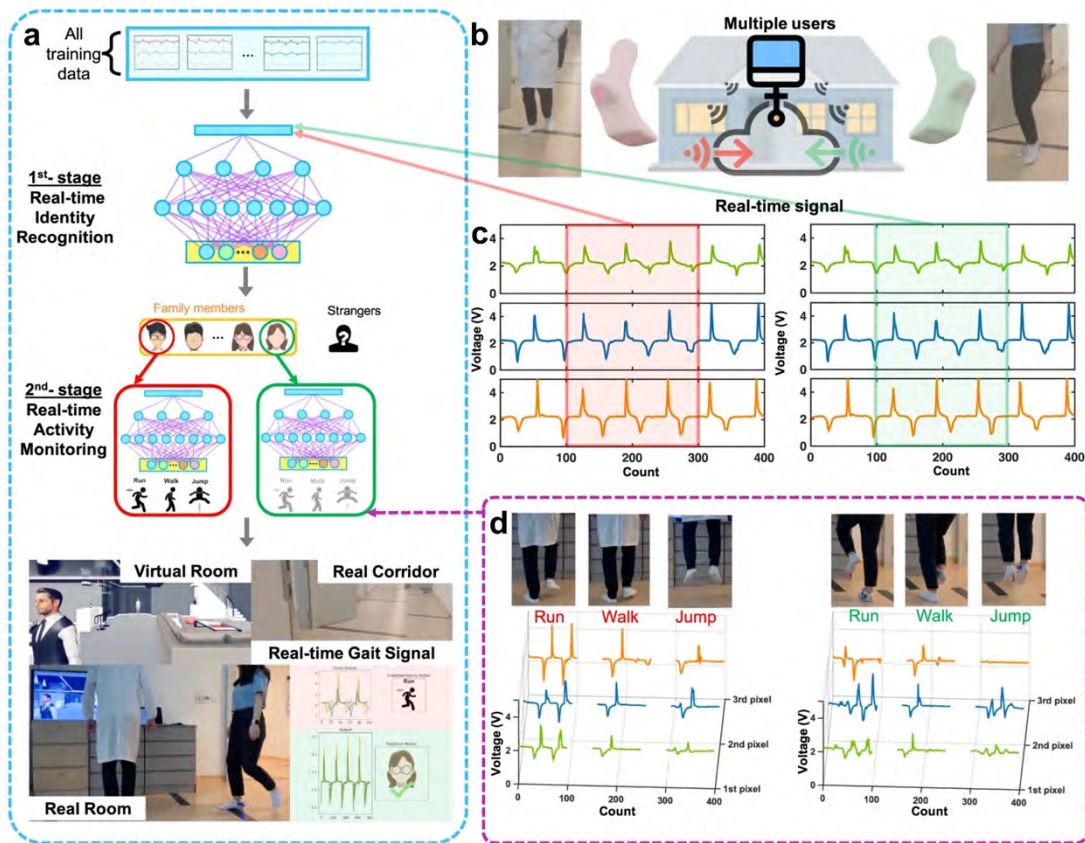


**Figure 75.** (a-b) Schematics of employing machine learning-enabled smart sock for gait signals identification with wireless communication. (c) The gait signal of two family members for gait identification in the first stage of smart home system. (d) The gait signals of recorded family members responding to different motions (run, walk, and jump) in the second stage of the smart home system. Reproduced with permission from ref <sup>868</sup>. Copyright 2020 Springer Nature.

### 5.3.3 Internets of Things

The advent of mobile devices, widespread internet access, and AI has ushered humanity into a new era of information.<sup>869</sup> The merging of wearable electronics and the internet has given rise to the emerging field of the IoT,<sup>416, 870</sup> enabling seamless connections between individuals and various internet-based systems. Currently, the IoT heavily relies on the personal terminals such as cellphones and portable electronics. To expand the horizons of the IoT, there is a growing demand for smart wearable electronics that possess sensing, computing, and communication capabilities, enabling continuous and ubiquitous interactions.<sup>871</sup> One significant application of such technology is in health monitoring, where wearable devices can continuously gather and transmit vital health data for improved patient care.<sup>872</sup> The integration of textile electronics in these areas offers a promising approach to collect personal health information during daily activities. Whereas various health monitoring applications have been demonstrated,<sup>832</sup>

achieving round-the-clock monitoring still presents great challenges in terms of continuous power supply and processing and storage of the collected big data. Regarding the wearable power supply issue, the rapid advancements in flexible energy devices would provide an elegant solution.<sup>873</sup> However, managing the enormous amount of data and data fusion from different sensors would be a hurdle. Efficient data processing and transmission devices are required to handle the data and facilitate seamless communication between sensors, while the development of novel all-textile based data processing units is challenged. Current solution still relies on the integration of conventional Si-based devices into textiles, and the integration strategy is detailed in above section. In addition, the machine learning-assisted data analysis would help to process and interpret the data, enabling effective solutions such as developing alarm systems based on the analyzed data. However, data privacy remains an important concern that needs to be addressed to ensure the security and confidentiality of personal information.

In short, with ongoing advancements in textile electronics and the increasing convergence of technologies, it is envisioned that smart textiles integrating HMI, VR/AR, and IoT functions will become a reality in the near future. This advancement holds the potential to bring us closer to a smarter world, revolutionizing how we perceive and interact with the world around us. However, achieving this goal requires systematic work and collaborative efforts by researchers, engineers, and industry experts. By working together, we can overcome challenges, optimize design and functionality, ensure reliability and user-friendliness, and thus pave the way for the widespread adoption of smart textiles in various applications.

#### **5.4 Extreme Environments**

We would like to highlight other potential application scenarios for wearable textile electronics in some extreme environments such as aerospace, military, and firefighting. These environments impose additional requirements on textile electronics such as radiation resistance, mechanical tolerance, and heat-resistance. In space, wearable electronics integrated into spacesuits offer crucial functions such as vital monitoring, environmental detection, and communications for astronauts. However, the aerospace environment presents formidable challenges including rarefied air, extreme temperatures, and radiation exposure. As a result, textile electronics must be capable of enduring these extreme conditions. In particular, radiation can largely disrupt the performance of electronics and reduce the lifespan of textiles. Therefore, designing wearable electronics for space necessitates the use of high-performance fibrous materials that withstand the extreme temperatures and provide effective radiation shielding. In

the military, textile electronics have the potential to provide advanced capabilities to soldiers in the field. These wearable devices can monitor physiological conditions of soldiers, track location, and facilitate communication among team members, which can enhance soldier safety, situational awareness, and communication efficiency. However, soldiers often stay in harsh environments in the wild, necessitating highly robust textile electronics capable of withstanding challenging mechanical abrasion and wet conditions. Additionally, maintaining anti-detection capabilities is crucial to prevent enemy detection. Therefore, the electronics should be equipped with electromagnetic shielding to ensure they remain undetectable. Furthermore, self-powered devices are essential for soldiers in case they become lost in the wilderness,<sup>874</sup> enabling them to rely on their own power source. In the field of firefighting, PCT-based wearable electronics can monitor vital signs, body temperature, and environmental conditions, consequently notifying the firefighters of potential hazards and mitigating the risk of heat-related injuries. In this case, the textile electronics need to be heat-resistant, and even flame-resistant to withstand high temperatures and fire conditions.<sup>875, 876</sup> He *et al.*<sup>875</sup> fabricated conductive aerogel fibers comprising calcium alginate, Fe<sub>3</sub>O<sub>4</sub> nanoparticles, and AgNWs by subsequent processes of solvent exchange, freeze drying, and spraying Ag NWs (**Figure 76a**). The conductive fibers have 3D porous network structure, and can be weaved into a conductive textile (**Figure 76b-e**). The conductive textile was integrated into firefighting protective clothing, and achieved temperature sensing at a wide range of 100~400 °C. This E-textile could timely transmit an alarm signal to the wearer before the firefighting protective clothing malfunctioned in extreme fire environments. In addition, a self-powered fire self-rescue location system was further established by constructing TENGs based on the conductive fibers. The TENG could not only serve as self-powered pressure sensors but also provide continuous power as high as 3 V for the fire location rescuing system (**Figure 76f**).

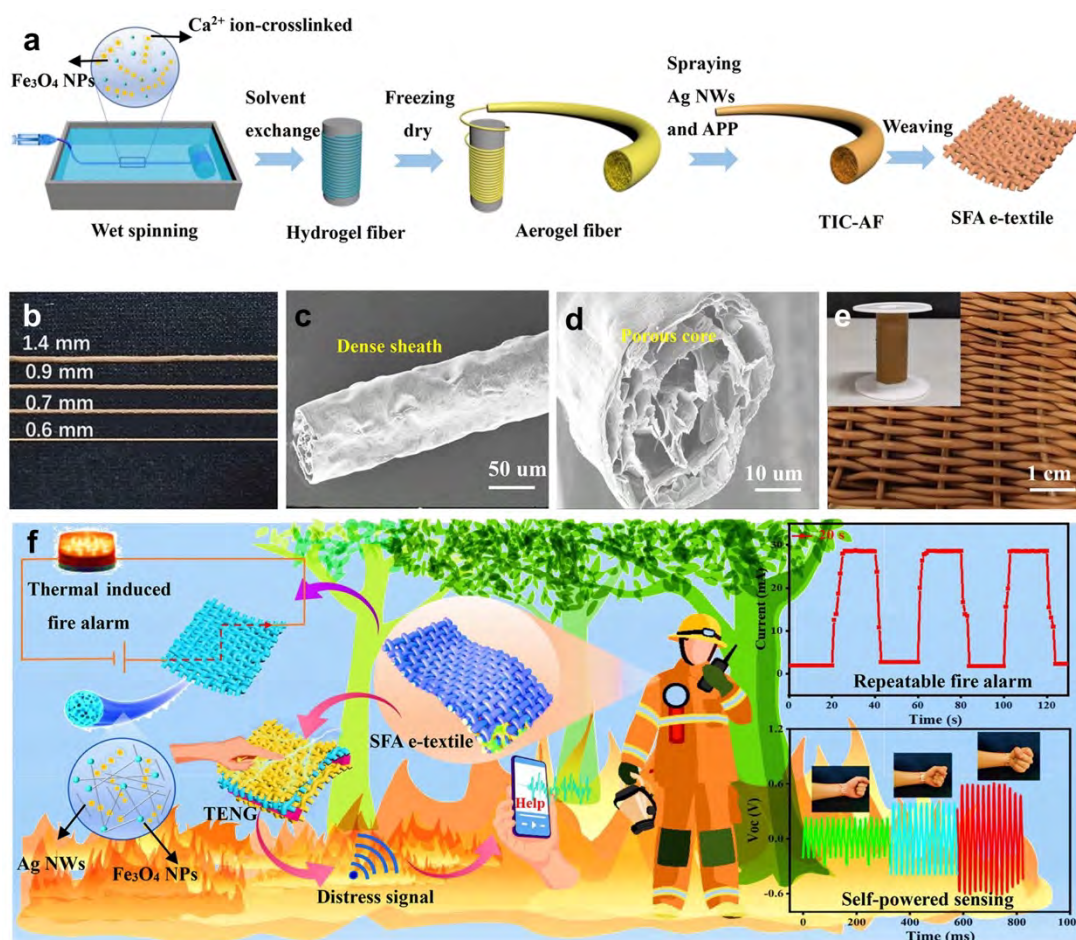


**Figure 76.** (a) Schematic description of the fabrication of conductive aerogel fiber. (b) Photo of the fibers fabricated with different diameters. (c-d) SEM images showing the surface and cross-sectional of the conductive aerogel fiber. (e) Photograph of an E-textile woven from the fibers. (f) Applications of the E-textile in smart firefighting clothing for energy harvesting, real-time fire warning, and precise rescue location. Reproduced with permission from ref. <sup>875</sup>. Copyright 2022 American Chemical Society.

The implementation of PCT-based wearable electronics in the demanding fields of aerospace, military, and firefighting offers the potential to enhance the safety, performance, and efficiency of personnel in these fields. It is imperative to continue dedicated research and innovation, particularly in materials development, to advance the deployment of highly advanced and dependable wearable electronics for extreme environments. One promising avenue is the utilization of high-performance fibers, such as aromatic polymer fibers (*e.g.*, polyimide, Kevlar),<sup>93, 877, 878</sup> inorganic fibers,<sup>879</sup> and carbon fibers, as the platform for developing textile-based electronics.



## 6. CHALLENGES AND PERSPECTIVES

Despite the fruitful results and progresses made in the past decades, the journey from materials discovery and development to devices and system-level integrations is still in its early stage. To further drive the development of this field, several challenges need to be addressed. These include ensuring the stability of PCTs and PCT-based electronic devices, addressing issues related to biocompatibility and sustainability, finding efficient wearable power supply solutions, enabling large-scale manufacturing, and deploying practical applications, *etc.* (**Figure 77**). Overcoming these challenges will be essential in propelling the field forward and bringing PCT-based wearable electronics to mainstream use.

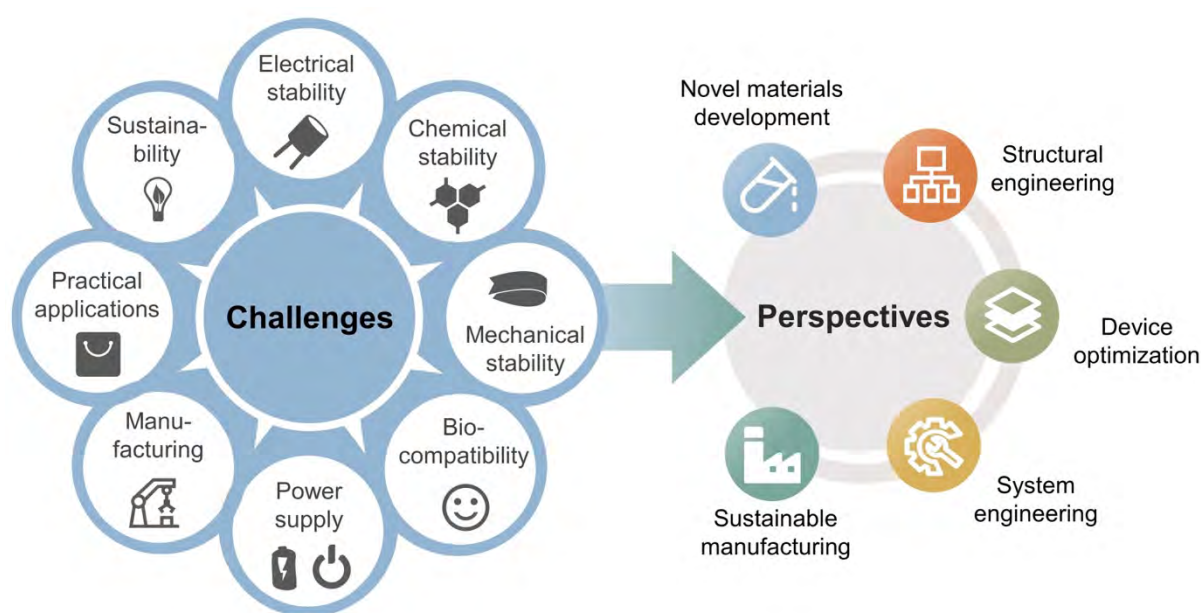


**Figure 77.** Challenges and perspectives of PCTs and PCT-based wearable electronics.

**Electrical Stability.** In comparison to their planar and flat solid counterparts, PCTs possess a high degree of porosity and numerous junctions between fibers and/or yarns. This unique porous structure makes them susceptible to changes in electrical properties during deformations, as the connectivity between fibers and the resulting conductive paths can vary. Additionally, the 3D hierarchical porous nature of PCTs can give rise to some unique electrical phenomena. For instance, when subjected to stretching, a textile not only undergoes shape changes along the stretching direction but also experiences vertical deformations due to its porous structure. These two factors can sometimes lead to balance in electrical conductivity, resulting in a relatively stable conductivity under stretching.<sup>24, 880</sup> Balancing the electrical stability of PCTs is crucial in device performance. On one hand, maintaining a stable electrical resistance is

essential to PCTs as electrodes, however, it is challenging to enable a strain-independent electrical property under high stretching strains. The pre-stretch process for forming bulking structure is a commonly used method to achieve this requirement. On the other hand, a desirable characteristic for PCTs that serve as active materials in resistive strain or pressure sensors is strain-responsive resistance. In addition, the porous structure of PCTs makes them vulnerable to environmental interferences, such as moisture absorption and exposure to wet conditions like body sweating, which can lead to fluctuations in electrical resistance. To address this, various strategies, such as applying a protective coating, have been explored to enhance the electrical stability and environmental tolerance of PCTs. However, it is important to note that such coating treatments can compromise the permeability of the textiles. Thus, striking a balance between coverage and permeability becomes a trade-off that needs to be considered. Nevertheless, the electrical stability of PCTs remains a critical factor to be taken into account during device design.

***Chemical Stability.*** The chemical stability of PCTs is primarily determined by the inherent chemical properties of the conductive materials, which can be additionally influenced by the post-treatments such as surface passivation and encapsulation approaches. Carbon materials show very high chemical stability under high humidity, acidic/basic environment, and high temperature. Therefore, PCTs made from carbon materials are promising building blocks for wearable electronics that require high electrochemical stability and flame resistivity.<sup>881, 882</sup> Metal-based PCTs, particularly those containing Cu and Ag nanomaterials, may suffer from oxidation problems under high temperature and high humidity, which makes their long-term applications challenging. The chemical stability of these metal-nanomaterial-based PCTs is also susceptible to degradation from acid/base corrosion and electrochemical corrosion under high humidity, leading to the deterioration of their electrical and mechanical properties.<sup>883, 884</sup> To enhance the chemical stability of metal-based PCTs, additional techniques, such as blending with carbon materials, surface passivation, and post-finishing treatments with inert coating, have been explored to enable the protection of metals in PCTs against oxidation and corrosion.<sup>201, 885-887</sup> While conducting polymers are resistant to oxidation due to their highest conductivity at oxidized states, they still encounter instability such as poor thermal stability, degradation in acid/base environment, and low resistance to water and organic solvents.<sup>888-890</sup> Encapsulating the conducting polymer-based PCTs and the associated electronic devices with protective coating is therefore highly essential, which in fact, is a universal solution to guarantee long-term chemical stability regardless for different types of PCTs, PCT-based



wearable electronic devices and systems. Nevertheless, it should be noted that the introduction of encapsulation may compromise the softness, permeability, and comfortability of PCTs and PCT-based wearable electronics, which has been mentioned in the previous section on electrical stability.<sup>891</sup> Therefore, when designing and fabricating PCT-based wearable electronics, it is highly essential to consider the coverage of the encapsulation (*i.e.*, protective coating) and its impact on the chemical stability, device performance, and wearable comfort of the PCTs and the associated devices.

Encapsulating the conducting polymer-based PCTs and the associated electronic devices with protective coating is therefore highly essential, which in fact, is a universal solution to guarantee long-term chemical stability regardless for different types of PCTs, PCT-based wearable electronic devices and systems. Nevertheless, it should be noted that the introduction of encapsulation may compromise the softness, permeability, and comfortability of PCTs and PCT-based wearable electronics, which has been mentioned in the previous section on electrical stability.<sup>891</sup> Therefore, when designing and fabricating PCT-based wearable electronics, it is highly essential to consider the coverage of the encapsulation (*i.e.*, protective coating) and its impact on the chemical stability, device performance, and wearable comfort of the PCTs and the associated devices.

***Mechanical Stability.*** Achieving the reasonable mechanical stability of PCTs can impart the associated wearable electronic devices and systems with the ability to withstand different types of mechanical deformations during daily wear. In the typical wearable application scenarios, PCTs and PCT-based wearable electronics will be subjected to various forms of external mechanical forces such as stretching, twisting, abrasion, and shearing. Such external forces can lead to the distortion and even breakage of textile fibers, which may cause the breakage of conductive path in PCTs and subsequently the failure of electronic devices. When taking prolonged use into consideration, PCT-based electronics may be required to be washable. However, friction, stress, as well as the use of detergent during the laundry can cause the delamination of the conductive coating on PCTs. This may subsequently degrade the electrical and mechanical properties of PCTs and the associated electronics. Moreover, harsh environments, such as extreme high/low temperatures and high humidity, may also degrade the mechanical properties (*e.g.*, strength, flexibility/stretchability) of PCTs, consequently impacting their electrical stability.

To address the challenge in mechanical stability, it is important to take material selection and structural design into consideration during the development of PCTs and PCT-based electronic devices. On one hand, the incorporation of high-strength conductive materials such as carbon and metals during the fabrication of conductive textiles can significantly enhance the mechanical strength of PCTs.<sup>892</sup> The use of strong fibrous materials, such as Kevlar and nylon, can further enable a stable and flexible building block of PCTs. Specific focus is required to be placed on ensuring a stable interface between fibrous building blockings and the conductive materials, through which the electrical connections within a PCT can be well sustained upon external mechanical deformations.<sup>186, 893</sup> On the other hand, employing reinforcement structures by loading extra fibers in the conductive composite matrix or laminating multilayered fabrics can benefit the stress distribution in PCTs, further strengthening the materials.<sup>894</sup> The encapsulation of PCTs and PCT-based electronic devices with protective coating is also a promising strategy to prevent mechanical failures. Nevertheless, while it is crucial to achieve a mechanically strong PCT for stable and durable PCT-based electronics devices, striving a balance between strength and flexibility/stretchability is the key to enable wearable electronic systems with desirable functionality and wearing comfortability.

**Biocompatibility.** Biocompatibility of PCTs and PCT-based wearable electronics refers to their ability to interact with human bodies without causing harm or adverse immune reactions, particularly in prolonged use.<sup>895</sup> The importance of such a feature lies in long-term wearable and on-skin applications, such as wearable/skin-attachable real-time health monitoring and therapeutic interventions for patients. Though most conventional textile materials are generally considered to be compatible with human skin, the addition of conductive and electronic materials may introduce toxicity and biosafety issues. For instance, some conductive materials, such as nickel, are likely to irritate the skin and cause allergies when in direct contact with the skin for a long time.<sup>896</sup> The residue of organic solvents left after the electrode and device fabrication may also pose a toxic risk to human health. Therefore, to minimize the harmful impact on human health, it is essential to take materials selection, device structural design, and handling methods into account when manufacturing PCTs and PCT-based electronics. Whereas introducing intrinsically non-toxic and safe materials for encapsulation can effectively avoid direct contact between harmful components and human bodies, it is highly feasible to adopt a series of biomaterials for the development of PCTs and the associated devices.<sup>897</sup> To date, biocompatible metals and metal alloys (*e.g.*, Au, Ag, Pt, and Ga-based LMs), stable polymers (*e.g.*, silicone elastomer), biomass materials derived from living

organisms, and biodegradable materials have been developed for biocompatible electronic applications, which can greatly benefit the non-toxic, non-irritant, and non-allergenic features of PCTs and PCT-based wearable electronics.<sup>895, 898</sup> In addition, imparting biosafe PCTs and the resultant wearable electronic systems with permeability, thermal-moisture comfort, and softness can further minimize the inconvenience and discomfort, which are also considered to be biocompatible with the human body. To advance the commercialization and practical applications of PCTs and PCT-based electronics, it is also necessary to establish testing protocols, standards, and regulations to assess their biocompatibility. This can ensure that the newly developed wearable electronic materials, devices, and systems are safe and effective for their intended on-body applications.

**Power Supply.** Batteries are the predominant power sources in current state-of-the-art wearable electronics. Though the development of flexible batteries on the basis of PCTs has shown great promise in enhancing the wearing comfort of wearable electronics, challenges still remain in achieving a balance among device flexibility, energy performance, durability and safety. While commercial LIBs can exhibit an energy density of over 600 Wh L<sup>-1</sup>, the energy density of state-of-the-art flexible PCT-based batteries reported in the literature are typically lower than 300 Wh L<sup>-1</sup>.<sup>546, 656</sup> Developing thin, lightweight, and soft current collectors and electrodes is one strategy to enhance the energy density with remaining mechanical flexibility, and several candidates such as CNT and graphene film, metal-coated porous fiber substrates have been demonstrated. Innovations in high-capacity and long-cycling-life electrode materials, for example, fibrous electrode compositing with Si, Li metal, and S, can also further endow high energy performance and durability to the flexible energy storage devices.<sup>546, 655, 899, 900</sup> It is also important to propose generic standards as well as testing protocol with a figure of merit to evaluate the energy performance and flexibility of flexible energy storages.<sup>546</sup> Safety is another critical issue when designing and applying these flexible energy storage devices into wearables. The use of combustible organic electrolytes poses the risk of leakage and safety hazard, while dendrite-related side reactions in the battery cells may lead to shorts and even severe consequent such as explosions and permanent damage to the circuits powered by the battery. The additional features of flexibility and daily uses under wearing conditions further increase the risk of safety hazards. To address this challenge, it is highly demanding to design solid-state electrolyte as well as other battery components with high thermal stability and low flammability.<sup>901</sup> For example, it has been demonstrated that the incorporation of polymer/inorganic composites, such as Li<sub>6.4</sub>La<sub>3</sub>Zr<sub>2</sub>Al<sub>0.2</sub>O<sub>12</sub>/polyethylene glycol electrolytes, can endow the flexibility and

safety of power supplies synchronously.<sup>902</sup>

Considering the limited life of batteries and their need to recharge, as well as the wearing conditions that require constant monitoring and data collection, research efforts should also be focused on developing alternative power supplies such as wireless charging technologies and energy harvesting systems. For the former, wireless charging enabled by RFID and NFC technologies can provide a convenient and user-friendly recharge for flexible batteries through the elimination of cable and external connectors. For the latter, the integration of energy harvesting systems can not only extend the battery life of wearable electronics but also reduce the need for frequent recharge and replacement, which can achieve a self-powered supply system for wearable electronics. The combinations of these power supply technologies are foreseen to enable the widespread use of wearable electronics in various applications.

**Manufacturing.** Multi-functional hybrid electronic devices have been demonstrated on fibrous substrates by utilizing PCT-based electronic devices and conventional microelectronics, however, their device functionality and system performance are still inferior to their rigid counterparts and far from the practical applications. This gap is primarily due to the limitation in the manufacturing processes, which have yet to develop compatible approaches for hybridizing and integrating components with vastly different form factors and mechanical properties onto textiles. Consequently, apart from focusing on the development of intrinsically flexible and stretchable PCT-based electronic devices, it is also necessary to research multilayer and high-integration-density hybrid E-textiles to simultaneously achieve multifunctionality, mechanical durability, and wear comfort.<sup>24, 58</sup> On the one hand, precise alignment design is required to ensure optimal electronic performance in multilayer hybrid electronic circuits. A proper package design, which includes encapsulating the stretchable interconnects, electronic chips, and VIAs between each circuit layer, is also critical for collecting accurate data with minimal noise or drift. On the other hand, it is desired to explore new fabrication techniques that are compatible with PCTs to enable high-resolution and high-density integration of different electronic components. In addition, new strategies have emerged for integrating microelectronics inside fibers, resulting in highly integrated multifunctional fibers with high device density and functionality.<sup>739, 903, 904</sup> These fibers can be further manufactured into a large textile system. However, the positioning and connection of large numbers of inserted devices pose great challenges. The optimization of materials and circuit design is the key to achieving such wearable hybrid electronic systems at a high

resolution.

Moreover, large-scale integration techniques are crucial for achieving commercialization and practical applications of integrated E-textiles.<sup>35, 80, 81, 699</sup> Different from the operations on rigid PCBs, integrating electronic components onto soft and flexible fibrous substrates requires complex and tedious processes. Scaling up these processes to automated manufacturing can be challenging, and optimization of the fabrication process is necessary to reduce manufacturing costs. During large-scale fabrication, the PCT-based devices must be robust enough to withstand harsh environments, including mechanical stress and chemical corrosion. Therefore, advanced material and structural designs are needed to ensure the reliability of the integrated systems. Additionally, testing standards are essential to achieving high and consistent quality of PCT-based wearable electronics.<sup>905</sup> However, there are technical and practical challenges in setting standards due to the complex functional components in wearable electronic systems and their interactions with versatile environments. For the reliable large-scale production of electronic textiles, it is urgent to explore the electrical and mechanical properties of electronic components, and the impact of environmental factors. Furthermore, machine learning can be used to improve the manufacturing process of electronic textiles by optimizing the design of materials and devices for functionality and durability, and to meet the needs of wearers.

***Practical Applications.*** The primary objective of wearable electronics is to incorporate them into our daily routines, ultimately enhancing human lifestyles and revolutionizing our way of life. Envisioned as a burgeoning market, flexible electronics continue to drive the increasing demand for wearable technology, fitness trackers, and health monitoring devices. PCT-based wearable electronics, which seamlessly incorporate flexible devices into everyday clothing, offering enhanced comfort, are undoubtedly poised to captivate a wide spectrum of consumers. Nevertheless, despite their promise, the deployment of PCT-based wearable electronics into practical applications, particularly commercial products, still encounters great challenges and desires more research and development input. In addition to the aforementioned endeavors required for exploring innovative PCT materials, improving the performance of individual PCT-based devices, and refining system integration, it is imperative to address various practical application aspects, including washability, aesthetic appeal, user-friendliness, cost-efficiency, and demand scenarios, when developing textile electronic products. Washability stands as an indispensable prerequisite for textile electronics for enduring applications. As discussed above, the washing process which involves vigorous mechanical agitation and use of detergents will

deteriorate the mechanical and electrical properties of PCTs. The encapsulation of conductive paths and electronic components appears to be the most effective approach for potentially resolving this issue. Nonetheless, while encapsulation treatments are generally effective for flexible and pliable components, they present challenges when it comes to the connections between soft and rigid elements, as well as the connection ports. Achieving a secure encapsulation for these areas can be particularly difficult. Additionally, it is important to note that not all electronic components can endure the demanding conditions of washing and prolonged water immersion. Therefore, an alternative approach may entail adopting a modular or plug-and-play design,<sup>25</sup> enabling the removal of specific components prior to washing. This strategy calls for specific circuit designs and connection methods to facilitate the seamless detachment and reattachment of these components.

Aesthetic appeal is a crucial aspect of textile electronics, as it plays a significant role in the adoption and acceptance of the products. Textile electronics seek to harmonize the realms of fashion and technology, aiming to create products that not only perform functions but also look appealing to consumers. Therefore, on one hand, it is essential to prioritize the incorporation of electronic components into textiles while preserving the overall design and aesthetics. Consequently, the miniaturization of devices and seamless system integration takes on significant importance. The creation of devices and/or systems by weaving and knitting fibrous units become a promising direction to design novel textile electronics.<sup>906</sup> On the other hand, the integration of versatile wearable display devices such as LEDs and electrochromic devices may have the potential to enhance the visual appeal of textiles, ushering in a fresh fashion trend. User-friendliness is another important aspect when it comes to delivering wearable products. It is essential that these products offer straightforward operations, without requiring users to possess professional skills for implementation and repair of PCT-based electronics. Integrating them with portable electronics like cellphones for device operation and data visualization, along with the incorporation of machine learning-based data processing, can be considered as design choices to enhance user-friendliness. Moreover, cost is an inevitable consideration for developing wearable electronic products. Consequently, the pursuit of innovative yet cost-effective materials, along with streamlined and scalable fabrication processes for manufacturing PCTs and assembling electronic devices, remains a perpetual aspiration. Last but not the least, the critical step of exploring particular application scenarios, crafting devices tailored to these contexts, and potentially creating personalized solutions to meet specific demands is indispensable in advancing the practical applications of PCT-based wearable

electronics.

**Sustainability.** While PCTs and PCT-based electronic devices are experiencing tremendous development in academia, the wearable markets have not yet witnessed a wide adoption of these novel E-textiles. One reason is that they are still facing the challenges in sustainability.<sup>907</sup> Though most of textile materials are recyclable, the incorporation of electronics into these existing textiles make end-of-life processing complicated.<sup>908</sup> Typically, a PCT-based electronic system is an integration of various types of non-textile components, such as conductive materials in PCTs as electrodes and interconnectors, batteries, and chips, into textile components. Because of the varying chemical/physical properties of these non-textile components, it is rather difficult and impractical to disassemble all of them from the textile substrates for specific recycling methods. Moreover, some electronic components contain heavy metals and organic compounds, which are hazardous and harmful to the individual health and the environment.<sup>909</sup> Therefore, it is highly necessary to have a sustainable design strategy for highly integrated E-textiles to ensure that they can be either recycled for other value-added product applications or deposited in the landfill without causing any negative environmental effects.

Sustainability is a multifaceted concept involving the better use of environmental-friendly materials, the development of durable/recyclable/biodegradable products, the adoption of manufacturing process with low carbon emissions, and the use of renewable resources.<sup>910</sup> Innovations in sustainable technologies are highly required for the development of environmentally safe electronic materials.<sup>911</sup> Special focus needs to be placed on achieving a balance among electronic performance, mechanical properties, and impacts to the environment. To date, researchers have made efforts on developing biocompatible and biodegradable electronic materials from low-cost natural materials by using low-energy approaches, leading to the emergence of “green” electronics.<sup>912, 913</sup> The applications of these green electronic materials in E-textiles can alleviate the adverse influences on the environment by reducing the toxic, harmful, and non-degradable electronic wastes (E-wastes). In addition, promoting the durability of wearable electronics can effectively prolong the life of devices to facilitate the reduction of E-wastes. It is also appealing to develop self-sustainable wearable electronic systems that can capture and store surrounding energy from sun, body heat and motion to power their device functions, through which wearable electronics can be operated in a low-carbon-emission and clean manner. Moreover, the disassembly of various electronic components from



the textiles needs to be taken into consideration to fully recycle the wearable electronics at the end of their use life.<sup>245, 532, 914</sup>

## 7. CONCLUSIONS

In this review, we have summarized and highlighted recent advances in developing PCTs for the application of flexible and wearable electronics. The utilization of textile materials in making flexible electronics represents a paradigm shift towards comfortable wearable electronics, of which the flexible electronics designed in the form factor of fiber or textile possess distinctive characteristics including good permeability, flexibility, and lightweight. PCTs lie in the fundamental in the fabrication of textile electronics. Therefore, research in this field is experiencing rapid growth.

We first introduced the fundamental aspects of PCTs in terms of building blocks, fabrication technologies, and key properties. Fibers are the basic unit of textiles, while yarns and fabrics are different aggregation levels of fibers spanning from 1D assembled bundles to 2D/3D customized textures, all of which can be used as the building block for the design of PCTs. Textiles can be configured in various forms, including regular structures of weaves and knits, or in the form of randomly overlaid non-wovens. In addition, the sources of fibers/textiles also have a broad range, ranging from natural materials like cotton, wool, and silk to synthetic ones such as nylon and polyester. However, these conventional textile materials usually lack conductivity. Consequently, conductive materials, such as conducting polymers, carbon materials, and metals, are another essential components to prepare PCTs. These conductive materials can be coated onto textiles through various methods such as dip coating, sputtering, polymerization, and chemical/electrochemical deposition. In addition, some intrinsically conductive materials such as CNTs, graphene, and metal nanowires can be self-assembled into free-standing fibers and textiles. Furthermore, the creation of conductive patterns on textile substrates via printing techniques represents another effective way to design electronics on textiles, wherein patterning with high resolution remains a challenge. It is crucial to render PCTs with excellent flexibility and stretchability to accommodate the demands of flexible electronics. While fibers and textiles with twisting and weaving/knitting structures inherently offer flexibility and a certain degree of stretchability, enhancing the stretchability of PCTs is always a desirable goal. Consequently, there is considerable interest in utilizing stretchable raw materials for preparing fibers, such as elastic polymers (*e.g.*, SBS, TPU) and hydrogels. Achieving good electrical conductivity, mechanical strength, and comfortability are the prerequisites to the fabrication of textile electronics. However, owing to the porous structure, PCTs usually exhibit inferior electrical conductivity and mechanical strength to their planar counterparts. Besides, establishing a durable interface between the conductive coatings and

fibers is imperative to withstand mechanical wear and chemical erosions, thereby ensuring stable conductivity. Surface modification and encapsulation are common approaches to address these challenges, while a balance between encapsulation and maintenance of permeability must be carefully considered. Overall, the continuous exploration of novel materials and methods for PCT fabrication and performance enhancement remains an ongoing endeavor.

PCTs play versatile roles in making wearable electronics, which can function as active sensing components, flexible electrodes, supporting substrates, current collectors, and interconnects, *etc.* Herein, we discussed the implementation of PCTs in various wearable electronic devices including sensors, actuators, therapeutic devices, energy harvesting and storage devices, and displays, detailing their working principles, device configurations, and performance. First, a variety of sensors involving biophysical sensors, chemical and biological sensors, and electrophysiological sensors are introduced. Pressure and strain sensors are the most common physical sensors for wearable applications, as they can detect motions such as body movements, gestures, and vital signs like pulse. The pressure and strain sensors can operate in different mechanisms including piezoresistive, capacitive, and electric (piezoelectric and triboelectric) ones. While the piezoresistive ones usually employ PCTs as the active sensing component as the porous structure can contribute to resistance change, the capacitive and electric ones usually utilize PCTs as the electrodes. Temperature sensor is another important physical sensor for monitoring body temperature. PCTs with thermal-resistive or thermoelectrical characteristic can be used as the active component to prepare temperature sensors. In addition, photodetectors are essential for the detection of environmental light intensity, especially in detecting the invisible lights of ultraviolet and infrared light. All these physical sensors can be assembled into different configurations and structures according to their working principles, ranging from 1D fiber shape, 2D planer structure, and 3D multilayer stacks. The remaining challenges in PCT-based physical sensors revolve around enhancing sensing stability, which includes mitigating environmental interferences and minimizing crosstalk between signals. Then, we introduced chemical and biological sensors for detecting versatile molecules and/or biomarkers contained in respiration gases and biofluids (*e.g.*, sweat), detection of which holds great potential for point-of-care diagnosis. The chemical and biological sensors can also operate in different principles including potentiometric, amperometric, impedimetric, and transistor-based. PCTs employed as the active component have the advantage of high surface area, which is beneficial to immobilize recognition elements like enzymes, thereby enhancing sensitivity. Multiple sensors targeting different substances can be incorporated into a textile through

methods like patterning, weaving, or embroidering various components. Continuous collection of analytes (*e.g.*, sweat) represents one of the biggest challenges of these wearable chemical/biological sensors. Electrophysiological sensors are capable of recording bioelectrical signals including ECG, EMG, EEG, and EOG, which are useful for disease diagnosis and HMI. PCT-based electrodes with good flexibility and permeability are a promising type of dry electrode for long-term applications, though they have the drawbacks of high contact impedance and susceptibility to motion artifacts owing to their poor adhesion to the skin. Afterward, various types of actuators that are developed based on PCTs are introduced. Actuators are devices that can execute motions in response to external stimuli and thus have applications for physical therapy, artificial muscle, and HMI. Actuators can be triggered by various external stimuli such as electric, electrochemical, thermal, and solvent inputs. PCT-based actuators have the advantages of high flexibility, lightweight, and fast response. Owing to the soft and porous structures, the forces generated by actuators based on PCTs are usually weak, thereby limiting their applications for artificial muscles and triggering heavy loadings.

Apart from sensors and actuators, PCTs can also be employed to fabricate therapeutic devices such as thermotherapy, electrical stimulation, and drug delivery systems. Joule heating devices are straightforward thermotherapy tools capable of producing heat through the application of voltage across a piece of PCT. Transcutaneous electrical stimulation devices can deliver electric charges through the skin to stimulate muscles or nerves, thereby offering therapeutic benefits for certain nerve-related issues, such as alleviating pain. In addition, drugs can be loaded in PCTs for drug delivery through the process of iontophoresis. While these types of therapeutic devices based on PCTs have received comparatively less attention in research, it is anticipated that they will find extensive applications in the future.

Power supply devices are an indispensable component of wearable devices. The predominant power supply devices for current portable electronics are miniaturized LIBs, which face challenges due to their inflexible nature and limited capacity, especially concerning future wearable applications. Recent research endeavors have yielded various solutions to address the need for flexible power sources. Notably, PCTs have played proactive roles in the advancement of flexible energy harvesting and storage devices. Solar cells are considered promising energy harvesting devices, capable of converting light into electricity. However, they have fatal limitations due to the intermittent and regional availability of light sources, and currently, textile-based solar cells exhibit low conversion efficiency. Nanogenerators including PENG,

TENG, and thermoelectric generators, are emerging energy harvesting devices capable of transforming mechanical variations and temperature disparities into electricity. Thus, they are promising for utilization as self-powered sensors. Nonetheless, their energy density remains significantly below the practical requirements for serving as power supply devices. Near-field energy harvesting devices like NFC and RFID offer wireless solutions for energizing wearable electronics without requiring complex energy devices, relying instead on an antenna printed on textiles. Notably, these antenna-based devices can withstand substantial deformations when employing stretchable PCTs prepared using LMs. Biofuel cells, which utilize biomolecules contained in sweat as the fuel, is effective to convert chemical energy into electricity. However, biocatalysts such as enzymes are usually required to facilitate the electrochemical reactions on the electrodes, thus may suffer from stability issues. In addition, the energy density of biofuel cells solely rely on sweat is usually low, as the concentrations of the biomolecules in sweat are low. Supercapacitors and batteries have been the predominant focus of research in the field of energy storage over the past two decades, leading to significant advancements in battery chemistry and material selection. PCTs show promise as replacements for conventional bulky metal foils as current collectors in the fabrication of flexible devices. Undoubtedly, PCT-based supercapacitors and batteries exhibit significantly improved flexibility compared to their planar counterparts. However, their energy density still lags behind that of planar devices. To achieve high-energy-density supercapacitors and batteries, further reduction in the density of PCTs and increase loading of active materials onto PCTs are required. Overall, although the individual devices among the mentioned energy solutions may not offer ideal performance as standalone wearable power sources, combining two or more of them may potentially provide an optimal solution for practical applications.

Wearable display devices based on PCTs offer a real-time acquisition of information, which is directly presented on clothing. LEDs with the core component of electroluminescent materials can be configured in various ways using fibers and PCTs as building blocks, including co-axial fiber-shaped LEDs, planar multi-layer structures, and inter-weaved textile LEDs. Notably, Peng's group recently achieved the development of scalable textile displays with meters-long capabilities through weaving.<sup>81</sup> Nonetheless, compared to the conventional planar LED displays manufactured by the micro-fabrication process, the textile displays still have much lower pixels and resolution, owing to the relatively large size of fiber diameter. Besides, electrochromic devices are optoelectronics capable of changing color upon applying voltage, which can be used for display, sensing, and camouflage, *etc.* Overall, the versatile textile LEDs

and electrochromic devices enhance the visual appeal and functionality of textiles, thereby opening doors to the convergence of textile fashion and technology.

Subsequently, we elaborated the strategies and fabrication approaches for the development of textile-based integrated electronic systems based on off-the-shelf microelectronics and PCT-based electronic devices. The initial approach to integrating electronic systems into textiles involved embedding pre-manufactured devices onto clothing. These devices are rigid and bulky, making them unsuitable for true flexible electronics. Then, researchers attempted to fabricate textile electronics by connecting off-the-shelf microelectronic components, which we refer to as the second generation of textile electronics. Since these microelectronic components are small, the resulting systems exhibit relatively good flexibility and wearability. However, due to the inherent rigidity of these components, significant challenges arise when integrating them with soft textiles, including addressing issues at the soft-hard interfaces. To enhance the strength of these connections, various methods such as soldering, welding, mechanical clamping, and adhesive bonding are developed. The third generation of textile electronic systems revolves around creating devices directly on textiles through two main approaches: assembling fibrous units into devices using techniques like weaving, knitting, and embroidery, or directly manufacturing devices onto textiles using patterning methods such as printing or laser engraving. This strategy largely eliminates the use of rigid microelectronic components, resulting in a seamless integration of wearable systems. However, the electronic component toolkits fabricated based on fibers are limited, thus the fabrication of an electronic system solely from fiber units is currently improbable. Therefore, there are two important aspects to consider: 1) further developing fibrous electronic components are needed to enrich the future design possibilities of all-textile electronic systems; 2) exploring novel bonding, connecting, and encapsulation technologies is essential as the use of conventional microelectronic components remains unavoidable for now. In addition to sensors, other components such as energy supply devices, processors, and data communication are also important for an integrated wearable system. Wireless communication systems offer a promising approach for real-time data collections. Besides, as continuous and long-term wearable sensing inevitably generates vast amounts of data, managing, processing, and interpreting this data pose significant challenges in real-world applications. Emerging machine-learning algorithms and IoT technologies hold promise as potential solutions to address these challenges.

We then highlighted and envisioned versatile applications of PCT-based wearable electronics.

Health monitoring seems to be the killer application of wearable electronics. Various environmental and body-related information including physical, chemical, and physiological ones can be collected by wearable sensors, which are essential for understanding human health conditions and diagnosis of diseases. PCT-based wearable sensors capable of real-time and continuous monitoring these conditions in daily life would largely trigger the development of personalized medicine. Additionally, in specific scenarios such as exercise and sports, PCT-based wearable electronics not only aid in training but also monitor athletes' health and provide valuable assistance in judgements. Recent technological convergence, encompassing HMI, XR, and IoT, is reshaping our lives, and the PCT-based wearables would thus serve as essential hardware for interacting with real-world objects. Furthermore, PCT-based wearable electronics find applications in extreme conditions like aerospace, military operations, and firefighting, aiding practitioners such as astronauts, soldiers, and firefighters in enhancing their operational skills and ensuring their safety. Although these applications hold promise for PCT-based wearable electronics, most of them remain at the prototype verification stage in laboratory research. The journey to making them a reality in real-world scenarios involves further engineering and design optimization, bridging the gap from lab development to practical implementation.

Finally, we discussed the challenges in the field of PCTs and E-textiles from the viewpoints of materials properties, device and system engineering, and manufacturing, and also provided our perspective on the future research directions that can effectively push PCT-based wearable electronics toward a commercially viable level. Further improvement of the electrical, chemical, and mechanical stability of PCTs is essential to enhance the performance of resulting devices. To achieve this, it is imperative to explore novel materials, fabrication processes, and post-modification techniques. Biocompatibility and comfort are crucial factors for wearable applications that are often overlooked in current studies. It is recommended that future research includes a comprehensive evaluation of these aspects. In addition, as an indispensable component, the existing PCT-based power devices can hardly meet the practical applications. Collaboration between researchers in the fields of flexible electronics and energy is necessary to address this practical challenge. The inevitable steps toward future product development involve system integration and large-scale fabrication of wearable electronics based on PCTs. Moreover, finding specific application scenarios and solving associated problems should serve as the driving force behind the development of PCT-based devices. Last but not the least, the ultimate goal for creating a green wearable world should encompass sustainability in all aspects,



including materials and manufacturing processes of PCTs.

In conclusion, PCTs have demonstrated their great potential as a platform for fabricating wearable electronics. Despite the notable progress in PCT-based wearable electronics, most studies still stay in the incubation period that requires further exploration and development. It is anticipated that with continuous innovations in materials science and engineering, electronic engineering, manufacturing, and product designs, along with the multidisciplinary and cross-disciplinary collaboration among scientists, engineers, and designers, wearable electronics on the basis of PCTs will become increasingly realistic and advanced in the near future. By addressing the challenges that persist in the field, we are optimistic that this novel type of wearable electronics will be soon ubiquitous in our daily lives, outperforming off-the-shell wearable electronic products.

## **AUTHOR INFORMATION**

### **Corresponding authors**

**Zijian Zheng** – Laboratory for Advanced Interfacial Materials and Devices, School of Fashion & Textiles; Department of Applied Biology and Chemical Technology, Faculty of Science; Research Institute for Intelligent Wearable Systems; Research Institute for Smart Energy, The Hong Kong Polytechnic University, Hong Kong SAR 999077, P.R. China; ORCID: [orcid.org/0000-0002-6653-7594](https://orcid.org/0000-0002-6653-7594); E-mail: [tczzheng@polyu.edu.hk](mailto:tczzheng@polyu.edu.hk).

**Qiyao Huang** – Laboratory for Advanced Interfacial Materials and Devices, School of Fashion & Textiles; Research Institute for Intelligent Wearable Systems; The Hong Kong Polytechnic University, Hong Kong SAR 999077, P.R. China; ORCID: [orcid.org/0000-0001-8233-1804](https://orcid.org/0000-0001-8233-1804); E-mail: [qi-yao.huang@polyu.edu.hk](mailto:qi-yao.huang@polyu.edu.hk).

### **Authors**

**Yichun Ding** – Laboratory for Advanced Interfacial Materials and Devices, School of Fashion & Textiles, The Hong Kong Polytechnic University, Hong Kong SAR 999077, P.R. China; Fujian Institute of Research on the Structure of Matter, Chinese Academy of Sciences, Fuzhou, Fujian 350108, P.R. China; Fujian Science & Technology Innovation Laboratory for Optoelectronic Information of China, Fuzhou, Fujian 350108, P.R. China; ORCID: [orcid.org/0000-0002-7441-800X](https://orcid.org/0000-0002-7441-800X)

**Jinxing Jiang** – Laboratory for Advanced Interfacial Materials and Devices, School of Fashion & Textiles, The Hong Kong Polytechnic University, Hong Kong SAR 999077, P.R. China; ORCID: [orcid.org/0000-0003-3272-6255](https://orcid.org/0000-0003-3272-6255)

**Yingsi Wu** – Laboratory for Advanced Interfacial Materials and Devices, School of Fashion & Textiles, The Hong Kong Polytechnic University, Hong Kong SAR 999077, P.R. China; ORCID: [orcid.org/0000-0001-7764-5710](https://orcid.org/0000-0001-7764-5710)

**Yaokang Zhang** – Laboratory for Advanced Interfacial Materials and Devices, School of Fashion & Textiles, The Hong Kong Polytechnic University, Hong Kong SAR 999077, P.R. China; ORCID: [orcid.org/0000-0002-6123-4789](https://orcid.org/0000-0002-6123-4789)

**Junhua Zhou** – Laboratory for Advanced Interfacial Materials and Devices, School of Fashion

& Textiles, The Hong Kong Polytechnic University, Hong Kong SAR 999077, P.R. China;  
ORCID: [orcid.org/0000-0003-1313-7746](https://orcid.org/0000-0003-1313-7746)

**Yufei Zhang** – Laboratory for Advanced Interfacial Materials and Devices, School of Fashion & Textiles, The Hong Kong Polytechnic University, Hong Kong SAR 999077, P.R. China;  
ORCID: [orcid.org/0000-0002-3578-3549](https://orcid.org/0000-0002-3578-3549)

### Author Contributions

<sup>§</sup>Y. Ding, J. Jiang, Y. Wu, Y. Zhang, J. Zhou, and Y. Zhang contributed equally to this article. CRediT: **Yichun Ding** writing-original draft, writing-review & editing; **Jinxing Jiang** writing-original draft, writing-review & editing; **Yingsi Wu** writing-original draft, writing-review & editing; **Yaokang Zhang** writing-original draft, writing-review & editing; **Junhua Zhou** writing-original draft, writing-review & editing; **Yufei Zhang** writing-original draft, writing-review & editing; **Qiyao Huang** writing-original draft, writing-review & editing, supervision; **Zijian Zheng** conceptualization, writing-review & editing, supervision.

### Notes

The authors declare no competing financial interest.

### Biographies

**Yichun Ding** is associate professor at the Fujian Institute of Research on the Structure of Matter, Chinese Academy of Sciences, and currently a postdoctoral fellow visiting at School of Fashion & Textiles, The Hong Kong Polytechnic University. He received his Ph.D. degree in Biomedical Engineering from South Dakota School of Mines & Technology (USA) in 2018. His research mainly focuses on exploring novel polymeric and fibrous materials for flexible and wearable electronics towards biomedical applications.

**Jinxing Jiang** received his B.Eng. degree in polymer material and engineering (2019) and M.S. degree (2022) in material science and engineering from Soochow University. Now he is a Ph.D. candidate in School of Fashion & Textiles, The Hong Kong Polytechnic University. His research interests mainly focus on fibrous devices for energy harvesting and healthcare monitoring applications.

**Yingsi Wu** received her B.E. and Ph.D. degrees from South China University of Technology

in 2009 and 2014, respectively. Then she worked as a research fellow in Singapore University of Technology and Design and Nanyang Technological University in Singapore. She is currently a research fellow in Prof. Zijian Zheng's group. Her research interests focus on flexible and stretchable electronics based on textiles for sensing applications.

**Yaokang Zhang** received his B.Sc. in chemistry from Renmin University of China in 2013 and his Ph.D. degree in 2018 under the supervision of Prof. Zijian Zheng in the Institute of Textiles and Clothing at The Hong Kong Polytechnic University. His research interest focuses on the fabrication of solution-processed flexible electronic devices.

**Junhua Zhou** received his Ph.D. degree from Soochow University in 2022. He is currently a postdoctoral fellow at The Hong Kong Polytechnic University. His research interests mainly focus on lithium-sulfur batteries and advanced electrolytes for high-voltage lithium metal batteries.

**Yufei Zhang** is currently a postdoctoral fellow of School of Fashion & Textiles, The Hong Kong Polytechnic University. She received her Ph.D. degree in Textile Science and Engineering from Donghua University, China, in 2021. Her current research interests include biomimetic nanofibrous materials, thermal and moisture comfort of smart textiles, wearable electronic textiles, and skin electronics.

**Qiyao Huang** is currently assistant professor at School of Fashion & Textiles, the Hong Kong Polytechnic University. She received her B.A. in fashion and textiles (2014) and Ph.D. (2019) in textile technology from The Hong Kong Polytechnic University. After a postdoctoral stay in Professor Zijian Zheng's group, she joined the Institute of Textiles and Clothing at The Hong Kong Polytechnic University as a research assistant professor in 2020. Her research interests include conductive textiles, flexible and stretchable electrodes, and textile-based devices for electrochemical energy storage and sensing applications.

**Zijian Zheng** received his B. Eng. in Chemical Engineering at Tsinghua University in 2003, and Ph.D. in Chemistry at University of Cambridge in 2007. In 2008-2009, he worked as Postdoctoral Research Associate with Prof. Chad A. Mirkin at the International Institute for Nanotechnology at Northwestern University. He joined PolyU as Assistant Professor in 2009, and currently he is Chair Professor at the Department of Applied Biology and Chemical

Technology, Associate Director of the Research Institute of Wearable Intelligent Systems, and Associate Director of the University Research Facility in Materials Characterization and Device Fabrication at The Hong Kong Polytechnic University (PolyU). His research interests include surface and polymer science, nanofabrication, flexible and wearable electronics, energy conversion and storage. He serves as Editor-in-Chief of *EcoMat* (a flagship open-access journal in green energy and environment published by Wiley), and Guest Editor of *Advanced Materials* and *Small*. He is Editorial Board Member of *Advanced Energy Materials* (Wiley) and *npj Flexible Electronics* (Springer Nature). Prof. Zheng is elected Founding Member of The Young Academy of Sciences of Hong Kong, and Chang Jiang Chair Professor by the Ministry of Education of China.

## ACKNOWLEDGMENTS

The authors acknowledge the financial support from RGC Senior Research Fellow Scheme of Hong Kong (SRF2122-5S04), General Research Fund of Hong Kong (15212021), National Natural Science Foundation of China/RGC Collaborative Research Scheme (CRS\_PolyU504/22), Research Impact Fund (R5019-22), National Natural Science Foundation of China (52203318), Innovation and Technology Fund-Guangdong-Hong Kong Technology Cooperation Funding Scheme (GHP/047/20GD), Shenzhen Science and Technology Innovation Committee (SGDX20210823103403033), The Hong Kong Polytechnic University (1-CD44, 1-CD8D, 1-YXA1, 1-W22Q), Hong Kong Scholar Program (XJ2021047), and Fujian Science & Technology Innovation Laboratory for Optoelectronic Information of China (2021ZR117).

## **ABBREVIATIONS USED**

1D = one-dimensional

2D = two-dimensional

3D = three-dimensional

AC = Active carbon

ACA = anisotropic conductive adhesives

ACEL = alternating current electroluminescent

ADC = Analog-to-digital converters

AgNFs = silver nanofibers

AgNP = silver nanoparticle

AgNWs = silver nanowires

AI = artificial intelligence

APGD = atmospheric-pressure glow discharge

APPJ = atmospheric-pressure plasma jet

AR = augmented reality

BEA = boundary element analysis

BLE = Bluetooth Low Energy

BOx = bilirubin oxidase

CAD = computer-aid design

CD = corona discharge

CF = cystic fibrosis

CMT = carbonized Modal textile

CNFs = carbon nanofibers

CNTs = carbon nanotubes

CKD = chronic kidney disease

CS = combustion synthesis

CT = cotton thread

CuNWs = copper nanowires

CVD = chemical vapor deposition

CVF = chitosan-viscose nonwoven fabric

DA = dopamine

DBD = dielectric-barrier discharge

DC = direct current

DPFs = date palm fibers

DSSCs = dye-sensitized solar cells  
EBG = electromagnetic bandgap  
ECG = electrocardiography  
EDL = electrical double layer  
EEG = electroencephalography  
EGaIn = eutectic-gallium-indium  
EIS = electrochemical impedance spectroscopy  
EMG = electromyography  
EMPA = Electrospun micropylamid array  
EOG = electrooculography  
E-skins = electronic skins  
ET = elastic thread  
FEA = finite element analysis  
FETs = field-effect transistors  
FOM = figure of merit  
FPCB = flexible printed circuit board  
GO = graphene oxide  
GOx = glucose oxidase  
HDPE = high density polyethylene  
HEA = hybrid element analysis  
HMI = human-machine interactions  
HoMSs = hollow multi-shelled structures  
HTP = hyperthermia patch  
IC = integrated circuit  
ICA = isotropic electrically conductive adhesives  
ILED = inorganic light-emitting diode  
IoT = internet of things  
ISF = interstitial fluid  
ISM = ion-selective membrane  
IT = information technology  
ITO = indium tin oxide  
LEC = light emitting electrochemical cell  
LED = light-emitting diode  
LIBs = lithium-ion batteries



LM = liquid metal  
LMFM = liquid-metal fiber mat  
MCU = microcontroller unit  
MEG = magnetoelastic generator  
MEMS = micro-electromechanical systems  
MIPs = molecular imprint polymers  
MMF = moisture management fabric  
MOFs = metal-organic frameworks  
MTA = microwave thermosphere ablation  
MWCNT = multi-walled carbon nanotube  
NCA = non-conductive adhesives  
NFC = near-field communication  
NRAs = nanorod arrays  
OCP = open circuit potential  
OFET = organic field-effective transistor  
OECT = organic electrochemical transistor  
OLED = organic light-emitting diode  
OSCs = organic solar cells  
PA = polyamide  
PAA = polyacrylate  
PAMD = polymer-assisted metal deposition  
PAN = polyacrylonitrile  
PANI = polyaniline  
PB = Prussian blue  
PCBs = printed circuit boards  
PCE = power conversion efficiency  
PCTs = porous conductive textiles  
PD = Parkinson's disease  
PDMS = polydimethylsiloxane  
PE = polyethylene  
PEDOT:PSS = poly(3,4-ethylenedioxythiophene) polystyrene sulfonate  
PEI = polyethyleneimine  
PEN = polyethylene naphthalate  
PENG = piezoelectric nanogenerator

PET = polyethylene terephthalate  
 PI = polyimide  
 PLED = polymer light-emitting diode  
 PMMA = polymethyl methacrylate  
 PSCs = perovskite solar cells  
 PTFE = polytetrafluoroethylene  
 pV3D3 = 1,3,5-trivinyl-1,3,5-trimethyl cyclotrisiloxane  
 PU = polyurethane  
 PVA = polyvinyl alcohol  
 PVDF = polyvinylidene fluoride  
 PVP = poly(vinyl pyrrolidone)  
 PPy = polypyrrole  
 RFA = radiofrequency ablation  
 RFID = Radio Frequency Identification  
 rHGO = reduced holey graphene oxides  
 rGO = reduced graphene oxide  
 SACNT = super-aligned CNT  
 SBS = poly(styrene-block-butadiene-block-styrene)  
 SBAS = poly(styrene-b-butyl acrylate-b-styrene) (SBAS)  
 SEBS = polystyrene-block-poly(ethylene-ran-butylene)-block-polystyrene  
 SEI = solid electrolyte interphase  
 SEM = scanning electron microscope  
 SIS = polystyrene-b-polyisoprene-b-polystyrene block copolymer  
 SMD = surface-mounted device  
 SMT = surface mount technology  
 SWCNT = single-walled carbon nanotube  
 TEM = transmission electron microscope  
 TENG = triboelectric nanogenerator  
 TENS = transcutaneous electrical nerve stimulation  
 TFT = thin-film transistors  
 THT = through-hole technology  
 TPU = thermoplastic polyurethane  
 UHMWPE = ultra-high molecular weight polyethylene  
 UV = ultraviolet

VIA = vertical interconnect access

VOCs = volatile organic compounds

VR = virtual reality

WBPU = waterborne polyurethane

XR = extended reality

ZIB = zinc-ion battery

ZIF = zero insertion force

## REFERENCES

- (1) Cima, M. J. Next-Generation Wearable Electronics. *Nat. Biotechnol.* **2014**, *32*, 642-643.
- (2) Malmivaara, M. The Emergence of Wearable Electronics and Intelligent Clothing. In *Smart Clothes and Wearable Technology (Second Edition)*, McCann, J., Bryson, D. Eds.; Woodhead Publishing, 2023; pp 39-66.
- (3) Tao, X. Wearable Electronics and Photonics. Tao, X., Ed.; Woodhead Publishing Limited: Cambridge, 2005; pp 1-12.
- (4) Tess, S.; Sam, D. *Wearable Technology Forecasts 2023-2033*; IDTechEx, 2023.
- (5) Ometov, A.; Shubina, V.; Klus, L.; Skibińska, J.; Saafi, S.; Pascacio, P.; Flueratoru, L.; Gaibor, D. Q.; Chukhno, N.; et al. A Survey on Wearable Technology: History, State-of-the-Art and Current Challenges. *Comput. Networks* **2021**, *193*, 108074.
- (6) Han, S. A.; Naqi, M.; Kim, S.; Kim, J. H. All-Day Wearable Health Monitoring System. *EcoMat* **2022**, *4*, e12198.
- (7) Guler, S. D.; Gannon, M.; Sicchio, K. A Brief History of Wearables. In *Crafting Wearables: Blending Technology with Fashion*, Guler, S. D., Gannon, M., Sicchio, K. Eds.; Apress, 2016; pp 3-10.
- (8) Heikenfeld, J.; Jajack, A.; Rogers, J.; Gutruf, P.; Tian, L.; Pan, T.; Li, R.; Khine, M.; Kim, J.; et al. Wearable Sensors: Modalities, Challenges, and Prospects. *Lab Chip* **2018**, *18*, 217-248.
- (9) Chen, G.; Xiao, X.; Zhao, X.; Tat, T.; Bick, M.; Chen, J. Electronic Textiles for Wearable Point-of-Care Systems. *Chem. Rev.* **2022**, *122*, 3259-3291.
- (10) Wang, Y.; Haick, H.; Guo, S.; Wang, C.; Lee, S.; Yokota, T.; Someya, T. Skin Bioelectronics towards Long-Term, Continuous Health Monitoring. *Chem. Soc. Rev.* **2022**, *51*, 3759-3793.
- (11) Bubnova, O. Stretching the Limits. *Nat. Nanotechnol.* **2017**, *12*, 101-101.
- (12) Ray, T.; Choi, J.; Reeder, J.; Lee, S. P.; Aranyosi, A. J.; Ghaffari, R.; Rogers, J. A. Soft, Skin-Interfaced Wearable Systems for Sports Science and Analytics. *Curr. Opin. Biomed. Eng.* **2019**, *9*, 47-56.
- (13) Rogers, J. A.; Someya, T.; Huang, Y. Materials and Mechanics for Stretchable Electronics. *Science* **2010**, *327*, 1603-1607.
- (14) Sun, Y.; Rogers, J. A. Inorganic Semiconductors for Flexible Electronics. *Adv. Mater.* **2007**, *19*, 1897-1916.
- (15) Jang, K.-I.; Han, S. Y.; Xu, S.; Mathewson, K. E.; Zhang, Y.; Jeong, J.-W.; Kim, G.-T.; Webb, R. C.; Lee, J. W.; et al. Rugged and Breathable Forms of Stretchable Electronics with

- Adherent Composite Substrates for Transcutaneous Monitoring. *Nat. Commun.* **2014**, *5*, 4779.
- (16) Fan, Z.; Ho, J. C.; Takahashi, T.; Yerushalmi, R.; Takei, K.; Ford, A. C.; Chueh, Y.-L.; Javey, A. Toward the Development of Printable Nanowire Electronics and Sensors. *Adv. Mater.* **2009**, *21*, 3730-3743.
- (17) Kim, Y.; Suh, J. M.; Shin, J.; Liu, Y.; Yeon, H.; Qiao, K.; Kum, H. S.; Kim, C.; Lee, H. E.; et al. Chip-Less Wireless Electronic Skins by Remote Epitaxial Freestanding Compound Semiconductors. *Science* **2022**, *377*, 859-864.
- (18) Hu, H.; Zhang, C.; Ding, Y.; Chen, F.; Huang, Q.; Zheng, Z. A Review of Structure Engineering of Strain-Tolerant Architectures for Stretchable Electronics. *Small Methods* **2023**, *n/a*, DOI: 10.1002/smtd.202300671.
- (19) Peng, H. Wearable Electronics. *Natl. Sci. Rev.* **2022**, *10*, nwac193.
- (20) Cheng, I. C.; Wagner, S. Overview of Flexible Electronics Technology. In *Flexible Electronics: Materials and Applications*, Wong, W. S., Salleo, A. Eds.; Springer US, 2009; pp 1-28.
- (21) Choudhry, N. A.; Arnold, L.; Rasheed, A.; Khan, I. A.; Wang, L. Textronics-A Review of Textile-Based Wearable Electronics. *Adv. Eng. Mater.* **2021**, *23*, 2100469.
- (22) Lin, Y.; Gritsenko, D.; Liu, Q.; Lu, X.; Xu, J. Recent Advancements in Functionalized Paper-Based Electronics. *ACS Appl. Mater. Interfaces* **2016**, *8*, 20501-20515.
- (23) Ling, H.; Liu, S.; Zheng, Z.; Yan, F. Organic Flexible Electronics. *Small Methods* **2018**, *2*, 1800070.
- (24) Ma, Z.; Huang, Q.; Xu, Q.; Zhuang, Q.; Zhao, X.; Yang, Y.; Qiu, H.; Yang, Z.; Wang, C.; et al. Permeable Superelastic Liquid-Metal Fibre Mat Enables Biocompatible and Monolithic Stretchable Electronics. *Nat. Mater.* **2021**, *20*, 859–868.
- (25) Jiang, Y.; Ji, S.; Sun, J.; Huang, J.; Li, Y.; Zou, G.; Salim, T.; Wang, C.; Li, W.; et al. A Universal Interface for Plug-and-Play Assembly of Stretchable Devices. *Nature* **2023**, *614*, 456-462.
- (26) Niu, S.; Matsuhisa, N.; Beker, L.; Li, J.; Wang, S.; Wang, J.; Jiang, Y.; Yan, X.; Yun, Y.; et al. A Wireless Body Area Sensor Network Based on Stretchable Passive Tags. *Nat. Electron.* **2019**, *2*, 361-368.
- (27) Hu, H.; Huang, H.; Li, M.; Gao, X.; Yin, L.; Qi, R.; Wu, R. S.; Chen, X.; Ma, Y.; et al. A Wearable Cardiac Ultrasound Imager. *Nature* **2023**, *613*, 667-675.
- (28) Liu, T.-L.; Dong, Y.; Chen, S.; Zhou, J.; Ma, Z.; Li, J. Battery-Free, Tuning Circuit–Inspired Wireless Sensor Systems for Detection of Multiple Biomarkers in Bodily Fluids. *Sci. Adv.* **2022**, *8*, eabo7049.

- (29) Zhao, G.; Ling, Y.; Su, Y.; Chen, Z.; Mathai, C. J.; Emeje, O.; Brown, A.; Alla, D. R.; Huang, J.; et al. Laser-Scribed Conductive, Photoactive Transition Metal Oxide on Soft Elastomers for Janus on-Skin Electronics and Soft Actuators. *Sci. Adv.* **2022**, *8*, eabp9734.
- (30) Wang, S. H.; Xu, J.; Wang, W. C.; Wang, G. J. N.; Rastak, R.; Molina-Lopez, F.; Chung, J. W.; Niu, S. M.; Feig, V. R.; et al. Skin Electronics from Scalable Fabrication of an Intrinsically Stretchable Transistor Array. *Nature* **2018**, *555*, 83-88.
- (31) Song, J.; Liu, H.; Zhao, Z.; Guo, X.; Liu, C.-k.; Griggs, S.; Marks, A.; Zhu, Y.; Law, H. K.-w.; et al. 2D Metal-Organic Frameworks for Ultraflexible Electrochemical Transistors with High Transconductance and Fast Response Speeds. *Sci. Adv.* **2023**, *9*, eadd9627.
- (32) Shen, Q.; Jiang, M.; Wang, R.; Song, K.; Vong, M. H.; Jung, W.; Krisnadi, F.; Kan, R.; Zheng, F.; et al. Liquid Metal-Based Soft, Hermetic, and Wireless-Communicable Seals for Stretchable Systems. *Science* **2023**, *379*, 488-493.
- (33) Xie, C.; Chang, J.; Shang, J.; Wang, L.; Gao, Y.; Huang, Q.; Zheng, Z. Hybrid Lithium-Ion/Metal Electrodes Enable Long Cycle Stability and High Energy Density of Flexible Batteries. *Adv. Funct. Mater.* **2022**, *32*, 2203242.
- (34) Khudiyev, T.; Grena, B.; Loke, G.; Hou, C.; Jang, H.; Lee, J.; Noel, G. H.; Alain, J.; Joannopoulos, J.; et al. Thermally Drawn Rechargeable Battery Fiber Enables Pervasive Power. *Mater. Today* **2022**, *52*, 80-89.
- (35) Liao, M.; Wang, C.; Hong, Y.; Zhang, Y.; Cheng, X.; Sun, H.; Huang, X.; Ye, L.; Wu, J.; et al. Industrial Scale Production of Fibre Batteries by a Solution-Extrusion Method. *Nat. Nanotechnol.* **2022**, *17*, 372-377.
- (36) Khudiyev, T.; Lee, J. T.; Cox, J. R.; Argentieri, E.; Loke, G.; Yuan, R.; Noel, G. H.; Tatara, R.; Yu, Y.; et al. 100 m Long Thermally Drawn Supercapacitor Fibers with Applications to 3D Printing and Textiles. *Adv. Mater.* **2020**, *32*, 2004971.
- (37) Xiong, T.; He, B.; Zhou, T.; Wang, Z.; Wang, Z.; Xin, J.; Zhang, H.; Zhou, X.; Liu, Y.; et al. Stretchable Fiber-Shaped Aqueous Aluminum Ion Batteries. *EcoMat* **2022**, *4*, e12218.
- (38) Dong, C.; Leber, A.; Yan, D.; Banerjee, H.; Laperrousaz, S.; Das Gupta, T.; Shadman, S.; Reis, P. M.; Sorin, F. 3D Stretchable and Self-Encapsulated Multimaterial Triboelectric Fibers. *Sci. Adv.* **2022**, *8*, eabo0869.
- (39) Shveda, R. A.; Rajappan, A.; Yap, T. F.; Liu, Z.; Bell, M. D.; Jumet, B.; Sanchez, V.; Preston, D. J. A Wearable Textile-Based Pneumatic Energy Harvesting System for Assistive Robotics. *Sci. Adv.* **2022**, *8*, eabo2418.
- (40) Yin, L.; Cao, M.; Kim, K. N.; Lin, M.; Moon, J.-M.; Sempionatto, J. R.; Yu, J.; Liu, R.; Wicker, C.; et al. A Stretchable Epidermal Sweat Sensing Platform with an Integrated Printed

Battery and Electrochromic Display. *Nat. Electron.* **2022**, *5*, 694-705.

(41) Hajiaghajani, A.; Afandizadeh Zargari, A. H.; Dautta, M.; Jimenez, A.; Kurdahi, F.; Tseng, P. Textile-Integrated Metamaterials for Near-Field Multibody Area Networks. *Nat. Electron.* **2021**, *4*, 808-817.

(42) Liu, S.; Shah, D. S.; Kramer-Bottiglio, R. Highly Stretchable Multilayer Electronic Circuits using Biphasic Gallium-Indium. *Nat. Mater.* **2021**, *20*, 851-858.

(43) Li, D.; Zhou, J.; Yao, K.; Liu, S.; He, J.; Su, J.; Qu, Q. a.; Gao, Y.; Song, Z.; et al. Touch IoT Enabled by Wireless Self-Sensing and Haptic-Reproducing Electronic Skin. *Sci. Adv.* **2022**, *8*, eade2450.

(44) Mattila, H. Chapter 15 - Yarn to Fabric: Intelligent Textiles. In *Textiles and Fashion*, Sinclair, R. Ed.; Woodhead Publishing, 2015; pp 355-376.

(45) Carr, D. J. Chapter One - Fibres, Yarns and Fabrics. In *Forensic Textile Science*, Carr, D. Ed.; Woodhead Publishing, 2017; pp 3-14.

(46) Gao, Y.; Xie, C.; Zheng, Z. Textile Composite Electrodes for Flexible Batteries and Supercapacitors: Opportunities and Challenges. *Adv. Energy Mater.* **2021**, *11*, 2002838.

(47) Huang, Q.; Wang, D.; Zheng, Z. Textile-Based Electrochemical Energy Storage Devices. *Adv. Energy Mater.* **2016**, *6*, 1600783.

(48) Wilson, J. Fibres, Yarns and Fabrics: Fundamental Principles for the Textile Designer. In *Textile Design*, Elsevier, 2011; pp 3-30.

(49) Ismar, E.; Kurşun Bahadır, S.; Kalaoglu, F.; Koncar, V. Futuristic Clothes: Electronic Textiles and Wearable Technologies. *Global chall.* **2020**, *4*, 1900092.

(50) Veit, D. Processes for the Production of Man-Made Fibers. In *Fibers: History, Production, Properties, Market*, Veit, D. Ed.; Springer International Publishing, 2022; pp 453-475.

(51) Eichhoff, J.; Hehl, A.; Jockenhoevel, S.; Gries, T. 7 - Textile Fabrication Technologies for Embedding Electronic Functions into Fibres, Yarns and Fabrics. In *Multidisciplinary Know-How for Smart-Textiles Developers*, Kirstein, T. Ed.; Woodhead Publishing, 2013; pp 191-226.

(52) McCann, J. 14 - Preparation for Smart Clothing Production. In *Smart Clothes and Wearable Technology (Second Edition)*, McCann, J., Bryson, D. Eds.; Woodhead Publishing, 2023; pp 371-404.

(53) Rosenberg, Z. B.; Knowles, C. G.; Mills, A. C.; Jur, J. S. 17 - Design Strategies for E-textile Manufacturing. In *Smart Clothes and Wearable Technology (Second Edition)*, McCann, J., Bryson, D. Eds.; Woodhead Publishing, 2023; pp 485-505.

(54) Stoppa, M.; Chiolerio, A. Wearable Electronics and Smart Textiles: A Critical Review. *Sensors* **2014**, *14*, 11957-11992.



- (55) Zheng, Z.; Jur, J.; Cheng, W. Smart Materials and Devices for Electronic Textiles. *MRS Bull.* **2021**, *46*, 488-490.
- (56) Agcayazi, T.; Chatterjee, K.; Bozkurt, A.; Ghosh, T. K. Flexible Interconnects for Electronic Textiles. *Adv. Mater. Technol.* **2018**, *3*, 1700277.
- (57) Li, Q.; Tao, X. M. Three-Dimensionally Deformable, Highly Stretchable, Permeable, Durable and Washable Fabric Circuit Boards. *Proc. R. Soc. A-Math. Phys. Eng. Sci.* **2014**, *470*, 22.
- (58) Roh, J.-S. All-Fabric Interconnection and One-Stop Production Process for Electronic Textile Sensors. *Text. Res. J.* **2017**, *87*, 1445-1456.
- (59) Uzun, S.; Seyedin, S.; Stoltzfus, A. L.; Levitt, A. S.; Alhabeb, M.; Anayee, M.; Strobel, C. J.; Razal, J. M.; Dion, G.; et al. Knittable and Washable Multifunctional MXene-Coated Cellulose Yarns. *Adv. Funct. Mater.* **2019**, *29*, 1905015.
- (60) Ma, Z.; Huang, Q.; Zhou, N.; Zhuang, Q.; Ng, S.-W.; Zheng, Z. Stretchable and Conductive Fibers Fabricated by a Continuous Method for Wearable Devices. *Cell Rep. Phys. Sci.* **2023**, *4*, 101300.
- (61) Fan, W.; He, Q.; Meng, K.; Tan, X.; Zhou, Z.; Zhang, G.; Yang, J.; Wang, Z. L. Machine-Knitted Washable Sensor Array Textile for Precise Epidermal Physiological Signal Monitoring. *Sci. Adv.* **2020**, *6*, eaay2840.
- (62) Gao, Y.; Hu, H.; Chang, J.; Huang, Q.; Zhuang, Q.; Li, P.; Zheng, Z. Realizing High-Energy and Stable Wire-Type Batteries with Flexible Lithium-Metal Composite Yarns. *Adv. Energy Mater.* **2021**, *11*, 2101809.
- (63) Lee, S.; Choi, H. W.; Figueiredo, C. L.; Shin, D.-W.; Moncunill, F. M.; Ullrich, K.; Sinopoli, S.; Jovančić, P.; Yang, J.; et al. Truly Form-Factor-Free Industrially Scalable System Integration for Electronic Textile Architectures with Multifunctional Fiber Devices. *Sci. Adv.* **2023**, *9*, eadf4049.
- (64) Shi, J. D.; Liu, S.; Zhang, L. S.; Yang, B.; Shu, L.; Yang, Y.; Ren, M.; Wang, Y.; Chen, J. W.; et al. Smart Textile-Integrated Microelectronic Systems for Wearable Applications. *Adv. Mater.* **2020**, *32*, 1901958.
- (65) Liu, S.; Ma, K.; Yang, B.; Li, H.; Tao, X. Textile Electronics for VR/AR Applications. *Adv. Funct. Mater.* **2020**, *31*, 2007254.
- (66) Gopalsamy, C.; Park, S.; Rajamanickam, R.; Jayaraman, S. The Wearable Motherboard™: The first Generation of Adaptive and Responsive Textile Structures (ARTS) for Medical Applications. *Virtual Reality* **1999**, *4*, 152-168.
- (67) Conroy, D. W.; García, A. A Golden Garment from Ancient Cyprus? Identifying New

Ways of Looking at the Past Through a Preliminary Report of Textile Fragments from the Pafos 'Erotes' Sarcophagus. In *The SInet 2010 eBook*, Yeatman, H. Ed.; Social Innovation Network (SInet), University of Wollongong, 2010; p 36.

(68) Fang, B.; Chang, D.; Xu, Z.; Gao, C. A Review on Graphene Fibers: Expectations, Advances, and Prospects. *Adv. Mater.* **2020**, *32*, 1902664.

(69) *Information on Textile Metallization Process.*  
[http://old.swicofil.com/textile\\_mettallization.html](http://old.swicofil.com/textile_mettallization.html) (accessed 2023 Oct. 5).

(70) *Development History of PAN based Carbon Fiber Technology.*  
<https://www.carbonfiber.gr.jp/english/tech/pan.html> (accessed 2023 Oct. 5).

(71) Andreatta, A.; Cao, Y.; Chiang, J. C.; Heeger, A. J.; Smith, P. Electrically-Conductive Fibers of Polyaniline Spun from Solutions in Concentrated Sulfuric Acid. *Synth. Met.* **1988**, *26*, 383-389.

(72) Liu, K.; Zhu, F.; Liu, L.; Sun, Y.; Fan, S.; Jiang, K. Fabrication and Processing of High-Strength Densely Packed Carbon Nanotube Yarns without Solution Processes. *Nanoscale* **2012**, *4*, 3389-3393.

(73) Coosemans, J.; Hermans, B.; Puers, R. Integrating Wireless ECG Monitoring in Textiles. *Sens. Actuator A Phys.* **2006**, *130-131*, 48-53.

(74) Hamed, M.; Forchheimer, R.; Inganäs, O. Towards Woven Logic from Organic Electronic Fibres. *Nat. Mater.* **2007**, *6*, 357-362.

(75) Hu, L.; Pasta, M.; La Mantia, F.; Cui, L.; Jeong, S.; Deshazer, H. D.; Choi, J. W.; Han, S. M.; Cui, Y. Stretchable, Porous, and Conductive Energy Textiles. *Nano Lett.* **2010**, *10*, 708-714.

(76) Xu, Z.; Gao, C. Graphene Chiral Liquid Crystals and Macroscopic Assembled Fibres. *Nat. Commun.* **2011**, *2*, 571.

(77) Kim, K. N.; Chun, J.; Kim, J. W.; Lee, K. Y.; Park, J.-U.; Kim, S.-W.; Wang, Z. L.; Baik, J. M. Highly Stretchable 2D Fabrics for Wearable Triboelectric Nanogenerator under Harsh Environments. *ACS Nano* **2015**, *9*, 6394-6400.

(78) Wang, Q.; Jian, M.; Wang, C.; Zhang, Y. Carbonized Silk Nanofiber Membrane for Transparent and Sensitive Electronic Skin. *Adv. Funct. Mater.* **2017**, *27*, 1605657.

(79) Miyamoto, A.; Lee, S.; Cooray, N. F.; Lee, S.; Mori, M.; Matsuhisa, N.; Jin, H.; Yoda, L.; Yokota, T.; et al. Inflammation-Free, Gas-Permeable, Lightweight, Stretchable on-Skin Electronics with Nanomeshes. *Nat. Nanotechnol.* **2017**, *12*, 907-913.

(80) He, J.; Lu, C.; Jiang, H.; Han, F.; Shi, X.; Wu, J.; Wang, L.; Chen, T.; Wang, J.; et al. Scalable Production of High-Performing Woven Lithium-Ion Fibre Batteries. *Nature* **2021**, *597*,

57-63.

- (81) Shi, X.; Zuo, Y.; Zhai, P.; Shen, J.; Yang, Y.; Gao, Z.; Liao, M.; Wu, J.; Wang, J.; et al. Large-Area Display Textiles Integrated with Functional Systems. *Nature* **2021**, *591*, 240-245.
- (82) Tabiei, A.; Ivanov, I. Computational Micro-Mechanical Model of Flexible Woven Fabric for Finite Element Impact Simulation. *Int. J. Numer. Methods Eng.* **2002**, *53*, 1259-1276.
- (83) Liu, Z.; Chen, K.; Fernando, A.; Gao, Y.; Li, G.; Jin, L.; Zhai, H.; Yi, Y.; Xu, L.; et al. Permeable Graphited Hemp Fabrics-Based, Wearing-Comfortable Pressure Sensors for Monitoring Human Activities. *Chem. Eng. J.* **2021**, *403*, 126191.
- (84) Lima, R. M. A. P.; Alcaraz-Espinoza, J. J.; da Silva, F. A. G., Jr.; de Oliveira, H. P. Multifunctional Wearable Electronic Textiles Using Cotton Fibers with Polypyrrole and Carbon Nanotubes. *ACS Appl. Mater. Interfaces* **2018**, *10*, 13783-13795.
- (85) Huang, Q.; Liu, L.; Wang, D.; Liu, J.; Huang, Z.; Zheng, Z. One-Step Electrospinning of Carbon Nanowebs on Metallic Textiles for High-Capacitance Supercapacitor Fabrics. *J. Mater. Chem. A* **2016**, *4*, 6802-6808.
- (86) Andrew, T. L.; Zhang, L.; Cheng, N.; Baima, M.; Kim, J. J.; Allison, L.; Hoxie, S. Melding Vapor-Phase Organic Chemistry and Textile Manufacturing To Produce Wearable Electronics. *Acc. Chem. Res.* **2018**, *51*, 850-859.
- (87) Wu, C.; Kim, T. W.; Li, F.; Guo, T. Wearable Electricity Generators Fabricated Utilizing Transparent Electronic Textiles Based on Polyester/Ag Nanowires/Graphene Core-Shell Nanocomposites. *ACS Nano* **2016**, *10*, 6449-6457.
- (88) Zhang, S.-W.; Yin, B.-S.; Liu, C.; Wang, Z.-B.; Gu, D.-M. A Low-Cost Wearable Yarn Supercapacitor Constructed by a Highly Bended Polyester Fiber Electrode and Flexible Film. *J. Mater. Chem. A* **2017**, *5*, 15144-15153.
- (89) Pu, X.; Li, L.; Song, H.; Du, C.; Zhao, Z.; Jiang, C.; Cao, G.; Hu, W.; Wang, Z. L. A Self-Charging Power Unit by Integration of a Textile Triboelectric Nanogenerator and a Flexible Lithium-Ion Battery for Wearable Electronics. *Adv. Mater.* **2015**, *27*, 2472-2478.
- (90) Yue, B.; Wang, C.; Ding, X.; Wallace, G. G. Polypyrrole Coated Nylon Lycra Fabric as Stretchable Electrode for Supercapacitor Applications. *Electrochim. Acta* **2012**, *68*, 18-24.
- (91) He, Z.; Chen, W.; Liang, B.; Liu, C.; Yang, L.; Lu, D.; Mo, Z.; Zhu, H.; Tang, Z.; et al. Capacitive Pressure Sensor with High Sensitivity and Fast Response to Dynamic Interaction Based on Graphene and Porous Nylon Networks. *ACS Appl. Mater. Interfaces* **2018**, *10*, 12816-12823.
- (92) Guo, Y.; Li, K.; Hou, C.; Li, Y.; Zhang, Q.; Wang, H. Fluoroalkylsilane-Modified Textile-Based Personal Energy Management Device for Multifunctional Wearable Applications. *ACS*

*Appl. Mater. Interfaces* **2016**, 8, 4676-4683.

(93) Wang, H.; Wang, H.; Wang, Y.; Su, X.; Wang, C.; Zhang, M.; Jian, M.; Xia, K.; Liang, X.; et al. Laser Writing of Janus Graphene/Kevlar Textile for Intelligent Protective Clothing. *ACS Nano* **2020**, 14, 3219-3226.

(94) Lee, J.; Kwon, H.; Seo, J.; Shin, S.; Koo, J. H.; Pang, C.; Son, S.; Kim, J. H.; Jang, Y. H.; et al. Conductive Fiber-Based Ultrasensitive Textile Pressure Sensor for Wearable Electronics. *Adv. Mater.* **2015**, 27, 2433-2439.

(95) Guo, X.; Facchetti, A. The Journey of Conducting Polymers from Discovery to Application. *Nat. Mater.* **2020**, 19, 922-928.

(96) Mokhtar, S. M. A.; Alvarez de Eulate, E.; Yamada, M.; Prow, T. W.; Evans, D. R. Conducting Polymers in Wearable Devices. *Med. Devices Sens.* **2021**, 4, e10160.

(97) Zhou, K.; Dai, K.; Liu, C.; Shen, C. Flexible Conductive Polymer Composites for Smart Wearable Strain Sensors. *SmartMat* **2020**, 1, e1010.

(98) Bhadra, S.; Khastgir, D.; Singha, N. K.; Lee, J. H. Progress in Preparation, Processing and Applications of Polyaniline. *Prog. Polym. Sci.* **2009**, 34, 783-810.

(99) Dall'Acqua, L.; Tonin, C.; Peila, R.; Ferrero, F.; Catellani, M. Performances and Properties of Intrinsic Conductive Cellulose-Polypyrrole Textiles. *Synth. Met.* **2004**, 146, 213-221.

(100) Kayser, L. V.; Lipomi, D. J. Stretchable Conductive Polymers and Composites Based on PEDOT and PEDOT:PSS. *Adv. Mater.* **2019**, 31, 1806133.

(101) Epstein, A. J. Conducting Polymers: Electrical Conductivity. In *Physical Properties of Polymers Handbook*, Mark, J. E. Ed.; Springer New York, 2007; pp 725-755.

(102) Le, T.-H.; Kim, Y.; Yoon, H. Electrical and Electrochemical Properties of Conducting Polymers. *Polymers* **2017**, 9, 150.

(103) Basescu, N.; Liu, Z. X.; Moses, D.; Heeger, A. J.; Naarmann, H.; Theophilou, N. High Electrical Conductivity in Doped Polyacetylene. *Nature* **1987**, 327, 403-405.

(104) Wang, X.-X.; Yu, G.-F.; Zhang, J.; Yu, M.; Ramakrishna, S.; Long, Y.-Z. Conductive Polymer Ultrafine Fibers via Electrospinning: Preparation, Physical Properties and Applications. *Prog. Mater. Sci.* **2021**, 115, 100704.

(105) Mirabedini, A.; Foroughi, J.; Wallace, G. G. Developments in Conducting Polymer Fibres: From Established Spinning Methods toward Advanced Applications. *RSC Adv.* **2016**, 6, 44687-44716.

(106) Paul, D. R. Diffusion During the Coagulation Step of Wet-Spinning. *J. App. Polym. Sci.* **1968**, 12, 383-402.

- (107) Phillips, D. M.; Drummy, L. F.; Naik, R. R.; Long, H. C. D.; Fox, D. M.; Trulove, P. C.; Mantz, R. A. Regenerated Silk Fiber Wet Spinning from an Ionic Liquid Solution. *J Mater Chem* **2005**, *15*, 4206-4208.
- (108) Islam, G. M. N.; Collie, S.; Qasim, M.; Ali, M. A. Highly Stretchable and Flexible Melt Spun Thermoplastic Conductive Yarns for Smart Textiles. *Nanomaterials* **2020**, *10*, 2324.
- (109) Xue, J.; Wu, T.; Dai, Y.; Xia, Y. Electrospinning and Electrospun Nanofibers: Methods, Materials, and Applications. *Chem. Rev.* **2019**, *119*, 5298-5415.
- (110) Xing, Y.; Xu, Y.; Wu, Q.; Wang, G.; Zhu, M. Optoelectronic Functional Fibers: Materials, Fabrication, and Application for Smart Textiles. *J. Mater. Chem. C* **2021**, *9*, 439-455.
- (111) Liu, B.; Zhang, J.; Wang, X.; Chen, G.; Chen, D.; Zhou, C.; Shen, G. Hierarchical Three-Dimensional ZnCo<sub>2</sub>O<sub>4</sub> Nanowire Arrays/Carbon Cloth Anodes for a Novel Class of High-Performance Flexible Lithium-Ion Batteries. *Nano Lett.* **2012**, *12*, 3005-3011.
- (112) Wang, G.; Wang, H.; Lu, X.; Ling, Y.; Yu, M.; Zhai, T.; Tong, Y.; Li, Y. Solid-State Supercapacitor Based on Activated Carbon Cloths Exhibits Excellent Rate Capability. *Adv. Mater.* **2014**, *26*, 2676-2682.
- (113) Yang, Y.; Huang, Q.; Niu, L.; Wang, D.; Yan, C.; She, Y.; Zheng, Z. Waterproof, Ultrahigh Areal-Capacitance, Wearable Supercapacitor Fabrics. *Adv. Mater.* **2017**, *29*, 1606679.
- (114) Wang, X.; Li, Z.; Xu, W.; Kulkarni, S. A.; Batabyal, S. K.; Zhang, S.; Cao, A.; Wong, L. H. TiO<sub>2</sub> Nanotube Arrays Based Flexible Perovskite Solar Cells with Transparent Carbon Nanotube Electrode. *Nano Energy* **2015**, *11*, 728-735.
- (115) Qiu, L.; Deng, J.; Lu, X.; Yang, Z.; Peng, H. Integrating Perovskite Solar Cells into a Flexible Fiber. *Angew. Chem., Int. Ed.* **2014**, *53*, 10425-10428.
- (116) Zhao, J.; Li, H.; Li, C.; Zhang, Q.; Sun, J.; Wang, X.; Guo, J.; Xie, L.; Xie, J.; et al. MOF for Template-Directed Growth of Well-Oriented Nanowire Hybrid Arrays on Carbon Nanotube Fibers for Wearable Electronics Integrated with Triboelectric Nanogenerators. *Nano Energy* **2018**, *45*, 420-431.
- (117) Pu, X.; Li, L.; Liu, M.; Jiang, C.; Du, C.; Zhao, Z.; Hu, W.; Wang, Z. L. Wearable Self-Charging Power Textile Based on Flexible Yarn Supercapacitors and Fabric Nanogenerators. *Adv. Mater.* **2016**, *28*, 98-105.
- (118) Cho, S.-Y.; Yu, H.; Choi, J.; Kang, H.; Park, S.; Jang, J.-S.; Hong, H.-J.; Kim, I.-D.; Lee, S.-K.; et al. Continuous Meter-Scale Synthesis of Weavable Tunicate Cellulose/Carbon Nanotube Fibers for High-Performance Wearable Sensors. *ACS Nano* **2019**, *13*, 9332-9341.

- (119) Wu, J.; Sun, Y.-M.; Wu, Z.; Li, X.; Wang, N.; Tao, K.; Wang, G. P. Carbon Nanocoil-Based Fast-Response and Flexible Humidity Sensor for Multifunctional Applications. *ACS Appl. Mater. Interfaces* **2019**, *11*, 4242-4251.
- (120) Zhang, S.; Xiao, S.; Li, D.; Liao, J.; Ji, F.; Liu, H.; Ci, L. Commercial Carbon Cloth: An Emerging Substrate for Practical Lithium Metal Batteries. *Energy Stor. Mater.* **2022**, *48*, 172-190.
- (121) Yusof, N.; Ismail, A. F. Post Spinning and Pyrolysis Processes of Polyacrylonitrile (PAN)-Based Carbon Fiber and Activated Carbon Fiber: A Review. *J. Anal. Appl. Pyrolysis* **2012**, *93*, 1-13.
- (122) Hunt, M. A.; Saito, T.; Brown, R. H.; Kumbhar, A. S.; Naskar, A. K. Patterned Functional Carbon Fibers from Polyethylene. *Adv. Mater.* **2012**, *24*, 2386-2389.
- (123) Bengtsson, A.; Bengtsson, J.; Sedin, M.; Sjöholm, E. Carbon Fibers from Lignin-Cellulose Precursors: Effect of Stabilization Conditions. *ACS Sustainable Chem. Eng.* **2019**, *7*, 8440-8448.
- (124) Khayyam, H.; Jazar, R. N.; Nunna, S.; Golkarnarenji, G.; Badii, K.; Fakhrhoseini, S. M.; Kumar, S.; Naebe, M. PAN Precursor Fabrication, Applications and Thermal Stabilization Process in Carbon Fiber Production: Experimental and Mathematical Modelling. *Prog. Mater. Sci.* **2020**, *107*, 100575.
- (125) Ding, Y.; Yang, J.; Tolle, C. R.; Zhu, Z. A Highly Stretchable Strain Sensor Based on Electrospun Carbon Nanofibers for Human Motion Monitoring. *RSC Adv.* **2016**, *6*, 79114-79120.
- (126) David, L. I. B.; Ismail, A. F. Influence of The Thermastabilization Process and Soak Time During Pyrolysis Process on the Polyacrylonitrile Carbon Membranes For O<sub>2</sub>/N<sub>2</sub> Separation. *J. Membr. Sci.* **2003**, *213*, 285-291.
- (127) Liao, X.; Ding, Y.; Chen, L.; Ye, W.; Zhu, J.; Fang, H.; Hou, H. Polyacrylonitrile-Derived Polyconjugated Ladder Structures for High Performance All-Organic Dielectric Materials. *Chem. Commun.* **2015**, *51*, 10127-10130.
- (128) Lu, W.; Zu, M.; Byun, J.-H.; Kim, B.-S.; Chou, T.-W. State of the Art of Carbon Nanotube Fibers: Opportunities and Challenges. *Adv. Mater.* **2012**, *24*, 1805-1833.
- (129) Baughman, R. H.; Zakhidov, A. A.; de Heer, W. A. Carbon Nanotubes--the Route Toward Applications. *Science* **2002**, *297*, 787-792.
- (130) Prasek, J.; Drbohlavova, J.; Chomoucka, J.; Hubalek, J.; Jasek, O.; Adam, V.; Kizek, R. Methods for Carbon Nanotubes Synthesis—Review. *J Mater Chem* **2011**, *21*, 15872-15884.
- (131) Liu, Q.; Shi, X.; Jiang, Q.; Li, R.; Zhong, S.; Zhang, R. Growth Mechanism and Kinetics

of Vertically Aligned Carbon Nanotube Arrays. *EcoMat* **2021**, 3, e12118.

(132) Zhang, X.; Lu, W.; Zhou, G.; Li, Q. Understanding the Mechanical and Conductive Properties of Carbon Nanotube Fibers for Smart Electronics. *Adv. Mater.* **2020**, 32, 1902028.

(133) Miaudet, P.; Badaire, S.; Maugey, M.; Derré, A.; Pichot, V.; Launois, P.; Poulin, P.; Zakri, C. Hot-Drawing of Single and Multiwall Carbon Nanotube Fibers for High Toughness and Alignment. *Nano Lett.* **2005**, 5, 2212-2215.

(134) Zhang, X.; Li, Q.; Tu, Y.; Li, Y.; Coulter, J. Y.; Zheng, L.; Zhao, Y.; Jia, Q.; Peterson, D. E.; et al. Strong Carbon-Nanotube Fibers Spun from Long Carbon-Nanotube Arrays. *Small* **2007**, 3, 244-248.

(135) Koziol, K.; Vilatela, J.; Moisala, A.; Motta, M.; Cunniff, P.; Sennett, M.; Windle, A. High-Performance Carbon Nanotube Fiber. *Science* **2007**, 318, 1892-1895.

(136) Vilatela, J. J.; Windle, A. H. Yarn-Like Carbon Nanotube Fibers. *Adv. Mater.* **2010**, 22, 4959-4963.

(137) Ryu, S.; Lee, P.; Chou, J. B.; Xu, R.; Zhao, R.; Hart, A. J.; Kim, S.-G. Extremely Elastic Wearable Carbon Nanotube Fiber Strain Sensor for Monitoring of Human Motion. *ACS Nano* **2015**, 9, 5929-5936.

(138) Zhou, J.; Xu, X.; Xin, Y.; Lubineau, G. Coaxial Thermoplastic Elastomer-Wrapped Carbon Nanotube Fibers for Deformable and Wearable Strain Sensors. *Adv. Funct. Mater.* **2018**, 28, 1705591.

(139) Zu, M.; Li, Q.; Wang, G.; Byun, J.-H.; Chou, T.-W. Carbon Nanotube Fiber Based Stretchable Conductor. *Adv. Funct. Mater.* **2013**, 23, 789-793.

(140) Xu, P.; Gu, T.; Cao, Z.; Wei, B.; Yu, J.; Li, F.; Byun, J.-H.; Lu, W.; Li, Q.; et al. Carbon Nanotube Fiber Based Stretchable Wire-Shaped Supercapacitors. *Adv. Energy Mater.* **2014**, 4, 1300759.

(141) Liu, Z. F.; Fang, S.; Moura, F. A.; Ding, J. N.; Jiang, N.; Di, J.; Zhang, M.; Lepró, X.; Galvão, D. S.; et al. Hierarchically Buckled Sheath-Core Fibers for Superelastic Electronics, Sensors, and Muscles. *Science* **2015**, 349, 400-404.

(142) Qi, H.; Schulz, B.; Vad, T.; Liu, J.; Mäder, E.; Seide, G.; Gries, T. Novel Carbon Nanotube/Cellulose Composite Fibers As Multifunctional Materials. *ACS Appl. Mater. Interfaces* **2015**, 7, 22404-22412.

(143) Xu, C.; Yang, S.; Li, P.; Wang, H.; Li, H.; Liu, Z. Wet-spun PEDOT:PSS/CNT Composite Fibers for Wearable Thermoelectric Energy Harvesting. *Compos. Commun.* **2022**, 32, 101179.

(144) Shin, Y.-E.; Cho, J. Y.; Yeom, J.; Ko, H.; Han, J. T. Electronic Textiles Based on Highly



Conducting Poly(vinyl alcohol)/Carbon Nanotube/Silver Nanobelt Hybrid Fibers. *ACS Appl. Mater. Interfaces* **2021**, *13*, 31051-31058.

(145) Zhang, D.; Miao, M.; Niu, H.; Wei, Z. Core-Spun Carbon Nanotube Yarn Supercapacitors for Wearable Electronic Textiles. *ACS Nano* **2014**, *8*, 4571-4579.

(146) Zhang, Q.; Wang, X.; Pan, Z.; Sun, J.; Zhao, J.; Zhang, J.; Zhang, C.; Tang, L.; Luo, J.; et al. Wrapping Aligned Carbon Nanotube Composite Sheets around Vanadium Nitride Nanowire Arrays for Asymmetric Coaxial Fiber-Shaped Supercapacitors with Ultrahigh Energy Density. *Nano Lett.* **2017**, *17*, 2719-2726.

(147) Shi, P.; Li, L.; Hua, L.; Qian, Q.; Wang, P.; Zhou, J.; Sun, G.; Huang, W. Design of Amorphous Manganese Oxide@Multiwalled Carbon Nanotube Fiber for Robust Solid-State Supercapacitor. *ACS Nano* **2017**, *11*, 444-452.

(148) Torrisi, F.; Hasan, T.; Wu, W.; Sun, Z.; Lombardo, A.; Kulmala, T. S.; Hsieh, G.-W.; Jung, S.; Bonaccorso, F.; et al. Inkjet-Printed Graphene Electronics. *ACS Nano* **2012**, *6*, 2992-3006.

(149) Avouris, P. Graphene: Electronic and Photonic Properties and Devices. *Nano Lett.* **2010**, *10*, 4285-4294.

(150) Wei, Z.; Wang, D.; Kim, S.; Kim, S.-Y.; Hu, Y.; Yakes, M. K.; Laracuenta, A. R.; Dai, Z.; Marder, S. R.; et al. Nanoscale Tunable Reduction of Graphene Oxide for Graphene Electronics. *Science* **2010**, *328*, 1373-1376.

(151) Meng, Y.; Zhao, Y.; Hu, C.; Cheng, H.; Hu, Y.; Zhang, Z.; Shi, G.; Qu, L. All-Graphene Core-Sheath Microfibers for All-Solid-State, Stretchable Fibriform Supercapacitors and Wearable Electronic Textiles. *Adv. Mater.* **2013**, *25*, 2326-2331.

(152) Avouris, P.; Dimitrakopoulos, C. Graphene: Synthesis and Applications. *Mater. Today* **2012**, *15*, 86-97.

(153) Hernandez, Y.; Nicolosi, V.; Lotya, M.; Blighe, F. M.; Sun, Z.; De, S.; McGovern, I. T.; Holland, B.; Byrne, M.; et al. High-Yield Production of Graphene by Liquid-Phase Exfoliation of Graphite. *Nat. Nanotechnol.* **2008**, *3*, 563-568.

(154) Yi, M.; Shen, Z. A Review on Mechanical Exfoliation for the Scalable Production of Graphene. *J. Mater. Chem. A* **2015**, *3*, 11700-11715.

(155) Eigler, S.; Enzelberger-Heim, M.; Grimm, S.; Hofmann, P.; Kroener, W.; Geworski, A.; Dotzer, C.; Röckert, M.; Xiao, J.; et al. Wet Chemical Synthesis of Graphene. *Adv. Mater.* **2013**, *25*, 3583-3587.

(156) Chen, L.; Hernandez, Y.; Feng, X.; Müllen, K. From Nanographene and Graphene Nanoribbons to Graphene Sheets: Chemical Synthesis. *Angew. Chem., Int. Ed.* **2012**, *51*, 7640-

7654.

- (157) Zhang, Y.; Zhang, L.; Zhou, C. Review of Chemical Vapor Deposition of Graphene and Related Applications. *Acc. Chem. Res.* **2013**, *46*, 2329-2339.
- (158) Yu, Q.; Lian, J.; Siriponglert, S.; Li, H.; Chen, Y. P.; Pei, S.-S. Graphene Segregated on Ni Surfaces and Transferred to Insulators. *Appl. Phys. Lett.* **2008**, *93*, 113103.
- (159) Xu, Z.; Gao, C. Graphene Fiber: A New Trend in Carbon Fibers. *Mater. Today* **2015**, *18*, 480-492.
- (160) Xu, Z.; Liu, Y.; Zhao, X.; Peng, L.; Sun, H.; Xu, Y.; Ren, X.; Jin, C.; Xu, P.; et al. Ultrastiff and Strong Graphene Fibers via Full-Scale Synergetic Defect Engineering. *Adv. Mater.* **2016**, *28*, 6449-6456.
- (161) Cong, H.-P.; Ren, X.-C.; Wang, P.; Yu, S.-H. Wet-Spinning Assembly of Continuous, Neat and Macroscopic Graphene Fibers. *Sci. Rep.* **2012**, *2*, 613.
- (162) Zhao, Y.; Jiang, C.; Hu, C.; Dong, Z.; Xue, J.; Meng, Y.; Zheng, N.; Chen, P.; Qu, L. Large-Scale Spinning Assembly of Neat, Morphology-Defined, Graphene-Based Hollow Fibers. *ACS Nano* **2013**, *7*, 2406-2412.
- (163) Hu, Y.; Cheng, H.; Zhao, F.; Chen, N.; Jiang, L.; Feng, Z.; Qu, L. All-in-One Graphene Fiber Supercapacitor. *Nanoscale* **2014**, *6*, 6448-6451.
- (164) Xin, G.; Yao, T.; Sun, H.; Scott, S. M.; Shao, D.; Wang, G.; Lian, J. Highly Thermally Conductive and Mechanically Strong Graphene Fibers. *Science* **2015**, *349*, 1083-1087.
- (165) Asmatulu, R.; Ceylan, M.; Nuraje, N. Study of Superhydrophobic Electrospun Nanocomposite Fibers for Energy Systems. *Langmuir* **2011**, *27*, 504-507.
- (166) Barakzahi, M.; Montazer, M.; Sharif, F.; Norby, T.; Chatzidakis, A. A Textile-Based Wearable Supercapacitor using Reduced Graphene Oxide/Polypyrrole Composite. *Electrochim. Acta* **2019**, *305*, 187-196.
- (167) Kwon, S.; Lee, T.; Choi, H.-J.; Ahn, J.; Lim, H.; Kim, G.; Choi, K.-B.; Lee, J. Scalable Fabrication of Inkless, Transfer-Printed Graphene-Based Textile Microsupercapacitors with High Rate Capabilities. *J. Power Sources* **2021**, *481*, 228939.
- (168) Karim, N.; Afroj, S.; Tan, S.; Novoselov, K. S.; Yeates, S. G. All Inkjet-Printed Graphene-Silver Composite Ink on Textiles for Highly Conductive Wearable Electronics Applications. *Sci. Rep.* **2019**, *9*, 8035.
- (169) Yao, D.; Tang, Z.; Zhang, L.; Li, R.; Zhang, Y.; Zeng, H.; Du, D.; Ouyang, J. Gas-Permeable and Highly Sensitive, Washable and Wearable Strain Sensors Based on Graphene/Carbon Nanotubes Hybrids E-Textile. *Compos. Part A Appl. Sci. Manuf.* **2021**, *149*, 106556.

- (170) Bian, X.-M.; Liu, L.; Li, H.-B.; Wang, C.-Y.; Xie, Q.; Zhao, Q.-L.; Bi, S.; Hou, Z.-L. Construction of Three-Dimensional Graphene Interfaces into Carbon Fiber Textiles for Increasing Deposition of Nickel Nanoparticles: Flexible Hierarchical Magnetic Textile Composites for Strong Electromagnetic Shielding. *Nanotechnology* **2017**, *28*, 045710.
- (171) Ji, X.; Xu, Y.; Zhang, W.; Cui, L.; Liu, J. Review of Functionalization, Structure and Properties of Graphene/Polymer Composite Fibers. *Compos. Part A Appl. Sci. Manuf.* **2016**, *87*, 29-45.
- (172) Qu, G.; Cheng, J.; Li, X.; Yuan, D.; Chen, P.; Chen, X.; Wang, B.; Peng, H. A Fiber Supercapacitor with High Energy Density Based on Hollow Graphene/Conducting Polymer Fiber Electrode. *Adv. Mater.* **2016**, *28*, 3646-3652.
- (173) Liu, L.; Yu, Y.; Yan, C.; Li, K.; Zheng, Z. Wearable Energy-Dense and Power-Dense Supercapacitor Yarns Enabled by Scalable Graphene-Metallic Textile Composite Electrodes. *Nat. Commun.* **2015**, *6*, 7260.
- (174) Wu, X.; Mu, F.; Zhao, H. Recent Progress in the Synthesis of Graphene/CNT Composites and the Energy-Related Applications. *J. Mater. Sci. Technol.* **2020**, *55*, 16-34.
- (175) Lu, Z.; Foroughi, J.; Wang, C.; Long, H.; Wallace, G. G. Superelastic Hybrid CNT/Graphene Fibers for Wearable Energy Storage. *Adv. Energy Mater.* **2018**, *8*, 1702047.
- (176) Zhang, Y.; Guo, X.; Huang, J.; Ren, Z.; Hu, H.; Li, P.; Lu, X.; Wu, Z.; Xiao, T.; et al. Solution Process Formation of High Performance, Stable Nanostructured Transparent Metal Electrodes via Displacement-Diffusion-Etch Process. *npj Flex. Electron.* **2022**, *6*, 4.
- (177) Wang, D.; Zhang, Y.; Lu, X.; Ma, Z.; Xie, C.; Zheng, Z. Chemical Formation of Soft Metal Electrodes for Flexible and Wearable Electronics. *Chem. Soc. Rev.* **2018**, *47*, 4611-4641.
- (178) Jalal Uddin, A. 9 - Novel Technical Textile Yarns. In *Technical Textile Yarns*, Alagirusamy, R., Das, A. Eds.; Woodhead Publishing, 2010; pp 259-297.
- (179) Guo, L.; Bashir, T.; Bresky, E.; Persson, N. K. 28 - Electroconductive Textiles and Textile-Based Electromechanical Sensors--Integration in as an Approach for Smart Textiles. In *Smart Textiles and their Applications*, Koncar, V. Ed.; Woodhead Publishing, 2016; pp 657-693.
- (180) Shabaridharan, K.; Bhattacharyya, A. Metallic Fibers for Composite Applications. In *Fibrous and Textile Materials for Composite Applications*, Rana, S., Figueiro, R. Eds.; Springer Singapore, 2016; pp 205-230.
- (181) Mishima, R.; Miyamura, H.; Sakai, T.; Kuriyama, N.; Ishikawa, H.; Uehara, I. Hydrogen Storage Alloys Rapidly Solidified by the Melt-Spinning Method and Their Characteristics as Metal Hydride Electrodes. *J. Alloys Compd.* **1993**, *192*, 176-178.

- (182) Zhou, J.; Zhai, M.; Wang, R.; Wang, Y.; Wang, Q.; Hu, Z.; Xiang, H.; Zhu, M. High Metal-Loaded Cu<sub>2</sub>O@Tm Hybrids for Melt-Spun Antibacterial Fibers Engineered towards Medical Protective Fabrics. *Compos. Part A Appl. Sci. Manuf.* **2022**, *161*, 107080.
- (183) Zhu, Y.; Zhao, Y.; Zhang, X.; Wang, L.; Wang, X.; Zhang, J.; Han, P.; Qiao, J. Metal Filaments/Nano-Filler Filled Hybrid Polymer Fibers with Improved Conductive Performance. *Mater. Lett.* **2016**, *173*, 26-30.
- (184) Jiang, S. Q.; Newton, E.; Yuen, C. W. M.; Kan, C. W. Chemical Silver Plating and Its Application to Textile Fabric Design. *J. App. Polym. Sci.* **2005**, *96*, 919-926.
- (185) Shahidi, S.; Moazzenchi, B.; Ghoranneviss, M. A Review-Application of Physical Vapor Deposition (PVD) and Related Methods in the Textile Industry. *EPJ. Applied Physics.* **2015**, *71*, 31302.
- (186) Li, P.; Zhang, Y.; Zheng, Z. Polymer-Assisted Metal Deposition (PAMD) for Flexible and Wearable Electronics: Principle, Materials, Printing, and Devices. *Adv. Mater.* **2019**, *31*, 1902987.
- (187) Beregoi, M.; Busuioc, C.; Evangelidis, A.; Matei, E.; Iordache, F.; Radu, M.; Dinischiotu, A.; Enculescu, I. Electrochromic Properties of Polyaniline-Coated Fiber Webs for Tissue Engineering Applications. *Int. J. Pharm.* **2016**, *510*, 465-473.
- (188) Liu, X.; Chang, H.; Li, Y.; Huck, W. T. S.; Zheng, Z. Polyelectrolyte-Bridged Metal/Cotton Hierarchical Structures for Highly Durable Conductive Yarns. *ACS Appl. Mater. Interfaces* **2010**, *2*, 529-535.
- (189) Meenambiga, S. S.; Sakthiselvan, P.; Hari, S.; Umai, D. Chapter 13 - Nanotechnology for Blood Test to Predict the Blood Diseases/Blood Disorders. In *Nanotechnology for Hematology, Blood Transfusion, and Artificial Blood*, Denizli, A., Nguyen, T. A., Rajan, M., Alam, M. F., Rahman, K. Eds.; Elsevier, 2022; pp 285-311.
- (190) Kawamura, G.; Muto, H.; Matsuda, A. Hard Template Synthesis of Metal Nanowires. *Front. Chem.* **2014**, *2*, 104.
- (191) Kline, T. R.; Tian, M.; Wang, J.; Sen, A.; Chan, M. W. H.; Mallouk, T. E. Template-Grown Metal Nanowires. *Inorg. Chem.* **2006**, *45*, 7555-7565.
- (192) Poolakkandy, R. R.; Menampambath, M. M. Soft-Template-Assisted Synthesis: A Promising Approach for the Fabrication of Transition Metal Oxides. *Nanoscale Adv.* **2020**, *2*, 5015-5045.
- (193) Sun, Y.; Mayers, B.; Herricks, T.; Xia, Y. Polyol Synthesis of Uniform Silver Nanowires: A Plausible Growth Mechanism and the Supporting Evidence. *Nano Lett.* **2003**, *3*, 955-960.

- (194) Bergin, S. M.; Chen, Y.-H.; Rathmell, A. R.; Charbonneau, P.; Li, Z.-Y.; Wiley, B. J. The Effect of Nanowire Length and Diameter on the Properties of Transparent, Conducting Nanowire Films. *Nanoscale* **2012**, *4*, 1996-2004.
- (195) Kwon, J.; Suh, Y. D.; Lee, J.; Lee, P.; Han, S.; Hong, S.; Yeo, J.; Lee, H.; Ko, S. H. Recent Progress in Silver Nanowire Based Flexible/Wearable Optoelectronics. *J. Mater. Chem. C* **2018**, *6*, 7445-7461.
- (196) Joo, S.-J.; Park, S.-H.; Moon, C.-J.; Kim, H.-S. A Highly Reliable Copper Nanowire/Nanoparticle Ink Pattern with High Conductivity on Flexible Substrate Prepared via a Flash Light-Sintering Technique. *ACS Appl. Mater. Interfaces* **2015**, *7*, 5674-5684.
- (197) Ye, S.; Rathmell, A. R.; Ha, Y.-C.; Wilson, A. R.; Wiley, B. J. The Role of Cuprous Oxide Seeds in the One-Pot and Seeded Syntheses of Copper Nanowires. *Small* **2014**, *10*, 1771-1778.
- (198) Fu, A.; Wang, C.; Peng, J.; Su, M.; Pei, F.; Cui, J.; Fang, X.; Li, J.-F.; Zheng, N. Lithiophilic and Antioxidative Copper Current Collectors for Highly Stable Lithium Metal Batteries. *Adv. Funct. Mater.* **2021**, *31*, 2009805.
- (199) Ye, D.-M.; Li, G.-Z.; Wang, G.-G.; Lin, Z.-Q.; Zhou, H.-L.; Han, M.; Liu, Y.-L.; Han, J.-C. One-Pot Synthesis of Copper Nanowire Decorated by Reduced Graphene Oxide with Excellent Oxidation Resistance and Stability. *Appl. Surf. Sci.* **2019**, *467-468*, 158-167.
- (200) Won, Y.; Kim, A.; Lee, D.; Yang, W.; Woo, K.; Jeong, S.; Moon, J. Annealing-Free Fabrication of Highly Oxidation-Resistive Copper Nanowire Composite Conductors for Photovoltaics. *NPG Asia Mater.* **2014**, *6*, e105-e105.
- (201) Chen, Z.; Ye, S.; Stewart, I. E.; Wiley, B. J. Copper Nanowire Networks with Transparent Oxide Shells That Prevent Oxidation without Reducing Transmittance. *ACS Nano* **2014**, *8*, 9673-9679.
- (202) Mirvakili, S. M.; Pazukha, A.; Sikkema, W.; Sinclair, C. W.; Spinks, G. M.; Baughman, R. H.; Madden, J. D. W. Niobium Nanowire Yarns and their Application as Artificial Muscles. *Adv. Funct. Mater.* **2013**, *23*, 4311-4316.
- (203) Saha, P.; Khan, M. F.; Patra, S. Truncated  $\alpha$ -Amylase: An Improved Candidate for Textile Processing. *Prep. Biochem. Biotechnol.* **2018**, *48*, 635-645.
- (204) Jiang, K.; Li, Q.; Fan, S. Spinning Continuous Carbon Nanotube Yarns. *Nature* **2002**, *419*, 801-801.
- (205) Ghemes, A.; Minami, Y.; Muramatsu, J.; Okada, M.; Mimura, H.; Inoue, Y. Fabrication and Mechanical Properties of Carbon Nanotube Yarns Spun from Ultra-Long Multi-Walled Carbon Nanotube Arrays. *Carbon* **2012**, *50*, 4579-4587.

- (206) Miao, M. 3 - Carbon Nanotube Yarns for Electronic Textiles. In *Electronic Textiles*, Dias, T. Ed.; Woodhead Publishing, 2015; pp 55-72.
- (207) Kim, S. H.; Haines, C. S.; Li, N.; Kim, K. J.; Mun, T. J.; Choi, C.; Di, J.; Oh, Y. J.; Oviedo, J. P.; et al. Harvesting Electrical Energy from Carbon Nanotube Yarn Twist. *Science* **2017**, *357*, 773-778.
- (208) Liu, K.; Sun, Y.; Lin, X.; Zhou, R.; Wang, J.; Fan, S.; Jiang, K. Scratch-Resistant, Highly Conductive, and High-Strength Carbon Nanotube-Based Composite Yarns. *ACS Nano* **2010**, *4*, 5827-5834.
- (209) Su, F.; Lv, X.; Miao, M. High-Performance Two-Ply Yarn Supercapacitors Based on Carbon Nanotube Yarns Dotted with Co<sub>3</sub>O<sub>4</sub> and NiO Nanoparticles. *Small* **2015**, *11*, 854-861.
- (210) Zhao, Z.; Yan, C.; Liu, Z.; Fu, X.; Peng, L. M.; Hu, Y.; Zheng, Z. Machine-Washable Textile Triboelectric Nanogenerators for Effective Human Respiratory Monitoring through Loom Weaving of Metallic Yarns. *Adv. Mater.* **2016**, *28*, 10267-10274.
- (211) Yang, A.; Li, Y.; Yang, C.; Fu, Y.; Wang, N.; Li, L.; Yan, F. Fabric Organic Electrochemical Transistors for Biosensors. *Adv. Mater.* **2018**, *30*, 1800051.
- (212) Jost, K.; Stenger, D.; Perez, C. R.; McDonough, J. K.; Lian, K.; Gogotsi, Y.; Dion, G. Knitted and Screen Printed Carbon-Fiber Supercapacitors for Applications in Wearable Electronics. *Energy Environ. Sci.* **2013**, *6*, 2698-2705.
- (213) Lin, R.; Kim, H.-J.; Achavananthadith, S.; Xiong, Z.; Lee, J. K. W.; Kong, Y. L.; Ho, J. S. Digitally-Embroidered Liquid Metal Electronic Textiles for Wearable Wireless Systems. *Nat. Commun.* **2022**, *13*, 2190.
- (214) Geetha, S.; Satheesh Kumar, K. K.; Rao, C. R. K.; Vijayan, M.; Trivedi, D. C. EMI Shielding: Methods and Materials—A Review. *J. App. Polym. Sci.* **2009**, *112*, 2073-2086.
- (215) Roh, J.-S.; Chi, Y.-S.; Kang, T. J. Wearable Textile Antennas. *Int. J. Fash. Des. Technol. Educ.* **2010**, *3*, 135-153.
- (216) Liu, T.; He, Z.; Liu, H.; Yang, J.; Zhang, S.; Yu, J.; Ji, M.; Zhu, C.; Xu, J. Heat-Resistant and High-Performance Solid-State Supercapacitors Based on Poly(para-phenylene terephthalamide) Fibers via Polymer-Assisted Metal Deposition. *ACS Appl. Mater. Interfaces* **2021**, *13*, 18100-18109.
- (217) McFarland, A. W.; Elumalai, A.; Miller, C. C.; Humayun, A.; Mills, D. K. Effectiveness and Applications of a Metal-Coated HNT/Poly(lactic Acid) Antimicrobial Filtration System. *Polymers* **2022**, *14*, 1603.
- (218) Miśkiewicz, P.; Frydrych, I.; Cichocka, A. Application of Physical Vapor Deposition in Textile Industry. *Autex Res. J.* **2022**, *22*, 42-54.

- (219) Taghavi Pourian Azar, G.; Fox, D.; Fedutik, Y.; Krishnan, L.; Cobley, A. J. Functionalised Copper Nanoparticle Catalysts for Electroless Copper Plating on Textiles. *Surf. Coat. Technol.* **2020**, *396*, 125971.
- (220) Yan, C.; Zheng, Z. Textile-Based Electronics. In *Handbook of Fibrous Materials*, 2020; pp 721-748.
- (221) Yan, C.; Zheng, Z. Polymer Brushes as Interfacial Materials for Soft Metal Conductors and Electronics. In *Polymer and Biopolymer Brushes*, 2017; pp 709-734.
- (222) Wang, X.; Yan, C.; Hu, H.; Zhou, X.; Guo, R.; Liu, X.; Xie, Z.; Huang, Z.; Zheng, Z. Aqueous and Air-Compatible Fabrication of High-Performance Conductive Textiles. *Chem. Asian J.* **2014**, *9*, 2170-2177.
- (223) Zhang, Y.; Luo, Y.; Wang, L.; Ng, P. F.; Hu, H.; Chen, F.; Huang, Q.; Zheng, Z. Destructive-Treatment-Free Rapid Polymer-Assisted Metal Deposition for Versatile Electronic Textiles. *ACS Appl. Mater. Interfaces* **2022**, *14*, 56193-56202.
- (224) Jia, L.-C.; Jia, X.-X.; Sun, W.-J.; Zhang, Y.-P.; Xu, L.; Yan, D.-X.; Su, H.-J.; Li, Z.-M. Stretchable Liquid Metal-Based Conductive Textile for Electromagnetic Interference Shielding. *ACS Appl. Mater. Interfaces* **2020**, *12*, 53230-53238.
- (225) Dong, C.; Leber, A.; Das Gupta, T.; Chandran, R.; Volpi, M.; Qu, Y.; Nguyen-Dang, T.; Bartolomei, N.; Yan, W.; et al. High-Efficiency Super-Elastic Liquid Metal Based Triboelectric Fibers and Textiles. *Nat. Commun.* **2020**, *11*, 3537.
- (226) Lim, T.; Kim, H. J.; Won, S.; Kim, C. H.; Yoo, J.; Lee, J. H.; Son, K. S.; Nam, I.-W.; Kim, K.; et al. Liquid Metal-Based Electronic Textiles Coated with Au Nanoparticles as Stretchable Electrode Materials for Healthcare Monitoring. *ACS Appl. Nano Mater.* **2023**, *6*, 8482–8494.
- (227) Zhuang, Q.; Ma, Z.; Gao, Y.; Zhang, Y.; Wang, S.; Lu, X.; Hu, H.; Cheung, C.; Huang, Q.; et al. Liquid–Metal-Superlyophilic and Conductivity–Strain-Enhancing Scaffold for Permeable Superelastic Conductors. *Adv. Funct. Mater.* **2021**, *31*, 2105587.
- (228) Afroj, S.; Tan, S.; Abdelkader, A. M.; Novoselov, K. S.; Karim, N. Highly Conductive, Scalable, and Machine Washable Graphene-Based E-Textiles for Multifunctional Wearable Electronic Applications. *Adv. Funct. Mater.* **2020**, *30*, 2000293.
- (229) Ryan, J. D.; Lund, A.; Hofmann, A. I.; Kroon, R.; Sarabia-Riquelme, R.; Weisenberger, M. C.; Müller, C. All-Organic Textile Thermoelectrics with Carbon-Nanotube-Coated n-Type Yarns. *ACS Appl. Energy Mater.* **2018**, *1*, 2934-2941.
- (230) Bashir, T.; Skrifvars, M.; Persson, N.-K. Production of Highly Conductive Textile Viscose Yarns by Chemical Vapor Deposition Technique: A Route to Continuous Process.



*Polym. Adv. Technol.* **2011**, 22, 2214-2221.

(231) Hu, B.; Li, D.; Manandharm, P.; Fan, Q.; Kasilingam, D.; Calvert, P. CNT/Conducting Polymer Composite Conductors Impart High Flexibility to Textile Electroluminescent Devices. *J Mater Chem* **2012**, 22, 1598-1605.

(232) Saini, P.; Choudhary, V.; Dhawan, S. K. Improved Microwave Absorption and Electrostatic Charge Dissipation Efficiencies of Conducting Polymer Grafted Fabrics Prepared via In Situ Polymerization. *Polym. Adv. Technol.* **2012**, 23, 343-349.

(233) Mule, A. R.; Dudem, B.; Patnam, H.; Graham, S. A.; Yu, J. S. Wearable Single-Electrode-Mode Triboelectric Nanogenerator via Conductive Polymer-Coated Textiles for Self-Power Electronics. *ACS Sustainable Chem. Eng.* **2019**, 7, 16450-16458.

(234) Zhu, S.; Wang, M.; Qiang, Z.; Song, J.; Wang, Y.; Fan, Y.; You, Z.; Liao, Y.; Zhu, M.; et al. Multi-Functional and Highly Conductive Textiles with Ultra-High Durability Through 'Green' Fabrication Process. *Chem. Eng. J.* **2021**, 406, 127140.

(235) Zhang, L.; Fairbanks, M.; Andrew, T. L. Rugged Textile Electrodes for Wearable Devices Obtained by Vapor Coating Off-the-Shelf, Plain-Woven Fabrics. *Adv. Funct. Mater.* **2017**, 27, 1700415.

(236) Vital, D.; Zhong, J.; Bhardwaj, S.; Volakis, J. L. Loss-Characterization and Guidelines for Embroidery of Conductive Textiles. In *2018 IEEE International Symposium on Antennas and Propagation & USNC/URSI National Radio Science Meeting*, 8-13 July 2018, 2018; pp 1301-1302.

(237) Lee, J. H.; Dzagbletey, P. A.; Jang, M.; Chung, J.-Y.; So, J.-H. Flat Yarn Fabric Substrates for Screen-Printed Conductive Textiles. *Adv. Eng. Mater.* **2020**, 22, 2000722.

(238) Kim, I.; Shahariar, H.; Ingram, W. F.; Zhou, Y.; Jur, J. S. Inkjet Process for Conductive Patterning on Textiles: Maintaining Inherent Stretchability and Breathability in Knit Structures. *Adv. Funct. Mater.* **2019**, 29, 1807573.

(239) Takamatsu, S.; Lonjaret, T.; Crisp, D.; Badier, J.-M.; Malliaras, G. G.; Ismailova, E. Direct Patterning of Organic Conductors on Knitted Textiles for Long-Term Electrocardiography. *Sci. Rep.* **2015**, 5, 15003.

(240) Choi, H. W.; Shin, D.-W.; Yang, J.; Lee, S.; Figueiredo, C.; Sinopoli, S.; Ullrich, K.; Jovančić, P.; Marrani, A.; et al. Smart Textile Lighting/Display System with Multifunctional Fibre Devices for Large Scale Smart Home and IoT Applications. *Nat. Commun.* **2022**, 13, 814.

(241) Sinha, S. K.; Noh, Y.; Reljin, N.; Treich, G. M.; Hajeb-Mohammadalipour, S.; Guo, Y.; Chon, K. H.; Sotzing, G. A. Screen-Printed PEDOT:PSS Electrodes on Commercial Finished Textiles for Electrocardiography. *ACS Appl. Mater. Interfaces* **2017**, 9, 37524-37528.

- (242) Matsuhisa, N.; Inoue, D.; Zalar, P.; Jin, H.; Matsuba, Y.; Itoh, A.; Yokota, T.; Hashizume, D.; Someya, T. Printable Elastic Conductors by in Situ Formation of Silver Nanoparticles from Silver Flakes. *Nat. Mater.* **2017**, *16*, 834-840.
- (243) Yu, Y.; Xiao, X.; Zhang, Y.; Li, K.; Yan, C.; Wei, X.; Chen, L.; Zhen, H.; Zhou, H.; et al. Photoreactive and Metal-Platable Copolymer Inks for High-Throughput, Room-Temperature Printing of Flexible Metal Electrodes for Thin-Film Electronics. *Adv. Mater.* **2016**, *28*, 4926-4934.
- (244) Zhuang, Q.; Yao, K.; Wu, M.; Lei, Z.; Chen, F.; Li, J.; Mei, Q.; Zhou, Y.; Huang, Q.; et al. Wafer-Patterned, Permeable, and Stretchable Liquid Metal Microelectrodes for Implantable Bioelectronics with Chronic Biocompatibility. *Sci. Adv.* **2023**, *9*, eadg8602.
- (245) Zhao, Z.; Xia, K.; Hou, Y.; Zhang, Q.; Ye, Z.; Lu, J. Designing Flexible, Smart and Self-Sustainable Supercapacitors for Portable/Wearable Electronics: From Conductive Polymers. *Chem. Soc. Rev.* **2021**, *50*, 12702-12743.
- (246) Shah, D. U.; Schubel, P. J.; Clifford, M. J. Modelling the Effect of Yarn Twist on the Tensile Strength of Unidirectional Plant Fibre Yarn Composites. *J. Compos. Mater.* **2013**, *47*, 425-436.
- (247) Miao, M. The Role of Twist in Dry Spun Carbon Nanotube Yarns. *Carbon* **2016**, *96*, 819-826.
- (248) Haines, C. S.; Lima, M. D.; Li, N.; Spinks, G. M.; Foroughi, J.; Madden, J. D. W.; Kim, S. H.; Fang, S.; Jung de Andrade, M.; et al. Artificial Muscles from Fishing Line and Sewing Thread. *Science* **2014**, *343*, 868-872.
- (249) Wang, R.; Zhou, X.; Wang, W.; Liu, Z. Twist-Based Cooling of Polyvinylidene Difluoride for Mechanothermochromic Fibers. *Chem. Eng. J.* **2021**, *417*, 128060.
- (250) Mun, T. J.; Kim, S. H.; Park, J. W.; Moon, J. H.; Jang, Y.; Huynh, C.; Baughman, R. H.; Kim, S. J. Wearable Energy Generating and Storing Textile Based on Carbon Nanotube Yarns. *Adv. Funct. Mater.* **2020**, *30*, 2000411.
- (251) Foroughi, J.; Spinks, G. M.; Wallace, G. G.; Oh, J.; Kozlov, M. E.; Fang, S.; Mirfakhrai, T.; Madden, J. D. W.; Shin, M. K.; et al. Torsional Carbon Nanotube Artificial Muscles. *Science* **2011**, *334*, 494-497.
- (252) Dixit, A.; Mali, H. S. Modeling Techniques for Predicting the Mechanical Properties of Woven-Fabric Textile Composites: A Review. *Mech. Compos. Mater.* **2013**, *49*, 1-20.
- (253) Hufenbach, W.; Böhm, R.; Thieme, M.; Winkler, A.; Mäder, E.; Rausch, J.; Schade, M. Polypropylene/Glass Fibre 3D-Textile Reinforced Composites for Automotive Applications. *Mater. Des.* **2011**, *32*, 1468-1476.

- (254) Nguyen, K. T. Q.; Navaratnam, S.; Mendis, P.; Zhang, K.; Barnett, J.; Wang, H. Fire Safety of Composites in Prefabricated Buildings: From Fibre Reinforced Polymer to Textile Reinforced Concrete. *Compos. B. Eng.* **2020**, *187*, 107815.
- (255) Peng, X. Q.; Cao, J.; Chen, J.; Xue, P.; Lussier, D. S.; Liu, L. Experimental and Numerical Analysis on Normalization of Picture Frame Tests for Composite Materials. *Compos. Sci. Technol.* **2004**, *64*, 11-21.
- (256) Gereke, T.; Döbrich, O.; Hübner, M.; Cherif, C. Experimental and Computational Composite Textile Reinforcement Forming: A review. *Compos. Part A Appl. Sci. Manuf.* **2013**, *46*, 1-10.
- (257) Peng, X.; Cao, J. A Dual Homogenization and Finite Element Approach for Material Characterization of Textile Composites. *Compos. B. Eng.* **2002**, *33*, 45-56.
- (258) Nilakantan, G.; Keefe, M.; Bogetti, T. A.; Gillespie, J. W. Multiscale Modeling of the Impact of Textile Fabrics Based on Hybrid Element Analysis. *Int. J. Impact Eng.* **2010**, *37*, 1056-1071.
- (259) Iarve, E. V.; Mollenhauer, D. H.; Zhou, E. G.; Breitzman, T.; Whitney, T. J. Independent Mesh Method-Based Prediction of Local and Volume Average Fields in Textile Composites. *Compos. Part A Appl. Sci. Manuf.* **2009**, *40*, 1880-1890.
- (260) Nilakantan, G.; Keefe, M.; Bogetti, T. A.; Adkinson, R.; Gillespie, J. W. On the Finite Element Analysis of Woven Fabric Impact using Multiscale Modeling Techniques. *Int. J. Solids Struct.* **2010**, *47*, 2300-2315.
- (261) Kumar, B.; Hu, J. 6 - Woven Fabric Structures and Properties. In *Engineering of High-Performance Textiles*, Miao, M., Xin, J. H. Eds.; Woodhead Publishing, 2018; pp 133-151.
- (262) Wang, L.; Zhao, B.; Wu, J.; Chen, C.; Zhou, K. Experimental and Numerical Investigation on Mechanical Behaviors of Woven Fabric Composites Under Off-Axial Loading. *Int. J. Mech. Sci.* **2018**, *141*, 157-167.
- (263) Maziz, A.; Concas, A.; Khaldi, A.; Stålhand, J.; Persson, N.-K.; Jager, E. W. H. Knitting and Weaving Artificial Muscles. *Sci. Adv.* **2017**, *3*, e1600327.
- (264) Wu, L.; Zhao, F.; Xie, J.; Wu, X.; Jiang, Q.; Lin, J.-H. The Deformation Behaviors and Mechanism of Weft Knitted Fabric Based on Micro-Scale Virtual Fiber Model. *Int. J. Mech. Sci.* **2020**, *187*, 105929.
- (265) Zhang, M.; Wang, C.; Liang, X.; Yin, Z.; Xia, K.; Wang, H.; Jian, M.; Zhang, Y. Weft-Knitted Fabric for a Highly Stretchable and Low-Voltage Wearable Heater. *Adv. Electron. Mater.* **2017**, *3*, 1700193.
- (266) Dong, K.; Wang, Y.-C.; Deng, J.; Dai, Y.; Zhang, S. L.; Zou, H.; Gu, B.; Sun, B.; Wang,

- Z. L. A Highly Stretchable and Washable All-Yarn-Based Self-Charging Knitting Power Textile Composed of Fiber Triboelectric Nanogenerators and Supercapacitors. *ACS Nano* **2017**, *11*, 9490-9499.
- (267) Shivers, J. J. C. Segmented Copolyetherester Elastomers. United States US3023192A, 1962.
- (268) Lv, F.; Yao, D.; Wang, Y.; Wang, C.; Zhu, P.; Hong, Y. Recycling of Waste Nylon 6/Spandex Blended Fabrics by Melt Processing. *Compos. B. Eng.* **2015**, *77*, 232-237.
- (269) Seyedin, S.; Razal, J. M.; Innis, P. C.; Jeiranikhameneh, A.; Beirne, S.; Wallace, G. G. Knitted Strain Sensor Textiles of Highly Conductive All-Polymeric Fibers. *ACS Appl. Mater. Interfaces* **2015**, *7*, 21150-21158.
- (270) Ding, Y.; Invernale, M. A.; Sotzing, G. A. Conductivity Trends of PEDOT-PSS Impregnated Fabric and the Effect of Conductivity on Electrochromic Textile. *ACS Appl. Mater. Interfaces* **2010**, *2*, 1588-1593.
- (271) Gupta, A. K.; Purwar, S. N. Crystallization of PP in PP/SEBS Blends and Its Correlation with Tensile Properties. *J. App. Polym. Sci.* **1984**, *29*, 1595-1609.
- (272) Zhang, Y.; Zhang, W.; Ye, G.; Tan, Q.; Zhao, Y.; Qiu, J.; Qi, S.; Du, X.; Chen, T.; et al. Core-Sheath Stretchable Conductive Fibers for Safe Underwater Wearable Electronics. *Adv. Mater. Technol.* **2020**, *5*, 1900880.
- (273) Lan, L.; Jiang, C.; Yao, Y.; Ping, J.; Ying, Y. A Stretchable and Conductive Fiber for Multifunctional Sensing and Energy Harvesting. *Nano Energy* **2021**, *84*, 105954.
- (274) Lee, S.; Shin, S.; Lee, S.; Seo, J.; Lee, J.; Son, S.; Cho, H. J.; Algadi, H.; Al-Sayari, S.; et al. Ag Nanowire Reinforced Highly Stretchable Conductive Fibers for Wearable Electronics. *Adv. Funct. Mater.* **2015**, *25*, 3114-3121.
- (275) Liu, K.; Wei, S.; Song, L.; Liu, H.; Wang, T. Conductive Hydrogels—A Novel Material: Recent Advances and Future Perspectives. *J. Agric. Food Chem.* **2020**, *68*, 7269-7280.
- (276) Duan, X.; Yu, J.; Zhu, Y.; Zheng, Z.; Liao, Q.; Xiao, Y.; Li, Y.; He, Z.; Zhao, Y.; et al. Large-Scale Spinning Approach to Engineering Knittable Hydrogel Fiber for Soft Robots. *ACS Nano* **2020**, *14*, 14929-14938.
- (277) Chen, G.; Wang, G.; Tan, X.; Hou, K.; Meng, Q.; Zhao, P.; Wang, S.; Zhang, J.; Zhou, Z.; et al. Integrated Dynamic Wet Spinning of Core-Sheath Hydrogel Fibers for Optical-to-Brain/Tissue Communications. *Natl. Sci. Rev.* **2020**, *8*, nwaa209.
- (278) Li, Y.; Wang, J.; Wang, Y.; Cui, W. Advanced Electrospun Hydrogel Fibers for Wound Healing. *Compos. B. Eng.* **2021**, *223*, 109101.
- (279) Guo, J.; Yu, Y.; Wang, H.; Zhang, H.; Zhang, X.; Zhao, Y. Conductive Polymer

Hydrogel Microfibers from Multiflow Microfluidics. *Small* **2019**, *15*, 1805162.

(280) Song, J.; Chen, S.; Sun, L.; Guo, Y.; Zhang, L.; Wang, S.; Xuan, H.; Guan, Q.; You, Z. Mechanically and Electronically Robust Transparent Organohydrogel Fibers. *Adv. Mater.* **2020**, *32*, 1906994.

(281) Zhao, X.; Chen, F.; Li, Y.; Lu, H.; Zhang, N.; Ma, M. Bioinspired Ultra-Stretchable and Anti-Freezing Conductive Hydrogel Fibers with Ordered and Reversible Polymer Chain Alignment. *Nat. Commun.* **2018**, *9*, 3579.

(282) Pietronero, L.; Strässler, S.; Zeller, H. R.; Rice, M. J. Electrical Conductivity of a Graphite Layer. *Phys. Rev. B* **1980**, *22*, 904-910.

(283) Chen, J.-H.; Jang, C.; Xiao, S.; Ishigami, M.; Fuhrer, M. S. Intrinsic and Extrinsic Performance Limits of Graphene Devices on SiO<sub>2</sub>. *Nat. Nanotechnol.* **2008**, *3*, 206-209.

(284) Wang, Y.; Chen, Y.; Lacey, S. D.; Xu, L.; Xie, H.; Li, T.; Danner, V. A.; Hu, L. Reduced Graphene Oxide Film with Record-High Conductivity and Mobility. *Mater. Today* **2018**, *21*, 186-192.

(285) Laird, E. A.; Kuemmeth, F.; Steele, G. A.; Grove-Rasmussen, K.; Nygård, J.; Flensberg, K.; Kouwenhoven, L. P. Quantum Transport in Carbon Nanotubes. *Rev. Mod. Phys.* **2015**, *87*, 703-764.

(286) Ebbesen, T. W.; Lezec, H. J.; Hiura, H.; Bennett, J. W.; Ghaemi, H. F.; Thio, T. Electrical Conductivity of Individual Carbon Nanotubes. *Nature* **1996**, *382*, 54-56.

(287) Wang, X.; Hu, H.; Shen, Y.; Zhou, X.; Zheng, Z. Stretchable Conductors with Ultrahigh Tensile Strain and Stable Metallic Conductance Enabled by Prestrained Polyelectrolyte Nanoplateforms. *Adv. Mater.* **2011**, *23*, 3090-3094.

(288) Liang, S.; Li, Y.; Zhou, T.; Yang, J.; Zhou, X.; Zhu, T.; Huang, J.; Zhu, J.; Zhu, D.; et al. Microfluidic Patterning of Metal Structures for Flexible Conductors by In Situ Polymer-Assisted Electroless Deposition. *Adv. Sci.* **2017**, *4*, 1600313.

(289) Li, E. Y.; Marzari, N. Improving the Electrical Conductivity of Carbon Nanotube Networks: A First-Principles Study. *ACS Nano* **2011**, *5*, 9726-9736.

(290) Krasheninnikov, A. V.; Nordlund, K.; Keinonen, J.; Banhart, F. Ion-Irradiation-Induced Welding of Carbon Nanotubes. *Phys. Rev. B* **2002**, *66*, 245403.

(291) Selzer, F.; Floresca, C.; Knepe, D.; Bormann, L.; Sachse, C.; Weiß, N.; Eychmüller, A.; Amassian, A.; Müller-Meskamp, L.; et al. Electrical Limit of Silver Nanowire Electrodes: Direct Measurement of the Nanowire Junction Resistance. *Appl. Phys. Lett.* **2016**, *108*, 163302.

(292) Garnett, E. C.; Cai, W.; Cha, J. J.; Mahmood, F.; Connor, S. T.; Greyson Christoforo, M.; Cui, Y.; McGehee, M. D.; Brongersma, M. L. Self-Limited Plasmonic Welding of Silver

Nanowire Junctions. *Nat. Mater.* **2012**, *11*, 241-249.

(293) Liu, Y.; Zhang, J.; Gao, H.; Wang, Y.; Liu, Q.; Huang, S.; Guo, C. F.; Ren, Z. Capillary-Force-Induced Cold Welding in Silver-Nanowire-Based Flexible Transparent Electrodes. *Nano Lett.* **2017**, *17*, 1090-1096.

(294) Bose, S.; Kuila, T.; Uddin, M. E.; Kim, N. H.; Lau, A. K. T.; Lee, J. H. In-Situ Synthesis and Characterization of Electrically Conductive Polypyrrole/Graphene Nanocomposites. *Polymer* **2010**, *51*, 5921-5928.

(295) Cao, M.; Xiong, D.-B.; Yang, L.; Li, S.; Xie, Y.; Guo, Q.; Li, Z.; Adams, H.; Gu, J.; et al. Ultrahigh Electrical Conductivity of Graphene Embedded in Metals. *Adv. Funct. Mater.* **2019**, *29*, 1806792.

(296) Liu, S.; Li, H.; He, C. Simultaneous Enhancement of Electrical Conductivity and Seebeck Coefficient in Organic Thermoelectric SWNT/PEDOT:PSS Nanocomposites. *Carbon* **2019**, *149*, 25-32.

(297) Nam, S.; Cho, H. W.; Lim, S.; Kim, D.; Kim, H.; Sung, B. J. Enhancement of Electrical and Thermomechanical Properties of Silver Nanowire Composites by the Introduction of Nonconductive Nanoparticles: Experiment and Simulation. *ACS Nano* **2013**, *7*, 851-856.

(298) Liang, Q.; Xia, X.; Sun, X.; Yu, D.; Huang, X.; Han, G.; Mugo, S. M.; Chen, W.; Zhang, Q. Highly Stretchable Hydrogels as Wearable and Implantable Sensors for Recording Physiological and Brain Neural Signals. *Adv. Sci.* **2022**, *9*, 2201059.

(299) Lee, C.; Wei, X.; Kysar, J. W.; Hone, J. Measurement of the Elastic Properties and Intrinsic Strength of Monolayer Graphene. *Science* **2008**, *321*, 385-388.

(300) Huang, Y.; Hu, H.; Huang, Y.; Zhu, M.; Meng, W.; Liu, C.; Pei, Z.; Hao, C.; Wang, Z.; et al. From Industrially Weavable and Knittable Highly Conductive Yarns to Large Wearable Energy Storage Textiles. *ACS Nano* **2015**, *9*, 4766-4775.

(301) Yun, Y. J.; Hong, W. G.; Kim, W.-J.; Jun, Y.; Kim, B. H. A Novel Method for Applying Reduced Graphene Oxide Directly to Electronic Textiles from Yarns to Fabrics. *Adv. Mater.* **2013**, *25*, 5701-5705.

(302) Park, K. H.; Seo, J. G.; Jung, S.; Yang, J. Y.; Song, S. H. Quaternary Artificial Nacre-Based Electronic Textiles with Enhanced Mechanical and Flame-Retardant Performance. *ACS Nano* **2022**, *16*, 5672-5681.

(303) Shang, J.; Yu, W.; Wang, L.; Xie, C.; Xu, H.; Wang, W.; Huang, Q.; Zheng, Z. Metallic Glass-Fiber Fabrics: A New Type of Flexible, Super-Lightweight, and 3D Current Collector for Lithium Batteries. *Adv. Mater.* **2023**, *35*, 2211748.

(304) Lu, X.; Shang, W.; Chen, G.; Wang, H.; Tan, P.; Deng, X.; Song, H.; Xu, Z.; Huang, J.;

et al. Environmentally Stable, Highly Conductive, and Mechanically Robust Metallized Textiles. *ACS Appl. Electron. Mater.* **2021**, *3*, 1477-1488.

(305) Xing, D.; Lu, L.; Teh, K. S.; Wan, Z.; Xie, Y.; Tang, Y. Highly Flexible and Ultra-Thin Ni-Plated Carbon-Fabric/Polycarbonate Film for Enhanced Electromagnetic Interference Shielding. *Carbon* **2018**, *132*, 32-41.

(306) Cai, L.; Song, A. Y.; Wu, P.; Hsu, P.-C.; Peng, Y.; Chen, J.; Liu, C.; Catrysse, P. B.; Liu, Y.; et al. Warming up Human Body by Nanoporous Metallized Polyethylene Textile. *Nat. Commun.* **2017**, *8*, 496.

(307) Yuen, C. W. M.; Jiang, S. Q.; Kan, C. W.; Tung, W. S. Influence of Surface Treatment on the Electroless Nickel Plating of Textile Fabric. *Appl. Surf. Sci.* **2007**, *253*, 5250-5257.

(308) Yip, J.; Jiang, S.; Wong, C. Characterization of Metallic Textiles Deposited by Magnetron Sputtering and Traditional Metallic Treatments. *Surf. Coat. Technol.* **2009**, *204*, 380-385.

(309) Bi, S.; Zhao, H.; Hou, L.; Lu, Y. Comparative Study of Electroless Co-Ni-P Plating on Tencel Fabric by Co<sup>0</sup>-Based and Ni<sup>0</sup>-Based Activation for Electromagnetic Interference Shielding. *Appl. Surf. Sci.* **2017**, *419*, 465-475.

(310) Chen, W.; Fan, W.; Wang, Q.; Yu, X.; Luo, Y.; Wang, W.; Lei, R.; Li, Y. A Nano-Micro Structure Engendered Abrasion Resistant, Superhydrophobic, Wearable Triboelectric Yarn for Self-Powered Sensing. *Nano Energy* **2022**, *103*, 107769.

(311) Zhang, D.; Yang, W.; Gong, W.; Ma, W.; Hou, C.; Li, Y.; Zhang, Q.; Wang, H. Abrasion Resistant/Waterproof Stretchable Triboelectric Yarns Based on Fermat Spirals. *Adv. Mater.* **2021**, *33*, 2100782.

(312) Tian, B.; Fang, Y.; Liang, J.; Zheng, K.; Guo, P.; Zhang, X.; Wu, Y.; Liu, Q.; Huang, Z.; et al. Fully Printed Stretchable and Multifunctional E-Textiles for Aesthetic Wearable Electronic Systems. *Small* **2022**, *18*, 2107298.

(313) Yang, W.; Gong, W.; Hou, C.; Su, Y.; Guo, Y.; Zhang, W.; Li, Y.; Zhang, Q.; Wang, H. All-Fiber Tribo-Ferroelectric Synergistic Electronics with High Thermal-Moisture Stability and Comfortability. *Nat. Commun.* **2019**, *10*, 5541.

(314) Cao, R.; Pu, X.; Du, X.; Yang, W.; Wang, J.; Guo, H.; Zhao, S.; Yuan, Z.; Zhang, C.; et al. Screen-Printed Washable Electronic Textiles as Self-Powered Touch/Gesture Tribo-Sensors for Intelligent Human-Machine Interaction. *ACS Nano* **2018**, *12*, 5190-5196.

(315) Xu, R.; She, M.; Liu, J.; Zhao, S.; Liu, H.; Qu, L.; Tian, M. Breathable Kirigami-Shaped Ionotronic e-Textile with Touch/Strain Sensing for Friendly Epidermal Electronics. *Adv. Fiber Mater.* **2022**, *4*, 1525-1534.



- (316) Huang, Q.; Zheng, Z. Pathway to Developing Permeable Electronics. *ACS Nano* **2022**, *16*, 15537–15544.
- (317) Hunter, L.; Fan, J. Waterproofing and Breathability of Fabrics and Garments. In *Engineering Apparel Fabrics and Garments*, 2009; pp 283-308.
- (318) Zhou, W.; Yao, S.; Wang, H.; Du, Q.; Ma, Y.; Zhu, Y. Gas-Permeable, Ultrathin, Stretchable Epidermal Electronics with Porous Electrodes. *ACS Nano* **2020**, *14*, 5798-5805.
- (319) Wang, Y.; Lee, S.; Wang, H.; Jiang, Z.; Jimbo, Y.; Wang, C.; Wang, B.; Kim, J. J.; Koizumi, M.; et al. Robust, Self-Adhesive, Reinforced Polymeric Nanofilms Enabling Gas-Permeable Dry Electrodes for Long-Term Application. *Proceed. Nat. Acad. Sci.* **2021**, *118*, e2111904118.
- (320) Chen, G.; Zhao, X.; Andalib, S.; Xu, J.; Zhou, Y.; Tat, T.; Lin, K.; Chen, J. Discovering Giant Magnetoelasticity in Soft Matter for Electronic Textiles. *Matter* **2021**, *4*, 3725-3740.
- (321) Li, Q.; Chen, G.; Cui, Y.; Ji, S.; Liu, Z.; Wan, C.; Liu, Y.; Lu, Y.; Wang, C.; et al. Highly Thermal-Wet Comfortable and Conformal Silk-Based Electrodes for On-Skin Sensors with Sweat Tolerance. *ACS Nano* **2021**, *15*, 9955-9966.
- (322) Chen, M.; Pang, D.; Chen, X.; Yan, H.; Yang, Y. Passive Daytime Radiative Cooling: Fundamentals, Material Designs, and Applications. *EcoMat* **2022**, *4*, e12153.
- (323) He, X.; Fan, C.; Xu, T.; Zhang, X. Biospired Janus Silk E-Textiles with Wet-Thermal Comfort for Highly Efficient Biofluid Monitoring. *Nano Lett.* **2021**, *21*, 8880-8887.
- (324) Zheng, S.; Li, W.; Ren, Y.; Liu, Z.; Zou, X.; Hu, Y.; Guo, J.; Sun, Z.; Yan, F. Moisture-Wicking, Breathable, and Intrinsically Antibacterial Electronic Skin Based on Dual-Gradient Poly(ionic liquid) Nanofiber Membranes. *Adv. Mater.* **2022**, *34*, 2106570.
- (325) Zhi, C.; Shi, S.; Zhang, S.; Si, Y.; Yang, J.; Meng, S.; Fei, B.; Hu, J. Bioinspired All-Fibrous Directional Moisture-Wicking Electronic Skins for Biomechanical Energy Harvesting and All-Range Health Sensing. *Nanomicro Lett.* **2023**, *15*, 60.
- (326) Kang, M. H.; Lee, G. J.; Lee, J. H.; Kim, M. S.; Yan, Z.; Jeong, J.-W.; Jang, K.-I.; Song, Y. M. Outdoor-Useable, Wireless/Battery-Free Patch-Type Tissue Oximeter with Radiative Cooling. *Adv. Sci.* **2021**, *8*, 2004885.
- (327) Chung, H. U.; Rwei, A. Y.; Hourlier-Fargette, A.; Xu, S.; Lee, K.; Dunne, E. C.; Xie, Z.; Liu, C.; Carlini, A.; et al. Skin-Interfaced Biosensors for Advanced Wireless Physiological Monitoring in Neonatal and Pediatric Intensive-Care Units. *Nat. Med.* **2020**, *26*, 418-429.
- (328) Xu, Y.; Sun, B.; Ling, Y.; Fei, Q.; Chen, Z.; Li, X.; Guo, P.; Jeon, N.; Goswami, S.; et al. Multiscale Porous Elastomer Substrates for Multifunctional on-Skin Electronics with Passive-Cooling Capabilities. *Proceed. Nat. Acad. Sci.* **2020**, *117*, 205-213.

- (329) Cai, L.; Song, A. Y.; Li, W.; Hsu, P.-C.; Lin, D.; Catrysse, P. B.; Liu, Y.; Peng, Y.; Chen, J.; et al. Spectrally Selective Nanocomposite Textile for Outdoor Personal Cooling. *Adv. Mater.* **2018**, *30*, 1802152.
- (330) Mandal, J.; Fu, Y.; Overvig, A. C.; Jia, M.; Sun, K.; Shi, N. N.; Zhou, H.; Xiao, X.; Yu, N.; et al. Hierarchically Porous Polymer Coatings for Highly Efficient Passive Daytime Radiative Cooling. *Science* **2018**, *362*, 315-319.
- (331) Zhang, J.-H.; Li, Z.; Xu, J.; Li, J.; Yan, K.; Cheng, W.; Xin, M.; Zhu, T.; Du, J.; et al. Versatile Self-Assembled Electrospun Micropyramid Arrays for High-Performance on-Skin Devices with Minimal Sensory Interference. *Nat. Commun.* **2022**, *13*, 5839.
- (332) Min, J.; Tu, J.; Xu, C.; Lukas, H.; Shin, S.; Yang, Y.; Solomon, S. A.; Mukasa, D.; Gao, W. Skin-Interfaced Wearable Sweat Sensors for Precision Medicine. *Chem. Rev.* **2023**, *123*, 5049-5138.
- (333) Xue, J.; Zou, Y.; Deng, Y.; Li, Z. Bioinspired Sensor System for Health Care and Human-Machine Interaction. *EcoMat* **2022**, *4*, e12209.
- (334) Heo, J. H.; Sung, M.; Trung, T. Q.; Lee, Y.; Jung, D. H.; Kim, H.; Kaushal, S.; Lee, N.-E.; Kim, J. W.; et al. Sensor Design Strategy for Environmental and Biological Monitoring. *EcoMat* **2023**, *5*, e12332.
- (335) Chen, F.; Huang, Q.; Zheng, Z. Permeable Conductors for Wearable and On-Skin Electronics. *Small Struct.* **2022**, *3*, 2100135.
- (336) Jiang, X.; Ren, Z.; Fu, Y.; Liu, Y.; Zou, R.; Ji, G.; Ning, H.; Li, Y.; Wen, J.; et al. Highly Compressible and Sensitive Pressure Sensor under Large Strain Based on 3D Porous Reduced Graphene Oxide Fiber Fabrics in Wide Compression Strains. *ACS Appl. Mater. Interfaces* **2019**, *11*, 37051-37059.
- (337) Jiang, J.; Sun, X.; Wen, Z. Perspectives of Triboelectric Sensors for Internet of Healthcare. *Adv. Sens. Res.* **2022**, *1*, 2200011.
- (338) Yi, J.; Dong, K.; Shen, S.; Jiang, Y.; Peng, X.; Ye, C.; Wang, Z. L. Fully Fabric-Based Triboelectric Nanogenerators as Self-Powered Human-Machine Interactive Keyboards. *Nanomicro Lett.* **2021**, *13*, 103.
- (339) Li, T.; Chen, L.; Yang, X.; Chen, X.; Zhang, Z.; Zhao, T.; Li, X.; Zhang, J. A Flexible Pressure Sensor Based on an Mxene-Textile Network Structure. *J. Mater. Chem. C* **2019**, *7*, 1022-1027.
- (340) Ding, Y.; Xu, T.; Onyilagha, O.; Fong, H.; Zhu, Z. Recent Advances in Flexible and Wearable Pressure Sensors Based on Piezoresistive 3D Monolithic Conductive Sponges. *ACS Appl. Mater. Interfaces* **2019**, *11*, 6685-6704.

- (341) Xu, T.; Ding, Y.; Wang, Z.; Zhao, Y.; Wu, W.; Fong, H.; Zhu, Z. Three-Dimensional and Ultralight Sponges with Tunable Conductivity Assembled from Electrospun Nanofibers for a Highly Sensitive Tactile Pressure Sensor. *J. Mater. Chem. C* **2017**, *5*, 10288-10294.
- (342) Zheng, Y.; Yin, R.; Zhao, Y.; Liu, H.; Zhang, D.; Shi, X.; Zhang, B.; Liu, C.; Shen, C. Conductive MXene/Cotton Fabric Based Pressure Sensor with Both High Sensitivity and Wide Sensing Range for Human Motion Detection and E-Skin. *Chem. Eng. J.* **2021**, *420*, 127720.
- (343) Chang, K.; Guo, M.; Pu, L.; Dong, J.; Li, L.; Ma, P.; Huang, Y.; Liu, T. Wearable Nanofibrous Tactile Sensors with Fast Response and Wireless Communication. *Chem. Eng. J.* **2023**, *451*, 138578.
- (344) Luo, Y.; Li, Y.; Sharma, P.; Shou, W.; Wu, K.; Foshey, M.; Li, B.; Palacios, T.; Torralba, A.; et al. Learning Human-Environment Interactions Using Conformal Tactile Textiles. *Nat. Electron.* **2021**, *4*, 193-201.
- (345) Song, Z.; Li, W.; Kong, H.; Chen, M.; Bao, Y.; Wang, N.; Wang, W.; Liu, Z.; Ma, Y.; et al. Merkel Receptor-Inspired Integratable and Biocompatible Pressure Sensor with Linear and Ultrahigh Sensitive Response for Versatile Applications. *Chem. Eng. J.* **2022**, *444*, 136481.
- (346) Liu, Z.; Zheng, Y.; Jin, L.; Chen, K.; Zhai, H.; Huang, Q.; Chen, Z.; Yi, Y.; Umar, M.; et al. Highly Breathable and Stretchable Strain Sensors with Insensitive Response to Pressure and Bending. *Adv. Funct. Mater.* **2021**, *31*, 2007622.
- (347) Hui, Z.; Wang, P.; Yang, J.; Zhou, J.; Huang, W.; Sun, G. Stiffness Engineering of  $\text{Ti}_3\text{C}_2\text{T}_x$  MXene-Based Skin-Inspired Pressure Sensor with Broad-Range Ultrasensitivity, Low Detection Limit, and Gas Permeability. *Adv. Mater. Inter.* **2022**, *9*, 2200261.
- (348) Kim, J.; Park, D.; Moon, S.; Park, C.; Thiyagarajan, K.; Choi, S.; Hwang, H.; Jeong, U. Omnidirectional Tactile Profiling Using a Deformable Pressure Sensor Array Based on Localized Piezoresistivity. *Adv. Mater. Technol.* **2021**, *7*, 2100688.
- (349) Hu, H.; Wang, D.; Tian, H.; Huang, Q.; Wang, C.; Chen, X.; Gao, Y.; Li, X.; Chen, X.; et al. Bioinspired Hierarchical Structures for Contact-Sensible Adhesives. *Adv. Funct. Mater.* **2022**, *32*, 2109076.
- (350) Chen, Y.; Wang, Z.; Xu, R.; Wang, W.; Yu, D. A Highly Sensitive and Wearable Pressure Sensor Based on Conductive Polyacrylonitrile Nanofibrous Membrane via Electroless Silver Plating. *Chem. Eng. J.* **2020**, *394*, 124960.
- (351) Sharma, S.; Chhetry, A.; Zhang, S.; Yoon, H.; Park, C.; Kim, H.; Sharifuzzaman, M.; Hui, X.; Park, J. Y. Hydrogen-Bond-Triggered Hybrid Nanofibrous Membrane-Based Wearable Pressure Sensor with Ultrahigh Sensitivity over a Broad Pressure Range. *ACS Nano*

**2021**, *15*, 4380-4393.

(352) Ding, H.; Wu, Z.; Wang, H.; Zhou, Z.; Wei, Y.; Tao, K.; Xie, X.; Wu, J. An Ultrastretchable, High-Performance, and Crosstalk-Free Proximity and Pressure Bimodal Sensor Based on Ionic Hydrogel Fibers for Human-Machine Interfaces. *Mater. Horiz.* **2022**, *9*, 1935-1946.

(353) Wu, R.; Ma, L.; Hou, C.; Meng, Z.; Guo, W.; Yu, W.; Yu, R.; Hu, F.; Liu, X. Y. Silk Composite Electronic Textile Sensor for High Space Precision 2D Combo Temperature-Pressure Sensing. *Small* **2019**, *15*, e1901558.

(354) Zhou, X.; Lee, P. S. Three Dimensional Printed Nanogenerators. *EcoMat* **2021**, *3*, e12098.

(355) Dong, K.; Peng, X.; Wang, Z. L. Fiber/Fabric-Based Piezoelectric and Triboelectric Nanogenerators for Flexible/Stretchable and Wearable Electronics and Artificial Intelligence. *Adv. Mater.* **2020**, *32*, 1902549.

(356) Hu, Y.; Zheng, Z. Progress in Textile-Based Triboelectric Nanogenerators for Smart Fabrics. *Nano Energy* **2019**, *56*, 16-24.

(357) Wang, Y.; Zhu, M.; Wei, X.; Yu, J.; Li, Z.; Ding, B. A Dual-Mode Electronic Skin Textile for Pressure and Temperature Sensing. *Chem. Eng. J.* **2021**, *425*, 130599.

(358) Huang, T.; Yang, S.; He, P.; Sun, J.; Zhang, S.; Li, D.; Meng, Y.; Zhou, J.; Tang, H.; et al. Phase-Separation-Induced PVDF/Graphene Coating on Fabrics toward Flexible Piezoelectric Sensors. *ACS Appl. Mater. Interfaces* **2018**, *10*, 30732-30740.

(359) Chao, S.; Ouyang, H.; Jiang, D.; Fan, Y.; Li, Z. Triboelectric Nanogenerator Based on Degradable Materials. *EcoMat* **2021**, *3*, e12072.

(360) Chen, C.; Chen, L.; Wu, Z.; Guo, H.; Yu, W.; Du, Z.; Wang, Z. L. 3D Double-Faced Interlock Fabric Triboelectric Nanogenerator for Bio-Motion Energy Harvesting and as Self-Powered Stretching and 3DTactile Sensors. *Mater. Today* **2020**, *32*, 84-93.

(361) Ning, C.; Dong, K.; Gao, W.; Sheng, F.; Cheng, R.; Jiang, Y.; Yi, J.; Ye, C.; Peng, X.; et al. Dual-Mode Thermal-Regulating and Self-Powered Pressure Sensing Hybrid Smart Fibers. *Chem. Eng. J.* **2021**, *420*, 129650.

(362) Peng, X.; Dong, K.; Ning, C.; Cheng, R.; Yi, J.; Zhang, Y.; Sheng, F.; Wu, Z.; Wang, Z. L. All-Nanofiber Self-Powered Skin-Interfaced Real-Time Respiratory Monitoring System for Obstructive Sleep Apnea-Hypopnea Syndrome Diagnosing. *Adv. Funct. Mater.* **2021**, *31*, 2103559.

(363) Ding, Y.; Zheng, Z. Stretchable Ionics: How to Measure the Electrical Resistance/Impedance. *Matter* **2022**, *5*, 2570-2573.

- (364) Liu, Z.; Zhu, T.; Wang, J.; Zheng, Z.; Li, Y.; Li, J.; Lai, Y. Functionalized Fiber-Based Strain Sensors: Pathway to Next-Generation Wearable Electronics. *Nanomicro Lett.* **2022**, *14*, 61.
- (365) Gong, S.; Zhang, X.; Nguyen, X. A.; Shi, Q.; Lin, F.; Chauhan, S.; Ge, Z.; Cheng, W. Hierarchically Resistive Skins as Specific And Multimetric on-Throat Wearable Biosensors. *Nat. Nanotechnol.* **2023**, *18*, 889–897.
- (366) Liu, Z.; Li, Z.; Yi, Y.; Li, L.; Zhai, H.; Lu, Z.; Jin, L.; Lu, J. R.; Xie, S. Q.; et al. Flexible Strain Sensing Percolation Networks towards Complicated Wearable Microclimate and Multi-Direction Mechanical Inputs. *Nano Energy* **2022**, *99*, 107444.
- (367) Gao, Y.; Guo, F.; Cao, P.; Liu, J.; Li, D.; Wu, J.; Wang, N.; Su, Y.; Zhao, Y. Winding-Locked Carbon Nanotubes/Polymer Nanofibers Helical Yarn for Ultrastretchable Conductor and Strain Sensor. *ACS Nano* **2020**, *14*, 3442-3450.
- (368) Yuan, L.; Zhang, M.; Zhao, T.; Li, T.; Zhang, H.; Chen, L.; Zhang, J. Flexible and Breathable Strain Sensor with High Performance Based on MXene/Nylon Fabric Network. *Sens. Actuator A Phys.* **2020**, *315*, 112192.
- (369) Li, H.; Chen, J.; Chang, X.; Xu, Y.; Zhao, G.; Zhu, Y.; Li, Y. A Highly Stretchable Strain Sensor with Both an Ultralow Detection Limit and an Ultrawide Sensing Range. *J. Mater. Chem. A* **2021**, *9*, 1795-1802.
- (370) Frutiger, A.; Muth, J. T.; Vogt, D. M.; Menguc, Y.; Campo, A.; Valentine, A. D.; Walsh, C. J.; Lewis, J. A. Capacitive Soft Strain Sensors via Multicore-Shell Fiber Printing. *Adv. Mater.* **2015**, *27*, 2440-2446.
- (371) Lee, J.; Ihle, S. J.; Pellegrino, G. S.; Kim, H.; Yea, J.; Jeon, C.-Y.; Son, H.-C.; Jin, C.; Eberli, D.; et al. Stretchable and Suturable Fibre Sensors for Wireless Monitoring of Connective Tissue Strain. *Nat. Electron.* **2021**, *4*, 291-301.
- (372) Liao, Q.; Mohr, M.; Zhang, X.; Zhang, Z.; Zhang, Y.; Fecht, H. J. Carbon Fiber-ZnO Nanowire Hybrid Structures for Flexible and Adaptable Strain Sensors. *Nanoscale* **2013**, *5*, 12350-12355.
- (373) Dong, K.; Hu, Y.; Yang, J.; Kim, S.-W.; Hu, W.; Wang, Z. L. Smart Textile Triboelectric Nanogenerators: Current Status and Perspectives. *MRS Bull.* **2021**, *46*, 512-521.
- (374) Ning, C.; Cheng, R.; Jiang, Y.; Sheng, F.; Yi, J.; Shen, S.; Zhang, Y.; Peng, X.; Dong, K.; et al. Helical Fiber Strain Sensors Based on Triboelectric Nanogenerators for Self-Powered Human Respiratory Monitoring. *ACS Nano* **2022**, *16*, 2811-2821.
- (375) Sheng, F.; Zhang, B.; Zhang, Y.; Li, Y.; Cheng, R.; Wei, C.; Ning, C.; Dong, K.; Wang, Z. L. Ultrastretchable Organogel/Silicone Fiber-Helical Sensors for Self-Powered Implantable

Ligament Strain Monitoring. *ACS Nano* **2022**, *16*, 10958-10967.

(376) Zhou, Z.; Chen, K.; Li, X.; Zhang, S.; Wu, Y.; Zhou, Y.; Meng, K.; Sun, C.; He, Q.; et al. Sign-to-Speech Translation Using Machine-Learning-Assisted Stretchable Sensor Arrays. *Nat. Electron.* **2020**, *3*, 571-578.

(377) Fang, Y.; Chen, G.; Bick, M.; Chen, J. Smart Textiles for Personalized Thermoregulation. *Chem. Soc. Rev.* **2021**, *50*, 9357-9374.

(378) Liu, H.; Sun, K.; Guo, X. L.; Liu, Z. L.; Wang, Y. H.; Yang, Y.; Yu, D.; Li, Y. T.; Ren, T. L. An Ultrahigh Linear Sensitive Temperature Sensor Based on PANI:Graphene and PDMS Hybrid with Negative Temperature Compensation. *ACS Nano* **2022**, *16*, 21527–21535.

(379) Persson, N.-K.; Martinez, J. G.; Zhong, Y.; Maziz, A.; Jager, E. W. H. Actuating Textiles: Next Generation of Smart Textiles. *Adv. Mater. Technol.* **2018**, *3*, 1700397.

(380) Kim, J.; Campbell, A. S.; de Ávila, B. E.-F.; Wang, J. Wearable Biosensors for Healthcare Monitoring. *Nat. Biotechnol.* **2019**, *37*, 389-406.

(381) Afroj, S.; Karim, N.; Wang, Z.; Tan, S.; He, P.; Holwill, M.; Ghazaryan, D.; Fernando, A.; Novoselov, K. S. Engineering Graphene Flakes for Wearable Textile Sensors via Highly Scalable and Ultrafast Yarn Dyeing Technique. *ACS Nano* **2019**, *13*, 3847-3857.

(382) Husain, M.; Kennon, R. Preliminary Investigations into the Development of Textile Based Temperature Sensor for Healthcare Applications. *Fibers* **2013**, *1*, 2-10.

(383) Wang, P.; Yu, W.; Li, G.; Meng, C.; Guo, S. Printable, Flexible, Breathable and Sweatproof Bifunctional Sensors Based on an All-Nanofiber Platform for Fully Decoupled Pressure-Temperature Sensing Application. *Chem. Eng. J.* **2023**, *452*, 139174.

(384) Jung, M.; Jeon, S.; Bae, J. Scalable and Facile Synthesis of Stretchable Thermoelectric Fabric for Wearable Self-Powered Temperature Sensors. *RSC Adv.* **2018**, *8*, 39992-39999.

(385) Li, M.; Chen, J.; Zhong, W.; Luo, M.; Wang, W.; Qing, X.; Lu, Y.; Liu, Q.; Liu, K.; et al. Large-Area, Wearable, Self-Powered Pressure-Temperature Sensor Based on 3D Thermoelectric Spacer Fabric. *ACS Sens.* **2020**, *5*, 2545-2554.

(386) Chen, H.; Liu, K.; Hu, L.; Al-Ghamdi, A. A.; Fang, X. New Concept Ultraviolet Photodetectors. *Mater. Today* **2015**, *18*, 493-502.

(387) Li, L.; Wang, D.; Zhang, D.; Ran, W.; Yan, Y.; Li, Z.; Wang, L.; Shen, G. Near-Infrared Light Triggered Self-Powered Mechano-Optical Communication System using Wearable Photodetector Textile. *Adv. Funct. Mater.* **2021**, *31*, 2104782.

(388) Peng, L.; Hu, L.; Fang, X. Low-Dimensional Nanostructure Ultraviolet Photodetectors. *Adv. Mater.* **2013**, *25*, 5321-5328.

(389) Ding, Y.; Zheng, F.; Zhu, Z. Low-Temperature Seeding and Hydrothermal Growth of

ZnO Nanorod on Poly(3,4-ethylene dioxythiophene):Poly(styrene sulfonic acid). *Mater. Lett.* **2016**, *183*, 197-201.

(390) Abid; Sehrawat, P.; Julien, C. M.; Islam, S. S. WS<sub>2</sub> Quantum Dots on e-Textile as a Wearable UV Photodetector: How Well Reduced Graphene Oxide Can Serve as a Carrier Transport Medium? *ACS Appl. Mater. Interfaces* **2020**, *12*, 39730-39744.

(391) Zhang, L.; Bai, S.; Su, C.; Zheng, Y.; Qin, Y.; Xu, C.; Wang, Z. L. A High-Reliability Kevlar Fiber-ZnO Nanowires Hybrid Nanogenerator and its Application on Self-Powered UV Detection. *Adv. Funct. Mater.* **2015**, *25*, 5794-5798.

(392) Zhu, Z.; Gu, Y.; Wang, S.; Zou, Y.; Zeng, H. Improving Wearable Photodetector Textiles via Precise Energy Level Alignment and Plasmonic Effect. *Adv. Electron. Mater.* **2017**, *3*, 1700281.

(393) Zhu, Z.; Ju, D.; Zou, Y.; Dong, Y.; Luo, L.; Zhang, T.; Shan, D.; Zeng, H. Boosting Fiber-Shaped Photodetectors via “Soft” Interfaces. *ACS Appl. Mater. Interfaces* **2017**, *9*, 12092-12099.

(394) Kim, H.-J.; Oh, H.; Kim, T.; Kim, D.; Park, M. Stretchable Photodetectors Based on Electrospun Polymer/Perovskite Composite Nanofibers. *ACS Appl. Nano Mater.* **2022**, *5*, 1308-1316.

(395) Xi, M.; Wang, X.; Zhao, Y.; Feng, Q.; Zheng, F.; Zhu, Z.; Fong, H. Mechanically Flexible Hybrid Mat Consisting of TiO<sub>2</sub> and SiO<sub>2</sub> Nanofibers Electrospun via Dual Spinnerets for Photo-detector. *Mater. Lett.* **2014**, *120*, 219-223.

(396) Zhu, Z.; Zhang, L.; Howe, J. Y.; Liao, Y.; Speidel, J. T.; Smith, S.; Fong, H. Aligned Electrospun ZnO Nanofibers for Simple and Sensitive Ultraviolet Nanosensors. *Chem. Commun.* **2009**, 2568-2570.

(397) He, J.; Xu, P.; Zhou, R.; Li, H.; Zu, H.; Zhang, J.; Qin, Y.; Liu, X.; Wang, F. Combustion Synthesized Electrospun InZnO Nanowires for Ultraviolet Photodetectors. *Adv. Electron. Mater.* **2022**, *8*, 2100997.

(398) Sharma, A.; Kumar, R.; Varadwaj, P. Smelling the Disease: Diagnostic Potential of Breath Analysis. *Mol. Diagn. Ther.* **2023**, *27*, 321-347.

(399) Khatib, M.; Haick, H. Sensors for Volatile Organic Compounds. *ACS Nano* **2022**, *16*, 7080-7115.

(400) Bag, A.; Lee, N.-E. Recent Advancements in Development of Wearable Gas Sensors. *Adv. Mater. Technol.* **2021**, *6*, 2000883.

(401) Alrammouz, R.; Podlecki, J.; Abboud, P.; Sorli, B.; Habchi, R. A Review on Flexible Gas Sensors: From Materials to Devices. *Sens. Actuator A Phys.* **2018**, *284*, 209-231.



- (402) Zhang, C.; Chen, P.; Hu, W. Organic Field-Effect Transistor-Based Gas Sensors. *Chem. Soc. Rev.* **2015**, *44*, 2087-2107.
- (403) Comini, E. Metal Oxides Nanowires Chemical/Gas Sensors: Recent Advances. *Mater. Today Adv.* **2020**, *7*, 100099.
- (404) Yuan, S.; Zhang, S. Recent Progress on Gas sensors Based on Graphene-Like 2D/2D Nanocomposites. *J. Semicond.* **2019**, *40*, 111608.
- (405) Majhi, S. M.; Ali, A.; Rai, P.; Greish, Y. E.; Alzamly, A.; Surya, S. G.; Qamhieh, N.; Mahmoud, S. T. Metal-Organic Frameworks for Advanced Transducer Based Gas Sensors: Review and Perspectives. *Nanoscale Adv.* **2022**, *4*, 697-732.
- (406) Tang, Y.; Xu, Y.; Yang, J.; Song, Y.; Yin, F.; Yuan, W. Stretchable and Wearable Conductometric VOC Sensors Based on Microstructured MXene/Polyurethane Core-Sheath fibers. *Sens. Actuator B Chem.* **2021**, *346*, 130500.
- (407) Indariti, N.; Kim, Y.-H.; Petchsang, N.; Jaisutti, R. Highly Sensitive Polyaniline-Coated Fiber Gas Sensors for Real-Time Monitoring of Ammonia Gas. *RSC Adv.* **2019**, *9*, 26773-26779.
- (408) Hatamie, A.; Angizi, S.; Kumar, S.; Pandey, C. M.; Simchi, A.; Willander, M.; Malhotra, B. D. Review-Textile Based Chemical and Physical Sensors for Healthcare Monitoring. *J. Electrochem. Soc.* **2020**, *167*, 037546.
- (409) Li, W.; Chen, R.; Qi, W.; Cai, L.; Sun, Y.; Sun, M.; Li, C.; Yang, X.; Xiang, L.; et al. Reduced Graphene Oxide/Mesoporous ZnO NSs Hybrid Fibers for Flexible, Stretchable, Twisted, and Wearable NO<sub>2</sub> E-Textile Gas Sensor. *ACS Sens.* **2019**, *4*, 2809-2818.
- (410) Wang, B.; Thukral, A.; Xie, Z.; Liu, L.; Zhang, X.; Huang, W.; Yu, X.; Yu, C.; Marks, T. J.; et al. Flexible and Stretchable Metal Oxide Nanofiber Networks for Multimodal and Monolithically Integrated Wearable Electronics. *Nat. Commun.* **2020**, *11*, 2405.
- (411) Kang, S.; Zhao, K.; Yu, D.-G.; Zheng, X.; Huang, C. Advances in Biosensing and Environmental Monitoring Based on Electrospun Nanofibers. *Adv. Fiber Mater.* **2022**, *4*, 404-435.
- (412) Chen, H.; Chen, J.; Liu, Y.; Li, B.; Li, H.; Zhang, X.; Lv, C.; Dong, H. Wearable Dual-Signal NH<sub>3</sub> Sensor with High Sensitivity for Non-invasive Diagnosis of Chronic Kidney Disease. *Langmuir* **2023**, *39*, 3420-3430.
- (413) Penner, R. M. A Nose for Hydrogen Gas: Fast, Sensitive H<sub>2</sub> Sensors Using Electrodeposited Nanomaterials. *Acc. Chem. Res.* **2017**, *50*, 1902-1910.
- (414) Nair, K. G.; Vishnuraj, R.; Pullithadathil, B. Highly Sensitive, Flexible H<sub>2</sub> Gas Sensors Based on Less Platinum Bimetallic Ni-Pt Nanocatalyst-Functionalized Carbon Nanofibers.

*ACS Appl. Electron. Mater.* **2021**, *3*, 1621-1633.

(415) Zhang, X.; Zhai, Z.; Wang, J.; Hao, X.; Sun, Y.; Yu, S.; Lin, X.; Qin, Y.; Li, C. Zr-MOF Combined with Nanofibers as an Efficient and Flexible Capacitive Sensor for Detecting SO<sub>2</sub>. *ChemNanoMat* **2021**, *7*, 1117-1124.

(416) Zhu, J.; Cho, M.; Li, Y.; He, T.; Ahn, J.; Park, J.; Ren, T.-L.; Lee, C.; Park, I. Machine Learning-Enabled Textile-Based Graphene Gas Sensing with Energy Harvesting-Assisted IoT Application. *Nano Energy* **2021**, *86*, 106035.

(417) Zhu, J.; Ren, Z.; Lee, C. Toward Healthcare Diagnoses by Machine-Learning-Enabled Volatile Organic Compound Identification. *ACS Nano* **2021**, *15*, 894-903.

(418) Qiao, L.; Benzigar, M. R.; Subramony, J. A.; Lovell, N. H.; Liu, G. Advances in Sweat Wearables: Sample Extraction, Real-Time Biosensing, and Flexible Platforms. *ACS Appl. Mater. Interfaces* **2020**, *12*, 34337-34361.

(419) Gao, W.; Emaminejad, S.; Nyein, H. Y. Y.; Challa, S.; Chen, K.; Peck, A.; Fahad, H. M.; Ota, H.; Shiraki, H.; et al. Fully Integrated Wearable Sensor Arrays for Multiplexed in situ Perspiration Analysis. *Nature* **2016**, *529*, 509-514.

(420) Legner, C.; Kalwa, U.; Patel, V.; Chesmore, A.; Pandey, S. Sweat Sensing in the Smart Wearables Era: Towards Integrative, Multifunctional and Body-Compliant Perspiration Analysis. *Sens. Actuator A Phys.* **2019**, *296*, 200-221.

(421) Shi, Y.; Zhang, Z.; Huang, Q.; Lin, Y.; Zheng, Z. Wearable Sweat Biosensors on Textiles for Health Monitoring. *J. Semicond.* **2023**, *44*, 021601.

(422) Zhang, S.; Tan, R.; Xu, X.; Iqbal, S.; Hu, J. Fibers/Textiles-Based Flexible Sweat Sensors: A Review. *ACS Mater. Lett.* **2023**, *5*, 1420-1440.

(423) Zhang, Y.; Liao, J.; Li, Z.; Hu, M.; Bian, C.; Lin, S. All Fabric and Flexible Wearable Sensors for Simultaneous Sweat Metabolite Detection and High-Efficiency Collection. *Talanta* **2023**, *260*, 124610.

(424) Cuartero, M.; Parrilla, M.; Crespo, G. A. Wearable Potentiometric Sensors for Medical Applications. *Sensors* **2019**, *19*, 363.

(425) Zdrachek, E.; Bakker, E. Potentiometric Sensing. *Anal. Chem.* **2019**, *91*, 2-26.

(426) Zdrachek, E.; Bakker, E. Potentiometric Sensing. *Anal. Chem.* **2021**, *93*, 72-102.

(427) Manjakkal, L.; Dang, W.; Yogeswaran, N.; Dahiya, R. Textile-Based Potentiometric Electrochemical pH Sensor for Wearable Applications. *Biosensors* **2019**, *9*, 14.

(428) Manjakkal, L.; Shakthivel, D.; Dahiya, R. Flexible Printed Reference Electrodes for Electrochemical Applications. *Adv. Mater. Technol.* **2018**, *3*, 1800252.

(429) Shao, Y.; Ying, Y.; Ping, J. Recent Advances in Solid-Contact Ion-Selective Electrodes:

Functional Materials, Transduction Mechanisms, and Development Trends. *Chem. Soc. Rev.* **2020**, *49*, 4405-4465.

(430) Ghoneim, M. T.; Nguyen, A.; Dereje, N.; Huang, J.; Moore, G. C.; Murzynowski, P. J.; Dagdeviren, C. Recent Progress in Electrochemical pH-Sensing Materials and Configurations for Biomedical Applications. *Chem. Rev.* **2019**, *119*, 5248-5297.

(431) Manjakkal, L.; Dervin, S.; Dahiya, R. Flexible Potentiometric pH Sensors for Wearable Systems. *RSC Adv.* **2020**, *10*, 8594-8617.

(432) Choi, M.-Y.; Lee, M.; Kim, J.-H.; Kim, S.; Choi, J.; So, J.-H.; Koo, H.-J. A Fully Textile-Based Skin pH Sensor. *J. Ind. Text.* **2022**, *51*, 441S-457S.

(433) Guinovart, T.; Valdés-Ramírez, G.; Windmiller, J. R.; Andrade, F. J.; Wang, J. Bandage-Based Wearable Potentiometric Sensor for Monitoring Wound pH. *Electroanalysis* **2014**, *26*, 1345-1353.

(434) Luo, D.; Sun, H.; Li, Q.; Niu, X.; He, Y.; Liu, H. Flexible Sweat Sensors: From Films to Textiles. *ACS Sens.* **2023**, *8*, 465-481.

(435) Alizadeh, A.; Burns, A.; Lenigk, R.; Gettings, R.; Ashe, J.; Porter, A.; McCaul, M.; Barrett, R.; Diamond, D.; et al. A Wearable Patch for Continuous Monitoring of Sweat Electrolytes During Exertion. *Lab Chip* **2018**, *18*, 2632-2641.

(436) Wang, S.; Bai, Y.; Yang, X.; Liu, L.; Li, L.; Lu, Q.; Li, T.; Zhang, T. Highly Stretchable Potentiometric Ion Sensor Based on Surface Strain Redistributed Fiber for Sweat Monitoring. *Talanta* **2020**, *214*, 120869.

(437) Xu, J.; Zhang, Z.; Gan, S.; Gao, H.; Kong, H.; Song, Z.; Ge, X.; Bao, Y.; Niu, L. Highly Stretchable Fiber-Based Potentiometric Ion Sensors for Multichannel Real-Time Analysis of Human Sweat. *ACS Sens.* **2020**, *5*, 2834-2842.

(438) Wang, L.; Wang, L.; Zhang, Y.; Pan, J.; Li, S.; Sun, X.; Zhang, B.; Peng, H. Weaving Sensing Fibers into Electrochemical Fabric for Real-Time Health Monitoring. *Adv. Funct. Mater.* **2018**, *28*, 1804456.

(439) Yang, Y.; Gao, W. Wearable and Flexible Electronics for Continuous Molecular Monitoring. *Chem. Soc. Rev.* **2019**, *48*, 1465-1491.

(440) Polat, E. O.; Cetin, M. M.; Tabak, A. F.; Bilget Güven, E.; Uysal, B. Ö.; Arsan, T.; Kabbani, A.; Hamed, H.; Gül, S. B. Transducer Technologies for Biosensors and Their Wearable Applications. *Biosensors* **2022**, *12*, 385.

(441) Terse-Thakoor, T.; Punjiya, M.; Matharu, Z.; Lyu, B.; Ahmad, M.; Giles, G. E.; Owyung, R.; Alaimo, F.; Shojaei Baghini, M.; et al. Thread-Based Multiplexed Sensor Patch for Real-Time Sweat Monitoring. *npj Flex. Electron.* **2020**, *4*, 18.

- (442) Khaliliazar, S.; Öberg Månsson, I.; Piper, A.; Ouyang, L.; Réu, P.; Hamed, M. M. Woven Electroanalytical Biosensor for Nucleic Acid Amplification Tests. *Adv. Healthc. Mater.* **2021**, *10*, 2100034.
- (443) Liu, X.; Lillehoj, P. B. Embroidered Electrochemical Sensors for Biomolecular Detection. *Lab Chip* **2016**, *16*, 2093-2098.
- (444) Zhao, Y.; Zhai, Q.; Dong, D.; An, T.; Gong, S.; Shi, Q.; Cheng, W. Highly Stretchable and Strain-Insensitive Fiber-Based Wearable Electrochemical Biosensor to Monitor Glucose in the Sweat. *Anal. Chem.* **2019**, *91*, 6569-6576.
- (445) Luo, X.; Yu, H.; Cui, Y. A Wearable Amperometric Biosensor on a Cotton Fabric for Lactate. *IEEE Electron Device Lett.* **2018**, *39*, 123-126.
- (446) Zheng, H.; Chen, H.; Pu, Z.; Li, D. A Breathable Flexible Glucose Biosensor with Embedded Electrodes for Long-Term and Accurate Wearable Monitoring. *Microchem. J.* **2022**, *181*, 107707.
- (447) He, W.; Wang, C.; Wang, H.; Jian, M.; Lu, W.; Liang, X.; Zhang, X.; Yang, F.; Zhang, Y. Integrated Textile Sensor Patch for Real-Time and Multiplex Sweat Analysis. *Sci. Adv.* **2019**, *5*, eaax0649.
- (448) Bertok, T.; Lorencova, L.; Chocholova, E.; Jane, E.; Vikartovska, A.; Kasak, P.; Tkac, J. Electrochemical Impedance Spectroscopy Based Biosensors: Mechanistic Principles, Analytical Examples and Challenges towards Commercialization for Assays of Protein Cancer Biomarkers. *ChemElectroChem* **2019**, *6*, 989-1003.
- (449) Migliorini, F. L.; Sanfelice, R. C.; Mercante, L. A.; Andre, R. S.; Mattoso, L. H. C.; Correa, D. S. Urea Impedimetric Biosensing Using Electrospun Nanofibers Modified with Zinc Oxide Nanoparticles. *Appl. Surf. Sci.* **2018**, *443*, 18-23.
- (450) Lee, M. Y.; Lee, H. R.; Park, C. H.; Han, S. G.; Oh, J. H. Organic Transistor-Based Chemical Sensors for Wearable Bioelectronics. *Acc. Chem. Res.* **2018**, *51*, 2829-2838.
- (451) Matsuhisa, N.; Kaltenbrunner, M.; Yokota, T.; Jinno, H.; Kuribara, K.; Sekitani, T.; Someya, T. Printable Elastic Conductors with a High Conductivity for Electronic Textile Applications. *Nat. Commun.* **2015**, *6*, 7461.
- (452) Ma, X.; Peng, R.; Mao, W.; Lin, Y.; Yu, H. Recent Advances in Ion-Sensitive Field-Effect Transistors for Biosensing Applications. *Electrochem. Sci. Adv.* **2022**, *3*, e2100163.
- (453) Song, J.; Liu, H.; Zhao, Z.; Lin, P.; Yan, F. Flexible Organic Transistors for Biosensing: Devices and Applications. *Adv. Mater.* **2023**, *n/a*, 2300034.
- (454) Sun, C.; Wang, X.; Auwalu, M. A.; Cheng, S.; Hu, W. Organic Thin Film Transistors-Based Biosensors. *EcoMat* **2021**, *3*, e12094.

- (455) Torricelli, F.; Adrahtas, D. Z.; Bao, Z.; Berggren, M.; Biscarini, F.; Bonfiglio, A.; Bortolotti, C. A.; Frisbie, C. D.; Macchia, E.; et al. Electrolyte-Gated Transistors for Enhanced Performance Bioelectronics. *Nat. Rev. Methods Primers* **2021**, *1*, 66.
- (456) Liao, C.; Zhang, M.; Niu, L.; Zheng, Z.; Yan, F. Highly Selective and Sensitive Glucose Sensors Based on Organic Electrochemical Transistors with Graphene-Modified Gate Electrodes. *Journal of Materials Chemistry B* **2013**, *1*, 3820-3829.
- (457) Gualandi, I.; Marzocchi, M.; Achilli, A.; Cavedale, D.; Bonfiglio, A.; Fraboni, B. Textile Organic Electrochemical Transistors as a Platform for Wearable Biosensors. *Sci. Rep.* **2016**, *6*, 33637.
- (458) Chen, H.; Geng, M.-Y.; Chen, Z.-M.; Chen, J.-Y.; Zhan, J.-L.; Yu, B.-Y.; Ju, L.; Ding, C.; Guan, Y.-S.; et al. Digitally Controlled Tunable Fabric Microwave Filter Based on Organic Electrochemical Transistors. *Adv. Mater. Technol.* **2023**, *8*, 2300428.
- (459) Qing, X.; Wang, Y.; Zhang, Y.; Ding, X.; Zhong, W.; Wang, D.; Wang, W.; Liu, Q.; Liu, K.; et al. Wearable Fiber-Based Organic Electrochemical Transistors as a Platform for Highly Sensitive Dopamine Monitoring. *ACS Appl. Mater. Interfaces* **2019**, *11*, 13105-13113.
- (460) Mei, X.; Yang, J.; Yu, X.; Peng, Z.; Zhang, G.; Li, Y. Wearable Molecularly Imprinted Electrochemical Sensor with Integrated Nanofiber-Based Microfluidic Chip for in situ Monitoring of Cortisol in Sweat. *Sens. Actuator B Chem.* **2023**, *381*, 133451.
- (461) Choi, J.; Ghaffari, R.; Baker, L. B.; Rogers, J. A. Skin-Interfaced Systems for Sweat Collection and Analytics. *Sci. Adv.* **2018**, *4*, eaar3921.
- (462) Son, J.; Bae, G. Y.; Lee, S.; Lee, G.; Kim, S. W.; Kim, D.; Chung, S.; Cho, K. Cactus-Spine-Inspired Sweat-Collecting Patch for Fast and Continuous Monitoring of Sweat. *Adv. Mater.* **2021**, *33*, 2102740.
- (463) Zhang, Y.; Tian, M.; Wang, L.; Zhao, H.; Qu, L. Flexible Janus Textile-Based Electroosmotic Pump for Large-Area Unidirectional Positive Water Transport. *Adv. Mater. Inter.* **2020**, *7*, 1902133.
- (464) Peng, Z.; Liu, R.; Xu, Z.; Chi, H.; Wang, Z.; Zhao, Y. Directional Sweat Transport Window Based on Hydrophobic/Hydrophilic Janus Fabric Enables Continuous Transfer and Monitoring of Sweat. *Appl. Mater. Today* **2022**, *29*, 101623.
- (465) He, X.; Yang, S.; Pei, Q.; Song, Y.; Liu, C.; Xu, T.; Zhang, X. Integrated Smart Janus Textile Bands for Self-Pumping Sweat Sampling and Analysis. *ACS Sens.* **2020**, *5*, 1548-1554.
- (466) Zhu, M.; Wang, H.; Li, S.; Liang, X.; Zhang, M.; Dai, X.; Zhang, Y. Flexible Electrodes for In Vivo and In Vitro Electrophysiological Signal Recording. *Adv. Healthc. Mater.* **2021**, *10*, 2100646.

- (467) Wu, H.; Yang, G.; Zhu, K.; Liu, S.; Guo, W.; Jiang, Z.; Li, Z. Materials, Devices, and Systems of On-Skin Electrodes for Electrophysiological Monitoring and Human–Machine Interfaces. *Adv. Sci.* **2021**, *8*, 2001938.
- (468) Pani, D.; Achilli, A.; Bonfiglio, A. Survey on Textile Electrode Technologies for Electrocardiographic (ECG) Monitoring, from Metal Wires to Polymers. *Adv. Mater. Technol.* **2018**, *3*, 1800008.
- (469) Cho, K. W.; Sunwoo, S.-H.; Hong, Y. J.; Koo, J. H.; Kim, J. H.; Baik, S.; Hyeon, T.; Kim, D.-H. Soft Bioelectronics Based on Nanomaterials. *Chem. Rev.* **2022**, *122*, 5068-5143.
- (470) Oh, J.; Jang, S. G.; Moon, S.; Kim, J.; Park, H. K.; Kim, H. S.; Park, S.-M.; Jeong, U. Air-Permeable Waterproofing Electrocardiogram Patch to Monitor Full-Day Activities for Multiple Days. *Adv. Healthc. Mater.* **2022**, *11*, 2102703.
- (471) Yang, X.; Wang, S.; Liu, M.; Li, L.; Zhao, Y.; Wang, Y.; Bai, Y.; Lu, Q.; Xiong, Z.; et al. All-Nanofiber-Based Janus Epidermal Electrode with Directional Sweat Permeability for Artifact-Free Biopotential Monitoring. *Small* **2022**, *18*, 2106477.
- (472) Eskandarian, L.; Pajootan, E.; Toossi, A.; Naguib, H. E. Dry Fiber-Based Electrodes for Electrophysiology Applications. *Adv. Fiber Mater.* **2023**, *5*, 819-846.
- (473) del Agua, I.; Mantione, D.; Ismailov, U.; Sanchez-Sanchez, A.; Aramburu, N.; Malliaras, G. G.; Mecerreyes, D.; Ismailova, E. DVS-Crosslinked PEDOT:PSS Free-Standing and Textile Electrodes toward Wearable Health Monitoring. *Adv. Mater. Technol.* **2018**, *3*, 1700322.
- (474) Chiu, C.-W.; Huang, C.-Y.; Li, J.-W.; Li, C.-L. Flexible Hybrid Electronics Nanofiber Electrodes with Excellent Stretchability and Highly Stable Electrical Conductivity for Smart Clothing. *ACS Appl. Mater. Interfaces* **2022**, *14*, 42441-42453.
- (475) Shi, S.; Wang, Y.; Meng, Q.; Lan, Z.; Liu, C.; Zhou, Z.; Sun, Q.; Shen, X. Conductive Cellulose-Derived Carbon Nanofibrous Membranes with Superior Softness for High-Resolution Pressure Sensing and Electrophysiology Monitoring. *ACS Appl. Mater. Interfaces* **2023**, *15*, 1903-1913.
- (476) Liu, L.; Xu, W.; Ding, Y.; Agarwal, S.; Greiner, A.; Duan, G. A Review of Smart Electrospun Fibers toward Textiles. *Compos. Commun.* **2020**, *22*, 100506.
- (477) Yao, S.; Yang, J.; Poblete, F. R.; Hu, X.; Zhu, Y. Multifunctional Electronic Textiles Using Silver Nanowire Composites. *ACS Appl. Mater. Interfaces* **2019**, *11*, 31028-31037.
- (478) La, T.-G.; Qiu, S.; Scott, D. K.; Bakhtiari, R.; Kuziek, J. W. P.; Mathewson, K. E.; Rieger, J.; Chung, H.-J. Two-Layered and Stretchable e-Textile Patches for Wearable Healthcare Electronics. *Adv. Healthc. Mater.* **2018**, *7*, 1801033.
- (479) Eskandarian, L.; Toossi, A.; Nassif, F.; Golmohammadi Rostami, S.; Ni, S.; Mahnam,

- A.; Alizadeh Meghraz, M.; Takarada, W.; Kikutani, T.; et al. 3D-Knit Dry Electrodes using Conductive Elastomeric Fibers for Long-Term Continuous Electrophysiological Monitoring. *Adv. Mater. Technol.* **2022**, *7*, 2101572.
- (480) Rahman, S. M. M.; Mattila, H.; Janka, M.; Virkki, J. Impedance Evaluation of Textile Electrodes for EEG Measurements. *Text. Res. J.* **2022**, *93*, 1878-1888.
- (481) Hossain, M. M.; Li, B. M.; Sennik, B.; Jur, J. S.; Bradford, P. D. Adhesive Free, Conformable and Washable Carbon Nanotube Fabric Electrodes for Biosensing. *npj Flex. Electron.* **2022**, *6*, 97.
- (482) Kisannagar, R. R.; Singh, M.; Gupta, D. Multifunctional, Wash Durable and Re-usable Conductive Textiles for Wearable Electro/Physiological Monitoring. *Macromol. Mater. Eng.* **2021**, *306*, 2000804.
- (483) Li, T.; Liang, B.; Ye, Z.; Zhang, L.; Xu, S.; Tu, T.; Zhang, Y.; Cai, Y.; Zhang, B.; et al. An Integrated and Conductive Hydrogel-Paper Patch for Simultaneous Sensing of Chemical–Electrophysiological Signals. *Biosens. Bioelectron.* **2022**, *198*, 113855.
- (484) Pan, S.; Zhang, F.; Cai, P.; Wang, M.; He, K.; Luo, Y.; Li, Z.; Chen, G.; Ji, S.; et al. Mechanically Interlocked Hydrogel–Elastomer Hybrids for On-Skin Electronics. *Adv. Funct. Mater.* **2020**, *30*, 1909540.
- (485) Chen, F.; Zhuang, Q.; Ding, Y.; Zhang, C.; Song, X.; Chen, Z.; Zhang, Y.; Mei, Q.; Zhao, X.; et al. Wet-Adaptive Electronic Skin. *Adv. Mater.* **2023**, *n/a*, 2305630.
- (486) Leng, X.; Mei, G.; Zhang, G.; Liu, Z.; Zhou, X. Tethering of Twisted-Fiber Artificial Muscles. *Chem. Soc. Rev.* **2023**, *52*, 2377-2390.
- (487) Huang, H.; Trentle, M.; Liu, Z.; Xiang, K.; Higgins, W.; Wang, Y.; Xue, B.; Yang, S. Polymer Complex Fiber: Property, Functionality, and Applications. *ACS Appl. Mater. Interfaces* **2023**, *15*, 7639-7662.
- (488) Cole, T.; Tang, S.-Y. Liquid Metals as Soft Electromechanical Actuators. *Mater. Adv.* **2022**, *3*, 173-185.
- (489) Apsite, I.; Salehi, S.; Ionov, L. Materials for Smart Soft Actuator Systems. *Chem. Rev.* **2022**, *122*, 1349-1415.
- (490) Arora, S.; Ghosh, T.; Muth, J. Dielectric Elastomer Based Prototype Fiber Actuators. *Sens. Actuator A Phys.* **2007**, *136*, 321-328.
- (491) He, J.; Chen, Z.; Xiao, Y.; Cao, X.; Mao, J.; Zhao, J.; Gao, X.; Li, T.; Luo, Y. Intrinsically Anisotropic Dielectric Elastomer Fiber Actuators. *ACS Mater. Lett.* **2022**, *4*, 472-479.
- (492) Chortos, A.; Mao, J.; Mueller, J.; Hajiesmaili, E.; Lewis, J. A.; Clarke, D. R. Printing Reconfigurable Bundles of Dielectric Elastomer Fibers. *Adv. Funct. Mater.* **2021**, *31*, 2010643.

- (493) Cakmak, E.; Fang, X.; Yildiz, O.; Bradford, P. D.; Ghosh, T. K. Carbon Nanotube Sheet Electrodes for Anisotropic Actuation of Dielectric Elastomers. *Carbon* **2015**, *89*, 113-120.
- (494) Mirfakhrai, T.; Oh, J.; Kozlov, M.; Fok, E. C. W.; Zhang, M.; Fang, S.; Baughman, R. H.; Madden, J. D. W. Electrochemical Actuation of Carbon Nanotube Yarns. *Smart Mater. Struct.* **2007**, *16*, S243-S249.
- (495) Lu, W.; Smela, E.; Adams, P.; Zuccarello, G.; Mattes, B. R. Development of Solid-in-Hollow Electrochemical Linear Actuators Using Highly Conductive Polyaniline. *Chem. Mater.* **2004**, *16*, 1615-1621.
- (496) Liu, J.; Wang, Z.; Xie, X.; Cheng, H.; Zhao, Y.; Qu, L. A Rationally-Designed Synergetic Polypyrrole/Graphene Bilayer Actuator. *J Mater Chem* **2012**, *22*, 4015.
- (497) Lima, M. D.; Li, N.; Jung de Andrade, M.; Fang, S.; Oh, J.; Spinks, G. M.; Kozlov, M. E.; Haines, C. S.; Suh, D.; et al. Electrically, Chemically, and Photonically Powered Torsional and Tensile Actuation of Hybrid Carbon Nanotube Yarn Muscles. *Science* **2012**, *338*, 928-932.
- (498) Yuan, J.; Neri, W.; Zakri, C.; Merzeau, P.; Kratz, K.; Lendlein, A.; Poulin, P. Shape Memory Nanocomposite Fibers for Untethered High-Energy Microengines. *Science* **2019**, *365*, 155-158.
- (499) Mirvakili, S. M.; Hunter, I. W. Fast Torsional Artificial Muscles from NiTi Twisted Yarns. *ACS Appl. Mater. Interfaces* **2017**, *9*, 16321-16326.
- (500) Cheng, H.; Liu, J.; Zhao, Y.; Hu, C.; Zhang, Z.; Chen, N.; Jiang, L.; Qu, L. Graphene Fibers with Predetermined Deformation as Moisture-Triggered Actuators and Robots. *Angew. Chem., Int. Ed.* **2013**, *52*, 10482-10486.
- (501) Cheng, H.; Hu, Y.; Zhao, F.; Dong, Z.; Wang, Y.; Chen, N.; Zhang, Z.; Qu, L. Moisture-Activated Torsional Graphene-Fiber Motor. *Adv. Mater.* **2014**, *26*, 2909-2913.
- (502) Fang, B.; Xiao, Y.; Xu, Z.; Chang, D.; Wang, B.; Gao, W.; Gao, C. Handedness-Controlled and Solvent-Driven Actuators with Twisted Fibers. *Mater. Horiz.* **2019**, *6*, 1207-1214.
- (503) He, S.; Chen, P.; Qiu, L.; Wang, B.; Sun, X.; Xu, Y.; Peng, H. A Mechanically Actuating Carbon-Nanotube Fiber in Response to Water and Moisture. *Angew. Chem., Int. Ed.* **2015**, *54*, 14880-14884.
- (504) Chen, P.; Xu, Y.; He, S.; Sun, X.; Pan, S.; Deng, J.; Chen, D.; Peng, H. Hierarchically Arranged Helical Fibre Actuators Driven by Solvents and Vapours. *Nat. Nanotechnol.* **2015**, *10*, 1077-1083.
- (505) Gschwend, P. M.; Hintze, J. M.; Herrmann, I. K.; Pratsinis, S. E.; Starsich, F. H. L. Precision in Thermal Therapy: Clinical Requirements and Solutions from Nanotechnology.



*Adv. Ther.* **2021**, *4*, 2000193.

(506) Choi, S.; Park, J.; Hyun, W.; Kim, J.; Kim, J.; Lee, Y. B.; Song, C.; Hwang, H. J.; Kim, J. H.; et al. Stretchable Heater Using Ligand-Exchanged Silver Nanowire Nanocomposite for Wearable Articular Thermotherapy. *ACS Nano* **2015**, *9*, 6626-6633.

(507) Li, L.; Zhang, X.; Zhou, J.; Zhang, L.; Xue, J.; Tao, W. Non-Invasive Thermal Therapy for Tissue Engineering and Regenerative Medicine. *Small* **2022**, *18*, 2107705.

(508) Liu, Q.; Tian, B.; Liang, J.; Wu, W. Recent Advances in Printed Flexible Heaters for Portable and Wearable Thermal Management. *Mater. Horiz.* **2021**, *8*, 1634-1656.

(509) Faruk, M. O.; Ahmed, A.; Jalil, M. A.; Islam, M. T.; Shamim, A. M.; Adak, B.; Hossain, M. M.; Mukhopadhyay, S. Functional Textiles and Composite Based Wearable Thermal Devices for Joule Heating: Progress and Perspectives. *Appl. Mater. Today* **2021**, *23*, 101025.

(510) Maurya, S. K.; Das, A.; Kumar, N.; Kumar, B. Electrothermal and Mechanical Characterization of Stainless Steel and Silver-Coated Cabled Yarns for Heating Application. *ACS Appl. Eng. Mater.* **2023**, *1*, 983-993.

(511) Ma, Z.; Xiang, X.; Shao, L.; Zhang, Y.; Gu, J. Multifunctional Wearable Silver Nanowire Decorated Leather Nanocomposites for Joule Heating, Electromagnetic Interference Shielding and Piezoresistive Sensing. *Angew. Chem., Int. Ed.* **2022**, *61*, e202200705.

(512) Lee, S.; Kim, S.-W.; Ghidelli, M.; An, H. S.; Jang, J.; Bassi, A. L.; Lee, S.-Y.; Park, J.-U. Integration of Transparent Supercapacitors and Electrodes Using Nanostructured Metallic Glass Films for Wirelessly Rechargeable, Skin Heat Patches. *Nano Lett.* **2020**, *20*, 4872-4881.

(513) Wang, Q.; Sheng, H.; Lv, Y.; Liang, J.; Liu, Y.; Li, N.; Xie, E.; Su, Q.; Ershad, F.; et al. A Skin-Mountable Hyperthermia Patch Based on Metal Nanofiber Network with High Transparency and Low Resistivity toward Subcutaneous Tumor Treatment. *Adv. Funct. Mater.* **2022**, *32*, 2111228.

(514) Yang, J.; Nithyanandam, P.; Kanetkar, S.; Kwon, K. Y.; Ma, J.; Im, S.; Oh, J.-H.; Shamsi, M.; Wilkins, M.; et al. Liquid Metal Coated Textiles with Autonomous Electrical Healing and Antibacterial Properties. *Adv. Mater. Technol.* **2023**, *8*, 2202183.

(515) He, Y.; Wan, C.; Yang, X.; Wang, Y.; Fang, J.; Liu, Y. Thermally Drawn Super-Elastic Multifunctional Fiber Sensor for Human Movement Monitoring and Joule Heating. *Adv. Mater. Technol.* **2023**, *8*, 2202079.

(516) Wang, Q.-W.; Zhang, H.-B.; Liu, J.; Zhao, S.; Xie, X.; Liu, L.; Yang, R.; Koratkar, N.; Yu, Z.-Z. Multifunctional and Water-Resistant MXene-Decorated Polyester Textiles with Outstanding Electromagnetic Interference Shielding and Joule Heating Performances. *Adv. Funct. Mater.* **2019**, *29*, 1806819.

- (517) Lian, Y.; Yu, H.; Wang, M.; Yang, X.; Li, Z.; Yang, F.; Wang, Y.; Tai, H.; Liao, Y.; et al. A Multifunctional Wearable E-textile via Integrated Nanowire-Coated Fabrics. *J. Mater. Chem. C* **2020**, *8*, 8399-8409.
- (518) Hsu, P.-C.; Liu, X.; Liu, C.; Xie, X.; Lee, H. R.; Welch, A. J.; Zhao, T.; Cui, Y. Personal Thermal Management by Metallic Nanowire-Coated Textile. *Nano Lett.* **2015**, *15*, 365-371.
- (519) Jalil, M. A.; Ahmed, A.; Hossain, M. M.; Adak, B.; Islam, M. T.; Moniruzzaman, M.; Parvez, M. S.; Shkir, M.; Mukhopadhyay, S. Synthesis of PEDOT:PSS Solution-Processed Electronic Textiles for Enhanced Joule Heating. *ACS Omega* **2022**, *7*, 12716-12723.
- (520) Li, Y.; Zhang, Z.; Li, X.; Zhang, J.; Lou, H.; Shi, X.; Cheng, X.; Peng, H. A Smart, Stretchable Resistive Heater Textile. *J. Mater. Chem. C* **2017**, *5*, 41-46.
- (521) Qiu, K.; Elhassan, A.; Tian, T.; Yin, X.; Yu, J.; Li, Z.; Ding, B. Highly Flexible, Efficient, and Sandwich-Structured Infrared Radiation Heating Fabric. *ACS Appl. Mater. Interfaces* **2020**, *12*, 11016-11025.
- (522) Wang, C.; Zhang, M.; Xia, K.; Gong, X.; Wang, H.; Yin, Z.; Guan, B.; Zhang, Y. Intrinsically Stretchable and Conductive Textile by a Scalable Process for Elastic Wearable Electronics. *ACS Appl. Mater. Interfaces* **2017**, *9*, 13331-13338.
- (523) Wang, C.; Xia, K.; Zhang, Y.; Kaplan, D. L. Silk-Based Advanced Materials for Soft Electronics. *Acc. Chem. Res.* **2019**, *52*, 2916-2927.
- (524) Sluka, K. A.; Walsh, D. Transcutaneous Electrical Nerve Stimulation: Basic Science Mechanisms and Clinical Effectiveness. *J. Pain* **2003**, *4*, 109-121.
- (525) Liu, M.; Ward, T.; Young, D.; Matos, H.; Wei, Y.; Adams, J.; Yang, K. Electronic Textiles Based Wearable Electrotherapy for Pain Relief. *Sens. Actuator A Phys.* **2020**, *303*, 111701.
- (526) Ciancibello, J.; King, K.; Meghraz, M. A.; Padmanaban, S.; Levy, T.; Ramdeo, R.; Straka, M.; Bouton, C. Closed-Loop Neuromuscular Electrical Stimulation using Feedforward-Feedback Control and Textile Electrodes to Regulate Grasp Force in Quadriplegia. *Bioelectron. Med.* **2019**, *5*, 19.
- (527) Yang, K.; Freeman, C.; Torah, R.; Beeby, S.; Tudor, J. Screen Printed Fabric Electrode Array for Wearable Functional Electrical Stimulation. *Sens. Actuator A Phys.* **2014**, *213*, 108-115.
- (528) Papaioordanidou, M.; Takamatsu, S.; Rezaei-Mazinani, S.; Lonjaret, T.; Martin, A.; Ismailova, E. Cutaneous Recording and Stimulation of Muscles Using Organic Electronic Textiles. *Adv. Healthc. Mater.* **2016**, *5*, 2001-2006.
- (529) Moineau, B.; Marquez-Chin, C.; Alizadeh-Meghraz, M.; Popovic, M. R. Garments for

Functional Electrical Stimulation: Design and Proofs of Concept. *J. Rehabil. Assist. Technol. Eng.* **2019**, *6*, 2055668319854340.

(530) Skrzetuska, E.; Michalak, D.; Krucińska, I. Design and Analysis of Electrodes for Electrostimulation (TENS) Using the Technique of Film Printing and Embroidery in Textiles. *Sensors* **2021**, *21*, 4789.

(531) Li, L.; Wai Man, A.; Yi, L.; Kam Man, W.; Sai Ho, W.; Kwok Shing, W. Design of Intelligent Garment with Transcutaneous Electrical Nerve Stimulation Function Based on the Intarsia Knitting Technique. *Text. Res. J.* **2009**, *80*, 279-286.

(532) He, T.; Wang, H.; Wang, J.; Tian, X.; Wen, F.; Shi, Q.; Ho, J. S.; Lee, C. Self-Sustainable Wearable Textile Nano-Energy Nano-System (NENS) for Next-Generation Healthcare Applications. *Adv. Sci.* **2019**, *6*, 1901437.

(533) Wang, Y.; Thakur, R.; Fan, Q.; Michniak, B. Transdermal Iontophoresis: Combination Strategies to Improve Transdermal Iontophoretic Drug Delivery. *Eur. J. Pharm. Biopharm.* **2005**, *60*, 179-191.

(534) De la Paz, E.; Saha, T.; Del Caño, R.; Seker, S.; Kshirsagar, N.; Wang, J. Non-Invasive Monitoring of Interstitial Fluid Lactate through an Epidermal Iontophoretic Device. *Talanta* **2023**, *254*, 124122.

(535) Yao, Y.; Chen, J.; Guo, Y.; Lv, T.; Chen, Z.; Li, N.; Cao, S.; Chen, B.; Chen, T. Integration of Interstitial Fluid Extraction and Glucose Detection in One Device for Wearable Non-invasive Blood Glucose Sensors. *Biosens. Bioelectron.* **2021**, *179*, 113078.

(536) Bolat, G.; De la Paz, E.; Azeredo, N. F.; Kartolo, M.; Kim, J.; de Loyola e Silva, A. N.; Rueda, R.; Brown, C.; Angnes, L.; et al. Wearable Soft Electrochemical Microfluidic Device Integrated with Iontophoresis for Sweat Biosensing. *Anal. Bioanal. Chem.* **2022**, *414*, 5411-5421.

(537) Tai, L.-C.; Gao, W.; Chao, M.; Bariya, M.; Ngo, Q. P.; Shahpar, Z.; Nyein, H. Y. Y.; Park, H.; Sun, J.; et al. Methylxanthine Drug Monitoring with Wearable Sweat Sensors. *Adv. Mater.* **2018**, *30*, 1707442.

(538) Zheng, H.; Pu, Z.; Wu, H.; Li, C.; Zhang, X.; Li, D. Reverse Iontophoresis with the Development of Flexible Electronics: A Review. *Biosens. Bioelectron.* **2023**, *223*, 115036.

(539) Dhal, S.; Pal, K.; Giri, S. Transdermal Delivery of Gold Nanoparticles by a Soybean Oil-Based Oleogel under Iontophoresis. *ACS Appl. Bio Mater.* **2020**, *3*, 7029-7039.

(540) An, Y.-H.; Lee, J.; Son, D. U.; Kang, D. H.; Park, M. J.; Cho, K. W.; Kim, S.; Kim, S.-H.; Ko, J.; et al. Facilitated Transdermal Drug Delivery Using Nanocarriers-Embedded Electroconductive Hydrogel Coupled with Reverse Electrodialysis-Driven Iontophoresis. *ACS*

*Nano* **2020**, *14*, 4523-4535.

(541) Kusama, S.; Sato, K.; Matsui, Y.; Kimura, N.; Abe, H.; Yoshida, S.; Nishizawa, M. Transdermal Electroosmotic Flow Generated by a Porous Microneedle Array Patch. *Nat. Commun.* **2021**, *12*, 658.

(542) Im, J. S.; Bai, B. C.; Lee, Y.-S. The Effect of Carbon Nanotubes on Drug Delivery in an Electro-Sensitive Transdermal Drug Delivery System. *Biomaterials* **2010**, *31*, 1414-1419.

(543) Wu, C.; Jiang, P.; Li, W.; Guo, H.; Wang, J.; Chen, J.; Prausnitz, M. R.; Wang, Z. L. Self-Powered Iontophoretic Transdermal Drug Delivery System Driven and Regulated by Biomechanical Motions. *Adv. Funct. Mater.* **2020**, *30*, 1907378.

(544) Zhou, Y.; Jia, X.; Pang, D.; Jiang, S.; Zhu, M.; Lu, G.; Tian, Y.; Wang, C.; Chao, D.; et al. An Integrated Mg Battery-Powered Iontophoresis Patch for Efficient and Controllable Transdermal Drug Delivery. *Nat. Commun.* **2023**, *14*, 297.

(545) Yang, J.; Li, Y.; Ye, R.; Zheng, Y.; Li, X.; Chen, Y.; Xie, X.; Jiang, L. Smartphone-Powered Iontophoresis-Microneedle Array Patch for Controlled Transdermal Delivery. *Microsyst. Nanoeng.* **2020**, *6*, 112.

(546) Chang, J.; Huang, Q.; Zheng, Z. A Figure of Merit for Flexible Batteries. *Joule* **2020**, *4*, 1346-1349.

(547) Yousif, B.; Abo-Elsoud, M. E. A.; Marouf, H. Triangle Grating for Enhancement the Efficiency in Thin Film Photovoltaic Solar Cells. *Opt. Quantum Electron.* **2019**, *51*, 276.

(548) Wu, Z.; Li, P.; Zhang, Y.; Zheng, Z. Flexible and Stretchable Perovskite Solar Cells: Device Design and Development Methods. *Small Methods* **2018**, *2*, 1800031.

(549) Zhang, Y.; Ng, S.-W.; Lu, X.; Zheng, Z. Solution-Processed Transparent Electrodes for Emerging Thin-Film Solar Cells. *Chem. Rev.* **2020**, *120*, 2049-2122.

(550) Hatamvand, M.; Kamrani, E.; Lira-Cantú, M.; Madsen, M.; Patil, B. R.; Vivo, P.; Mehmood, M. S.; Numan, A.; Ahmed, I.; et al. Recent Advances in Fiber-Shaped and Planar-Shaped Textile Solar Cells. *Nano Energy* **2020**, *71*, 104609.

(551) Zhai, W.; Zhu, Z.; Sun, X.; Peng, H. Fiber Solar Cells from High Performances Towards Real Applications. *Adv. Fiber Mater.* **2022**, *4*, 1293-1303.

(552) O'Connor, B.; Pipe, K. P.; Shtein, M. Fiber Based Organic Photovoltaic Devices. *Appl. Phys. Lett.* **2008**, *92*, 193306.

(553) Weintraub, B.; Wei, Y.; Wang, Z. L. Optical Fiber/Nanowire Hybrid Structures for Efficient Three-Dimensional Dye-Sensitized Solar Cells. *Angew. Chem., Int. Ed.* **2009**, *121*, 9143-9147.

- (554) Zhang, Z.; Chen, X.; Chen, P.; Guan, G.; Qiu, L.; Lin, H.; Yang, Z.; Bai, W.; Luo, Y.; et al. Integrated Polymer Solar Cell and Electrochemical Supercapacitor in a Flexible and Stable Fiber Format. *Adv. Mater.* **2014**, *26*, 466-470.
- (555) Liu, D.; Zhao, M.; Li, Y.; Bian, Z.; Zhang, L.; Shang, Y.; Xia, X.; Zhang, S.; Yun, D.; et al. Solid-State, Polymer-Based Fiber Solar Cells with Carbon Nanotube Electrodes. *ACS Nano* **2012**, *6*, 11027-11034.
- (556) Li, R.; Xiang, X.; Tong, X.; Zou, J.; Li, Q. Wearable Double-Twisted Fibrous Perovskite Solar Cell. *Adv. Mater.* **2015**, *27*, 3831-3835.
- (557) Dong, B.; Hu, J.; Xiao, X.; Tang, S.; Gao, X.; Peng, Z.; Zou, D. High-Efficiency Fiber-Shaped Perovskite Solar Cell by Vapor-Assisted Deposition with a Record Efficiency of 10.79%. *Adv. Mater. Technol.* **2019**, *4*, 1900131.
- (558) Saberi Motlagh, M.; Mottaghitalab, V.; Rismanchi, A.; Rafieepoor Chirani, M.; Hasanzadeh, M. Performance Modelling of Textile Solar Cell Developed by Carbon Fabric/Polypyrrole Flexible Counter Electrode. *Int. J. Sustain. Energy* **2022**, *41*, 1106-1126.
- (559) Fu, X.; Sun, H.; Xie, S.; Zhang, J.; Pan, Z.; Liao, M.; Xu, L.; Li, Z.; Wang, B.; et al. A fiber-Shaped Solar Cell Showing a Record Power Conversion Efficiency of 10%. *J. Mater. Chem. A* **2018**, *6*, 45-51.
- (560) Zhang, J.; Wang, Z.; Li, X.; Yang, J.; Song, C.; Li, Y.; Cheng, J.; Guan, Q.; Wang, B. Flexible Platinum-Free Fiber-Shaped Dye Sensitized Solar Cell with 10.28% Efficiency. *ACS Appl. Energy Mater.* **2019**, *2*, 2870-2877.
- (561) Kang, X.; Zhu, Z.; Zhao, T.; Zhai, W.; Xu, J.; Lin, Z.; Zeng, K.; Wang, B.; Sun, X.; et al. Hierarchically Assembled Counter Electrode for Fiber Solar Cell Showing Record Power Conversion Efficiency. *Adv. Funct. Mater.* **2022**, *32*, 2207763.
- (562) Zhu, Z.; Lin, Z.; Zhai, W.; Kang, X.; Song, J.; Lu, C.; Jiang, H.; Chen, P.; Sun, X.; et al. Indoor Photovoltaic Fiber with An Efficiency of 25.53% Under 1500 Lux Illumination. *Adv. Mater.* **2023**, *n/a*, 2304876.
- (563) Zhu, Z.; Lin, Z.; Gu, Y.; Song, J.; Kang, X.; Jiang, H.; Peng, H. Designing Reflective Hybrid Counter Electrode for Fiber Dye-Sensitized Solar Cell with Record Efficiency. *Adv. Funct. Mater.* **2023**, *n/a*, 2306742.
- (564) Yun, M. J.; Cha, S. I.; Seo, S. H.; Kim, H. S.; Lee, D. Y. Insertion of Dye-Sensitized Solar Cells in Textiles using a Conventional Weaving Process. *Sci. Rep.* **2015**, *5*, 11022.
- (565) Chen, J.; Huang, Y.; Zhang, N.; Zou, H.; Liu, R.; Tao, C.; Fan, X.; Wang, Z. L. Micro-Cable Structured Textile for Simultaneously Harvesting Solar and Mechanical Energy. *Nat. Energy* **2016**, *1*, 16138.

- (566) Fan, X.; Wang, F.; Chu, Z.; Chen, L.; Zhang, C.; Zou, D. Conductive Mesh Based Flexible Dye-Sensitized Solar Cells. *Appl. Phys. Lett.* **2007**, *90*, 073501.
- (567) Chen, T.-Y.; Huang, Y.-J.; Li, C.-T.; Kung, C.-W.; Vittal, R.; Ho, K.-C. Metal-Organic Framework/Sulfonated Polythiophene on Carbon Cloth as a Flexible Counter Electrode for Dye-Sensitized Solar Cells. *Nano Energy* **2017**, *32*, 19-27.
- (568) Domanski, K.; Correa-Baena, J.-P.; Mine, N.; Nazeeruddin, M. K.; Abate, A.; Saliba, M.; Tress, W.; Hagfeldt, A.; Grätzel, M. Not All That Glitters Is Gold: Metal-Migration-Induced Degradation in Perovskite Solar Cells. *ACS Nano* **2016**, *10*, 6306-6314.
- (569) Gholipour, S.; Correa-Baena, J.-P.; Domanski, K.; Matsui, T.; Steier, L.; Giordano, F.; Tajabadi, F.; Tress, W.; Saliba, M.; et al. Highly Efficient and Stable Perovskite Solar Cells based on a Low-Cost Carbon Cloth. *Adv. Energy Mater.* **2016**, *6*, 1601116.
- (570) Liu, S.; Huang, W.; Liao, P.; Pootrakulchote, N.; Li, H.; Lu, J.; Li, J.; Huang, F.; Shai, X.; et al. 17% Efficient Printable Mesoscopic Pin Metal Oxide Framework Perovskite Solar Cells using Cesium-Containing Triple Cation Perovskite. *J. Mater. Chem. A* **2017**, *5*, 22952-22958.
- (571) Arumugam, S.; Li, Y.; Senthilarasu, S.; Torah, R.; Kanibolotsky, A. L.; Inigo, A. R.; Skabara, P. J.; Beeby, S. P. Fully Spray-Coated Organic Solar Cells on Woven Polyester Cotton Fabrics for Wearable Energy Harvesting Applications. *J. Mater. Chem. A* **2016**, *4*, 5561-5568.
- (572) Zhen, H.; Li, K.; Chen, C.; Yu, Y.; Zheng, Z.; Ling, Q. Water-Borne Foldable Polymer Solar Cells: One-Step Transferring Free-Standing Polymer Films onto Woven Fabric Electrodes. *J. Mater. Chem. A* **2017**, *5*, 782-788.
- (573) Chen, G.; Li, Y.; Bick, M.; Chen, J. Smart Textiles for Electricity Generation. *Chem. Rev.* **2020**, *120*, 3668-3720.
- (574) Chen, C.; Zhao, S.; Pan, C.; Zi, Y.; Wang, F.; Yang, C.; Wang, Z. L. A Method for Quantitatively Separating the Piezoelectric Component from the As-Received "Piezoelectric" Signal. *Nat. Commun.* **2022**, *13*, 1391.
- (575) Siddiqui, S.; Lee, H. B.; Kim, D.-I.; Duy, L. T.; Hanif, A.; Lee, N.-E. An Omnidirectionally Stretchable Piezoelectric Nanogenerator Based on Hybrid Nanofibers and Carbon Electrodes for Multimodal Straining and Human Kinematics Energy Harvesting. *Adv. Energy Mater.* **2018**, *8*, 1701520.
- (576) Du, Y.; Fu, C.; Gao, Y.; Liu, L.; Liu, Y.; Xing, L.; Zhao, F. Carbon Fibers/ZnO Nanowires Hybrid Nanogenerator Based on an Insulating Interface Barrier. *RSC Adv.* **2017**, *7*, 21452-21458.
- (577) Liao, Q.; Zhang, Z.; Zhang, X.; Mohr, M.; Zhang, Y.; Fecht, H.-J. Flexible Piezoelectric

Nanogenerators Based on a Fiber/ZnO Nanowires/Paper Hybrid Structure for Energy Harvesting. *Nano Res.* **2014**, 7, 917-928.

(578) Sim, H. J.; Choi, C.; Lee, C. J.; Kim, Y. T.; Spinks, G. M.; Lima, M. D.; Baughman, R. H.; Kim, S. J. Flexible, Stretchable and Weavable Piezoelectric Fiber. *Adv. Eng. Mater.* **2015**, 17, 1270-1275.

(579) Egusa, S.; Wang, Z.; Chocat, N.; Ruff, Z. M.; Stolyarov, A. M.; Shemuly, D.; Sorin, F.; Rakich, P. T.; Joannopoulos, J. D.; et al. Multimaterial Piezoelectric Fibres. *Nat. Mater.* **2010**, 9, 643-648.

(580) Kim, M.; Wu, Y. S.; Kan, E. C.; Fan, J. Breathable and Flexible Piezoelectric ZnO@PVDF Fibrous Nanogenerator for Wearable Applications. *Polymers* **2018**, 10, 745.

(581) Song, S.; Yun, K.-S. Design and Characterization of Scalable Woven Piezoelectric Energy Harvester for Wearable Applications. *Smart Mater. Struct.* **2015**, 24, 045008.

(582) Wan, X.; Wang, Z.; Zhao, X.; Hu, Q.; Li, Z.; Lin Wang, Z.; Li, L. Flexible and Highly Piezoelectric Nanofibers with Organic-Inorganic Coaxial Structure for Self-Powered Physiological Multimodal Sensing. *Chem. Eng. J.* **2023**, 451, 139007.

(583) Zhang, Z.; Chen, Y.; Guo, J. ZnO Nanorods Patterned-Textile Using a Novel Hydrothermal Method for Sandwich Structured-Piezoelectric Nanogenerator for Human Energy Harvesting. *Physica E Low Dimens. Syst. Nanostruct.* **2019**, 105, 212-218.

(584) Chen, C.; Wen, Z.; Shi, J.; Jian, X.; Li, P.; Yeow, J. T. W.; Sun, X. Micro Triboelectric Ultrasonic Device for Acoustic Energy Transfer and Signal Communication. *Nat. Commun.* **2020**, 11, 4143.

(585) Li, S.; Jiang, J.; Zhai, N.; Liu, J.; Feng, K.; Chen, Y.; Wen, Z.; Sun, X.; Zhong, J. A Half-Wave Rectifying Triboelectric Nanogenerator for Self-Powered Water Splitting Towards Hydrogen Production. *Nano Energy* **2022**, 93, 106870.

(586) Jiang, J.; Guan, Q.; Liu, Y.; Sun, X.; Wen, Z. Abrasion and Fracture Self-Healable Triboelectric Nanogenerator with Ultrahigh Stretchability and Long-Term Durability. *Adv. Funct. Mater.* **2021**, 31, 2105380.

(587) Liao, W.; Liu, X.; Li, Y.; Xu, X.; Jiang, J.; Lu, S.; Bao, D.; Wen, Z.; Sun, X. Transparent, Stretchable, Temperature-Stable and Self-Healing Ionogel-Based Triboelectric Nanogenerator for Biomechanical Energy Collection. *Nano Res.* **2021**, 15, 2060-2068.

(588) Wang, J.; Shi, J.; Deng, X.; Xie, L.; Jiang, J.; Tang, J.; Liu, J.; Wen, Z.; Sun, X.; et al. Transition Metal Pincer Complex Based Self-Healable, Stretchable and Transparent Triboelectric Nanogenerator. *Nano Energy* **2020**, 78, 105348.

(589) Lv, T.; Cheng, R.; Wei, C.; Su, E.; Jiang, T.; Sheng, F.; Peng, X.; Dong, K.; Wang, Z. L.

All-Fabric Direct-Current Triboelectric Nanogenerators Based on the Tribovoltaic Effect as Power Textiles. *Adv. Energy Mater.* **2023**, *13*, 2301178.

(590) Wen, Z.; Yeh, M.-H.; Guo, H.; Wang, J.; Zi, Y.; Xu, W.; Deng, J.; Zhu, L.; Wang, X.; et al. Self-Powered Textile for Wearable Electronics by Hybridizing Fiber-Shaped Nanogenerators, Solar Cells, and Supercapacitors. *Sci. Adv.* **2016**, *2*, e1600097.

(591) Yang, Y.; Sun, N.; Wen, Z.; Cheng, P.; Zheng, H.; Shao, H.; Xia, Y.; Chen, C.; Lan, H.; et al. Liquid-Metal-Based Super-Stretchable and Structure-Designable Triboelectric Nanogenerator for Wearable Electronics. *ACS Nano* **2018**, *12*, 2027-2034.

(592) Dong, K.; Deng, J.; Zi, Y.; Wang, Y. C.; Xu, C.; Zou, H.; Ding, W.; Dai, Y.; Gu, B.; et al. 3D Orthogonal Woven Triboelectric Nanogenerator for Effective Biomechanical Energy Harvesting and as Self-Powered Active Motion Sensors. *Adv. Mater.* **2017**, *29*, 1702648.

(593) Dong, K.; Peng, X.; An, J.; Wang, A. C.; Luo, J.; Sun, B.; Wang, J.; Wang, Z. L. Shape Adaptable and Highly Resilient 3D Braided Triboelectric Nanogenerators As E-Textiles for Power and Sensing. *Nat. Commun.* **2020**, *11*, 2868.

(594) Dong, K.; Peng, X.; Cheng, R.; Ning, C.; Jiang, Y.; Zhang, Y.; Wang, Z. L. Advances in High-Performance Autonomous Energy and Self-Powered Sensing Textiles with Novel 3D Fabric Structures. *Adv. Mater.* **2022**, *34*, 2109355.

(595) Huang, T.; Zhang, J.; Yu, B.; Yu, H.; Long, H.; Wang, H.; Zhang, Q.; Zhu, M. Fabric Texture Design for Boosting the Performance of a Knitted Washable Textile Triboelectric Nanogenerator as Wearable Power. *Nano Energy* **2019**, *58*, 375-383.

(596) Jung, S.; Lee, J.; Hyeon, T.; Lee, M.; Kim, D. H. Fabric-Based Integrated Energy Devices for Wearable Activity Monitors. *Adv. Mater.* **2014**, *26*, 6329-6334.

(597) Sheng, F.; Zhang, B.; Cheng, R.; Wei, C.; Shen, S.; Ning, C.; Yang, J.; Wang, Y.; Wang, Z. L.; et al. Wearable Energy Harvesting-Storage Hybrid Textiles as on-Body Self-Charging Power Systems. *Nano Res. Energy* **2023**, *2*, e9120079.

(598) Zhu, J. X.; Zhu, M. L.; Shi, Q. F.; Wen, F.; Liu, L.; Dong, B. W.; Haroun, A.; Yang, Y. Q.; Vachon, P.; et al. Progress in TENG Technology-A Journey from Energy Harvesting to Nanoenergy and Nanosystem. *EcoMat* **2020**, *2*, e12058.

(599) Dong, K.; Peng, X.; Cheng, R.; Wang, Z. L. Smart Textile Triboelectric Nanogenerators: Prospective Strategies for Improving Electricity Output Performance. *Nano energy Adv.* **2022**, *2*, 133-164.

(600) Komatsu, N.; Ichinose, Y.; Dewey, O. S.; Taylor, L. W.; Trafford, M. A.; Yomogida, Y.; Wehmeyer, G.; Pasquali, M.; Yanagi, K.; et al. Macroscopic Weavable Fibers of Carbon Nanotubes with Giant Thermoelectric Power Factor. *Nat. Commun.* **2021**, *12*, 4931.



- (601) Wang, L.; Zhang, K. Textile-Based Thermoelectric Generators and Their Applications. *Energy Environ. Mater.* **2020**, *3*, 67-79.
- (602) Ding, T.; Chan, K. H.; Zhou, Y.; Wang, X.-Q.; Cheng, Y.; Li, T.; Ho, G. W. Scalable Thermoelectric Fibers for Multifunctional Textile-Electronics. *Nat. Commun.* **2020**, *11*, 6006.
- (603) Lee, T.; Park, K. T.; Ku, B. C.; Kim, H. Carbon Nanotube Fibers with Enhanced Longitudinal Carrier Mobility for High-Performance All-Carbon Thermoelectric Generators. *Nanoscale* **2019**, *11*, 16919-16927.
- (604) Jung, J.; Hyun Suh, E.; Jeong, Y.; Yun, D.-J.; Chan Park, S.; Gyu Oh, J.; Jang, J. Ionic-Liquid Doping of Carbon Nanotubes with [HMIM][BF<sub>4</sub>] for Flexible Thermoelectric Generators. *Chem. Eng. J.* **2022**, *438*, 135526.
- (605) Jin, L.; Sun, T.; Zhao, W.; Wang, L.; Jiang, W. Durable and Washable Carbon Nanotube-Based Fibers toward Wearable Thermoelectric Generators Application. *J. Power Sources* **2021**, *496*, 229838.
- (606) Sun, T.; Zhou, B.; Zheng, Q.; Wang, L.; Jiang, W.; Snyder, G. J. Stretchable Fabric Generates Electric Power from Woven Thermoelectric Fibers. *Nat. Commun.* **2020**, *11*, 572.
- (607) Wang, K.; Hou, C.; Zhang, Q.; Li, Y.; Wang, H. Highly Integrated Fiber-Shaped Thermoelectric Generators with Radially Heterogeneous Interlayers. *Nano Energy* **2022**, *95*, 107055.
- (608) Allison, L. K.; Andrew, T. L. A Wearable All-Fabric Thermoelectric Generator. *Adv. Mater. Technol.* **2019**, *4*, 1800615.
- (609) Lu, Z.; Zhang, H.; Mao, C.; Li, C. M. Silk Fabric-Based Wearable Thermoelectric Generator for Energy Harvesting from the Human Body. *Appl. Energy* **2016**, *164*, 57-63.
- (610) Kim, Y.; Lund, A.; Noh, H.; Hofmann, A. I.; Craighero, M.; Darabi, S.; Zokaei, S.; Park, J. I.; Yoon, M. H.; et al. Robust PEDOT:PSS Wet-Spun Fibers for Thermoelectric Textiles. *Macromol. Mater. Eng.* **2020**, *305*.
- (611) Alsharif, M. H.; Kim, S.; Kuruoğlu, N. Energy Harvesting Techniques for Wireless Sensor Networks/Radio-Frequency Identification: A Review. *Symmetry* **2019**, *11*, 865.
- (612) Xu, L.; Liu, Z.; Chen, X.; Sun, R.; Hu, Z.; Zheng, Z.; Ye, T. T.; Li, Y. Deformation-Resilient Embroidered Near Field Communication Antenna and Energy Harvesters for Wearable Applications. *Adv. Intell. Syst.* **2019**, *1*, 1900056.
- (613) Lin, R.; Kim, H.-J.; Achavananthadith, S.; Kurt, S. A.; Tan, S. C. C.; Yao, H.; Tee, B. C. K.; Lee, J. K. W.; Ho, J. S. Wireless Battery-Free Body Sensor Networks using Near-Field-Enabled Clothing. *Nat. Commun.* **2020**, *11*, 444.

- (614) Garnier, B.; Mariage, P.; Rault, F.; Cochrane, C.; Koncar, V. Textile NFC Antenna for Power and Data Transmission Across Clothes. *Smart Mater. Struct.* **2020**, *29*, 085017.
- (615) Jiang, Y.; Pan, K.; Leng, T.; Hu, Z. Smart Textile Integrated Wireless Powered Near Field Communication Body Temperature and Sweat Sensing System. *IEEE J. Electromagn. RF Microw. Med.* **2020**, *4*, 164-170.
- (616) Tian, X.; Lee, P. M.; Tan, Y. J.; Wu, T. L. Y.; Yao, H.; Zhang, M.; Li, Z.; Ng, K. A.; Tee, B. C. K.; et al. Wireless Body Sensor Networks Based on Metamaterial Textiles. *Nat. Electron.* **2019**, *2*, 243-251.
- (617) Winter, M.; Brodd, R. J. What Are Batteries, Fuel Cells, and Supercapacitors? *Chem. Rev.* **2004**, *104*, 4245-4270.
- (618) Jeerapan, I.; Sempionatto, J. R.; Wang, J. On-Body Bioelectronics: Wearable Biofuel Cells for Bioenergy Harvesting and Self-Powered Biosensing. *Adv. Funct. Mater.* **2020**, *30*, 1906243.
- (619) Zhong, L.; Tang, L.; Yang, S.; Zhao, Z.; Zheng, Z.; Jiang, X. Stretchable Liquid Metal-Based Metal-Polymer Conductors for Fully Screen-Printed Biofuel Cells. *Anal. Chem.* **2022**, *94*, 16738-16745.
- (620) Wu, H.; Zhang, Y.; Kjøniksen, A.-L.; Zhou, X.; Zhou, X. Wearable Biofuel Cells: Advances from Fabrication to Application. *Adv. Funct. Mater.* **2021**, *31*, 2103976.
- (621) Kwon, C. H.; Ko, Y.; Shin, D.; Kwon, M.; Park, J.; Bae, W. K.; Lee, S. W.; Cho, J. High-Power Hybrid Biofuel Cells using Layer-by-Layer Assembled Glucose Oxidase-Coated Metallic Cotton Fibers. *Nat. Commun.* **2018**, *9*, 4479.
- (622) Yin, S.; Jin, Z.; Miyake, T. Wearable High-Powered Biofuel Cells Using Enzyme/Carbon Nanotube Composite Fibers on Textile Cloth. *Biosens. Bioelectron.* **2019**, *141*, 111471.
- (623) Kwon, C. H.; Ko, Y.; Shin, D.; Lee, S. W.; Cho, J. Highly Conductive Electrocatalytic Gold Nanoparticle-Assembled Carbon Fiber Electrode for High-Performance Glucose-based Biofuel Cells. *J. Mater. Chem. A* **2019**, *7*, 13495-13505.
- (624) Jia, W.; Wang, X.; Imani, S.; Bandodkar, A. J.; Ramírez, J.; Mercier, P. P.; Wang, J. Wearable Textile Biofuel Cells for Powering Electronics. *J. Mater. Chem. A* **2014**, *2*, 18184-18189.
- (625) Jeerapan, I.; Sempionatto, J. R.; Pavinatto, A.; You, J.-M.; Wang, J. Stretchable Biofuel Cells as Wearable Textile-Based Self-Powered Sensors. *J. Mater. Chem. A* **2016**, *4*, 18342-18353.
- (626) Chen, Z.; Yao, Y.; Lv, T.; Yang, Y.; Liu, Y.; Chen, T. Flexible and Stretchable Enzymatic Biofuel Cell with High Performance Enabled by Textile Electrodes and Polymer Hydrogel

Electrolyte. *Nano Lett.* **2022**, *22*, 196-202.

(627) Wang, C.; Shim, E.; Chang, H.-K.; Lee, N.; Kim, H. R.; Park, J. Sustainable and High-Power Wearable Glucose Biofuel Cell Using Long-Term and High-Speed Flow in Sportswear Fabrics. *Biosens. Bioelectron.* **2020**, *169*, 112652.

(628) Ogawa, Y.; Takai, Y.; Kato, Y.; Kai, H.; Miyake, T.; Nishizawa, M. Stretchable Biofuel Cell with Enzyme-Modified Conductive Textiles. *Biosens. Bioelectron.* **2015**, *74*, 947-952.

(629) Yin, S.; Liu, X.; Kaji, T.; Nishina, Y.; Miyake, T. Fiber-Crafted Biofuel Cell Bracelet for Wearable Electronics. *Biosens. Bioelectron.* **2021**, *179*, 113107.

(630) Sharifi, M.; Pothu, R.; Boddula, R.; Bardajee, G. R. Trends of Biofuel Cells for Smart Biomedical Devices. *Int. J. Hydrogen Energy* **2021**, *46*, 3220-3229.

(631) Chu, T.-F.; Rajendran, R.; Kuznetsova, I.; Wang, G.-J. High-Power, Non-Enzymatic Glucose Biofuel Cell Based on a Nano/Micro Hybrid-Structured Au Anode. *J. Power Sources* **2020**, *453*, 227844.

(632) U S, J.; Goel, S. Microfluidic Non-Enzymatic Biofuel Cell Integrated with Electrodeposited Metallic Catalysts on a Paper Based Platform. *J. Power Sources* **2021**, *510*, 230405.

(633) Huang, Q.; Yang, Y.; Chen, R.; Wang, X. High Performance Fully Paper-Based All-Solid-State Supercapacitor Fabricated by a Papermaking Process with Silver Nanoparticles and Reduced Graphene Oxide-Modified Pulp Fibers. *EcoMat* **2021**, *3*, e12076.

(634) Yang, Y.; Ng, S.-W.; Chen, D.; Chang, J.; Wang, D.; Shang, J.; Huang, Q.; Deng, Y.; Zheng, Z. Freestanding Lamellar Porous Carbon Stacks for Low-Temperature-Foldable Supercapacitors. *Small* **2019**, *15*, 1902071.

(635) Yao, L.; Lin, J.; Yang, H.; Wu, Q.; Wang, D.; Li, X.; Deng, L.; Zheng, Z. Two-Dimensional Hierarchically Porous Carbon Nanosheets for Flexible Aqueous Supercapacitors with High Volumetric Capacitance. *Nanoscale* **2019**, *11*, 11086-11092.

(636) Yao, L.; Wu, Q.; Zhang, P.; Zhang, J.; Wang, D.; Li, Y.; Ren, X.; Mi, H.; Deng, L.; et al. Scalable 2D Hierarchical Porous Carbon Nanosheets for Flexible Supercapacitors with Ultrahigh Energy Density. *Adv. Mater.* **2018**, *30*, 1706054.

(637) Wang, D. W.; Li, F.; Liu, M.; Lu, G. Q.; Cheng, H. M. 3D Aperiodic Hierarchical Porous Graphitic Carbon Material for High-Rate Electrochemical Capacitive Energy Storage. *Angew. Chem., Int. Ed.* **2008**, *47*, 373-376.

(638) Chen, R.; Tang, H.; He, P.; Zhang, W.; Dai, Y.; Zong, W.; Guo, F.; He, G.; Wang, X. Interface Engineering of Biomass-Derived Carbon used as Ultrahigh-Energy-Density and

- Practical Mass-Loading Supercapacitor Electrodes. *Adv. Funct. Mater.* **2022**, *33*, 2212078.
- (639) Zou, M.; Zhao, W.; Wu, H.; Zhang, H.; Xu, W.; Yang, L.; Wu, S.; Wang, Y.; Chen, Y.; et al. Single Carbon Fibers with a Macroscopic-Thickness, 3D Highly Porous Carbon Nanotube Coating. *Adv. Mater.* **2018**, *30*, 1704419.
- (640) Zhou, J.; Chen, Z.; Yu, G.; Ma, K.; Lian, X.; Li, S.; Shi, Q.; Wang, J.; Guo, L.; et al. Accelerating O-Redox Kinetics with Carbon Nanotubes for Stable Lithium-Rich Cathodes. *Small Methods* **2022**, *6*, 2200449.
- (641) Huang, Q.; Wang, D.; Hu, H.; Shang, J.; Chang, J.; Xie, C.; Yang, Y.; Lepró, X.; Baughman, R. H.; et al. Additive Functionalization and Embroidery for Manufacturing Wearable and Washable Textile Supercapacitors. *Adv. Funct. Mater.* **2020**, *30*, 1910541.
- (642) Wu, Z.-S.; Wang, D.-W.; Ren, W.; Zhao, J.; Zhou, G.; Li, F.; Cheng, H.-M. Anchoring Hydrous RuO<sub>2</sub> on Graphene Sheets for High-Performance Electrochemical Capacitors. *Adv. Funct. Mater.* **2010**, *20*, 3595-3602.
- (643) Hu, L.; Chen, W.; Xie, X.; Liu, N.; Yang, Y.; Wu, H.; Yao, Y.; Pasta, M.; Alshareef, H. N.; et al. Symmetrical MnO<sub>2</sub>-Carbon Nanotube-Textile Nanostructures for Wearable Pseudocapacitors with High Mass Loading. *ACS Nano* **2011**, *5*, 8904–8913.
- (644) Paleo, A. J.; Staiti, P.; Brigandì, A.; Ferreira, F. N.; Rocha, A. M.; Lufrano, F. Supercapacitors based on AC/MnO<sub>2</sub> Deposited onto Dip-Coated Carbon Nanofiber Cotton Fabric Electrodes. *Energy Stor. Mater.* **2018**, *12*, 204-215.
- (645) Zhang, Y.; Wang, W.; Wang, L.; Guo, Q.; Hu, H.; Xie, C.; Shang, J.; Xu, J.; Zhang, Y.; et al. Inverse Opaline Metallic Membrane Addresses the Tradeoff Between Volumetric Capacitance and Areal Capacitance of Supercapacitor. *Adv. Energy Mater.* **2022**, *12*, 2102802.
- (646) Zhang, W.; Guo, R.; Dang, L.; Sun, J.; Liu, Z.; Lei, Z. Cotton Fabric-Derived Hybrid Carbon Network with N-Doped Carbon Nanotubes Grown Vertically as Flexible Multifunctional Electrodes for High-Rate Capacitive Energy Storage. *J. Power Sources* **2021**, *507*, 230303.
- (647) Gao, Y.; Zhou, R.; Wang, D.; Huang, Q.; Cheng, C.-H.; Zheng, Z. Boosting the Energy Density of Flexible Asymmetric Supercapacitor with Three Dimensional Fe<sub>2</sub>O<sub>3</sub> Composite Brush Anode. *Chem. Res. Chin. Univ.* **2020**, *36*, 97-104.
- (648) Ko, Y.; Kwon, M.; Bae, W. K.; Lee, B.; Lee, S. W.; Cho, J. Flexible Supercapacitor Electrodes Based on Real Metal-Like Cellulose Papers. *Nat. Commun.* **2017**, *8*, 536.
- (649) Shang, J.; Huang, Q.; Wang, L.; Yang, Y.; Li, P.; Zheng, Z. Soft Hybrid Scaffold (SHS) Strategy for Realization of Ultrahigh Energy Density of Wearable Aqueous Supercapacitors.

*Adv. Mater.* **2020**, *32*, 1907088.

(650) Wang, J.; Dong, L.; Xu, C.; Ren, D.; Ma, X.; Kang, F. Polymorphous Supercapacitors Constructed from Flexible Three-Dimensional Carbon Network/Polyaniline/MnO<sub>2</sub> Composite Textiles. *ACS Appl. Mater. Interfaces* **2018**, *10*, 10851-10859.

(651) Zhang, Q.; Liu, D.; Pei, H.; Pan, W.; Liu, Y.; Xu, S.; Cao, S. Swelling-Reconstructed Chitosan-Viscose Nonwoven Fabric for High-Performance Quasi-Solid-State Supercapacitors. *J. Colloid Interface Sci.* **2022**, *617*, 489-499.

(652) Yao, B.; Wang, H.; Zhou, Q.; Wu, M.; Zhang, M.; Li, C.; Shi, G. Ultrahigh-Conductivity Polymer Hydrogels with Arbitrary Structures. *Adv. Mater.* **2017**, *29*, 1700974.

(653) Tebyetekerwa, M.; Xu, Z.; Li, W.; Wang, X.; Marriam, I.; Peng, S.; Ramkrishna, S.; Yang, S.; Zhu, M. Surface Self-Assembly of Functional Electroactive Nanofibers on Textile Yarns as a Facile Approach toward Super Flexible Energy Storage. *ACS Appl. Energy Mater.* **2018**, *1*, 377-386.

(654) Wu, D.; Zhong, W. A New Strategy for Anchoring a Functionalized Graphene Hydrogel in a Carbon Cloth Network to Support a Lignosulfonate/Polyaniline Hydrogel as an Integrated Electrode for Flexible High Areal-Capacitance Supercapacitors. *J. Mater. Chem. A* **2019**, *7*, 5819-5830.

(655) Chang, J.; Huang, Q.; Gao, Y.; Zheng, Z. Pathways of Developing High-Energy-Density Flexible Lithium Batteries. *Adv. Mater.* **2021**, *33*, 2004419.

(656) Xie, C.; Guo, Y.; Zheng, Z. Pushing the Limit of Flexible Batteries. *CCS Chemistry* **2023**, *5*, 531-543.

(657) Wang, L.; Zhang, Y.; Bruce, P. G. Batteries for Wearables. *Natl. Sci. Rev.* **2023**, *10*, nwac062.

(658) Zhu, Y.; Cao, K.; Cheng, W.; Zeng, S.; Dou, S.; Chen, W.; Zhao, D.; Yu, H. A Non-Newtonian Fluidic Cellulose-Modified Glass Microfiber Separator for Flexible Lithium-Ion Batteries. *EcoMat* **2021**, *3*, e12126.

(659) Li, D.; Xie, C.; Gao, Y.; Hu, H.; Wang, L.; Zheng, Z. Inverted Anode Structure for Long-Life Lithium Metal Batteries. *Adv. Energy Mater.* **2022**, *12*, 2200584.

(660) Gao, Y.; Guo, Q.; Zhang, Q.; Cui, Y.; Zheng, Z. Fibrous Materials for Flexible Li-S Battery. *Adv. Energy Mater.* **2021**, *11*, 2002580.

(661) Lin, D.; Liu, Y.; Cui, Y. Reviving the Lithium Metal Anode for High-Energy Batteries. *Nat. Nanotechnol.* **2017**, *12*, 194-206.

(662) Chang, J.; Hu, H.; Shang, J.; Fang, R.; Shou, D.; Xie, C.; Gao, Y.; Yang, Y.; Zhuang, Q. N.; et al. Rational Design of Li-Wicking Hosts for Ultrafast Fabrication of Flexible and Stable

Lithium Metal Anodes. *Small* **2022**, *18*, 2105308.

(663) Chang, J.; Shang, J.; Sun, Y.; Ono, L. K.; Wang, D.; Ma, Z.; Huang, Q.; Chen, D.; Liu, G.; et al. Flexible and Stable High-Energy Lithium-Sulfur Full Batteries with Only 100% Oversized Lithium. *Nat. Commun.* **2018**, *9*, 4480.

(664) Li, D.; Xie, C.; Gao, Y.; Hu, H.; Wang, L.; Zheng, Z. Inverted Anode Structure for Long-Life Lithium Metal Batteries. *Adv. Energy Mater.* **2022**, *12*, 2200584.

(665) Wang, L.; Shang, J.; Huang, Q.; Hu, H.; Zhang, Y.; Xie, C.; Luo, Y.; Gao, Y.; Wang, H.; et al. Smoothing the Sodium-Metal Anode with a Self-Regulating Alloy Interface for High-Energy and Sustainable Sodium-Metal Batteries. *Adv. Mater.* **2021**, *33*, 2102802.

(666) Zhu, J.; Lu, Y.; Chen, C.; Ge, Y.; Jasper, S.; Leary, J. D.; Li, D.; Jiang, M.; Zhang, X. Porous One-Dimensional Carbon/Iron Oxide Composite for Rechargeable Lithium-Ion Batteries With High and Stable Capacity. *J. Alloys Compd.* **2016**, *672*, 79-85.

(667) Zhou, J.; You, Y.; Lian, X.; Shi, Q.; Liu, Y.; Yang, X.; Bachmatiuk, A.; Liu, L.; Sun, J.; et al. Toward Stable Lithium-Ion Batteries: Accelerating the Transfer and Alloying Reactions of Sn-Based Anodes via Coordination Atom Regulation and Carbon Hybridization. *J. Power Sources* **2022**, *519*, 230778.

(668) Balogun, M. S.; Qiu, W.; Jian, J.; Huang, Y.; Luo, Y.; Yang, H.; Liang, C.; Lu, X.; Tong, Y. Vanadium Nitride Nanowire Supported SnS<sub>2</sub> Nanosheets with High Reversible Capacity as Anode Material for Lithium Ion Batteries. *ACS Appl. Mater. Interfaces* **2015**, *7*, 23205-23215.

(669) Zhou, J.; Wang, L.; Yang, M.; Wu, J.; Chen, F.; Huang, W.; Han, N.; Ye, H.; Zhao, F.; et al. Hierarchical VS<sub>2</sub> Nanosheet Assemblies: A Universal Host Material for the Reversible Storage of Alkali Metal Ions. *Adv. Mater.* **2017**, *29*, 1702061.

(670) Hua, X.; Eggeman, A. S.; Castillo-Martinez, E.; Robert, R.; Geddes, H. S.; Lu, Z.; Pickard, C. J.; Meng, W.; Wiaderek, K. M.; et al. Revisiting Metal Fluorides as Lithium-Ion Battery Cathodes. *Nat. Mater.* **2021**, *20*, 841-850.

(671) Nguyen, V. P.; Park, J. S.; Yuk, J. M.; Oh, M.; Kim, J.-H.; Lee, S.-M. Boosted Zn<sup>2+</sup> Storage Performance of Hydrated Vanadium Oxide by Defect and Heterostructure. *J. Mater. Chem. A* **2022**, *10*, 13428-13438.

(672) Nguyen, V. P.; Kim, I. H.; Shim, H. C.; Park, J. S.; Yuk, J. M.; Kim, J.-H.; Kim, D.; Lee, S.-M. Porous Carbon Textile Decorated with VC/V<sub>2</sub>O<sub>3-x</sub> Hybrid Nanoparticles: Dual-Functional Host for Flexible Li-S Full Batteries. *Energy Stor. Mater.* **2022**, *46*, 542-552.

(673) Zhu, T.; Cheng, Y.; Cao, C.; Mao, J.; Li, L.; Huang, J.; Gao, S.; Dong, X.; Chen, Z.; et al. A Semi-Interpenetrating Network Ionic Hydrogel for Strain Sensing with High Sensitivity,

- Large Strain Range, and Stable Cycle Performance. *Chem. Eng. J.* **2020**, *385*, 123912.
- (674) Zhu, Y.; Yang, M.; Huang, Q.; Wang, D.; Yu, R.; Wang, J.; Zheng, Z.; Wang, D. V<sub>2</sub>O<sub>5</sub> Textile Cathodes with High Capacity and Stability for Flexible Lithium-Ion Batteries. *Adv. Mater.* **2020**, *32*, 1906205.
- (675) Gao, Z.; Song, N.; Zhang, Y.; Li, X. Cotton-Textile-Enabled, Flexible Lithium-Ion Batteries with Enhanced Capacity and Extended Lifespan. *Nano Lett.* **2015**, *15*, 8194-8203.
- (676) Cho, S.; Chang, T.; Yu, T.; Lee, C. H. Smart Electronic Textiles for Wearable Sensing and Display. *Biosensors* **2022**, *12*, 222.
- (677) Gu, C.; Jia, A.-B.; Zhang, Y.-M.; Zhang, S. X.-A. Emerging Electrochromic Materials and Devices for Future Displays. *Chem. Rev.* **2022**, *122*, 14679-14721.
- (678) Kwon, S.; Hwang, Y. H.; Nam, M.; Chae, H.; Lee, H. S.; Jeon, Y.; Lee, S.; Kim, C. Y.; Choi, S.; et al. Recent Progress of Fiber Shaped Lighting Devices for Smart Display Applications—A Fibertronic Perspective. *Adv. Mater.* **2020**, *32*, 1903488.
- (679) Yoo, J.; Li, S.; Kim, D.-H.; Yang, J.; Choi, M. K. Materials and Design Strategies for Stretchable Electroluminescent Devices. *Nanoscale Horiz.* **2022**, *7*, 801-821.
- (680) Wang, Z.; Shi, X.; Peng, H. Alternating Current Electroluminescent Fibers for Textile Displays. *Natl. Sci. Rev.* **2023**, *10*, nwac113.
- (681) Yin, H.; Zhu, Y.; Youssef, K.; Yu, Z.; Pei, Q. Structures and Materials in Stretchable Electroluminescent Devices. *Adv. Mater.* **2022**, *34*, 2106184.
- (682) Choi, S.; Jeon, Y.; Kwon, J. H.; Ihm, C.; Kim, S. Y.; Choi, K. C. Wearable Photomedicine for Neonatal Jaundice Treatment Using Blue Organic Light-Emitting Diodes (OLEDs): Toward Textile-Based Wearable Phototherapeutics. *Adv. Sci.* **2022**, *9*, 2204622.
- (683) Ko, K.-J.; Lee, H. B.; Kang, J.-W. Flexible, Wearable Organic Light-Emitting Fibers Based on PEDOT:PSS/Ag-Fiber Embedded Hybrid Electrodes for Large-Area Textile Lighting. *Adv. Mater. Technol.* **2020**, *5*, 2000168.
- (684) Kim, W.; Kwon, S.; Lee, S.-M.; Kim, J. Y.; Han, Y.; Kim, E.; Choi, K. C.; Park, S.; Park, B.-C. Soft Fabric-Based Flexible Organic Light-Emitting Diodes. *Org. Electron.* **2013**, *14*, 3007-3013.
- (685) O'Connor, B.; An, K. H.; Zhao, Y.; Pipe, K. P.; Shtein, M. Fiber Shaped Light Emitting Device. *Adv. Mater.* **2007**, *19*, 3897-3900.
- (686) Meier, S. B.; Tordera, D.; Pertegás, A.; Roldán-Carmona, C.; Ortí, E.; Bolink, H. J. Light-Emitting Electrochemical Cells: Recent Progress and Future Prospects. *Mater. Today* **2014**, *17*, 217-223.
- (687) Zhang, Z.; Guo, K.; Li, Y.; Li, X.; Guan, G.; Li, H.; Luo, Y.; Zhao, F.; Zhang, Q.; et al.

A Colour-Tunable, Weavable Fibre-Shaped Polymer Light-Emitting Electrochemical Cell. *Nat. Photonics* **2015**, 9, 233-238.

(688) Jayathilaka, W. A. D. M.; Chinnappan, A.; Tey, J. N.; Wei, J.; Ramakrishna, S. Alternative Current Electroluminescence and Flexible Light Emitting Devices. *J. Mater. Chem. C* **2019**, 7, 5553-5572.

(689) Torres Alonso, E.; Rodrigues, D. P.; Khetani, M.; Shin, D.-W.; De Sanctis, A.; Joulie, H.; de Schrijver, I.; Baldycheva, A.; Alves, H.; et al. Graphene Electronic Fibres with Touch-Sensing and Light-Emitting Functionalities for Smart Textiles. *npj Flex. Electron.* **2018**, 2, 25.

(690) Hu, B.; Li, D.; Ala, O.; Manandhar, P.; Fan, Q.; Kasilingam, D.; Calvert, P. D. Textile-Based Flexible Electroluminescent Devices. *Adv. Funct. Mater.* **2011**, 21, 305-311.

(691) Mi, H.; Zhong, L.; Tang, X.; Xu, P.; Liu, X.; Luo, T.; Jiang, X. Electroluminescent Fabric Woven by Ultrastretchable Fibers for Arbitrarily Controllable Pattern Display. *ACS Appl. Mater. Interfaces* **2021**, 13, 11260-11267.

(692) Ma, F.; Lin, Y.; Yuan, W.; Ding, C.; Su, W.; Meng, X.; Cui, Z. Fully Printed, Large-Size Alternating Current Electroluminescent Device on Fabric for Wearable Textile Display. *ACS Appl. Electron. Mater.* **2021**, 3, 1747-1757.

(693) Kline, W. M.; Lorenzini, R. G.; Sotzing, G. A. A Review of Organic Electrochromic Fabric Devices. *Color. Technol* **2014**, 130, 73-80.

(694) Fan, H.; Wei, W.; Hou, C.; Zhang, Q.; Li, Y.; Li, K.; Wang, H. Wearable Electrochromic Materials and Devices: from Visible to Infrared Modulation. *J. Mater. Chem. C* **2023**, 11, 7183-7210.

(695) Yan, C.; Kang, W.; Wang, J.; Cui, M.; Wang, X.; Foo, C. Y.; Chee, K. J.; Lee, P. S. Stretchable and Wearable Electrochromic Devices. *ACS Nano* **2014**, 8, 316-322.

(696) Li, K.; Zhang, Q.; Wang, H.; Li, Y. Red, Green, Blue (RGB) Electrochromic Fibers for the New Smart Color Change Fabrics. *ACS Appl. Mater. Interfaces* **2014**, 6, 13043-13050.

(697) Sinha, S.; Daniels, R.; Yassin, O.; Baczkowski, M.; Tefferi, M.; Deshmukh, A.; Cao, Y.; Sotzing, G. Electrochromic Fabric Displays from a Robust, Open-Air Fabrication Technique. *Adv. Mater. Technol.* **2022**, 7, 2100548.

(698) Cherenack, K.; Zysset, C.; Kinkeldei, T.; Münzenrieder, N.; Tröster, G. Woven Electronic Fibers with Sensing and Display Functions for Smart Textiles. *Adv. Mater.* **2010**, 22, 5178-5182.

(699) Wicaksono, I.; Tucker, C. I.; Sun, T.; Guerrero, C. A.; Liu, C.; Woo, W. M.; Pence, E. J.; Dagdeviren, C. A Tailored, Electronic Textile Conformable Suit for Large-Scale Spatiotemporal Physiological Sensing in vivo. *npj Flex. Electron.* **2020**, 4, 5.



- (700) Lacour, S. P.; Jones, J.; Wagner, S.; Teng, L.; Zhigang, S. Stretchable Interconnects for Elastic Electronic Surfaces. *Proc. IEEE* **2005**, *93*, 1459-1467.
- (701) Xu, S.; Zhang, Y.; Cho, J.; Lee, J.; Huang, X.; Jia, L.; Fan, J. A.; Su, Y.; Su, J.; et al. Stretchable Batteries with Self-Similar Serpentine Interconnects and Integrated Wireless Recharging Systems. *Nat. Commun.* **2013**, *4*, 1543.
- (702) Jang, K.-I.; Li, K.; Chung, H. U.; Xu, S.; Jung, H. N.; Yang, Y.; Kwak, J. W.; Jung, H. H.; Song, J.; et al. Self-Assembled Three Dimensional Network Designs for Soft Electronics. *Nat. Commun.* **2017**, *8*, 15894.
- (703) Song, Z.; Ma, T.; Tang, R.; Cheng, Q.; Wang, X.; Krishnaraju, D.; Panat, R.; Chan, C. K.; Yu, H.; et al. Origami Lithium-Ion Batteries. *Nat. Commun.* **2014**, *5*, 3140.
- (704) Guo, H.; Yeh, M.-H.; Lai, Y.-C.; Zi, Y.; Wu, C.; Wen, Z.; Hu, C.; Wang, Z. L. All-in-One Shape-Adaptive Self-Charging Power Package for Wearable Electronics. *ACS Nano* **2016**, *10*, 10580-10588.
- (705) Wang, Y.; Yokota, T.; Someya, T. Electrospun Nanofiber-Based Soft Electronics. *NPG Asia Mater.* **2021**, *13*, 22.
- (706) Cao, J.; Liang, F.; Li, H.; Li, X.; Fan, Y.; Hu, C.; Yu, J.; Xu, J.; Yin, Y.; et al. Ultra-Robust Stretchable Electrode for E-Skin: In Situ Assembly Using a Nanofiber Scaffold and Liquid Metal to Mimic Water-To-Net Interaction. *InfoMat* **2022**, *4*, e12302.
- (707) Stanley, J.; Hunt, J. A.; Kunovski, P.; Wei, Y. A Review of Connectors and Joining Technologies for Electronic Textiles. *Eng. Rep.* **2022**, *4*, e12491.
- (708) Silvestre, R.; Llinares Llopis, R.; Contat Rodrigo, L.; Serrano Martínez, V.; Ferri, J.; Garcia-Breijo, E. Low-Temperature Soldering of Surface Mount Devices on Screen-Printed Silver Tracks on Fabrics for Flexible Textile Hybrid Electronics. *Sensors* **2022**, *22*, 5766.
- (709) Tao, X.; Koncar, V.; Huang, T.-H.; Shen, C.-L.; Ko, Y.-C.; Jou, G.-T. How to Make Reliable, Washable, and Wearable Textronic Devices. *Sensors* **2017**, *17*, 673.
- (710) Nashed, M.-N.; Hardy, D. A.; Hughes-Riley, T.; Dias, T. A Novel Method for Embedding Semiconductor Dies within Textile Yarn to Create Electronic Textiles. *Fibers* **2019**, *7*, 12.
- (711) Kang, H.; Rajendran, S. H.; Jung, J. P. Low Melting Temperature Sn-Bi Solder: Effect of Alloying and Nanoparticle Addition on the Microstructural, Thermal, Interfacial Bonding, and Mechanical Characteristics. *Metals* **2021**, *11*, 364.
- (712) Hirman, M.; Navratil, J.; Steiner, F.; Reboun, J.; Soukup, R.; Hamacek, A. Study of Low-Temperature Interconnection Techniques for Instant Assembly of Electronics on Stretchable E-Textile Ribbons. *Text. Res. J.* **2022**, *92*, 4269-4287.

- (713) Liu, Y.; Tu, K. N. Low Melting Point Solders Based on Sn, Bi, and In Elements. *Mater. Today Adv.* **2020**, *8*, 100115.
- (714) Molla, M. T. I.; Goodman, S.; Schleif, N.; Berglund, M. E.; Zacharias, C.; Compton, C.; Dunne, L. E. Surface-Mount Manufacturing for E-Textile Circuits. In Proceedings of the 2017 ACM International Symposium on Wearable Computers, Maui, Hawaii; 2017.
- (715) Lanin, V. L. Infrared Heating in the Technology of Soldering Components in Electronics. *Surf. Eng. Appl. Electrochem.* **2007**, *43*, 381-386.
- (716) Micus, S.; Haupt, M.; Gresser, G. T. Soldering Electronics to Smart Textiles by Pulsed Nd:YAG Laser. *Materials* **2020**, *13*, 2429.
- (717) Micus, S.; Haupt, M.; Gresser, G. T. Automatic Joining of Electrical Components to Smart Textiles by Ultrasonic Soldering. *Sensors* **2021**, *21*, 545.
- (718) Boley, J. W.; White, E. L.; Chiu, G. T. C.; Kramer, R. K. Direct Writing of Gallium-Indium Alloy for Stretchable Electronics. *Adv. Funct. Mater.* **2014**, *24*, 3501-3507.
- (719) Gui, H.; Tan, S.; Wang, Q.; Yu, Y.; Liu, F.; Lin, J.; Liu, J. Spraying Printing of Liquid Metal Electronics on Various Clothes to Compose Wearable Functional Device. *Sci. China Technol. Sci.* **2017**, *60*, 306-316.
- (720) Wang, Q.; Yu, Y.; Yang, J.; Liu, J. Fast Fabrication of Flexible Functional Circuits Based on Liquid Metal Dual-Trans Printing. *Adv. Mater.* **2015**, *27*, 7109-7116.
- (721) Linz, T.; Kallmayer, C. New Interconnection Technologies for the Integration of Electronics on Textile Substrates. In Ambience 2005, 2005.
- (722) Simon, E. P.; Kallmayer, C.; Schneider-Ramelow, M.; Lang, K. D. Development of A Multi-Terminal Crimp Package for Smart Textile Integration. In *2012 4th Electronic System-Integration Technology Conference*, 17-20 Sept. 2012, 2012; pp 1-6.
- (723) Linz, T.; Kallmayer, C.; Aschenbrenner, R.; Reichl, H. Embroidering Electrical Interconnects with Conductive Yarn for the Integration of Flexible Electronic Modules into Fabric. In *Ninth IEEE International Symposium on Wearable Computers (ISWC'05)*, 18-21 Oct. 2005, 2005; pp 86-89.
- (724) Linz, T.; Simon, E.; Walter, H. Fundamental Analysis of Embroidered Contacts for Electronics in Textiles. In *3rd Electronics System Integration Technology Conference ESTC*, 13-16 Sept. 2010, 2010; pp 1-5.
- (725) Buechley, L.; Eisenberg, M. The LilyPad Arduino: Toward Wearable Engineering for Everyone. *IEEE Pervasive Comput.* **2008**, *7*, 12-15.
- (726) Buechley, L.; Eisenberg, M. Fabric PCBs, Electronic Sequins, and Socket Buttons: Techniques for E-Textile Craft. *Pers. Ubiquitous. Comput.* **2009**, *13*, 133-150.

- (727) Briedis, U.; Valisevskis, A.; Grecka, M. Development of a Smart Garment Prototype with Enuresis Alarm Using an Embroidery-machine-based Technique for the Integration of Electronic Components. *Procedia Comput Sci* **2017**, *104*, 369-374.
- (728) Linz, T.; von Krshiwoblozki, M.; Walter, H.; Foerster, P. Contacting Electronics to Fabric Circuits with Nonconductive Adhesive Bonding. *J. Text. Inst.* **2012**, *103*, 1139-1150.
- (729) Hirman, M.; Navratil, J.; Steiner, F.; Hamacek, A. Effect of Washing Cycles on Glued Conductive Joints Used on Stretchable Smart Textile Ribbons. In *2020 IEEE 8th Electronics System-Integration Technology Conference (ESTC)*, 15-18 Sept. 2020, 2020; pp 1-4.
- (730) Zysset, C.; Kinkeldei, T. W.; Munzenrieder, N.; Cherenack, K.; Troster, G. Integration Method for Electronics in Woven Textiles. *IEEE Trans. Compon., Packag., Manuf. Technol.* **2012**, *2*, 1107-1117.
- (731) Merritt, C. R.; Nagle, H. T.; Grant, E. Fabric-Based Active Electrode Design and Fabrication for Health Monitoring Clothing. *IEEE Trans. Inf. Technol.* **2009**, *13*, 274-280.
- (732) Aradhana, R.; Mohanty, S.; Nayak, S. K. A Review on Epoxy-Based Electrically Conductive Adhesives. *Int. J. Adhes. Adhes.* **2020**, *99*, 102596.
- (733) Stennergmann, A.; Balder, D.; Stennergmann, M.; Tabor, C.; Stoffel, N.; Al-Haidari, R.; Garakani, B.; Abbara, U. S. E. M.; Alhendi, M.; et al. Robustness and Reliability of Novel Anisotropic Conductive Epoxy for Stretchable Wearable Electronics. In *2022 IEEE 72nd Electronic Components and Technology Conference (ECTC)*, 31 May-3 June 2022, 2022; pp 762-768.
- (734) Li, Z.; Le, T.; Wu, Z.; Yao, Y.; Li, L.; Tentzeris, M.; Moon, K.-S.; Wong, C. P. Rational Design of a Printable, Highly Conductive Silicone-based Electrically Conductive Adhesive for Stretchable Radio-Frequency Antennas. *Adv. Funct. Mater.* **2015**, *25*, 464-470.
- (735) Li, Z.; Zhang, R.; Moon, K.-S.; Liu, Y.; Hansen, K.; Le, T.; Wong, C. P. Highly Conductive, Flexible, Polyurethane-Based Adhesives for Flexible and Printed Electronics. *Adv. Funct. Mater.* **2013**, *23*, 1459-1465.
- (736) Wang, M.; Wang, K.; Ma, C.; Uzabakiriho, P. C.; Chen, X.; Zhao, G. Mechanical Gradients Enable Highly Stretchable Electronics Based on Nanofiber Substrates. *ACS Appl. Mater. Interfaces* **2022**, *14*, 35997-36006.
- (737) Zhang, N.; Chen, J.; Huang, Y.; Guo, W.; Yang, J.; Du, J.; Fan, X.; Tao, C. A Wearable All-Solid Photovoltaic Textile. *Adv. Mater.* **2016**, *28*, 263-269.
- (738) Chen, C.; Guo, H.; Chen, L.; Wang, Y.-C.; Pu, X.; Yu, W.; Wang, F.; Du, Z.; Wang, Z. L. Direct Current Fabric Triboelectric Nanogenerator for Biomotion Energy Harvesting. *ACS Nano* **2020**, *14*, 4585-4594.

- (739) Rein, M.; Favrod, V. D.; Hou, C.; Khudiyev, T.; Stolyarov, A.; Cox, J.; Chung, C.-C.; Chhav, C.; Ellis, M.; et al. Diode Fibres for Fabric-Based Optical Communications. *Nature* **2018**, *560*, 214-218.
- (740) Han, J.; Xu, C.; Zhang, J.; Xu, N.; Xiong, Y.; Cao, X.; Liang, Y.; Zheng, L.; Sun, J.; et al. Multifunctional Coaxial Energy Fiber toward Energy Harvesting, Storage, and Utilization. *ACS Nano* **2021**, *15*, 1597-1607.
- (741) Kou, L.; Huang, T.; Zheng, B.; Han, Y.; Zhao, X.; Gopalsamy, K.; Sun, H.; Gao, C. Coaxial Wet-Spun Yarn Supercapacitors for High-Energy Density and Safe Wearable Electronics. *Nat. Commun.* **2014**, *5*, 3754.
- (742) Nayeem, M. O. G.; Lee, S.; Jin, H.; Matsuhisa, N.; Jinno, H.; Miyamoto, A.; Yokota, T.; Someya, T. All-Nanofiber-Based, Ultrasensitive, Gas-Permeable Mechanoacoustic Sensors for Continuous Long-Term Heart Monitoring. *Proceed. Nat. Acad. Sci.* **2020**, *117*, 7063-7070.
- (743) Jiang, C.; Wu, C.; Li, X.; Yao, Y.; Lan, L.; Zhao, F.; Ye, Z.; Ying, Y.; Ping, J. All-Electrospun Flexible Triboelectric Nanogenerator Based on Metallic MXene Nanosheets. *Nano Energy* **2019**, *59*, 268-276.
- (744) Laforgue, A. All-Textile Flexible Supercapacitors Using Electrospun Poly(3,4-ethylenedioxythiophene) Nanofibers. *J. Power Sources* **2011**, *196*, 559-564.
- (745) Liu, Q.; Wang, Y.; Dai, L.; Yao, J. Scalable Fabrication of Nanoporous Carbon Fiber Films as Bifunctional Catalytic Electrodes for Flexible Zn-Air Batteries. *Adv. Mater.* **2016**, *28*, 3000-3006.
- (746) Chen, J.-Y.; Hsieh, H.-C.; Chiu, Y.-C.; Lee, W.-Y.; Hung, C.-C.; Chueh, C.-C.; Chen, W.-C. Electrospinning-Induced Elastomeric Properties of Conjugated Polymers for Extremely Stretchable Nanofibers and Rubbery Optoelectronics. *J. Mater. Chem. C* **2020**, *8*, 873-882.
- (747) He, X.; Zhou, N.; Li, Y.; Xiong, P.; Zhang, S.; Ma, Z. An Electrically Stable and Mechanically Robust Stretchable Fiber Conductor Prepared by Dip-Coating Silver Nanowires on Porous Elastomer Yarn. *Mater. Adv.* **2023**, *4*, 1978-1988.
- (748) Kim, D.; Yang, Z.; Cho, J.; Park, D.; Kim, D. H.; Lee, J.; Ryu, S.; Kim, S.-W.; Kim, M. High-Performance Piezoelectric Yarns for Artificial Intelligence-Enabled Wearable Sensing and Classification. *EcoMat* **2023**, *5*, e12384.
- (749) Zhang, C.; Zhang, L.; Pu, Z.; Bao, B.; Ouyang, W.; Li, D. Fabricating 1D Stretchable Fiber-Shaped Electronics Based on Inkjet Printing Technology for Wearable Applications. *Nano Energy* **2023**, *113*, 108574.
- (750) Wang, Y.; Wang, Z.; Wang, Z.; Xiong, T.; Shum, P. P.; Wei, L. Multifunctional Electronic Textiles by Direct 3D Printing of Stretchable Conductive Fibers. *Adv. Electron.*

*Mater.* **2023**, *9*, 2201194.

(751) Hwang, S.; Kang, M.; Lee, A.; Bae, S.; Lee, S.-K.; Lee, S. H.; Lee, T.; Wang, G.; Kim, T.-W. Integration of Multiple Electronic Components on a Microfibre Towards an Emerging Electronic Textile Platform. *Nat. Commun.* **2022**, *13*, 3173.

(752) Zhang, N.; Huang, F.; Zhao, S.; Lv, X.; Zhou, Y.; Xiang, S.; Xu, S.; Li, Y.; Chen, G.; et al. Photo-Rechargeable Fabrics as Sustainable and Robust Power Sources for Wearable Bioelectronics. *Matter* **2020**, *2*, 1260-1269.

(753) Jo, A.; Seo, Y.; Ko, M.; Kim, C.; Kim, H.; Nam, S.; Choi, H.; Hwang, C. S.; Lee, M. J. Textile Resistance Switching Memory for Fabric Electronics. *Adv. Funct. Mater.* **2017**, *27*, 1605593.

(754) Zhang, L.; Andrew, T. Vapor-Coated Monofilament Fibers for Embroidered Electrochemical Transistor Arrays on Fabrics. *Adv. Electron. Mater.* **2018**, *4*, 1800271.

(755) Yoon, J.; Jeong, Y.; Kim, H.; Yoo, S.; Jung, H. S.; Kim, Y.; Hwang, Y.; Hyun, Y.; Hong, W.-K.; et al. Robust and Stretchable Indium Gallium Zinc Oxide-Based Electronic Textiles Formed by Cilia-Assisted Transfer Printing. *Nat. Commun.* **2016**, *7*, 11477.

(756) Dils, C.; Kalas, D.; Reboun, J.; Suchy, S.; Soukup, R.; Moravcova, D.; Krshiwoblozki, M. v.; Schneider-Ramelow, M. Interconnecting Embroidered Hybrid Conductive Yarns by Ultrasonic Plastic Welding for e-Textiles. *Text. Res. J.* **2022**, *92*, 4501-4520.

(757) Muñoz, E.; García-Manrique, J. A. Water Absorption Behaviour and Its Effect on the Mechanical Properties of Flax Fibre Reinforced Bioepoxy Composites. *Int. J. Polym. Sci.* **2015**, *2015*, 390275.

(758) Kim, J. K.; Pal, K. *Recent Advances in the Processing of Wood-Plastic Composites*; Springer Berlin, Heidelberg, 2010.

(759) Molina, R.; Esquena, J.; Erra, P. Interfacial Processes in Textile Materials: Relevance to Adhesion. *J. Adhes. Sci. Technol.* **2010**, *24*, 7-33.

(760) Wang, W.; Wang, S.; Rastak, R.; Ochiai, Y.; Niu, S.; Jiang, Y.; Arunachala, P. K.; Zheng, Y.; Xu, J.; et al. Strain-Insensitive Intrinsically Stretchable Transistors and Circuits. *Nat. Electron.* **2021**, *4*, 143-150.

(761) Libanori, R.; Erb, R. M.; Reiser, A.; Le Ferrand, H.; Süess, M. J.; Spolenak, R.; Studart, A. R. Stretchable Heterogeneous Composites with Extreme Mechanical Gradients. *Nat. Commun.* **2012**, *3*, 1265.

(762) Ashori, A.; Nourbakhsh, A. Preparation and Characterization of Polypropylene/Wood Flour/Nanoclay Composites. *Eur. J. Wood Wood Prod.* **2011**, *69*, 663-666.

(763) Signorini, C.; Nobili, A.; Cedillo González, E. I.; Siligardi, C. Silica Coating for

Interphase Bond Enhancement of Carbon and AR-Glass Textile Reinforced Mortar (TRM). *Compos. B. Eng.* **2018**, *141*, 191-202.

(764) Vilakati, G. D.; Mishra, A. K.; Mishra, S. B.; Mamba, B. B.; Thwala, J. M. Influence of TiO<sub>2</sub>-Modification on the Mechanical and Thermal Properties of Sugarcane Bagasse–EVA Composites. *J. Inorg. Organomet. Polym. Mater.* **2010**, *20*, 802-808.

(765) Tania, I. S.; Ali, M. Coating of ZnO Nanoparticle on Cotton Fabric to Create a Functional Textile with Enhanced Mechanical Properties. *Polymers* **2021**, *13*, 2701.

(766) Javanshour, F.; Ramakrishnan, K. R.; Layek, R. K.; Laurikainen, P.; Prapavesis, A.; Kanerva, M.; Kallio, P.; Van Vuure, A. W.; Sarlin, E. Effect of Graphene Oxide Surface Treatment on the Interfacial Adhesion and the Tensile Performance of Flax Epoxy Composites. *Compos. Part A Appl. Sci. Manuf.* **2021**, *142*, 106270.

(767) Birenboim, M.; Alatawna, A.; Sripada, R.; Nahum, L.; Cullari, L. L.; Peled, A.; Regev, O. Enhancement of Fabric–Mortar Interfacial Adhesion by Particle Decoration: Insights from Pull-Off Measurements. *Mater. Struct.* **2021**, *54*, 200.

(768) Tian, Y.; Huang, X.; Cheng, Y.; Niu, Y.; Ma, J.; Zhao, Y.; Kou, X.; Ke, Q. Applications of Adhesives in Textiles: A Review. *Eur. Polym. J.* **2022**, *167*, 111089.

(769) Saheb, D. N.; Jog, J. P. Natural Fiber Polymer Composites: A Review. *Adv. Polym. Technol.* **1999**, *18*, 351-363.

(770) Mohammed, M.; Rasidi, M.; Mohammed, A. M.; Rahman, R.; Osman, A. F.; Adam, T.; Betar, B. O.; Dahham, O. S. Interfacial Bonding Mechanisms of Natural Fibre-Matrix Composites: An Overview. *BioResources* **2022**, *17*, 7031-7090.

(771) Oushabi, A.; Oudrhiri Hassani, F.; Abboud, Y.; Sair, S.; Tanane, O.; El Bouari, A. Improvement of the Interface Bonding Between Date Palm Fibers and Polymeric Matrices Using Alkali-Silane Treatments. *Int. J. Ind. Chem.* **2018**, *9*, 335-343.

(772) Moyano, M. A.; París, R.; Martín-Martínez, J. M. Viscoelastic and Adhesion Properties of Hot-Melts Made with Blends of Ethylene-Co-N-Butyl Acrylate (EBA) and Ethylene-Co-Vinyl Acetate (EVA) Copolymers. *Int. J. Adhes. Adhes.* **2019**, *88*, 34-42.

(773) Staeger, M.; Finot, E.; Brachais, C.-H.; Auguste, S.; Durand, H. Surface Investigation of Adhesive Formulation Consisting of UV Sensitive Triblock Poly(Styrene-b-Butadiene-b-Styrene) Copolymer. *Appl. Surf. Sci.* **2002**, *185*, 231-242.

(774) Galante, A. J.; Pilsbury, B. C.; Li, M.; LeMieux, M.; Liu, Q.; Leu, P. W. Achieving Highly Conductive, Stretchable, and Washable Fabric from Reactive Silver Ink and Increased Interfacial Adhesion. *ACS Appl. Polym. Mater.* **2022**, *4*, 5253-5260.

(775) Kan, C. W. Evaluating Antistatic Performance of Plasma-Treated Polyester. *Fibers*

*Polym.* **2007**, *8*, 629-634.

(776) Bhat, N.; Netravali, A.; Gore, A.; Sathianarayanan, M.; Arolkar, G.; Deshmukh, R. Surface Modification of Cotton Fabrics Using Plasma Technology. *Text. Res. J.* **2011**, *81*, 1014-1026.

(777) Jelil, R. A. A Review of Low-Temperature Plasma Treatment of Textile Materials. *J. Mater. Sci.* **2015**, *50*, 5913-5943.

(778) Shin, Y.; Yoo, D. I. Surface Characterization of Pet Nonwoven Fabric Treated by He/O<sub>2</sub> Atmospheric Pressure Plasma. *J. App. Polym. Sci.* **2008**, *108*, 785-790.

(779) Karahan, H. A.; Özdoğan, E. Improvements of Surface Functionality of Cotton Fibers by Atmospheric Plasma Treatment. *Fibers Polym.* **2008**, *9*, 21-26.

(780) Kim, M. S.; Kang, T. J. Dimensional and Surface Properties of Plasma and Silicone Treated Wool Fabric. *Text. Res. J.* **2002**, *72*, 113-120.

(781) Bozaci, E.; Sever, K.; Sarikanat, M.; Seki, Y.; Demir, A.; Ozdogan, E.; Tavman, I. Effects of the Atmospheric Plasma Treatments on Surface and Mechanical Properties of Flax Fiber and Adhesion Between Fiber-Matrix for Composite Materials. *Compos. B. Eng.* **2013**, *45*, 565-572.

(782) Felix, J. M.; Carlsson, C. M. G.; Gatenholm, P. Adhesion Characteristics of Oxygen Plasma-Treated Rayon Fibers. *J. Adhes. Sci. Technol.* **1994**, *8*, 163-180.

(783) Ráhel', J.; Černák, M.; Hudec, I.; Štefečka, M.; Kando, M.; Chodák, I. Surface Modification of Polyester Monofilaments by Atmospheric-Pressure Nitrogen Plasma. *Plasmas Polym.* **2000**, *5*, 119-127.

(784) Huang, C.-Y.; Wu, J.-Y.; Tsai, C.-S.; Hsieh, K.-H.; Yeh, J.-T.; Chen, K.-N. Effects of Argon Plasma Treatment on the Adhesion Property of Ultra High Molecular Weight Polyethylene (UHMWPE) Textile. *Surf. Coat. Technol.* **2013**, *231*, 507-511.

(785) Locher, I.; Troster, G. Fundamental Building Blocks for Circuits on Textiles. *IEEE Trans. Adv. Packag.* **2007**, *30*, 541-550.

(786) Stanley, J.; Hunt, J. A.; Kunovski, P.; Wei, Y. Novel Interposer for Modular Electronic Textiles: Enabling Detachable Connections Between Flexible Electronics and Conductive Textiles. *IEEE Sens. Lett.* **2022**, *6*, 1-4.

(787) Takamatsu, S.; Sato, S.; Itoh, T. Stress Concentration-Relocating Interposer in Electronic Textile Packaging using Thermoplastic Elastic Polyurethane Film With via Holes For Bearing Textile Stretch. *Sci. Rep.* **2022**, *12*, 9269.

(788) Vervust, T.; Buyle, G.; Bossuyt, F.; Vanfleteren, J. Integration of Stretchable and Washable Electronic Modules for Smart Textile Applications. *J. Text. Inst.* **2012**, *103*, 1127-

1138.

(789) Vanfleteren, J.; Gonzalez, M.; Bossuyt, F.; Hsu, Y. Y.; Vervust, T.; De Wolf, I.; Jablonski, M. Printed Circuit Board Technology Inspired Stretchable Circuits. *MRS Bull.* **2012**, *37*, 254-260.

(790) Cotton, D. P. J.; Popel, A.; Graz, I. M.; Lacour, S. P. Photopatterning the Mechanical Properties of Polydimethylsiloxane Films. *J. Appl. Phys.* **2011**, *109*, 054905.

(791) Gu, M.; Song, W.-J.; Hong, J.; Kim, S. Y.; Shin, T. J.; Kotov, N. A.; Park, S.; Kim, B.-S. Stretchable Batteries with Gradient Multilayer Conductors. *Sci. Adv.* **2019**, *5*, eaaw1879.

(792) Jin, H.; Matsuhisa, N.; Lee, S.; Abbas, M.; Yokota, T.; Someya, T. Enhancing the Performance of Stretchable Conductors for E-Textiles by Controlled Ink Permeation. *Adv. Mater.* **2017**, *29*, 1605848.

(793) Yang, K.; Torah, R.; Wei, Y.; Beeby, S.; Tudor, J. Waterproof and Durable Screen Printed Silver Conductive Tracks on Textiles. *Text. Res. J.* **2013**, *83*, 2023-2031.

(794) Suo, Z.; Ma, E. Y.; Gleskova, H.; Wagner, S. Mechanics of Rollable and Foldable Film-on-Foil Electronics. *Appl. Phys. Lett.* **1999**, *74*, 1177-1179.

(795) Kallmayer, C.; Pisarek, R.; Neudeck, A.; Cichos, S.; Gimpel, S.; Aschenbrenner, R.; Reichlt, H. New Assembly Technologies for Textile Transponder Systems. In *53rd Electronic Components and Technology Conference, 2003. Proceedings.*, 27-30 May 2003, 2003; pp 1123-1126.

(796) Jeong, S. Y.; Shim, H. R.; Na, Y.; Kang, K. S.; Jeon, Y.; Choi, S.; Jeong, E. G.; Park, Y. C.; Cho, H.-E.; et al. Foldable and Washable Textile-Based OLEDs with a Multi-Functional Near-Room-Temperature Encapsulation Layer for Smart E-Textiles. *npj Flex. Electron.* **2021**, *5*, 15.

(797) Wu, Q.; Hu, J. Waterborne Polyurethane Based Thermoelectric Composites and Their Application Potential in Wearable Thermoelectric Textiles. *Compos. B. Eng.* **2016**, *107*, 59-66.

(798) Lin, Z.; Yang, J.; Li, X.; Wu, Y.; Wei, W.; Liu, J.; Chen, J.; Yang, J. Large-Scale and Washable Smart Textiles Based on Triboelectric Nanogenerator Arrays for Self-Powered Sleeping Monitoring. *Adv. Funct. Mater.* **2018**, *28*, 1704112.

(799) Wang, M.; Ma, C.; Uzabakiriho, P. C.; Chen, X.; Chen, Z.; Cheng, Y.; Wang, Z.; Zhao, G. Stencil Printing of Liquid Metal upon Electrospun Nanofibers Enables High-Performance Flexible Electronics. *ACS Nano* **2021**, *15*, 19364–19376.

(800) Jiang, Y.; Xu, L.; Pan, K.; Leng, T.; Li, Y.; Danoon, L.; Hu, Z. e-Textile Embroidered Wearable Near-Field Communication RFID Antennas. *IET Microwaves, Antennas & Propagation* **2019**, *13*, 99-104.



- (801) Ashyap, A. Y. I.; Abidin, Z. Z.; Dahlan, S. H.; Majid, H. A.; Shah, S. M.; Kamarudin, M. R.; Alomainy, A. Compact and Low-Profile Textile EBG-Based Antenna for Wearable Medical Applications. *IEEE Antennas Wirel. Propag. Lett.* **2017**, *16*, 2550-2553.
- (802) Ashyap, A. Y. I.; Abidin, Z. Z.; Dahlan, S. H.; Majid, H. A.; Waddah, A. M. A.; Kamarudin, M. R.; Oguntala, G. A.; Abd-Alhameed, R. A.; Noras, J. M. Inverted E-Shaped Wearable Textile Antenna for Medical Applications. *IEEE Access* **2018**, *6*, 35214-35222.
- (803) Plant, L.; Noriega, B.; Sonti, A.; Constant, N.; Mankodiya, K. Smart E-Textile Gloves for Quantified Measurements in Movement Disorders. In *2016 IEEE MIT Undergraduate Research Technology Conference (URTC)*, 4-6 Nov. 2016, 2016; pp 1-4.
- (804) Tao, X.; Huang, T.-H.; Shen, C.-L.; Ko, Y.-C.; Jou, G.-T.; Koncar, V. Bluetooth Low Energy-Based Washable Wearable Activity Motion and Electrocardiogram Textronic Monitoring and Communicating System. *Adv. Mater. Technol.* **2018**, *3*, 1700309.
- (805) Fang, Y.; Zou, Y.; Xu, J.; Chen, G.; Zhou, Y.; Deng, W.; Zhao, X.; Roustaei, M.; Hsiai, T. K.; et al. Ambulatory Cardiovascular Monitoring via a Machine-Learning-Assisted Textile Triboelectric Sensor. *Adv. Mater.* **2021**, *33*, 2104178.
- (806) Zhu, M.; Shi, Q.; He, T.; Yi, Z.; Ma, Y.; Yang, B.; Chen, T.; Lee, C. Self-Powered and Self-Functional Cotton Sock Using Piezoelectric and Triboelectric Hybrid Mechanism for Healthcare and Sports Monitoring. *ACS Nano* **2019**, *13*, 1940-1952.
- (807) Zhou, F.; Chai, Y. Near-Sensor and in-Sensor Computing. *Nat. Electron.* **2020**, *3*, 664-671.
- (808) Yang, H.; Li, J.; Xiao, X.; Wang, J.; Li, Y.; Li, K.; Li, Z.; Yang, H.; Wang, Q.; et al. Topographic Design in Wearable Mxene Sensors with in-Sensor Machine Learning for Full-Body Avatar Reconstruction. *Nat. Commun.* **2022**, *13*, 5311.
- (809) Shuvo, I. I.; Shah, A.; Dagdeviren, C. Electronic Textile Sensors for Decoding Vital Body Signals: State-of-the-Art Review on Characterizations and Recommendations. *Adv. Intell. Syst.* **2022**, *4*, 2100223.
- (810) Yang, Y.; Wei, X.; Zhang, N.; Zheng, J.; Chen, X.; Wen, Q.; Luo, X.; Lee, C.-Y.; Liu, X.; et al. A Non-Printed Integrated-Circuit Textile for Wireless Theranostics. *Nat. Commun.* **2021**, *12*, 4876.
- (811) Lee, S.; Kim, S.-R.; Jeon, K.-H.; Jeon, J.-W.; Lee, E.-I.; Jeon, J.; Oh, J.-H.; Yoo, J.-H.; Kil, H.-J.; et al. A Fabric-Based Wearable Sensor for Continuous Monitoring of Decubitus Ulcer of Subjects Lying on a Bed. *Sci. Rep.* **2023**, *13*, 5773.
- (812) Libanori, A.; Chen, G.; Zhao, X.; Zhou, Y.; Chen, J. Smart Textiles for Personalized Healthcare. *Nat. Electron.* **2022**, *5*, 142-156.

- (813) Wang, H.; Zhang, Y.; Liang, X.; Zhang, Y. Smart Fibers and Textiles for Personal Health Management. *ACS Nano* **2021**, *15*, 12497-12508.
- (814) Hasanpour, S.; Karperien, L.; Walsh, T.; Jahanshahi, M.; Hadisi, Z.; Neale, K. J.; Christie, B. R.; Djilali, N.; Akbari, M. A Hybrid Thread-Based Temperature and Humidity Sensor for Continuous Wound Monitoring. *Sens. Actuator B Chem.* **2022**, *370*, 132414.
- (815) Wang, F.; Zhu, B.; Shu, L.; Li, Y.; Lai, X.; Ma, L.; Ji, P.; Zhou, Q.; Yu, T.; et al. Smart Clothing with Built-In Soft Sensing Network for Measuring Temporal and Spatial Distribution of Pressure under Impact Scenarios. *Adv. Sens. Res.* **2023**, *2*, 2200019.
- (816) Fay, C. D.; Mannering, N.; Jeiranikhameneh, A.; Mokhtari, F.; Foroughi, J.; Baughman, R. H.; Choong, P. F. M.; Wallace, G. G. Wearable Carbon Nanotube-Spandex Textile Yarns for Knee Flexion Monitoring. *Adv. Sens. Res.* **2023**, *2*, 2200021.
- (817) Nie, B.; Huang, R.; Yao, T.; Zhang, Y.; Miao, Y.; Liu, C.; Liu, J.; Chen, X. Textile-Based Wireless Pressure Sensor Array for Human-Interactive Sensing. *Adv. Funct. Mater.* **2019**, *29*, 1808786.
- (818) Zheng, Q.; Dai, X.; Wu, Y.; Liang, Q.; Wu, Y.; Yang, J.; Dong, B.; Gao, G.; Qin, Q.; et al. Self-Powered High-Resolution Smart Insole System for Plantar Pressure Mapping. *BMEMat* **2023**, *1*, e12008.
- (819) Wei, C.; Cheng, R.; Ning, C.; Wei, X.; Peng, X.; Lv, T.; Sheng, F.; Dong, K.; Wang, Z. L. A Self-Powered Body Motion Sensing Network Integrated with Multiple Triboelectric Fabrics for Biometric Gait Recognition and Auxiliary Rehabilitation Training. *Adv. Funct. Mater.* **2023**, *33*, 2303562.
- (820) Kwon, S.; Kim, H.; Yeo, W.-H. Recent Advances in Wearable Sensors and Portable Electronics for Sleep Monitoring. *iScience* **2021**, *24*, 102461.
- (821) Liu, T.; Gou, G.-y.; Gao, F.; Yao, P.; Wu, H.; Guo, Y.; Yin, M.; Yang, J.; Wen, T.; et al. Multichannel Flexible Pulse Perception Array for Intelligent Disease Diagnosis System. *ACS Nano* **2023**, *17*, 5673-5685.
- (822) Song, X.; Li, B.; Wang, P.; Zhou, Y.; Wang, J.; Wang, Y.; Fang, C.; Jin, M. Flexible Piezoelectric Sensor for Pregnant Recognition Based on the Pulse-Taking Procedure in Traditional Chinese Medicine. *Eng. Rep.* **2023**, *n/a*, e12645.
- (823) Li, S.; Wang, H.; Ma, W.; Qiu, L.; Xia, K.; Zhang, Y.; Lu, H.; Zhu, M.; Liang, X.; et al. Monitoring Blood Pressure and Cardiac Function without Positioning via a Deep Learning-Assisted Strain Sensor Array. *Sci. Adv.* **2023**, *9*, eadh0615.
- (824) Qiao, Z.; Chen, S.; Fan, S.; Xiong, Z.; Lim, C. T. Epidermal Bioelectronics for Management of Chronic Diseases: Materials, Devices and Systems. *Adv. Sens. Res.* **2023**, *2*,

2200068.

(825) Nguyen, P. Q.; Soenksen, L. R.; Donghia, N. M.; Angenent-Mari, N. M.; de Puig, H.; Huang, A.; Lee, R.; Slomovic, S.; Galbersanini, T.; et al. Wearable Materials with Embedded Synthetic Biology Sensors for Biomolecule Detection. *Nat. Biotechnol.* **2021**, *39*, 1366-1374.

(826) Alshabouna, F.; Lee, H. S.; Barandun, G.; Tan, E.; Cotur, Y.; Asfour, T.; Gonzalez-Macia, L.; Coatsworth, P.; Núñez-Bajo, E.; et al. PEDOT:PSS-Modified Cotton Conductive Thread for Mass Manufacturing of Textile-Based Electrical Wearable Sensors by Computerized Embroidery. *Mater. Today* **2022**, *59*, 56-67.

(827) Kim, J.-H.; Marcus, C.; Ono, R.; Sadat, D.; Mirzazadeh, A.; Jens, M.; Fernandez, S.; Zheng, S.; Durak, T.; et al. A Conformable Sensory Face Mask for Decoding Biological and Environmental Signals. *Nat. Electron.* **2022**, *5*, 794-807.

(828) Ma, X.; Wang, P.; Huang, L.; Ding, R.; Zhou, K.; Shi, Y.; Chen, F.; Zhuang, Q.; Huang, Q.; et al. A Monolithically Integrated in-Textile Wristband for Wireless Epidermal Biosensing. *Sci. Adv.* **2023**, *9*, eadj2763.

(829) Feng, B.; Wei, H.; Shi, B.; Zhao, D.; Ye, S.; Wu, G.; Wang, R.; Zuo, G.; Wu, Z.; et al. Sleeping Heart Monitoring Using Hydrogel-Textile Capacitive ECG Electrodes. *IEEE Sens. J.* **2022**, *22*, 9255-9267.

(830) Zhao, Z.; Wang, J.; Wang, S.; Wang, R.; Lu, Y.; Yuan, Y.; Chen, J.; Dai, Y.; Liu, Y.; et al. Multimodal Sensing in Stroke Motor Rehabilitation. *Adv. Sens. Res.* **2023**, *2*, 2200055.

(831) Chen, W.; Cai, M.; Wu, J.; Ma, H.; Liu, W.; Xu, F. Highly Conductive, Durable, Washable, and Scalable Composite Yarn for Multifunctional Wearable Electronic Applications. *Compos. Sci. Technol.* **2023**, *241*, 110115.

(832) De Fazio, R.; Mastronardi, V. M.; De Vittorio, M.; Visconti, P. Wearable Sensors and Smart Devices to Monitor Rehabilitation Parameters and Sports Performance: An Overview. *Sensors* **2023**, *23*, 1856.

(833) Xu, D.; Ouyang, Z.; Dong, Y.; Yu, H.-Y.; Zheng, S.; Li, S.; Tam, K. C. Robust, Breathable and Flexible Smart Textiles as Multifunctional Sensor and Heater for Personal Health Management. *Adv. Fiber Mater.* **2023**, *5*, 282-295.

(834) Liang, Q.; Zhang, D.; Wu, Y.; Qu, X.; Jia, Y.; Chen, S.; Wang, H.; Lee, C. Stretchable Helical Fibers with Skin-Core Structure for Pressure and Proximity Sensing. *Nano Energy* **2023**, *113*, 108598.

(835) Ye, X.; Shi, B.; Li, M.; Fan, Q.; Qi, X.; Liu, X.; Zhao, S.; Jiang, L.; Zhang, X.; et al. All-Textile Sensors for Boxing Punch Force and Velocity Detection. *Nano Energy* **2022**, *97*, 107114.

- (836) Shathi, M. A.; Chen, M.; Khoso, N. A.; Rahman, M. T.; Bhattacharjee, B. Graphene Coated Textile Based Highly Flexible and Washable Sports Bra for Human Health Monitoring. *Mater. Des.* **2020**, *193*, 108792.
- (837) Wang, R.; Zhai, Q.; An, T.; Gong, S.; Cheng, W. Stretchable Gold Fiber-Based Wearable Textile Electrochemical Biosensor for Lactate Monitoring in Sweat. *Talanta* **2021**, *222*, 121484.
- (838) Zhang, J.; Chen, M.; Peng, Y.; Li, S.; Han, D.; Ren, S.; Qin, K.; Li, S.; Han, T.; et al. Wearable Biosensors for Human Fatigue Diagnosis: A Review. *Bioeng. Transl. Med.* **2023**, *8*, e10318.
- (839) Zhao, Z.; Li, Q.; Dong, Y.; Gong, J.; Li, Z.; Zhang, J. Core-Shell Structured Gold Nanorods on Thread-Embroidered Fabric-Based Microfluidic Device for ex situ Detection Of Glucose and Lactate in Sweat. *Sens. Actuator B Chem.* **2022**, *353*, 131154.
- (840) Zhao, C.; Li, X.; Wu, Q.; Liu, X. A Thread-Based Wearable Sweat Nanobiosensor. *Biosens. Bioelectron.* **2021**, *188*, 113270.
- (841) Qu, C.; Wang, S.; Liu, L.; Bai, Y.; Li, L.; Sun, F.; Hao, M.; Li, T.; Lu, Q.; et al. Bioinspired Flexible Volatile Organic Compounds Sensor Based on Dynamic Surface Wrinkling with Dual-Signal Response. *Small* **2019**, *15*, 1900216.
- (842) Tat, T.; Chen, G.; Zhao, X.; Zhou, Y.; Xu, J.; Chen, J. Smart Textiles for Healthcare and Sustainability. *ACS Nano* **2022**, *16*, 13301-13313.
- (843) Li, F.; Xue, H.; Lin, X.; Zhao, H.; Zhang, T. Wearable Temperature Sensor with High Resolution for Skin Temperature Monitoring. *ACS Appl. Mater. Interfaces* **2022**, *14*, 43844-43852.
- (844) Zhang, Z.; Cui, L.; Shi, X.; Tian, X.; Wang, D.; Gu, C.; Chen, E.; Cheng, X.; Xu, Y.; et al. Textile Display for Electronic and Brain-Interfaced Communications. *Adv. Mater.* **2018**, *30*, 1800323.
- (845) Xu, K.; Lu, Y.; Takei, K. Flexible Hybrid Sensor Systems with Feedback Functions. *Adv. Funct. Mater.* **2021**, *31*, 2007436.
- (846) Wang, M.; Wang, T.; Luo, Y.; He, K.; Pan, L.; Li, Z.; Cui, Z.; Liu, Z.; Tu, J.; et al. Fusing Stretchable Sensing Technology with Machine Learning for Human–Machine Interfaces. *Adv. Funct. Mater.* **2021**, *31*, 2008807.
- (847) Kim, K. K.; Suh, Y.; Ko, S. H. Smart Stretchable Electronics for Advanced Human–Machine Interface. *Adv. Intell. Syst.* **2021**, *3*, 2000157.
- (848) Yin, R.; Wang, D.; Zhao, S.; Lou, Z.; Shen, G. Wearable Sensors-Enabled Human–Machine Interaction Systems: From Design to Application. *Adv. Funct. Mater.* **2021**, *31*,

2008936.

(849) Li, T.; Su, Y.; Chen, F.; Zheng, H.; Meng, W.; Liu, Z.; Ai, Q.; Liu, Q.; Tan, Y.; et al. Bioinspired Stretchable Fiber-Based Sensor toward Intelligent Human–Machine Interactions. *ACS Appl. Mater. Interfaces* **2022**, *14*, 22666–22677.

(850) Zhu, C.; Li, R.; Chen, X.; Chalmers, E.; Liu, X.; Wang, Y.; Xu, B. B.; Liu, X. Ultraelastic Yarns from Curcumin-Assisted ELD toward Wearable Human-Machine Interface Textiles. *Adv. Sci.* **2020**, *7*, 2002009.

(851) Duan, S.; Lin, Y.; Zhang, C.; Li, Y.; Zhu, D.; Wu, J.; Lei, W. Machine-Learned, Waterproof MXene Fiber-Based Glove Platform for Underwater Interactivities. *Nano Energy* **2022**, *91*, 106650.

(852) Pang, Y.; Xu, X.; Chen, S.; Fang, Y.; Shi, X.; Deng, Y.; Wang, Z.-L.; Cao, C. Skin-Inspired Textile-Based Tactile Sensors Enable Multifunctional Sensing of Wearables and Soft Robots. *Nano Energy* **2022**, *96*, 107137.

(853) Zhong, W.; Ming, X.; Li, W.; Jia, K.; Jiang, H.; Ke, Y.; Li, M.; Wang, D. Wearable Human-Machine Interaction Device Integrated by All-Textile-Based Tactile Sensors Array via Facile Cross-Stitch. *Sens. Actuator A Phys.* **2022**, *333*, 113240.

(854) Chen, Y.; Chen, E.; Wang, Z.; Ling, Y.; Fisher, R.; Li, M.; Hart, J.; Mu, W.; Gao, W.; et al. Flexible, Durable, and Washable Triboelectric Yarn and Embroidery for Self-Powered Sensing and Human-Machine Interaction. *Nano Energy* **2022**, *104*, 107929.

(855) He, Q.; Wu, Y.; Feng, Z.; Fan, W.; Lin, Z.; Sun, C.; Zhou, Z.; Meng, K.; Wu, W.; et al. An All-Textile Triboelectric Sensor for Wearable Teleoperated Human-Machine Interaction. *J. Mater. Chem. A* **2019**, *7*, 26804–26811.

(856) Ning, C.; Zheng, G.; Dong, K. Emerging Self-Powered Autonomous Sensing Triboelectric Fibers toward Future Wearable Human-Computer Interaction Devices. *Adv. Sens. Res.* **2023**, *2*, 2200044.

(857) Lim, T.; Won, S.; Kim, M.; Trout, M. A.; Kim, J.; George, J. A.; Zhang, H. Multiscale Material Engineering of a Conductive Polymer and a Liquid Metal Platform for Stretchable and Biostable Human-Machine-Interface Bioelectronic Applications. *ACS Mater. Lett.* **2022**, *4*, 2289–2297.

(858) Lu, L.; Jiang, C.; Hu, G.; Liu, J.; Yang, B. Flexible Noncontact Sensing for Human–Machine Interaction. *Adv. Mater.* **2021**, *33*, 2100218.

(859) Biswas, S.; Visell, Y. Haptic Perception, Mechanics, and Material Technologies for Virtual Reality. *Adv. Funct. Mater.* **2021**, *31*, 2008186.

(860) Liu, Y.; Yiu, C. K.; Zhao, Z.; Park, W.; Shi, R.; Huang, X.; Zeng, Y.; Wang, K.; Wong,

- T. H.; et al. Soft, Miniaturized, Wireless Olfactory Interface for Virtual Reality. *Nat. Commun.* **2023**, *14*, 2297.
- (861) Yu, X.; Xie, Z.; Yu, Y.; Lee, J.; Vazquez-Guardado, A.; Luan, H.; Ruban, J.; Ning, X.; Akhtar, A.; et al. Skin-Integrated Wireless Haptic Interfaces for Virtual and Augmented Reality. *Nature* **2019**, *575*, 473-479.
- (862) Yang, P.; Shi, Y.; Tao, X.; Liu, Z.; Li, S.; Chen, X.; Wang, Z. L. Self-Powered Virtual Olfactory Generation System Based on Bionic Fibrous Membrane and Electrostatic Field Accelerated Evaporation. *EcoMat* **2023**, *5*, e12298.
- (863) Duan, S.; Zhao, F.; Yang, H.; Hong, J.; Shi, Q.; Lei, W.; Wu, J. A Pathway into Metaverse: Gesture Recognition Enabled by Wearable Resistive Sensors. *Adv. Sens. Res.* **2023**, *2*, 2200054.
- (864) Kim, J. J.; Wang, Y.; Wang, H.; Lee, S.; Yokota, T.; Someya, T. Skin Electronics: Next-Generation Device Platform for Virtual and Augmented Reality. *Adv. Funct. Mater.* **2021**, *31*, 2009602.
- (865) Zhou, Y.; Xiao, X.; Chen, G.; Zhao, X.; Chen, J. Self-powered sensing technologies for human Metaverse interfacing. *Joule* **2022**, *6*, 1381-1389.
- (866) Fang, H.; Guo, J.; Wu, H. Wearable Triboelectric Devices for Haptic Perception and VR/AR Applications. *Nano Energy* **2022**, *96*, 107112.
- (867) Wen, F.; Sun, Z.; He, T.; Shi, Q.; Zhu, M.; Zhang, Z.; Li, L.; Zhang, T.; Lee, C. Machine Learning Glove Using Self-Powered Conductive Superhydrophobic Triboelectric Textile for Gesture Recognition in VR/AR Applications. *Adv. Sci.* **2020**, *7*, 2000261.
- (868) Zhang, Z.; He, T.; Zhu, M.; Sun, Z.; Shi, Q.; Zhu, J.; Dong, B.; Yuce, M. R.; Lee, C. Deep Learning-Enabled Triboelectric Smart Socks for IoT-based Gait Analysis and VR Applications. *npj Flex. Electron.* **2020**, *4*, 29.
- (869) Chen, M.; Cui, D.; Haick, H.; Tang, N. Artificial Intelligence-Based Medical Sensors for Healthcare System. *Adv. Sens. Res.* **2023**, *n/a*, 2300009.
- (870) Zhan, Y.; Mei, Y.; Zheng, L. Materials Capability and Device Performance in Flexible Electronics for the Internet of Things. *J. Mater. Chem. C* **2014**, *2*, 1220-1232.
- (871) Lin, Y.; Bariya, M.; Javey, A. Wearable Biosensors for Body Computing. *Adv. Funct. Mater.* **2021**, *31*, 2008087.
- (872) Wen, F.; He, T.; Liu, H.; Chen, H.-Y.; Zhang, T.; Lee, C. Advances in Chemical Sensing Technology for Enabling the Next-Generation Self-Sustainable Integrated Wearable System in the IoT Era. *Nano Energy* **2020**, *78*, 105155.
- (873) Portilla, L.; Loganathan, K.; Faber, H.; Eid, A.; Hester, J. G. D.; Tentzeris, M. M.; Fattori, M.; Cantatore, E.; Jiang, C.; et al. Wirelessly Powered Large-Area Electronics for the Internet

of Things. *Nat. Electron.* **2023**, *6*, 10-17.

(874) Zopf, S. F.; Manser, M. Screen-printed Military Textiles for Wearable Energy Storage. *J. Eng. Fibers Fabr.* **2016**, *11*, 155892501601100303.

(875) He, H.; Liu, J.; Wang, Y.; Zhao, Y.; Qin, Y.; Zhu, Z.; Yu, Z.; Wang, J. An Ultralight Self-Powered Fire Alarm e-Textile Based on Conductive Aerogel Fiber with Repeatable Temperature Monitoring Performance Used in Firefighting Clothing. *ACS Nano* **2022**, *16*, 2953-2967.

(876) Yang, J.; Rong, L.; Huang, W.; Wu, Z.; Ding, Q.; Zhang, H.; Lin, Y.; Li, F.; Li, C.; et al. Flame-Retardant, Flexible, and Breathable Smart Humidity Sensing Fabrics Based on Hydrogels for Respiratory Monitoring and Non-Contact Sensing. *VIEW* **2023**, *4*, 20220060.

(877) Sun, K.; Wang, F.; Yang, W.; Liu, H.; Pan, C.; Guo, Z.; Liu, C.; Shen, C. Flexible Conductive Polyimide Fiber/MXene Composite Film for Electromagnetic Interference Shielding and Joule Heating with Excellent Harsh Environment Tolerance. *ACS Appl. Mater. Interfaces* **2021**, *13*, 50368-50380.

(878) Ding, Y.; Hou, H.; Zhao, Y.; Zhu, Z.; Fong, H. Electrospun Polyimide Nanofibers and Their Applications. *Prog. Polym. Sci.* **2016**, *61*, 67-103.

(879) Wang, X.; Zhang, Y.; Zhao, Y.; Li, G.; Yan, J.; Yu, J.; Ding, B. A General Strategy to Fabricate Flexible Oxide Ceramic Nanofibers with Gradient Bending-Resilience Properties. *Adv. Funct. Mater.* **2021**, *31*, 2103989.

(880) Ding, Y.; Xu, W.; Wang, W.; Fong, H.; Zhu, Z. Scalable and Facile Preparation of Highly Stretchable Electrospun PEDOT:PSS@PU Fibrous Nonwovens toward Wearable Conductive Textile Applications. *ACS Appl. Mater. Interfaces* **2017**, *9*, 30014-30023.

(881) Liang, X.; Li, H.; Dou, J.; Wang, Q.; He, W.; Wang, C.; Li, D.; Lin, J.-M.; Zhang, Y. Stable and Biocompatible Carbon Nanotube Ink Mediated by Silk Protein for Printed Electronics. *Adv. Mater.* **2020**, *32*, 2000165.

(882) Ge, Q.; Chu, J.; Cao, W.; Yi, F.; Ran, Z.; Jin, Z.; Mao, B.; Li, Z.; Novoselov, K. S. Graphene-Based Textiles for Thermal Management and Flame Retardancy. *Adv. Funct. Mater.* **2022**, *32*, 2205934.

(883) Asif, M.; Aziz, A.; Ashraf, G.; Iftikhar, T.; Sun, Y.; Xiao, F.; Liu, H. Unveiling Microbiologically Influenced Corrosion Engineering to Transfigure Damages into Benefits: A Textile Sensor For H<sub>2</sub>O<sub>2</sub> Detection in Clinical Cancer Tissues. *Chem. Eng. J.* **2022**, *427*, 131398.

(884) Jiang, S. X.; Guo, R. H. Electromagnetic Shielding and Corrosion Resistance of Electroless Ni-P/Cu-Ni Multilayer Plated Polyester Fabric. *Surf. Coat. Technol.* **2011**, *205*,

4274-4279.

(885) Jiang, S.; Miao, D.; Li, A.; Guo, R.; Shang, S. Adhesion and Durability of Cu Film on Polyester Fabric Prepared by Finishing Treatment with Polyester-Polyurethane and Aqueous Acrylate. *Fibers Polym.* **2016**, *17*, 1397-1402.

(886) Ahn, Y.; Jeong, Y.; Lee, Y. Improved Thermal Oxidation Stability of Solution-Processable Silver Nanowire Transparent Electrode by Reduced Graphene Oxide. *ACS Appl. Mater. Interfaces* **2012**, *4*, 6410-6414.

(887) Zhao, F.-G.; Kong, Y.-T.; Xu, Z.-W.; Yao, X.; Zuo, B.; Li, W.-S. High-Performance Flexible Transparent Conductive Films Achieved by Cooperation Between 1D Copper Nanowires and 2D Graphene Materials. *J. Mater. Chem. C* **2017**, *5*, 5509-5516.

(888) Yang, C. Y.; Reghu, M.; Heeger, A. J.; Cao, Y. Thermal Stability of Polyaniline Networks in Conducting Polymer Blends. *Synth. Met.* **1996**, *79*, 27-32.

(889) Mawad, D.; Mansfield, C.; Lauto, A.; Perbellini, F.; Nelson, G. W.; Tonkin, J.; Bello, S. O.; Carrad, D. J.; Micolich, A. P.; et al. A Conducting Polymer with Enhanced Electronic Stability Applied in Cardiac Models. *Sci. Adv.* **2016**, *2*, e1601007.

(890) Chiang, C.-J.; Tsai, K.-T.; Lee, Y.-H.; Lin, H.-W.; Yang, Y.-L.; Shih, C.-C.; Lin, C.-Y.; Jeng, H.-A.; Weng, Y.-H.; et al. In Situ Fabrication of Conducting Polymer Composite Film as a Chemical Resistive CO<sub>2</sub> Gas Sensor. *Microelectron. Eng.* **2013**, *111*, 409-415.

(891) Sang, M.; Kim, K.; Shin, J.; Yu, K. J. Ultra-Thin Flexible Encapsulating Materials for Soft Bio-Integrated Electronics. *Adv. Sci.* **2022**, *9*, 2202980.

(892) Tseghai, G. B.; Mengistie, D. A.; Malengier, B.; Fante, K. A.; Van Langenhove, L. PEDOT:PSS-Based Conductive Textiles and Their Applications. *Sensors* **2020**, *20*, 1881.

(893) Yu, Y.; Yan, C.; Zheng, Z. Polymer-Assisted Metal Deposition (PAMD): A Full-Solution Strategy for Flexible, Stretchable, Compressible, and Wearable Metal Conductors. *Adv. Mater.* **2014**, *26*, 5508-5516.

(894) Yu, A.; Sukigara, S.; Shirakihara, M. Effect of Silicone Inlaid Materials on Reinforcing Compressive Strength of Weft-Knitted Spacer Fabric for Cushioning Applications. *Polymers* **2021**, *13*, 3645.

(895) Lim, H.-R.; Kim, H. S.; Qazi, R.; Kwon, Y.-T.; Jeong, J.-W.; Yeo, W.-H. Advanced Soft Materials, Sensor Integrations, and Applications of Wearable Flexible Hybrid Electronics in Healthcare, Energy, and Environment. *Adv. Mater.* **2020**, *32*, 1901924.

(896) Torres, F.; das Graças, M.; Melo, M.; Tosti, A. Management of Contact Dermatitis Due to Nickel Allergy: an Update. *Clinical, Cosmetic and Investigational Dermatology* **2009**, *2*, 39-48.



- (897) Mao, S.; Sun, B.; Zhou, G.; Guo, T.; Wang, J.; Zhao, Y. Applications of Biomemristors in Next Generation Wearable Electronics. *Nanoscale Horiz.* **2022**, *7*, 822-848.
- (898) Oh, J. Y.; Bao, Z. Second Skin Enabled by Advanced Electronics. *Adv. Sci.* **2019**, *6*, 1900186.
- (899) Wang, D.; Chang, J.; Huang, Q.; Chen, D.; Li, P.; Yu, Y.-W. D.; Zheng, Z. Crumpled, High-Power, and Safe Wearable Lithium-Ion Battery Enabled by Nanostructured Metallic Textiles. *Fundam. Res.* **2021**, *1*, 399-407.
- (900) Luo, Y.; Wang, L.; Wei, Z.; Huang, Q.; Deng, Y.; Zheng, Z. Cracking-Controlled Slurry Coating of Mosaic Electrode for Flexible and High-Performance Lithium–Sulfur Battery. *Adv. Energy Mater.* **2023**, *13*, 2203621.
- (901) Guo, Q.; Zheng, Z. Rational Design of Binders for Stable Li-S and Na-S Batteries. *Adv. Funct. Mater.* **2020**, *30*, 1907931.
- (902) Fu, K.; Gong, Y.; Dai, J.; Gong, A.; Han, X.; Yao, Y.; Wang, C.; Wang, Y.; Chen, Y.; et al. Flexible, Solid-State, Ion-Conducting Membrane with 3D Garnet Nanofiber Networks for Lithium Batteries. *Proceed. Natl. Acad. Sci.* **2016**, *113*, 7094-7099.
- (903) Qian, S.; Liu, M.; Dou, Y.; Fink, Y.; Yan, W. A ‘Moore's law’ for Fibers Enables Intelligent Fabrics. *Natl. Sci. Rev.* **2023**, *10*, nwac202.
- (904) Sahasrabudhe, A.; Rupprecht, L. E.; Orguc, S.; Khudiyev, T.; Tanaka, T.; Sands, J.; Zhu, W.; Tabet, A.; Manthey, M.; et al. Multifunctional Microelectronic Fibers Enable Wireless Modulation of Gut And Brain Neural Circuits. *Nat. Biotechnol.* **2023**, 10.1038/s41587-41023-01833-41585.
- (905) Ikra Iftekhhar, S.; Justine, D.; Dominic, L.; Patricia, I. D. Smart Textiles Testing: A Roadmap to Standardized Test Methods for Safety and Quality-Control. In *Textiles for Functional Applications*, Bipin, K. Ed.; IntechOpen, 2021; p Ch. 7.
- (906) Zeng, K.; Shi, X.; Tang, C.; Liu, T.; Peng, H. Design, Fabrication and Assembly Considerations for Electronic Systems Made of Fibre Devices. *Nat. Rev. Mater.* **2023**, *8*, 552-561.
- (907) Meena, J. S.; Choi, S. B.; Jung, S.-B.; Kim, J.-W. Electronic Textiles: New Age of Wearable Technology for Healthcare and Fitness Solutions. *Mater. Today Bio* **2023**, *19*, 100565.
- (908) Dulal, M.; Afroj, S.; Ahn, J.; Cho, Y.; Carr, C.; Kim, I.-D.; Karim, N. Toward Sustainable Wearable Electronic Textiles. *ACS Nano* **2022**, *16*, 19755-19788.
- (909) Timmins, M. Environmental and Waste Issues Concerning the Production of Smart Clothes and Wearable Technology. In *Smart Clothes and Wearable Technology*; McCann, J.,

Bryson, D., Eds.; Woodhead Publishing, 2009; pp 319-331. DOI: 10.1533/9781845695668.3.319.

(910) Tao, X.; Liao, S.; Wang, Y. Polymer-Assisted Fully Recyclable Flexible Sensors. *EcoMat* **2021**, 3, e12083.

(911) Zhang, L.; Leung, M. Y.; Boriskina, S.; Tao, X. Advancing Life Cycle Sustainability of Textiles Through Technological Innovations. *Nat. Sustain.* **2023**, 6, 243-253.

(912) Zarei, M.; Lee, G.; Lee, S. G.; Cho, K. Advances in Biodegradable Electronic Skin: Material Progress and Recent Applications in Sensing, Robotics, and Human-Machine Interfaces. *Adv. Mater.* **2023**, 35, 2203193.

(913) Chen, S.; Wu, Z.; Chu, C.; Ni, Y.; Neisiany, R. E.; You, Z. Biodegradable Elastomers and Gels for Elastic Electronics. *Adv. Sci.* **2022**, 9, 2105146.

(914) Köhler, A. R.; Hilty, L. M.; Bakker, C. Prospective Impacts of Electronic Textiles on Recycling and Disposal. *J. Ind. Ecol.* **2011**, 15, 496-511.